

**Characterisation of the Oxidation State of Hepatitis C
Virus (HCV) Envelope Glycoproteins E1 and E2 during
Glycoprotein Biosynthesis and Virus Entry**

Johanna Elisabeth Dean, BSc (Hons)

A thesis submitted for the degree of Doctor of Philosophy

2011

Department of Microbiology

Faculty of Medicine, Nursing, and Health Sciences

Monash University

Clayton, VIC 3800

Copyright Notices

Notice 1

Under the Copyright Act 1968, this thesis must be used only under the normal conditions of scholarly fair dealing. In particular no results or conclusions should be extracted from it, nor should it be copied or closely paraphrased in whole or in part without the written consent of the author. Proper written acknowledgement should be made for any assistance obtained from this thesis.

Notice 2

I certify that I have made all reasonable efforts to secure copyright permissions for third-party content included in this thesis and have not knowingly added copyright content to my work without the owner's permission.

Contents

Abstract	7
Declaration	9
Acknowledgements	10
Abbreviations	12
List of Figures	16
List of Tables.....	19
Chapter 1 – Introduction and Literature Review	20
1.1 Overview of Hepatitis C Virus	20
1.1.1 Epidemiology	20
1.1.2 Disease description and therapy.....	22
1.2 HCV Genomic Organisation and Structure	24
1.2.1 Classification.....	24
1.2.2 Virus structure.....	25
1.3 HCV Lifecycle	26
1.3.1 Receptor binding and viral fusion.....	26
1.3.2 Translation and processing.....	28
1.3.3 RNA replication.....	30
1.3.4 Virion assembly and egress.....	32
1.4 Structure and Function of Non-Structural Proteins	33
1.5 HCV Structural Proteins.....	35
1.5.1 Core	35
1.5.2 Envelope glycoproteins E1 and E2: biosynthesis.....	35
1.5.3 Structural and functional determinants of E2	43
1.5.4 Structural and functional determinants of E1	51

1.6 HCV Host Cell Receptors	54
1.6.1 Cellular attachment factors	54
1.6.2 CD81	55
1.6.3 Scavenger Receptor Class B Type 1 (SR-BI)	57
1.6.4 Claudin-1 and occludin.....	58
1.7 Virus-Cell Membrane Fusion	61
1.7.1 Structure and function of viral fusion proteins	61
1.7.2 Fusion activation triggers	67
1.8 Hypotheses and Aims	69
Chapter 2 – Materials and Methods.....	71
2.1 Construction of pE1E2H77c Encoding HCV Envelope Glycoproteins....	71
2.2 Construction of Full Length HCV Vector pJC1FLAG2(p7-NS-GLUC2A).	71
2.3 Construction of pMBP-E1	72
2.4 Construction of pcE1myc	72
2.5 Additional Plasmids	73
2.6 Cloning Procedures	74
2.6.1 Restriction digestion of DNA	74
2.6.2 Site directed mutagenesis by overlap extension PCR	74
2.6.3 Site directed mutagenesis by QuikChange II Site-Directed Mutagenesis Kit ..	
.....	77
2.6.4 DNA cycle sequencing.....	78
2.6.5 Agarose gel electrophoresis of DNA	79
2.6.6 Preparation of competent cells.....	79
2.6.7 Plasmid transformation into competent cells.....	79
2.6.8 Small scale plasmid purification (mini-prep).....	80
2.6.9 Large scale plasmid purification (midi-prep).....	80
2.7 RNA Transcription.....	80
2.7.1 RNA gel electrophoresis	80
2.7.2 RNA quantification by quantitative reverse transcriptase PCR (qRT-PCR).	81
2.8 Antibodies	82
2.9 Cell Lines and Transient Transfections.....	82
2.9.1 FuGene-6 DNA transfection.....	83

2.9.2 DMRIE-C RNA transfection.....	83
2.10 Protein Analysis.....	84
2.10.1 Sodium dodecyl sulphate polyacrylamide gel electrophoresis (SDS-PAGE).	84
2.10.2 Radio-immunoprecipitation (RIP)	85
2.10.3 Deglycosylation of mammalian expressed, secreted proteins	86
2.10.4 Biotinylation of E1E2	87
2.10.5 Solid phase E1E2-CD81 binding assay.....	87
2.11 E1E2-Pseudotyped HIV-1 Particle Entry Assay.....	88
2.12 HCVcc Quantification	90
2.12.1 HCVcc TCID ₅₀ /ml	90
2.12.2 Core ELISA assay	90
2.13 HCVcc Infection	91
2.14 Huh-7.5 Viability Assays	92
2.15 Bacterial Protein Expression	92
2.15.1 Small scale purification of MBP-tagged proteins	93
2.15.2 Large scale purification of MBP-tagged proteins	93
2.15.3 Large scale purification of His-tagged proteins.....	93
2.16 Limited Proteolysis of MBP-E1₂₅₉	94
2.17 Insulin Reduction Assay	94
Chapter 3 – Oxidation State of HCV Envelope Glycoproteins E1 and E2	95
3.1 Introduction	95
3.2 Results	96
3.2.1 E1E2 contain free sulfhydryl groups that are essential for HCV entry.....	96
3.2.2 Free sulfhydryl groups are present on HCVpp incorporated forms of E1 and E2.....	101
3.2.3 E1 and E2 are not linked via a labile disulfide bond.....	104
3.2.4 Non-covalent E1 and E2 contain free sulfhydryl groups in mature HCVpp105	
3.2.5 HCVpp but not HCVcc remains sensitive to M135 labelling following attachment to cells	109
3.2.6 DTT does not rescue entry of alkylated virus	110
3.2.7 Characterisation of free sulfhydryls in E1 and E2 post CD81 binding	113

3.2.8	Characterisation of free sulfhydryls in E1 and E2 post heparin binding	115
3.3	Discussion and Conclusions	118
3.4	Supplementary Data.....	128
Chapter 4 – Characterisation of a Conserved CXXC Thiol-Disulfide Exchange Motif in E1		
130		
4.1	Introduction	130
4.2	Results - Role of C²²⁶VPC Cys Residues in Glycoprotein Biosynthesis and Virus Entry	132
4.2.1	Expression of E1 and E2 containing C ²²⁶ VPC Cys to Ala mutations.....	132
4.2.2	Heterodimerisation of E1E2 containing E1 Cys to Ala mutations.....	133
4.2.3	HCVpp incorporation of conformational and non-conformational E1E2 for E1 Cys to Ala mutants	134
4.2.4	Expression of E1 and E2 containing C ²²⁶ VPC Cys to Ser mutations	137
4.2.5	Heterodimerisation of E1E2 containing C ²²⁶ VPC Cys to Ser mutations....	138
4.2.6	HCVpp incorporation of conformational E1E2 containing Cys to Ser mutations	139
4.2.7	Pulse chase analysis of AVPC and CVPA mutants	140
4.2.8	Pulse chase analysis of AVPA mutant	145
4.2.9	CD81 binding by C ²²⁶ VPC Cys to Ala mutants.....	147
4.2.10	Entry competence of C ²²⁶ VPC cysteine mutants.....	148
4.3	Results - Role of C²²⁶VPC Val, Pro Dipeptide in Glycoprotein Biosynthesis and Virus Entry	151
4.3.1	Western blot analysis of Val227, Pro228 mutants.....	152
4.3.2	Expression of E1E2 heterodimers from Val, Pro mutants	153
4.3.3	HCVpp incorporation of conformational E1E2 from Val, Pro mutants	154
4.3.4	HCVpp incorporation of total E1E2 from Val, Pro mutants.....	157
4.3.5	CD81 binding by Val227, Pro228 mutants	159
4.3.6	Formation of immunologically distinct domains in C ²²⁶ VPC mutants	160
4.3.7	Entry competence of Val227 and Pro228 mutants.....	162
4.4	Results - Maleimide Biotinylation of Val227 Mutants	165
4.5	Discussion and Conclusions	168

Chapter 5 – Expression of Recombinant E1 for Redox Activity Assays	176
5.1 Introduction	176
5.2 Results - Bacterial Expression of E1	179
5.2.1 Small scale expression of MBP-E1 proteins	180
5.2.2 Large scale expression and purification of MBP-E1 proteins	183
5.2.3 Analysis of MBP-E1 ₃₂₉ FPLC fractions.....	185
5.2.4 Analysis of MBP-E1 ₃₄₀ FPLC fractions.....	188
5.2.5 Analysis of MBP-E1 ₃₅₁ FPLC fractions.....	190
5.2.6 Identification of MBP-E1 truncation products	192
5.2.7 Small scale expression of MBP-E1 ₂₅₉	193
5.2.8 Large scale expression of MBP-E1 ₂₅₉	196
5.2.9 Limited proteolysis of MBP-E1 ₂₅₉	198
5.2.10 Insulin reduction assay	201
5.3 Results - Mammalian Expression of E1	202
5.3.1 Expression of E1-myc in HEK 293T cells.....	202
5.3.2 Expression of E1-myc in CHO-K1 and Lec-8 cells	204
5.3.3 Deglycosylation of E1-myc expressed in CHO-K1 and Lec-8 cells	206
5.4 Discussion and Conclusions	210
Chapter 6 – General Conclusions.....	218
Chapter 7 - References	218

Abstract

Hepatitis C virus (HCV) is a major cause of chronic liver disease, including cirrhosis and hepatocellular carcinoma (HCC) and is a leading reason for liver transplantation in industrialised countries. The most recent estimate of global prevalence is 2-3% representing 130-170 million HCV-positive people [1].

HCV is an enveloped, positive strand RNA virus which comprises the hepacivirus genus within the *Flaviviridae* family. The virus displays two glycoproteins on its surface, E1 and E2, which are required to mediate entry into hepatocytes [2,3,4]. Cellular infection is dependent on receptors CD81, SR-BI, claudin-1, 6 or 9, and occludin [5,6,7,8,9,10]. Following attachment HCV is thought to be internalised via clathrin mediated endocytosis where the low pH of the endosome is required for fusion of the viral and cellular membranes [11]. Productive infection occurs following delivery of the viral nucleocapsid to the cytoplasm where RNA translation, replication and virus assembly takes place.

This project investigated the significance of the redox state of HCV envelope glycoproteins E1 and E2 during glycoprotein biosynthesis and virus entry. It was found that virion incorporated forms of E1 and E2 contain at least one free cysteine residue each prior to cellular attachment. Alkylation of reduced sulfhydryl groups prior to cellular attachment abolished virus infectivity. However, it was found that cell culture derived HCV (HCVcc) became insensitive to thiol-reactive agents after binding to cells indicating that the thiol groups were no longer available for modification following receptor engagement. These data suggest that free sulfhydryl groups within E1 and/or E2 are required to mediate virus entry and that receptor engagement may induce a switch in glycoprotein redox state from reduced to oxidised.

A highly conserved C²²⁶VPC thiol isomerisation motif was identified in E1 critical for formation of a functional E1E2 heterodimer. Mutation of Val227 to Ile or Leu allowed normal E1 and E2 biosynthesis and virion incorporation. However,

mutant viruses demonstrated significantly reduced entry compared to wild type. These findings indicate that the C²²⁶VPC motif is required to function during virus entry.

Domain organisation within E1 was examined by expression of E1 ectodomain residues in bacteria. A stable domain consisting of N-terminal amino acids 191-259 was identified and produced as a soluble monomer. When expressed in mammalian cells, ectodomain residues 191-329 were efficiently expressed and secreted from cells suggesting that when glycosylated these residues may fold independently from other HCV protein sequences.

The findings from this study indicate that HCV functionality is highly dependent on careful regulation of the redox state of the viral envelope glycoproteins, possibly mediated by the E1 C²²⁶VPC motif.

Declaration

The work described in this thesis was conducted at the Burnet Institute, Melbourne, in affiliation with the Department of Microbiology at Monash University, Clayton Campus. This thesis contains no material which has been accepted for the award of any other degree or diploma in any other university or institution. To the best of my knowledge and belief, this thesis contains no material previously published or written by another person, except where due reference has been made in the text.

Signed _____

Acknowledgements

Firstly, I am very grateful to Monash University for providing me with a Monash Graduate Scholarship for the duration of my PhD studies. Thank you also to the Burnet Institute, for providing me with lab space and all the tools required for me to conduct my research.

I would like to thank my primary supervisor Associate Professor Heidi Drummer for her expertise, support, encouragement and positivity towards this project. I have learnt more than I could have hoped for while being in your lab. I would also like to thank Dr. Pantelis Pountourios for his input into this work, especially in manuscript preparation and conference proceedings.

All the members of the Drummer/Pountourios lab have been very supportive throughout the last 4 years. I would especially like to thank Irene Boo and Kevin te Wierik for their technical help.

Many of the experiments described were dependent on reagents that were kind gifts from other researchers. I am forever grateful to Professor Jean Dubuisson for the provision of antibodies H53, H52 and A4, and to Professor Charles Rice for supplying the pJC1FLAG2(p7-NS-GLUC2A) construct and Huh-7.5 cells.

I am sure I would not have made it to the end of this degree without the infinite support of my family. Thanks Mum, Dad, Alex, Oli and Josh for never doubting that I could complete this marathon. Josh, I will do my best to be as forgiving towards you when your time comes.

To all my friends, especially Carrie, Carla, Courtney, Jess W, Jess A, Jas, and fellow PhD'er Kitty, thanks for all the coffee/wine/email/phone dates that have kept me going. I am particularly grateful to Jas for proofreading my final thesis draft so efficiently.

Lastly, I would like to thank my fiancée Arran, for waiting for me. I can't wait to begin the rest of our lives together.

Abbreviations

A	Alanine
AIDS	Acquired immunodeficiency virus
Ala	Alanine
ALT	Alanine aminotransferase
Arg	Arginine
ASGP-R	Asialoglycoprotein receptor
Asp	Asparagine
bp	Base pair
BVDV	Bovine viral diarrhoea virus
C	Cysteine
°C	Degrees centigrade
cCMP	Cyclic cytidine 3',5'-monophosphate
CD	Circular dichroism
CD4	Cluster of differentiation 4
CD81	Cluster of differentiation 81
cDNA	Complementary deoxyribonucleic acid
CMV	Cytomegalovirus
Cys	Cysteine
Da	Dalton
DAB	3-3'-diaminobenzidine tetrahydrochloride
DC-SIGN	Dendritic cell-specific intercellular adhesion molecule-3-grabbing non-integrin
DMEM	Dulbecco's minimal essential medium
DMF10	DMEM with 10% fetal calf serum and 2 mM L-glutamine
DMF20	DMEM with 20% fetal calf serum and 2 mM L-glutamine
DMF10NEA	DMF10 with non-essential amino acids
DMF20NEA	DMF20 with non-essential amino acids
DNA	Deoxyribonucleic acid
dNTP	Deoxynucleotide triphosphate
dsRNA	Double stranded ribonucleic acid
DTT	Dithiothreitol
dUTP	Deoxyuridine triphosphate
E	Glutamate
E1	Envelope glycoprotein 1
E2	Envelope glycoprotein 2
E1/E2	Disulfide linked, high molecular weight forms of E1 and E2
<i>E. coli</i>	<i>Escherichia coli</i>
EDTA	Ethylenediaminetetraacetic acid
ELISA	Enzyme linked immunosorbent assay
Endo H	Endoglycosidase H
ER	Endoplasmic reticulum
F	Phenylalanine
FTIR	Fourier transform infrared (spectroscopy)
FPLC	Fast protein liquid chromatography
g	Gram

g	Relative centrifugal force (xg)
G	Glycine
GAG	Glycosaminoglycan
Gln	Glutamine
Glu	Glutamate
Gly	Glycine
gp	Glycoprotein
GTP	Guanosine triphosphate
h	Hour
H	Histidine
HCC	Hepatocellular carcinoma
HCV	Hepatitis C virus
HCVcc	Cell culture derived HCV
HCV-LP	HCV-like particle
HCVpp	HCV pseudotype particle
HEK	Human embryonic kidney
His	Histidine
HIV	Human immunodeficiency virus
HTLV	Human T-cell leukaemia virus
HVR	Hypervariable region
I	Isoleucine
IFN α	Interferon alpha
Ig	Immunoglobulin
igVR	Intergenotypic variable region
Ile	Isoleucine
IPTG	Isopropyl- β -D -thiogalactopyranoside
IRES	Internal ribosome entry site
K	Lysine
kb	KiloBase
kDa	KiloDalton
LD	Lipid droplet
L	Litre
L	Leucine
LB	Luria Bertani
LDL	Low density lipoprotein
LDLr	Low density lipoprotein receptor
LEL	Large extracellular loop
Leu	Leucine
LI-COR	Odyssey infrared imaging system
L-SIGN	Liver-specific intracellular adhesion molecule-3 grabbing non-integrin
Lys	Lysine
M	Molar
M	Methionine
M135	4-(N-Maleimido)benzyl- α -trimethylammonium iodide
MAb	Monoclonal antibody
Maleimide-biotin	EZ-Link Maleimide-PEG2-Biotin
MBP	Maltose binding protein
Met	Methionine
μ g	Microgram

mg	Milligram
min	Minute
µl	Microlitre
ml	Millilitre
mM	Millimolar
MPHR	Membrane proximal heptad repeat
MLV	Murine leukaemia virus
MoMLV	Molony murine leukaemia virus
MWCO	Molecular weight cut off
N	Asparagine
nAb	Neutralising antibody
NEM	N-Ethylmaleimide
NHS-biotin	Sulfo-NHS-LC-Biotin
nm	Nanometer
NMR	Nuclear magnetic resonance
NS	Non-structural
NTP	Nucleoside triphosphate
OD	Optical density
P	Proline
PBS	Phosphate buffered saline
PBST	Phosphate buffered saline + 0.05% Tween-80
PCR	Polymerase chain reaction
PDI	Protein disulfide isomerase
PEG	Polyethylene glycol
PEG-IFN α	PEGylated interferon alpha
pH	Potential of hydrogen
Phe	Phenylalanine
pKa	Acid dissociation constant
PMSF	Phenylmethanesulfonylfluoride
PNGase F	Peptide: N-glycosidase F
Pro	Proline
Q	Glutamine
R	Arginine
RBD	Receptor binding domain
RIP	Radioimmunoprecipitation
RLU	Relative light units
RNA	Ribonucleic acid
RNase	Ribonuclease
RdRp	RNA dependent RNA polymerase
rpm	Revolutions per minute
RT-PCR	Reverse transcriptase polymerase chain reaction
SDS	Sodium dodecyl sulfate
SDS-PAGE	Sodium dodecyl sulfate polyacrylamide gel electrophoresis
sE2	E2 ectodomain lacking the TMD
SR-BI	Scavenger receptor class B type I
SU	Surface receptor binding glycoprotein
SVR	Sustained virological response
TB	Terrific broth
TBEV	Tick-borne encephalitis virus

TCID ₅₀	50% tissue culture infectious dose
TM	Transmembrane protein
TMD	Transmembrane domain
tRNA	Transfer ribonucleic acid
Trp	Tryptophan
Trx	Thioredoxin
Tyr	Tyrosine
U	Units
V	Volts
V	Valine
v/v	Volume to volume ratio
Val	Valine
VLDL	Very low density lipoprotein
VSV	Vesicular stomatitis virus
VSVg	Vesicular stomatitis virus envelope protein G
W	Tryptophan
WHO	World Health Organization
WT	Wild type
Y	Tyrosine

List of Figures

Figure 1-1. Schematic representation of HCV entry into hepatocytes.....	28
Figure 1-2. Genomic organisation and polypeptide processing of HCV	30
Figure 1-3. Schematic representation of the localisation and orientation of HCV structural and non-structural proteins at the ER membrane	43
Figure 1-4. Schematic representation of E2.....	50
Figure 1-5. Schematic representation of E1	53
Figure 1-6. Virus-cell membrane fusion	62
Figure 1-7. Schematic representation of a class II fusion protein pre and post fusion activation	65
Figure 3-1. HCV entry is dependent on the presence of free sulfhydryl groups .	100
Figure 3-2. Free sulfhydryl groups are present on both E1 and E2 in mature virus particles	103
Figure 3-3. E1 and E2 are not linked via a labile disulfide bond.....	105
Figure 3-4. Non-covalent and multimeric oligomers of HCVpp incorporated E1 and E2 contain free sulfhydryl groups.....	107, 108
Figure 3-5. HCVpp but not HCVcc remains sensitive to M135 labelling following attachment to cells.....	110
Figure 3-6. DTT treatment of alkylated HCVcc does not rescue HCVcc entry ...	112
Figure 3-7. E1 and E2 contain free sulfhydryl groups post CD81 binding	114
Figure 3-8. E1 and E2 contain free sulfhydryl groups post heparin binding	117
Figure 4-1. Schematic representation of E1 and Clustal X alignment of prototype strains representative of each HCV genotype.....	131
Figure 4-2. Expression of E1 and E2 containing C ²²⁶ VPC Cys to Ala mutations	133
Figure 4-3. Heterodimerisation of E1E2 containing C ²²⁶ VPC Cys to Ala mutations	134
Figure 4-4. HCVpp incorporation of conformational and non-conformational E1E2 containing C ²²⁶ VPC Cys to Ala mutations.....	136
Figure 4-5. Expression of E1 and E2 containing C ²²⁶ VPC Cys to Ser mutations	138
Figure 4-6. Heterodimerisation of E1E2 containing C ²²⁶ VPC Cys to Ser mutations	139

Figure 4-7. HCVpp incorporation of conformational E1E2 containing C ²²⁶ VPC Cys to Ser mutations.....	140
Figure 4-8. Pulse chase analysis of CVPC-wt, AVPC and CVPA mutants.....	144
Figure 4-9. Pulse chase analysis of CVPC-wt and AVPA mutant	146
Figure 4-10. Solid phase E2-CD81 binding assay for Cys to Ala mutants	148
Figure 4-11. Effect of cysteine mutagenesis on HCVpp and HCVcc entry.....	150
Figure 4-12. Western blot analysis of Val227, Pro228 mutants	153
Figure 4-13. Analysis of E1E2 heterodimerisation of Val, Pro mutant E1E2 in HEK 293T cell lysates	154
Figure 4-14. Characterisation of conformational E1E2 incorporation into mature HCVpp for V227, P228 mutants.....	156
Figure 4-15. Characterisation of total E1E2 incorporation into mature HCVpp for V227, P228 mutants	158
Figure 4-16. Solid phase E2-CD81 binding assay for Val227, Pro228 mutants .	160
Figure 4-17. Characterisation of E1 and E2 incorporated into HCVpp by domain specific, conformational antibodies	162
Figure 4-18. Effect of Val, Pro mutagenesis on HCVpp and HCVcc entry	164
Figure 4-19. Characterisation of free sulfhydryl groups in E1 and E2 of Val227 mutants	167
Figure 5-1. Schematic representation of various E1 ectodomain lengths expressed as MBP-tagged proteins in <i>E. coli</i>	180
Figure 5-2. Small scale expression and purification of MBP-E1 constructs from <i>E. coli</i>	182
Figure 5-3. FPLC profiles of MBP-E1 proteins	184
Figure 5-4. Purification of MBP-E1 ₃₂₉ and separation of oligomeric forms	187
Figure 5-5. Purification of MBP-E1 ₃₄₀ and separation of oligomeric forms	189
Figure 5-6. Purification of MBP-E1 ₃₅₁ and separation of oligomeric forms	191
Figure 5-7. Mass spectrometry analysis of MBP-E1 ₃₂₉ fractions 3 and 4	193
Figure 5-8. Expression and purification of MBP-E1 ₂₅₉	195
Figure 5-9. Purification of MBP-E1 ₂₅₉ and separation of oligomeric forms	197
Figure 5-10. Analysis of MBP-E1 ₂₅₉ by limited proteolysis	200
Figure 5-11. Insulin reducing activity of MBP-E1 ₂₅₉	202
Figure 5-12. Expression of E1-myc in HEK 293T cells.....	204
Figure 5-13. Expression of E1-myc in CHO-K1 cells and Lec-8 cells.....	206

Figure 5-14. Deglycosylation of E1myc proteins expressed in CHO-K1 and Lec-8 cells	209
Figure 5-15. NMR structures of thioredoxin in reduced and oxidised forms	213
Figure 6-1. Schematic model demonstrating the predicated role of thiol isomerisation in fusion activation of HCV glycoproteins E1 and E2	221

List of Tables

Table 2-1. pMBP-E1 primers	72
Table 2-2. pcE1myc primers.....	73
Table 2-3. Primers used for site directed mutagenesis of pE1E2H77c.....	76
Table 2-4. PCR cycle conditions for reactions 1, 2 and 3 of overlap extension PCR.....	77
Table 2-5. Quikchange primers used for site directed mutagenesis of pJC1FLAG2(p7-NS-GLUC2A)	78
Table 2-6. BigDye Terminator cycle sequencing conditions.	79
Table 2-7. Cycle conditions for quantitative real-time RT PCR.....	81
Table 3-1. Quantification of free sulfhydryl groups in E1 and E2 post CD81 binding	114
Table 4-1. Replication rate and concentration of structural protein core in HCVcc CVPC-wt and Cys mutant viruses.....	151
Table 4-2. Replication rate and concentration of structural protein core in HCVcc CVPC-wt and Val227, Pro228 mutant viruses	165
Table 4-3. Quantitative comparison of Maleimide-biotin labelling of E1 and E2 from V227I/L HCVpp.....	167

Chapter 1 – Introduction and Literature Review

1.1 Overview of Hepatitis C Virus

1.1.1 Epidemiology

Hepatitis C Virus (HCV) was first identified in 1989 as the causative agent of post-transfusion non-A, non-B type hepatitis infection [12,13]. According to the most recent estimates from the World Health Organization (WHO) global prevalence of HCV infection stands at 2-3% with 130-170 million HCV-positive people worldwide [1]. HCV is a major cause of chronic liver disease, including cirrhosis and hepatocellular carcinoma (HCC), and is a leading reason for liver transplantation in industrialised countries. A study performed in 2006 estimates 27% of cirrhosis and 25% of HCC cases worldwide are attributable to HCV infection [14]. There is currently no vaccine available to prevent or treat HCV.

Region specific prevalence of HCV is highly varied and there is an absence of reported infection data for many countries. According to the WHO, African and Eastern Mediterranean regions have the highest infection rates (>10%), while Egypt has the highest seroprevalence worldwide with estimates of 15-20% [15]. Developed countries including Canada, Australia and those in Northern and Western Europe report low seroprevalence rates of <1% [16], while slightly higher rates have been estimated for the United States (1.6%), Japan (2%) and China (3%) [17,18,19,20,21]. It should be noted that the validity of each estimate is limited by factors such as study sample size, population bias and population accessibility. Therefore in some cases, particularly in developing countries where few epidemiological studies have been performed, these rates are likely to underestimate the true prevalence.

HCV is a blood borne disease and as such disease prevalence appears to closely track medical and social behaviour. For example, previous routine use of reusable syringes for injections and unscreened blood products are likely to

account for the observation that the prevalence of HCV antibodies in persons from Japan, China and Italy steadily increases with age [21,22,23,24]. In addition, the high rate of HCV infection in Egypt has been attributed to extensive use of parenteral antischistosomal therapy from the 1920s until the 1980s [15]. In developed countries where safe medical practices have been adopted for some time, newly acquired infections are most common in young adults who are injecting drug users [25,26].

In Australia, the 2010 HIV/AIDS, Viral Hepatitis and Sexually Transmissible Infections in Australia Annual Surveillance Report released by the National Centre in HIV Epidemiology and Clinical Research, estimated the national HCV prevalence at 217 000 including 46 000 living with moderate to severe liver disease. The report found that the *per capita* rate of diagnosis of HCV infection in Australia declined by 12% in 2009 to 51.9 per 100 000 population. Based on these reported cases, HCV transmission in Australia is considered to occur predominantly among people with a recent history of injecting drug use [27].

While improved health care procedures continue to result in an overall reduction in newly acquired HCV infections in developed countries, risk of transmission from unsafe injecting drug use, unsterile tattoos or body piercing, needlestick injuries or other accidental blood-blood contact events is still high. Furthermore, developing countries are still at risk from unsafe therapeutic injections and contaminated blood [28]. A recent study indicated that the rate of HCV transmission in Egypt remains exceptionally high suggesting a resistance to adopt infection control measures [29]. The chronic nature of HCV means that despite an overall decrease in rates of infection, significant numbers of people around the world continue to live with the disease. It is predicted that as the current HCV-positive population ages, rates of HCV-related deaths will also increase [30]. As such, further clinical research of the virus, development of anti-viral drugs, and prophylactic and therapeutic vaccines are all essential to eliminate the burden of HCV disease.

1.1.2 Disease description and therapy

In many cases, HCV infection results in liver disease caused by the body's immune response to the virus. The extent of liver damage in patients can be determined by histological analyses following liver biopsy where a score from 0 to 4 is assigned based on fibrotic content (where 0 refers to a liver with no scarring and 4 represents a liver with advanced scarring or cirrhosis) [31].

HCV can cause both acute and chronic infections. Acute HCV is defined as the first 6 months immediately following infection after which a continuing infection is classified as chronic. Between 20-50% of acute infections are cleared completely within 2-6 months, while the remaining 50-80% will progress to chronic infections at which stage viral clearance is very rare. Between 40-60% of chronically infected people experience some level of liver disease within 15 years of acquiring HCV. Five to 10% of chronically infected people will develop cirrhosis and 2-5% will experience liver failure or hepatocellular carcinoma after 20 years of infection [32].

Acute HCV infection is characterised by the presence of viral RNA in the blood 1-2 weeks after virus exposure [33,34,35,36], elevated levels of the liver enzyme alanine aminotransferase (ALT; indicative of liver damage) and production of anti-HCV antibodies 6-8 weeks following infection [37]. In patients that clear acute infections, HCV RNA levels drop below detectable levels and ALT levels return to normal. However, in chronic infections, persistent or fluctuating levels of ALT are seen despite the disease frequently remaining asymptomatic [38]. In these patients RNA levels can also alter significantly sometimes dropping below detectable levels [34,36,39]. As such, diagnosis and monitoring of infections can be difficult.

The current standard of care for HCV is a combination of PEGylated-interferon- α (PEG-IFN α) and ribavirin. HCV has been treated with anti-viral interferon since 1986, 3 years prior to the identification of non-A non-B hepatitis [40]. However, treatment of HCV with interferon alone results in limited virus

clearance; a 6-month course leads to sustained virological response rates (SVR; associated with removal of the virus) of 6–12% while extending treatment time to 12 months improves this rate to just 16–20% [41]. Addition of ribavirin (a broad spectrum antiviral guanosine analogue) into the treatment regime has doubled the sustained response rate [42], and pegylated interferon is now used to increase the half life of circulating interferon [43]. Even still, current estimates of SVR stand at just 50% [44]. A long treatment regime (up to 48 weeks) and frequent side effects including neuropsychiatric events, flu-like symptoms and blood toxicities, cause many patients to discontinue treatment prior to completion [45].

There are 6 major HCV genotypes [46] and although virus genotype is not a predictor of the outcome of infection, it does predict the likelihood of treatment response. Infections with genotype 1a virus are the most common in developed countries and are also the least likely to be cleared with the current standard of care [47].

Significant advances in the treatment of HCV are expected in the near future with the recent development of inhibitors directed against the HCV polymerase and protease proteins. These drugs are likely to provide a better outcome, especially for genotype 1a infections, than the current standard of care [48,49,50,51]. It is inevitable that drug resistance will emerge upon the introduction of these therapies due to the high mutation rate and heterogeneity of HCV sequences, therefore combination therapies will be essential in order to limit the rate of emergence of resistant virus.

1.2 HCV Genomic Organisation and Structure

1.2.1 Classification

HCV comprises the hepacivirus genus within the *Flaviviridae* family which also consists of the pestivirus and flavivirus genera [52] as well as the GB viruses [53]. HCV is further divided into 6 genotypes that differ by up to 30% at the nucleotide level as well as many more subtypes that differ by up to 20% [46]. HCV is an enveloped virus that has a positive strand ~9.6 kb RNA genome encoding a single open reading frame. The genome is expressed as one long ~3 000 amino acid polyprotein that is cleaved into structural proteins (core and envelope glycoproteins E1 and E2) and non-structural proteins (NS2, NS3, NS4A, NS4B, NS5A and NS5B, p7 and F) by host cell signalases and viral proteases.

The classification of HCV was initially proposed in 1991 based on genomic similarity to flaviviruses [54]. All viruses classified within the *Flaviviridae* family are enveloped and contain a single stranded, positive sense RNA genome that encodes a single open reading frame. The genome arrangement encodes structural proteins at the N-terminal end of the polypeptide followed by the non-structural proteins [55]. Furthermore, the arrangement of HCV envelope glycoproteins E1 and E2 in tandem in the polypeptide is characteristic of flaviviruses including tick borne encephalitis virus (TBEV), dengue virus, West Nile virus and yellow fever virus. Despite little sequence homology, flaviviruses show high structural similarity to viruses from a separate family of enveloped, positive strand RNA viruses, the *Togaviridae* [56]. Well characterised members of the *Togaviridae* include the alphaviruses Semliki Forest virus, Sindbis virus and chikungunya virus. Together, these viruses demonstrate important paradigms that have provided insights into the structure and function of HCV.

1.2.2 Virus structure

HCV particles are believed to be 40-70 nm in diameter [57] consisting of the viral RNA genome encapsulated by the structural protein core [58,59]. The viral membrane which surrounds this nucleocapsid is host derived and displays the membrane bound envelope glycoproteins E1 and E2.

There is little information regarding the 3D structure of HCV particles due to the low virus titre produced in cell culture. Cryo-electron microscopy (cryo-EM) studies have been performed by Yu *et al.* (2007) and Bonnafous *et al.* (2010) on HCV-like particles (HCV-LPs) and retroviral particles displaying HCV E1 and E2 (HCVpp), respectively. These studies indicate that the envelope glycoproteins arrange in a smooth outer layer on the virus [60,61] similar to the envelope proteins of dengue and West Nile flaviviruses [62,63]. This contrasts to the glycoprotein spikes observed on the surface of HIV and influenza virus [64,65].

HCV derived from infected patients demonstrates significant heterogeneity in density due to varying associations with low-density and very low density lipoproteins (LDL and VLDL) [66,67,68] and immunoglobulins [69]. Circulating free virus has also been identified [70]. LDL and VLDL are large particles 22-80 nm in diameter that are produced in the liver to allow transport of triglycerides and cholesterol through the blood stream [71,72]. In addition to these lipids, LDL and VLDL incorporate apolipoproteins. Viral proteins and RNA isolated from circulating HCV appear in the same fraction as apolipoproteins ApoB, ApoB48, ApoCII, ApoCIII and ApoE [73]. It is not currently understood how these large lipoprotein particles associate with HCV but they appear to play an important role in virus infectivity [74,75].

1.3 HCV Lifecycle

1.3.1 Receptor binding and viral fusion

Following attachment to target cells enveloped viruses must mediate fusion between viral and target cell membranes in order to induce productive infection. This can occur at either the plasma membrane of cells as has been described for paramyxo- [76] and corona viruses [77], or within an endocytic compartment as occurs for influenza [78] and flaviviruses [79].

HCV entry into hepatocytes is dependent on cellular receptors CD81 [5], the scavenger receptor class B type 1 (SR-BI) [6,7] and tight junction proteins claudin-1, 6 or 9 [8,9] and occludin [10] (schematically represented in Figure 1-1). In addition, a number of cellular attachment factors have been proposed that promote adsorption of HCV to the cell surface including the LDL receptor (LDLr) [80,81], glycosaminoglycans (GAGs) such as heparan sulfate, [82,83,84,85], lectin receptors DC-SIGN and L-SIGN [86,87] and the asialoglycoprotein receptor (ASGP-R) [88].

Following attachment to cells, HCV entry is thought to proceed via specific interactions between HCV envelope glycoprotein E2 and receptors CD81 and SR-BI, and indirect contacts with claudin-1 and occludin. The timing and order of involvement of each of the four receptors during HCV entry remains unclear. A kinetic study using nAb directed towards CD81 and SR-BI indicated that these receptors are likely to be involved in close succession [7]. It has been proposed that the virus-receptor complex then relocalises to the tight junctions of hepatocytes, possibly mediated by CD81 signalled actin reorganisation [89], where claudin-1 and occludin are required for a late stage in entry [8,90]. However, a recent report demonstrated association of claudin-1 with CD81 at the basolateral membrane of polarized HepG2 cells [91]. The group determined that the half-maximal time for antibody directed towards each of these receptors to neutralise HCV entry occurred within 3 minutes of each other. This would suggest that

claudin-1 may be involved in an earlier stage of entry than first thought (discussed in detail in section 1.6.4).

Internalisation of HCV occurs via clathrin mediated endocytosis with the low pH of the endosome required to induce fusion between viral and cellular membranes for delivery of the viral nucleocapsid into target cells [11,92]. HCV entry cannot be efficiently induced at the plasma membrane following low pH exposure suggesting that entry of HCV is likely to require a specific sequence of events involving the various cellular factors described above [11].

The viral fusion glycoproteins present on the surface of enveloped viruses mediate fusion between viral and cellular membranes. Characteristic of all fusion proteins is the presence of an N-terminal or internal hydrophobic peptide which is able to insert into target cell membranes following a specific activation trigger [56] such as exposure to low pH [78]. The viral fusion glycoproteins then undergo major conformational changes adopting a lower energy hairpin conformation that draws the viral and target cell membranes into close proximity [56]. The conformational changes are thought to release sufficient energy to drive reorganisation of the two lipid bilayers allowing for formation of a fusion pore through which the nucleocapsid can pass [93]. HCV envelope glycoproteins E1 and E2 function as a heterodimer to mediate these events [2,3,4]. However, in the absence of structural information the glycoprotein rearrangements that occur during HCV entry are not known.

Due to the relatedness of HCV to flaviviruses as well as additional antibody [94] and mutagenesis studies [95] it has been proposed that HCV uses a class II fusion mechanism (discussed in more detail in section 1.7.1). Data also indicates that E2 may represent a class II fusion protein activated by low pH and an additional mechanism yet to be determined.

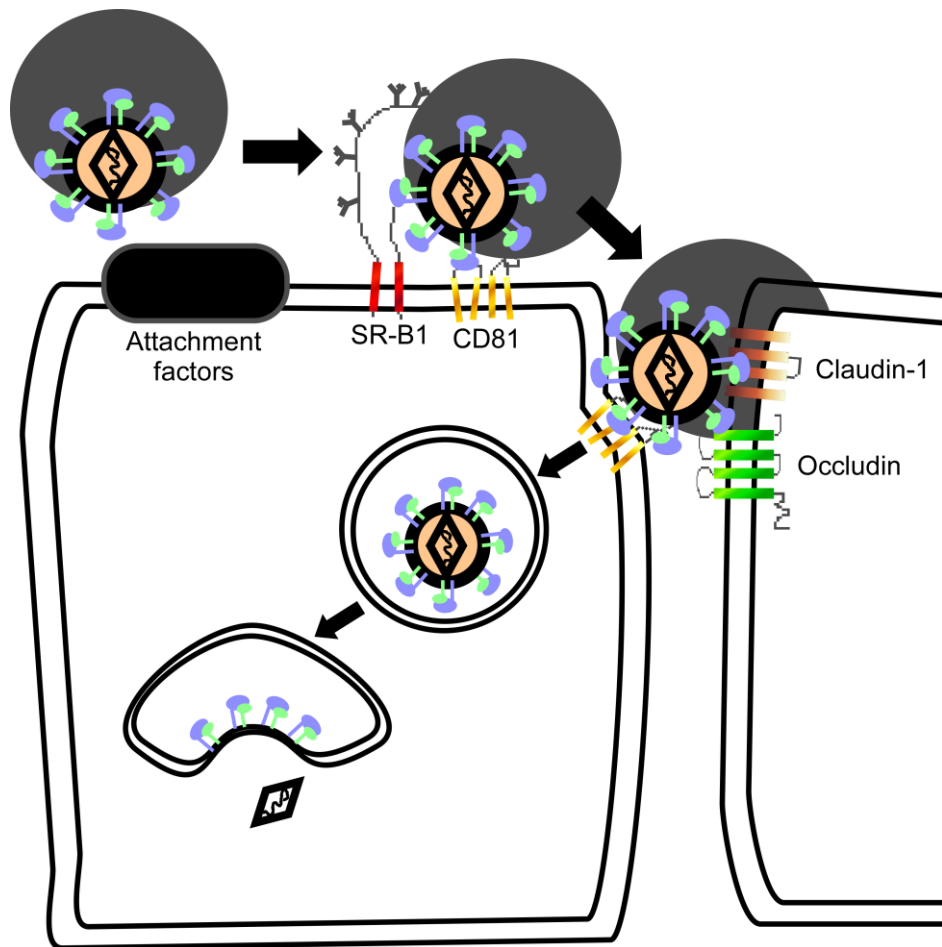


Figure 1-1. Schematic representation of HCV entry into hepatocytes. HCV associated with VLDL/LDL (dark grey) adheres to hepatocytes via potential factors including LDLr, GAGs and/or L-SIGN. Virus interactions with cellular receptors SR-B1 (red) and CD81 (gold) promotes translocation to tight junctions where claudin-1 (brown) and occludin (green) are localised. HCV is internalised via clathrin mediated endocytosis. Low endosomal pH drives fusion of viral and cellular membranes resulting in delivery of the viral nucleocapsid into the cytoplasm. Alternatively, following adherence to cells, HCV may associate with SR-B1, and claudin-1-CD81 complexes at the basolateral surface of cells, followed by translocation to occludin at tight junctions and internalisation.

1.3.2 Translation and processing

Following delivery of the viral nucleocapsid into the target cell cytoplasm, virus uncoating occurs to release the viral RNA. The RNA genome of positive strand viruses is required for translation of viral proteins and also acts as a template for production of further viral genomes [96].

HCV RNA lacks a 5' cap and therefore translation depends on an internal ribosome entry site (IRES) in the 5' non-coding region. The small subunit of cellular ribosome binds the HCV IRES directly then recruits eukaryotic initiation factor (eIF) 3 and the ternary complex of Met-tRNA-eIF2-GTP to the AUG initiation codon. Formation of the translationally active 80S complex is slow and highly dependent on IRES structure [97,98,99].

Translation occurs in association with ER membranes producing a ~3 000 amino acid polypeptide that encodes 3 structural proteins at its N-terminus followed by 7 non-structural proteins (schematically represented in Figure 1-2). Structural proteins core, E1 and E2 are required for formation of functional virus while non-structural proteins coordinate virus replication and assembly. Polypeptide processing occurs both co- and post-translationally with host signal peptidases releasing core, E1 and E2 [100]. Signal sequences located between core-E1 and E1-E2 and E2-p7 direct the structural proteins co-translationally to the ER membrane where E1 and E2 are translocated into the ER lumen [101,102]. The polypeptide encodes non-structural proteins NS2 and NS3 that demonstrate protease activity [103,104]. NS2 undergoes autocatalytic cleavage processing at the junction between NS2 and NS3, allowing NS3 to release the remaining non-structural proteins.

Following translation, all HCV proteins (except E1 and E2 that are translocated to the ER lumen) appear to associate with the ER membrane with a cytosolic orientation [105,106,107,108,109,110] (schematically represented in Figure 1-3). An additional processing event by host signal peptide peptidases releases core from this association where it redirects to the membrane of lipid droplets, essential for virus assembly [111,112,113].

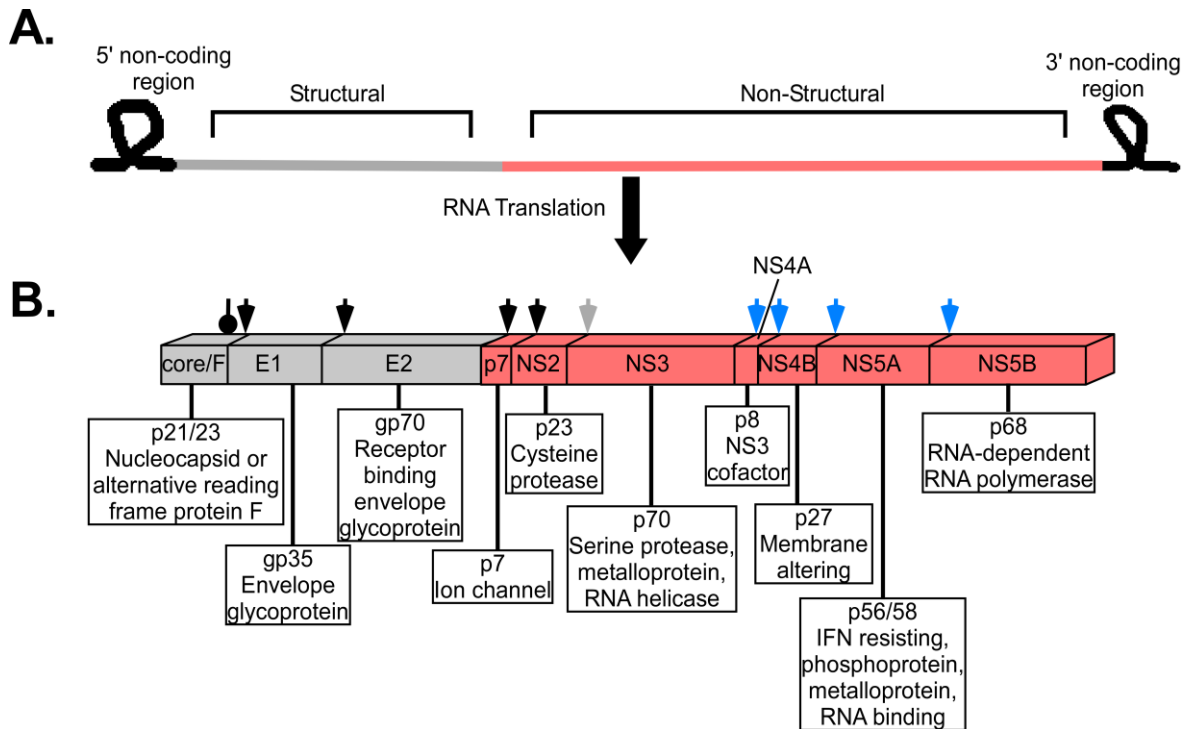


Figure 1-2. Genomic organisation and polypeptide processing of HCV. Schematic representation of the 9.6 kb RNA genome (A) and proteins produced by translation and polypeptide processing (B). Non-coding regions of RNA are indicated. Structural proteins are shown in grey and non-structural proteins in pink. Black arrowheads indicate sites processed by host signal peptidases, black pin-head indicates the site cleaved by signal peptide peptidases, the grey arrowhead indicates the site cleaved by NS2/3 autocatalysis, blue arrowheads indicate polypeptide sites cleaved by NS3. Approximate protein sizes and protein functions are shown in boxes.

1.3.3 RNA replication

Until recently it was not possible to grow HCV in cell culture, therefore many studies on HCV replication have been performed using a self-replicating RNA replicon system [114]. Using this system it was possible to determine the minimal complex required to mediate HCV RNA replication which includes the subset of non-structural proteins NS3, NS4A, NS4B, NS5A and NS5B. More recent studies have employed full length replication competent HCV which produces infectious virus (HCVcc) [57,115,116].

Replication of HCV RNA is mediated by NS5B which is an RNA dependent RNA polymerase (RdRp) [117]. HCV RdRp is responsible for production of a

negative-strand RNA intermediate from the positive strand RNA genome. The negative strand RNA then serves as a template for the production of new positive-strand viral genomes. Nascent genomes can then be translated, further replicated, or packaged within new virus particles.

HCV RNA replication is dependent on the structure of 2 of 4 domains located in the 5' non-coding region of the positive strand RNA [118]. In addition, conserved elements in the 3' non-coding region have been shown to be essential for replication in cell culture [119,120] and *in vivo* [121,122]. RNA synthesis by NS5B *in vitro* can be divided into distinct steps including RNA binding, initiation, elongation, and termination.

HCV replication has been shown to occur on ER-derived membrane structures termed a membranous web that are specifically induced by NS4B [123,124]. These structures have been shown to contain the majority of non-structural proteins produced upon polyprotein processing [123], and represents the major site of RNA synthesis in Huh-7 cells harbouring HCV replicons [124]. Formation of replication complexes on cellular membranes that incorporate viral RNA and viral and cellular proteins is characteristic of positive-strand RNA viruses including flaviviruses [125,126].

Structural protein core has long been known to associate with cytoplasmic lipid droplets [111,127]. However the significance of this association in virus replication is only beginning to be understood. Lipid droplets are cellular organelles that store neutral lipids and have been shown to move throughout the cytoplasm associating with various other organelles including the ER [128]. After signal peptide peptidase cleavage core protein relocates from the ER membrane to the membrane of lipid droplets. Miyanari *et al.* (2007) showed that this association was essential for the production of infectious virus and were able to demonstrate recruitment of non-structural proteins as well as plus and minus strand RNA to the lipid droplet membrane in a core dependent manner [113]. Therefore it is currently believed that the HCV replication complex resides on ER membranes in close association with lipid droplets, mediated by core.

1.3.4 Virion assembly and egress

Formation of all enveloped *Flaviviridae* family members including HCV, is thought to occur by accumulation of core protein in association with viral RNA at ER-derived membranes followed by budding into the secretory system [129,130]. It is assumed that this budding process collects envelope glycoproteins that are retained in the ER membrane [131,132,133].

Flaviviruses such as TBEV undergo significant maturation during transit through the Golgi apparatus including oligomeric reorganisation of the envelope glycoproteins and cleavage of the precursor envelope protein prM by furin [134,135,136]. While the glycans of infectious HCV appear to be modified in the Golgi compartment [3,137] there is no evidence for further polyprotein cleavage or maturation requirements for the HCV envelope glycoproteins [138].

A possible link between lipoprotein metabolism and viral assembly and egress has recently been proposed [139,140]. Studies suggest that HCV maturation may occur in a manner very similar to the formation of VLDL which is also assembled at the cytoplasmic surface of the ER prior to secretion [141]. In fact, HCV production in cell culture has been shown to be reduced by two agents that block VLDL assembly [139]. Furthermore, HCV maturation and assembly stages have been shown to be dependent on the presence of apolipoprotein B (an essential component of VLDL) and microsomal transfer protein (required for assembly of VLDL). The finding that HCV isolated from the supernatant of infected cell cultures has biophysical properties similar to those of particles circulating in infected patients supports an association between HCV and VLDL maturation pathways, resulting in a low-density form of HCV being produced prior to cellular egress [68,142].

1.4 Structure and Function of Non-Structural Proteins

p7 is a small 63 amino acid protein that is essential for productive HCV infection *in vivo* [143]. While the role of p7 during the virus lifecycle is unclear, it is not required for RNA replication *in vitro* [114]. Recent data shows that virus entry is largely independent of p7 with the protein likely to play an important role in virus assembly rather than as a structural component of virus particles [144]. p7 is predicted to form ion channels across membranes and has been shown to conduct cations across artificial membranes *in vitro* [145,146]. This activity can be blocked by ion channel inhibitor amantidine [145] and imino-sugar derivatives, although reports of amantidine specificity are controversial [147] and may be genotype specific [148]. The significance of this activity and how p7 functions to promote virus assembly are not yet understood.

NS2 is the first of two encoded proteases produced by the HCV polyprotein sequence. NS2 is not required for HCV genomic replication [114,149]. However, its activity is required for persistent HCV infection in chimpanzees [122]. Recent studies show that NS2 can be co-precipitated with structural and non-structural proteins indicating that NS2 may act as a scaffold to mediate virus assembly [150,151,152,153].

NS3 is the second virally encoded protease in the polyprotein and is essential for HCV replication [115,154], releasing the remaining non-structural proteins from the polyprotein [155]. NS3 folding, activity and membrane localisation is dependent on the incorporation of a β -strand from membrane bound NS4A [106,156]. NS3 additionally demonstrates RNA helicase activity which may promote RNA replication [157,158,159,160], and a pro-viral role interfering with innate immune responses [161,162].

NS4B is a small, highly hydrophobic 27 kDa membrane bound protein [107,163] that is essential for HCV replication [164,165,166]. NS4B has been shown to specifically induce localised perturbations in the ER membrane producing membranous web structures that support the replication complex

[123,124]. Although largely studied in the context of the replicon system, these structures are believed to be physiologically relevant as similar membrane perturbations have been identified by electron microscopy analysis of the liver of HCV infected chimpanzees [167]. Recent studies indicate that NS4B may also play an additional role in virus assembly [164].

NS5A is a large 56-58 kDa phosphoprotein. It is essential for HCV RNA replication although no clear enzymatic function has been described [168,169,170]. The earliest reports of NS5A described the protein as an interferon resisting protein [171,172,173]. This may partially explain why treatment of HCV with PEG-IFN α is not successful in obtaining a sustained virological response in a number of patients [174,175].

NS5A is predicted to be largely hydrophilic and contains no transmembrane domain but is instead anchored to the ER membrane by an N-terminal amphipathic α -helix [108]. A role as a scaffold protein in the replication complex has been proposed as mutations on the hydrophilic side of the α -helix that do not disrupt membrane association have been shown to inhibit HCV replication [169]. Indeed, direct associations between NS5A and NS5B have been reported [176,177]. Recently it was shown that NS5A associates with, and appears to activate, a lipid kinase required for maintenance of the membranous web and the HCV replication complex [178].

NS5B is an RNA dependent RNA polymerase (RdRp) that is critical for HCV replication [117]. HCV RdRp is responsible for production of a negative-strand RNA intermediate from the positive strand RNA genome. The crystal structure for RdRp shows a 531 amino acid catalytic domain which forms fingers, palm and thumb subdomains [179,180] characteristic of other polymerases [181]. HCV RdRp is anchored to the ER membrane by a C-terminal hydrophobic tail. Removal of the transmembrane domain (TMD) of RdRp does not inhibit RNA polymerase activity *in vitro* [182]. However, HCV replication is abrogated [183], likely due to the loss of localisation with other members of the replication complex.

In addition to the non-structural proteins described, an alternative reading frame in the gene encoding structural protein core has been identified that could encode a 160 amino acid protein termed F (frameshift protein) or ARF (alternative reading frame protein) [184]. This is likely to be expressed during infection *in vivo* as antibodies directed towards F have been detected in HCV-positive patients [185]. However, the relevance of this protein is unclear as it is not required for either *in vitro* or *in vivo* RNA replication [186].

1.5 HCV Structural Proteins

1.5.1 Core

Core is predicted to be a major constituent of HCV virions, oligomerising to encompass and protect the viral RNA and forming the viral nucleocapsid [58,59]. N-terminal residues of core are highly basic and are thought to bind the 5' end of viral RNA [187,188,189]. This is likely to be important for initiation of RNA encapsulation by core protein.

Like other HCV proteins, core has been shown to be involved in many other cellular processes. Some of those described include activity as a transcriptional activator [190,191,192], pro- and anti-apoptotic regulator (see [193,194] for example), cell growth regulator [195] and immunomodulator [196].

1.5.2 Envelope glycoproteins E1 and E2: biosynthesis

Envelope glycoproteins E1 and E2 are encoded immediately after core in the polypeptide sequence and consist of residues 191-383 (E1; prototype strain H77c polyprotein numbering used throughout this study) and 384-746 (E2). E1 and E2 form a heterodimeric complex on the surface of HCV [3,197,198,199,200] with both glycoproteins required to mediate membrane fusion for delivery of the viral nucleocapsid into target cells [2,3,4]. E1 and E2 are type 1 transmembrane proteins with heavily glycosylated ectodomains [197,198,199,200,201,202,203]. The biosynthesis of these glycoproteins is discussed in detail below.

Upon translation of structural proteins core and E1, the signal sequence located between the two proteins directs the polyprotein co-translationally to the ER where this sequence is cleaved by a host signal peptidase, freeing the E1 ectodomain to translocate into the ER lumen [100,204]. The extreme C-terminal 30 amino acids of each glycoprotein contain an additional polypeptide signal sequence essential for directing the glycoproteins to the ER membrane [101,102]. The signal sequence at the C-terminus of E1 directs the continuing polypeptide sequence encoding E2 towards the translocon of the ER. Cleavage of this signal sequence by a host signal peptidase allows the E2 ectodomain to translocate into the ER lumen while host signal peptidases are additionally required to release E2 from p7.

The C-terminal signal sequences of the two glycoproteins remain embedded in the ER membrane forming TMDs with the ectodomain of each protein facing the ER lumen. In addition to anchoring E1 and E2 to the ER membrane the TMDs of each glycoprotein function as ER retention signals, preventing the proteins from entering the secretory pathway prior to RNA replication and assembly of viral components. Interestingly, E1 and E2 do not contain classical ER retention signals such as KDEL [205] or KKXX [206] which cause retrieval of proteins from post-ER compartments [207]. Instead charged residues within the E1 and E2 TMDs prevent progression of the glycoproteins through the ER [132,208].

The TMDs have been shown to be sufficient to retain E1 and E2 in the ER, as attachment of the C-terminal residues of E1 or E2 to cell surface expressed protein CD4 causes relocalisation of CD4 to the Golgi network [102,209]. Furthermore, truncation of E1 at residue 311 or E2 at residue 661 induces efficient secretion of the glycoproteins from mammalian cells [210]. An additional sequence in the juxtamembrane region of E1 has also been shown to independently influence the localisation of E1 to the ER [211]. Although the TMDs are sufficient to restrict the glycoproteins to the ER this additional sequence in E1 may stabilise retention. Most localisation studies of E1 and E2 have been performed in

heterologous expression systems. Recent studies have confirmed the role of the E1 and E2 TMDs using replication competent HCV [133].

The topology of E1 and E2 TMDs has long been debated as the TMD of each glycoprotein consists of two C-terminal hydrophobic segments separated by a very short polar sequence (at least one conserved charged residue) [208]. Sequence analysis of the C-terminal regions of E1 and E2 led the field to believe that the C-terminus of the glycoproteins may span the ER membrane twice with the short polar sequence facing the cytosol and the ectodomain of the protein directed towards the ER lumen. This arrangement has been described for E2 from alphaviruses [212], as well as the glycoproteins from the related flaviviruses [213]. However, further analyses using mutagenesis and epitope localisation studies suggest that both E1 and E2 span the ER membrane just once [214]. As such, E1 and E2 are referred to as type 1 transmembrane proteins. Interestingly, the orientation of the TMDs appears to change after cleavage of signal sequences by signal peptidase in the ER. Epitope tagging studies suggest that the TMD of E1 and E2 transiently adopt a hairpin like structure as the ectodomains of the glycoproteins translocate into the ER lumen. Following cleavage of the signal sequences the hairpin structures are thought to open out to relocate the most C-terminal region of the TMDs back towards the cytosol [214]. This reorientation is predicted to allow the signal sequences to function in other processes more efficiently, such as heterodimerisation of E1 and E2 (discussed below), and is likely to facilitate stronger ER retention [214].

E1 and E2 contain 5 and 11 potential N-linked glycosylation sites, respectively. These are encoded by the amino acid sequence Asn-X-Thr/Ser, where X is any amino acid except Pro [215,216]. While the E1 sequence from all genotypes encodes 5 common sequons, one site is immediately followed by a Pro which precludes efficient modification (sequon beginning at residue 324). In addition, genotypes 1b and 6 encode a 6th potential N-linked glycosylation site in E1 (sequon beginning at residue 249) [217,218,219]. A preformed oligosaccharide precursor containing 14 sugar residues is immediately added to Asn residues within the Asn-X-Thr/Ser motif upon import of the newly synthesised protein into

the ER, catalysed by oligosaccharyl transferase [220]. This precursor oligosaccharide consists of 3 glucose, 9 mannose and 2 *N*-acetylglucosamine molecules and is the common structure added to proteins encoding an N-linked glycosylation site in animal cells [215]. Interestingly, it has been reported that glycosylation of E1 can occur up to 1 h post translation when expressed in the absence of E2 suggesting that association of E1 with E2 may facilitate oligosaccharide attachment, possibly by modulating exposure of the attachment sites [221].

Immediately following attachment of the oligosaccharide precursor, the three glucose residues and one mannose residue are enzymatically removed [222]. Further modifications of attached carbohydrate can occur upon trafficking of glycoproteins through the *cis*-, *medial*- and *trans*-Golgi cisternae by glucosyl hydrolase and glucosyl transferase enzymes to produce high-mannose, complex or hybrid type glycans. In fact, specific modifications provide information about the trafficking process of a particular protein; proteins with high-mannose glycans are located in the ER or *cis*-Golgi compartment, while complex or hybrid glycans indicate the protein has progressed through the *trans*-Golgi network [223].

An early study on E1E2 expression, performed using recombinant vaccinia virus which induces high levels of cytoplasmic transcription and translation of the encoded DNA, suggested that E1 and E2 were strictly retained in the ER or a *cis*-Golgi compartment based on immunofluorescence and endoglycosidase H (Endo H) sensitivity of the E1 and E2 carbohydrate attachments [197]. In 2003, Drummer *et al.* studied expression of E1 and E2 by transient transfection of HEK 293T cells with a plasmid encoding E1E2 driven by a cytomegalovirus promoter [3]. This system allows high levels of nuclear transcription of the transfected DNA, followed by RNA translation by host cell factors. In this system it was found that a proportion of E1 and E2 escapes the ER, likely due to saturation of the ER retention machinery, and can be incorporated into retroviral pseudotyped particles (HCVpp). This allowed characterisation of glycosylation on virion incorporated forms of the glycoproteins. It was found that E1 appeared to contain mostly high-mannose glycans while the majority of glycans on E2 were insensitive to endo H,

consistent with the presence of complex/hybrid type modifications. It was therefore suggested that within the E1E2 heterodimer, E2 may shield E1 from further glycan modifications in the Golgi. Since HCV is not expected to bud from the surface membrane of cells this is not likely to represent the native maturation and egress pathway of HCV. However, given that this form is functionally active in virus entry it is believed to be relevant. In addition, this finding is consistent with an early study of the glycan content on HCV from infected patients [224]. More recently, the glycosylation state of E1 and E2 from full length replication competent HCV (HCVcc) has been reported. [137]. High-mannose glycan forms were detected on intracellular E1 and E2 and virion incorporated E1 consistent with studies in HCVpp. In this system, E2 was found to harbour a range of glycans ranging from completely endo H resistant (complex and/or hybrid) to completely endo H sensitive, indicative of high-mannose glycans. The finding that E2 from HCVpp contains mostly complex/hybrid type modification compared to a range of complex/hybrid and high-mannose forms of E2 in HCVcc, suggests that the different maturation processes employed by E1E2 destined for incorporation into HCVpp or HCVcc result in variability in the exposure of E1 and E2 to various Golgi glycosidases and/or glycosyl transferases. Alternatively, it is possible that the analysis of cell-free HCVcc was contaminated with intracellular material containing immature and mature glycoforms.

N-linked glycans are large, hydrophilic attachments that comprise an essential functional component of HCV. There is evidence that HCV glycans can modulate the exposure of epitopes recognised by nAb aiding in immune evasion [225,226] as well as facilitating glycoprotein folding and virus entry [218,227]. Glycans can directly affect the folding of a protein by influencing the positioning of peptide sequences [228,229]. Mutagenesis studies performed on both E1 and E2 have identified key glycosylation sites essential for correct folding and E1 and E2 heterodimer formation [218,227]. Although reports appear to be contradictory in the identification of which glycans are critical for E1 and E2 folding, it is apparent that removal of just one glycan from either E1 or E2 is sufficient to interfere with production of infectious particles [217,218,227].

As well as facilitating protein folding directly, N-linked glycans mediate interactions with ER resident lectin-chaperones such as calnexin and calreticulin [230]. The rate of folding and association of E1 and E2 with ER chaperones has been investigated by a number of groups with mixed findings, discussed below.

Studies performed by Choukhi *et al.* (1998) and Dubuisson and Rice (1996) were performed using a vaccinia expression system for E1 and E2 which exhibits exceptionally high levels of cytoplasmic viral protein expression while shutting down host protein synthesis [231,232]. Associations were demonstrated between E1 and E2 and chaperone proteins BiP, calnexin and calreticulin. However, this expression system results in the formation of a large amount of protein aggregates, and it was shown that BiP and calreticulin associations occurred only with these high molecular weight forms of E1E2. As such, Choukhi *et al.* (1998) concluded that E1 and E2 associated with BiP and calreticulin were involved in a non-productive folding pathway. Calnexin was found to associate with non-covalent forms of E1 and E2 and as such was deemed to be a relevant chaperone involved in facilitating productive folding of the glycoproteins. Dubuisson and Rice (1996) observed a fast rate of folding for E2, while a much slower folding rate for E1 was determined [231,232].

Analysis of E1 and E2 folding in an *in vitro* cell-free system using rabbit reticulocytes also determined the folding rate of E1 to be very slow (5 h) [233]. In contrast to earlier studies, folding of E2 was also observed to be slow, oxidising at a similar rate to E1. In this system it was found that E1 folding was facilitated by the presence of core and E2 when expressed as a polypeptide. However, E2 was not required for oxidation of non-covalent E1. This is distinct to the findings of a previous study that showed E1 lacking its TMD required the presence of E2 in order to fold and escape the ER for secretion [210]. Rather, in the cell-free expression system it was found that core was required to direct E1 oxidation. This may suggest that core can structurally influence ER translocation of E1 and as such promote correct folding of the glycoprotein. In this system, E1 was shown to associate with calnexin and briefly with calreticulin.

In an attempt to avoid potential caveats associated with protein over-expression systems, Brazzoli *et al.* (2005) used a CHO cell line stably transfected with E1 and E2 to examine glycoprotein folding [234]. In this system E1-calnexin co-precipitation was demonstrated but E2 was not found in association with any chaperone. These experiments showed E1 to fold much faster than E2 (2 h compared with 6 h for E2), and found E1 to be associated with unoxidised forms of E2. These data suggest that E1 may function as a chaperone to facilitate E2 folding

These variations in folding rates and chaperone associations are likely to be a reflection of the different expression systems used. Over-expression systems generate a cell stress response that may result in impaired folding and maturation of proteins [235]. As a result there may be enhanced association of proteins with chaperones in order to retain the misfolded proteins in the ER. The observation that E1 associates with calnexin appears to be a consistent finding from all groups and is therefore likely to represent a true association in native infection.

These studies have assessed the folding of E1 and E2 in terms of formation of oxidised non-covalent forms of the glycoproteins. As described above, the TMDs of the HCV glycoproteins are multifunctional, forming the membrane anchor, encoding signal sequences for ER localisation and peptidase cleavage, as well as encoding ER retention signals. In a true demonstration of multifunctionality, the TMD from each glycoprotein has been shown to be an essential heterodimerisation determinant [236,237,238]. The E1 TMD encodes a GXXXG motif associated with formation of helical regions [239] as well as homo- and hetero-oligomerisation [240]. There have been reports of association between truncated forms of E1 and E2 that lack their TMDs [241,242] although whether these represent correctly folded forms of the glycoproteins remains controversial [210,242]. Whether or not E1 and E2 are capable of associating in the absence of their TMDs, there is evidence that disruption of the predicted α -helical transmembrane region by alanine insertion mutagenesis in full length E1 and E2 results in significant disruption to E1E2 heterodimer formation [236]. This suggests

that the native fold of the glycoprotein TMDs is critical for correct glycoprotein association.

Furthermore, a highly conserved hydrophobic heptad repeat located near the C-terminus of E2 (termed the membrane proximal heptad repeat; MPHR) has been shown to function as a heterodimerisation determinant in addition to the E1 and E2 TMDs [95]. Although this region was not found to be sufficient to mediate wild-type levels of E1E2 heterodimerisation alone, disruption of the predicted α -helical structure by Pro and Ala substitution abrogated heterodimerisation and formation of a functional heterodimer [95].

The non-covalent heterodimeric form of E1E2 has long been assumed to represent the functional form of the glycoproteins incorporated into virus particles [3,131,138,197,232,243] although disulfide linked forms of the glycoproteins are also evident in HCVpp [138]. Recently, the first analysis of intracellular and virion incorporated E1 and E2 from replication competent HCV was reported [137]. It was shown that while the majority of intracellular glycoprotein assembled as non-covalently associated heterodimers, once incorporated into infectious particles E1 and E2 appeared to form large covalently linked complexes of up to, and larger than, 440 kDa. The group suggested that although intracellular covalently linked E1E2 appear to form aggregates retained in the ER, on the surface of particles covalent linkages may allow formation of ordered oligomers and proposed that this arrangement may facilitate budding during assembly. These high molecular weight forms were observed in protein samples prepared without boiling prior to SDS-PAGE analysis. However, to ensure these findings are not artefacts resulting from extraction and SDS-PAGE processes, further analysis of HCVcc derived glycoproteins should be performed using a stringent biochemical approach. For example, alkylation of any free sulfhydryl groups prior to glycoprotein extraction, and analysis by native SDS-PAGE. This would prevent formation of opportunistic disulfide bonds and further disulfide rearrangements upon protein extraction. Identification of the functionally relevant oligomer of E1 and E2 is essential for understanding the structure of HCV as well as future development of drugs targeted towards the envelope glycoproteins.

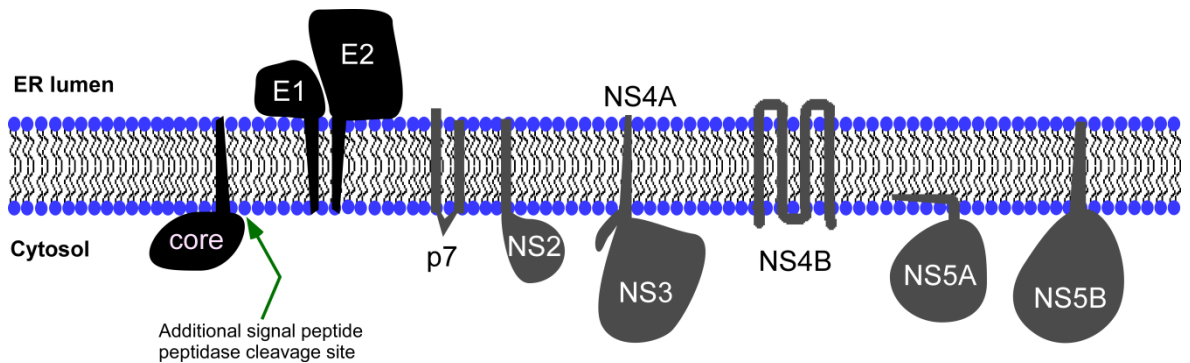


Figure 1-3. Schematic representation of the localisation and orientation of HCV structural and non-structural proteins at the ER membrane. Structural proteins are shown in black, non-structural proteins are in grey. Membrane interactive regions are indicated. Note that core undergoes further cleavage by a host peptide peptidase to release a soluble form of core that localises to lipid droplets.

1.5.3 Structural and functional determinants of E2

E2 residues 384-746 comprise an ectodomain (residues 384-715) linked to the C-terminal TMD (schematically represented in Figure 1-4A). Michalak *et al.* (1997) examined expression of a soluble form of the E2 ectodomain, including constructs terminating at residues 661, 688, 704 and 715. Although secreted forms could be obtained for each of these truncated forms, only E2 residues 384-661 retained conformational epitopes [210]. Since this finding, several groups have shown that this form of E2 can be efficiently expressed and secreted from mammalian cells and has the ability to bind cellular receptors CD81 [2,244,245,246,247] and SR-BI [6,248]. Therefore, E2 residues 384-661 are considered to form an independent receptor binding domain (RBD), termed E2₆₆₁ RBD.

Tetraspanin CD81 was first identified as an attachment factor for HCV in 1998 [5]. CD81 has since been validated as essential for entry of HCVpp, HCVcc and serum derived virus into liver cells using siRNA knockdown, antibody and mutagenesis studies [115,249,250,251,252,253]. The function of CD81 will be discussed in detail in section 1.6.2. The E2 residues that are essential for the

interaction with CD81 have been mapped to at least four different regions within the E2₆₆₁ RBD and include residues W⁴²⁰ [254], G⁴³⁶WLAGLFY [247], Y⁵²⁷SWGANDTD [254] and Y⁶¹³RLWHY [255,256]. It is believed that the disparate locations of these residues are brought together by the tertiary fold of the glycoprotein to form the CD81 binding surface [257].

Despite the essential requirement of CD81 for virus infectivity, it has been observed that the affinity of E2 for CD81 is genotype specific [255,256,258]. This may reflect sequence and structural variation between the HCV genotypes. Alternatively, the finding may be an artefact resulting from subtle conformational differences between recombinant soluble CD81 used in the assays, and full length CD81 [246,259]. In any case, it has been confirmed that all genotypes of HCV require CD81 to enter hepatocytes [260,261].

Within the E2₆₆₁ RBD are three regions that show high variability in amino acid sequence termed hypervariable regions 1, 2 and the intergenotypic variable region (igVR). Hypervariable region 1 (HVR1) is located at the extreme N-terminus of the glycoprotein and comprises polypeptide residues 384-410. This region has been described as immunodominant and demonstrates a high rate of mutation throughout the course of infection allowing for accumulation of neutralisation escape mutations [262]. Despite this, HVR1 appears to retain an overall positive charge that is important for virus entry [263,264]. It is thought that the positive charge of HVR1 may play an important role in coordinating SR-BI-mediated virus entry [252,265,266]. Recombinant, soluble forms of E2 have been shown to directly interact with SR-BI, while removal of HVR1 greatly reduces this interaction, and antibody directed towards HVR1 can out compete binding of E2₆₆₁ RBD to SR-BI [6,248,263]. However, the relevance of the E2-SR-BI interaction remains unclear as it has not been replicated using virion incorporated forms of heterodimeric E1E2. Mechanisms by which SR-BI may influence HCV entry will be discussed in more detail in section 1.6.3.

Hypervariable region 2 (HVR2) is located between polypeptide residues 474 and 482 [246,267] and is flanked by conserved Cys residues Cys459 and

Cys486. While there is a large degree of sequence diversity in HVR2 across different genotypes, the presence of a highly conserved N-linked glycosylation site in most genotypes, and a G⁴⁶⁸WG motif in all genotypes indicates that various structural features in HVR2 are important for function. This is reflected in the observation that the HVR2 sequence appears to demonstrate relative stability throughout infections [268].

The igVR, consisting of polypeptide residues 570 to 580, is also flanked by conserved Cys residues at positions 569 and 581. This region shows significant sequence diversity between genotypes but is relatively conserved within genotypes [246].

Each of these variable regions can be simultaneously deleted from the ectodomain of E2 in the context of E2₆₆₁ RBD leaving a functional form of E2 that can bind full length and a recombinant soluble form of CD81 (residues 113-201 of the large extracellular loop of CD81 expressed in fusion with maltose binding protein; MBP-LEL¹¹³⁻²⁰¹). Furthermore, E2₆₆₁ RBD is recognised by conformation sensitive monoclonal antibodies (MAbs) [246]. It is therefore predicated that these variable regions form mobile disulfide bonded loops that are excluded from the core domain of E2 in a manner analogous to the variable loops in HIV-1 gp120 [246,269,270,271,272,273]. These may function to shield the CD81 binding site from neutralising antibodies. Interestingly, it was observed that removal of HVR1 and HVR2 only, resulted in a ~50% reduction in binding of E2 to full length CD81 suggesting a functional interplay between the variable regions that may regulate exposure of the CD81 binding site [246]. A recent publication has shown that independent deletion of HVR2 or igVR in the context of HCVpp results in a loss of E1E2 heterodimerisation, CD81 binding and entry competence demonstrating an essential role for these variable regions in heterodimer assembly [274]. In contrast, when HVR1 was removed E1E2 heterodimerisation and CD81 binding were retained but HCVpp entry was abolished. When these deletions were introduced into E2 in the context of HCVcc, replication proceeded at wild-type levels, although the infectivity of HCVcc lacking HVR2 or the igVR was abolished. By contrast, deletion of HVR1 alone reduced infectivity 5-10 fold. This is consistent with an

earlier finding that HCV lacking HVR1 was infectious but attenuated in chimpanzees [275]. Together these findings indicate that HVR2 and the igVR, but not HVR1, are essential for the formation of a functional glycoprotein complex.

A role for several E2 N-linked glycans in virus entry has been described [226,276]. In one study by Falkowska *et al.* (2007) it was found that mutations preventing glycosylation at N417, N423, N448 and N556 significantly impaired HCVpp entry while largely retaining E1E2 heterodimerisation and incorporation into virus particles. This indicates that these glycans are likely to modulate virus attachment to cellular receptors possibly by regulating exposure of the receptor binding site(s). Furthermore, removal of several glycans from E2 resulted in significantly higher sensitivity of HCVpp to neutralisation by sera from HCV-positive individuals. As such, glycans including, but not limited to those at N417 and N532 may mask particular nAb epitopes.

Structural insight into the domain organisation of E2 was achieved in a study by Keck *et al.* (2004) who used a panel of human MAbs to characterise the function of distinct regions in E2 [94]. The group identified three immunologically discrete domains within E2 incorporated into HCVpp in association with E1. Two of these domains contained neutralising epitopes that could block E2-CD81 binding. Furthermore, one domain was found to be pH sensitive, with a 40% reduction in epitope recognition after exposure of HCVpp to low pH, indicating that this region of E2 is likely to undergo a structural change after endocytosis of the virus. Together this data indicates that HCV E2 contains three immunogenic domains with distinct functions, reminiscent of the three domain architecture of other class II fusion proteins [277,278,279].

The presence of a highly conserved hydrophobic heptad repeat sequence located between the E2 RBD and the C-terminal TMD provides further evidence to suggest that E2 may represent a class II fusion protein [95]. The MPHR is predicted to form an α -helix and has structure similarity to the stem region of flavivirus glycoprotein E [280] (discussed in section 1.7.1). Mutagenesis studies have indicated that the MPHR region of HCV E2 is essential for E2

heterodimerisation with E1 as described above. In addition, the E2 MPHR may function in a post CD81 binding stage of entry. Mutation of the highly conserved MPHR residue Pro683 to Ala allowed wild-type expression of E1 and E2, incorporation of E1E2 heterodimers into HCVpp and E2 from these mutants bound recombinant CD81 at normal levels but the mutant virus was entry incompetent. Given that proline incorporation causes the helical axis to bend by an average of 26° [281], it appears that interruption of the N-terminal helical region of the MPHR is important for HCV infectivity. The findings from this study indicate that the MPHR from E2 is essential for virus entry and suggests that the MPHR may operate in a manner analogous to the stem region of flavivirus glycoprotein E.

In order for envelope glycoproteins to mediate entry into target cells, an internal or N-terminal hydrophobic fusion peptide is required to insert into the target cell membrane to initiate the conformational changes required for the merging of the two membranes [56]. The location of the fusion peptide has not been confirmed in either glycoprotein E1 or E2 from HCV although several membrane interactive sequences have been proposed. Given the apparent structural and functional similarities between HCV E2 and flavivirus and alphavirus fusion proteins E and E1, respectively, it is reasonable to predict that E2 will contain the fusion peptide. A variety of sequences within the E2 ectodomain have been proposed as membrane interactive elements. An early modelling study performed on E2 suggested residues 476-494 aligned with the fusion peptide of TBEV glycoprotein E [255]. However, the function of this region has not experimentally investigated. Additionally, the E2 sequence G⁴³⁶WLAGLFY was identified as having several features in common with fusion peptides from TBEV and dengue-2 envelope glycoproteins. Examination of this region in a mutagenesis study indicated that it was instead required to form hydrophobic contacts with receptor CD81 [247]. Sequence analysis and mutagenesis of the HCV glycoproteins performed by Lavillette *et al.* (2006) identified at least two hydrophobic regions in E2 that appeared to be required to mediate membrane fusion [282]. Residues 416-430 and 600-620 were shown to be functionally important during membrane fusion events as demonstrated with the use of cell-cell and liposome/HCVpp fusion assays.

The absence of a crystal structure has hampered insights into the structure and function of the HCV glycoproteins. Recently Krey *et al.* (2010) published circular dichroism and infrared spectroscopy analyses of recombinantly expressed E2 lacking the TMD (sE2) [273]. Their data indicated that this soluble form of E2 contains approximately 28% β -sheet consistent with the expected secondary structure of a class II fusion protein. Using sE2 from three different genotypes, the group mapped the disulfide bonding arrangement within the 18 conserved cysteine residues of E2 using tryptic digestion followed by identification of the peptide fragments by mass spectrometry. Cysteines involved in eight of nine disulfides were unambiguously identified while the remaining two Cys residues at 597 and 620 were assumed to be disulfide linked. Whidby *et al.* (2009) reported a similar finding for a recombinant form of E2 (residues 384-664, incorporating 17 of the 18 conserved cysteines) whereby 16 of the Cys residues were apparently oxidised and unable to be modified by sulfhydryl reactive agents [283]

By combining this information with knowledge of the residues involved in the composite CD81 binding site, antibody mapping studies, and apparent exclusion of the variable regions from the E2 core structure, Krey *et al.* (2010) were able to model the polypeptide sequence of E2 onto a class II fusion protein scaffold consisting of 3 domains (discussed in section 1.7.1). Domain I is predicted to contain 8 anti-parallel β -sheets and the majority of known CD81 binding determinants (Figure 1-4B). Domain II is connected to domain I via an extension of two β -strands and contains highly conserved hydrophobic residues 502-520, predicted by the group to form the fusion peptide. Confirmation of the involvement of this region in virus entry will require a mutagenesis study. Domain III is linked to domain I and is separated from the TMD via the MPHR. Domain III also includes part of the predicted CD81 binding site. Interestingly, with the CD81 binding site mapped to regions overlapping domains I and III, this model indicates that E2 will likely need to dissociate from CD81 prior to fusion activation assuming E2 will undergo domain rotation to draw the C-terminal and fusion peptide regions together. This information provides the first insight into the structure of HCV glycoprotein E2. Validation of this model will require further mutagenic and crystallographic studies.

The C-terminal residues of E2 form a TMD essential for glycoprotein biosynthesis as described above. This region has also been implicated with a role in virus entry [238]. Ciczora *et al.* (2007) performed tryptophan replacement mutagenesis on the E2 TMD to identify residues that are required for protein-protein interactions. The group identified several residues that retained normal E1E2 heterodimerisation in HCVpp, indicative of correct glycoprotein folding, but were impaired for entry. The group predicted that the TMD may be required to facilitate reorganisation events between the HCV envelope glycoproteins prior to or during virus entry as has been described for other viruses such as the alphavirus, Semliki Forest virus [284]. While such events have not been described for HCV to date, the recent observation that E1 and E2 from HCVcc appear to rearrange from non-covalently linked heterodimers in intracellular glycoforms, to disulfide linked multimers on cell free HCVcc [137] may suggest a late maturation stage at which the E1 and E2 TMDs are required. Until further structural information is obtained for the HCV glycoproteins it will not be possible to confirm whether such a TMD-mediated rearrangement occurs.

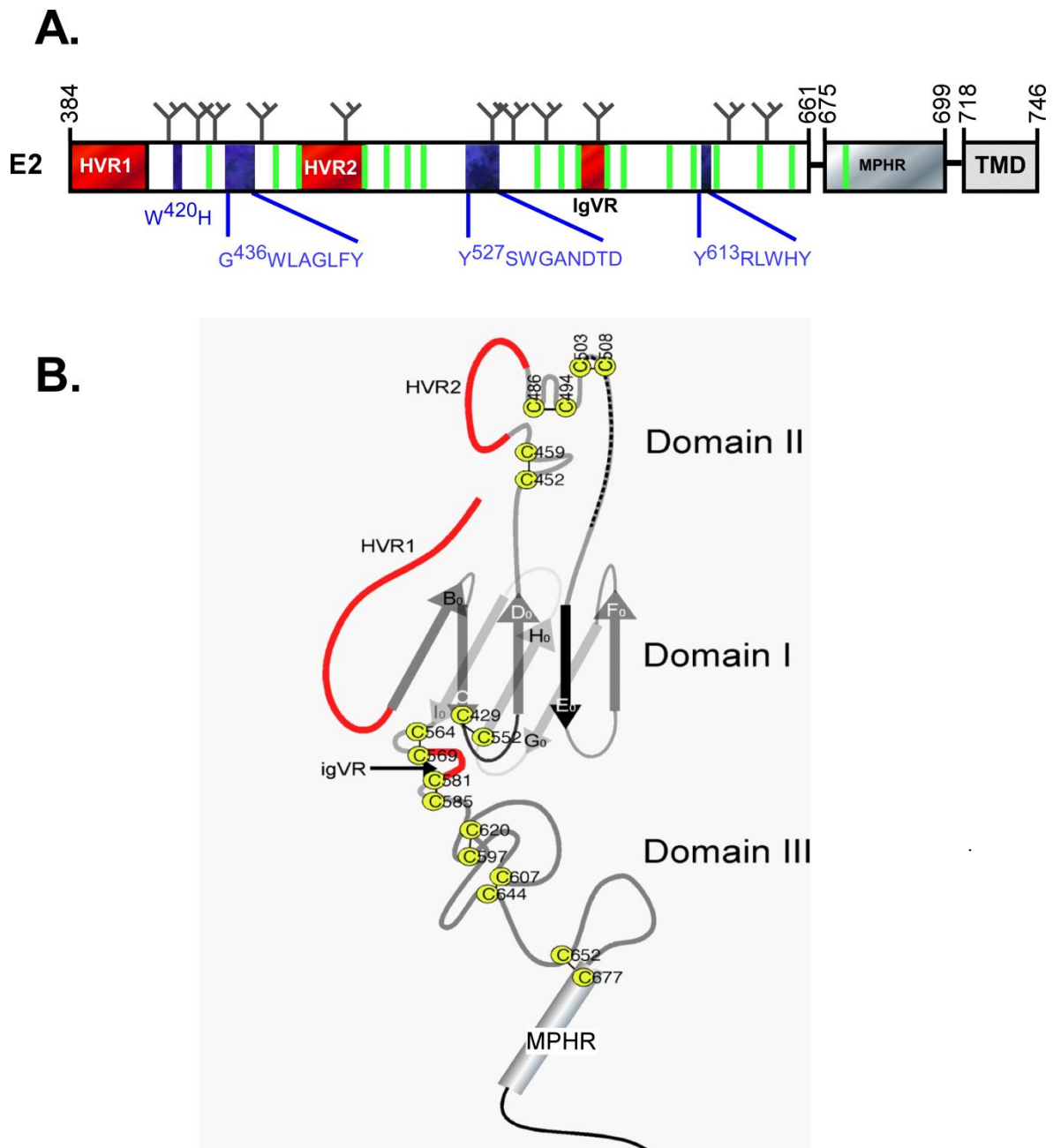


Figure 1-4. Schematic representation of E2. **A.** Polypeptide numbering from prototype strain H77c is indicated above, as are conserved N-linked glycosylation sites (Y). Conserved Cys residues are represented by green vertical lines. Proposed residues involved in CD81 binding are indicated in blue. HVR1, HVR2 and igVR are shown in red. The MPHR is in grey shading and the TMD is in light grey. **B.** Schematic representation of the three dimensional structure of the E2 ectodomain predicted by disulfide mapping and molecular modelling proposed by Krey *et al.* (2010). Variable regions are shown in red, the conserved Cys residues are shown in yellow and the 9 intramolecular disulfides are indicated by solid lines. The proposed fusion peptide is represented by a black dashed line. Modified from McCaffrey *et al.* (2010) [274].

1.5.4 Structural and functional determinants of E1

E1 is an essential component of the HCV envelope glycoprotein complex that is strictly required along with E2 to facilitate entry into hepatocytes [2,3,4] (schematically represented in Figure 1-5). However, the precise role of E1 during these events is not known.

The functions of the E1 TMD during glycoprotein biosynthesis have already been described. However, like E2, several mutations have been identified that could be introduced into the E1 TMD resulting in significantly impaired virus entry while retaining normal levels of E1E2 heterodimer incorporation into HCVpp [238]. This finding suggests that the E1 TMD may have additional roles in the virus lifecycle.

The structure of polypeptide residues 350-370 within the E1 TMD has been solved by NMR [238]. The data strongly suggests that the TMD of E1 anchors the ectodomain to the ER membrane by a single transmembrane α -helix. Residues 359-367 were shown to form a stable α -helix. The structure of residues 354-358 was not as clear but indicated that the region had a tendency to adopt a helical fold. This data supports earlier studies that suggest after cleavage by host signal peptidases the TMD straightens out into a single membrane-spanning helix [214]. It should be noted that the structural detail of this region may differ in the tertiary arrangement of full length E1.

E1 is not likely to be large enough to constitute a typical class II fusion protein. In the absence of a confirmed fusion peptide sequence in E2 the possibility that E1 may function as a truncated class II protein, coordinating fusion events with E2, has been investigated [285]. In support of this hypothesis, it was found that E1 also contains a conserved MPHR (polypeptide residues 330–347) [286]. The NMR structure of a peptide encoding polypeptide residues 314-342 which overlaps this short MPHR has been solved [287]. Heptad repeat sequences typically form helical structures and consistent with this, the peptide was found to contain two helical sections encompassing residues 319-323 and 329-338.

Mutagenesis of this region in E1 found that disruption of the MPHR did not affect formation of E1E2 heterodimers. However, introduction of proline at hydrophobic *a* and *d* positions (A330, V333, L337, I340, I344 and M347), inducing a kink of approximately 26° in the helix [281], inhibited entry in all cases. This indicates that the helical region of the E1 MPHR is functionally important during virus entry [286]. In the absence of a crystal structure of pre and post fusion conformations of E1 and E2 it is unclear whether the E1 MPHR is likely to function in a manner similar to the stem region of flaviviruses. However, given that the E1 MPHR is not required for heterodimerisation with E2 this does not seem likely.

Despite several investigations into membrane interactive sequences in E1, identification of a fusion peptide has remained elusive. A computer modelling study performed by Garry and Dash (2003) identified E1 polypeptide residues 272-281 that aligned with the well-characterised class II flavivirus TBEV glycoprotein E fusion peptide residues 385-396. Both the proposed TBEV glycoprotein E and HCV E1 fusion peptide sequences have flanking cysteine residues and consist of mostly aromatic and hydrophobic amino acids [285]. A subsequent study suggested that while this sequence showed similarities to a class II fusion peptide, extension of the sequence to incorporate residues 272-286 would include further fusion peptide elements. These include a VFLVG motif (similar to a GLFG fusion peptide motif in flavivirus glycoprotein E [277,288] and influenza glycoprotein HA [289,290]), three conserved cysteine residues (as found in TBEV [288] and Semliki Forest virus [291,292] fusion peptides), and a central proline residue believed to be a general feature of internal fusion peptides [293]. However, mutagenesis of hydrophobic residues Y276, V217, F285 and L286 contained in this sequence, in all but one instance (F285A), had no significant effect on entry [286]. This finding suggests that E1 residues 272-286 are unlikely to function as a typical fusion peptide. Despite this, a second mutagenesis study showed that Y276F and G282A mutations introduced into the putative fusion peptide are important for mediating cell-cell fusion [282]. Furthermore, a study that investigated the membrane interactive regions of E1 and E2 by using a series of 18-mer peptides also identified E1 polypeptide residues 265-296 as highly membranotropic [294]. Together these studies indicate that although it is unlikely that E1 functions as a

truncated class II fusion protein it is possible that E1 amino acid F285 and possibly Y276 and G282 may supply important hydrophobic contacts to facilitate entry.

In contrast to E2 there is no evidence for the direct involvement of E1 in virus attachment to cellular receptors. Despite this, neutralising antibodies have been described that are directed towards E1 [295,296,297]. One explanation for the strict requirement for E1 with E2 during entry is that E1 may facilitate conformational changes in the glycoprotein complex or it may act sterically to support and/or orientate E2. Alternatively, E1 may be required to protect E2 from undergoing premature fusion activation in a similar manner to envelope glycoprotein prM from TBEV [298].

Other than NMR structures for the two short peptides encoding E1 sequence described above, there is no structural information available for E1. Elucidation of the E1 crystal structure, including the disulfide bonding arrangement of 8 highly conserved Cys residues, will likely provide substantial insight into potential roles of E1 during virus entry by allowing structural comparisons with other virus envelope glycoprotein paradigms.

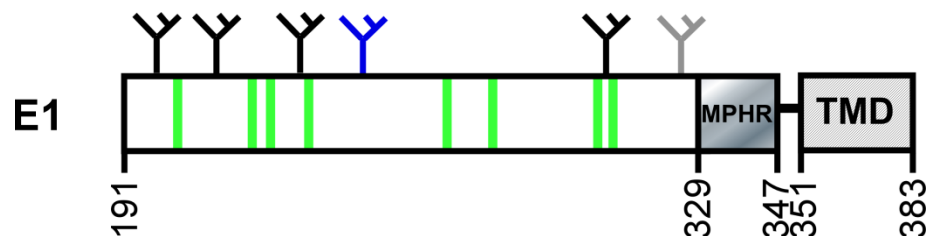


Figure 1-5. Schematic representation of E1. Polypeptide numbering is indicated below. Conserved Cys residues are represented by green vertical lines and N-linked glycosylation sites that are utilised are indicated in black above (Y). A fifth site utilised in genotypes where a Pro does not immediately follow the sequon, is shown in light grey. A sixth N-linked glycosylation site that is used in genotype 1b and 6 viruses is shown in blue. The MPHR is shown in grey shading and the TMD is in light grey.

1.6 HCV Host Cell Receptors

1.6.1 Cellular attachment factors

Several cellular factors have been described that appear to promote attachment of HCV to target cells and may represent initial docking receptors for HCV.

Lectin receptors DC-SIGN and L-SIGN have been shown to interact with high-mannose glycans on HCV envelope glycoproteins [86,87]. DC-SIGN and L-SIGN are selectively expressed on immature dendritic cells and liver endothelial cells, respectively. It is possible that attachment of the virus to dendritic cells may facilitate transport of the virus through the blood system, concentrating the virus at the liver.

Another carbohydrate binding protein asialoglycoprotein receptor (ASGP-R) has been proposed as a virus adhesion factor. ASGP-R was reported to internalise insect-derived HCV-like particles into hepatocytes [88]. However, the physiological relevance of this finding remains unclear as carbohydrate modification differs significantly between insect and mammalian cells. Furthermore, this finding has not been replicated using current HCV model systems to date.

Several groups have investigated a potential role for heparan sulfate proteoglycans in virus attachment [82,85,263]. Removal of cell surface heparan sulfate has been shown to significantly reduce HCVpp attachment and entry into hepatocytes, with several residues spanning E2 shown to be required for binding events [83,84]. Furthermore, addition of soluble heparin (a homolog of highly sulfated heparan sulfate) or highly sulfated heparan sulphate itself to infection assays has been shown by multiple groups to inhibit HCVcc and HCVpp entry [7,84,299,300]. Inhibition only occurs when these factors are present at the time of virus addition indicating that this molecule is involved in initiating attachment of the virus to cells.

A large body of evidence supports the involvement of the LDL receptor (LDLr) in HCV entry [80,81]. The natural ligand for LDLr is LDL, therefore the involvement of this receptor in HCV-hepatocyte attachment is consistent with the observed association of HCV with LDL and VLDL *in vitro* and *in vivo* [66,67,68,81,301]. Addition of exogenous LDL has been shown to inhibit patient-derived HCV entry into LDLr positive MOLT-4 cells, presumably by saturating available LDL receptor molecules [81]. In addition, siRNA knockdown of LDLr and anti-LDLr antibodies have also been shown to abrogate serum derived HCV entry [302].

It is important to note that LDLr is not required for HCVpp entry [252,303]. HCVpp are produced in HEK 293T cells that are a non-VLDL producing embryonic kidney cell line. Furthermore, E1 and E2 destined for HCVpp incorporation escape through the secretory pathway, becoming incorporated into retrovirus particles at the plasma membrane. By contrast, HCVcc virion assembly and secretion is thought to be tightly linked to VLDL synthesis at ER membranes [139]. Therefore HCVpp are unlikely to associate with lipoproteins and use LDLr as an entry receptor. This would suggest that LDLr is not an essential component of the entry pathway. However, there has been no direct association demonstrated between HCV glycoproteins and LDLr and it is highly conceivable that the HCV-associated lipoprotein interacts with LDLr to initiate viral attachment to hepatocytes by inducing exposure of the glycoproteins for further interactions with cellular receptors. In the case of HCVpp, if there is no virus-associated lipoprotein this initial attachment to LDLr may not be required. Another explanation is that HCV entry via LDLr may represent an alternative entry pathway whereby virus attachment induces internalisation by LDLr-mediated endocytosis [304,305]. Further work is required to determine the involvement of LDLr in HCV entry.

1.6.2 CD81

CD81 is a member of the tetraspanin family; a large family of surface expressed molecules involved in cell adhesion, motility, and metastasis, as well as cell activation and signal transduction [306]. Tetraspanins such as CD81 are small

molecules characterised by four transmembrane domains linked by small and large extracellular loops (LEL). While the structure of the small extracellular loop is not known, the LEL has been shown to contain a constant region of 3 α -helices and a variable region that is frequently involved in protein-protein interactions [306].

CD81 has been shown by multiple groups to be an essential entry factor for HCV, mediated by interactions with E2 [5,247,254,255,256]. Using model systems such as HCVpp as well as HCVcc and serum derived virus, HCV entry into liver cells has been shown to be severely impaired by siRNA knockdown of CD81, anti-CD81 antibody, and mutagenesis of various E2 and CD81 residues [115,249,250,251,252,253]. Therefore it is widely accepted that a direct interaction between E2 and CD81 is required for HCV entry.

CD81-LEL can be expressed in a soluble form independently from the rest of the molecule, assembling as a homodimer [245,259,307]. Crystallisation of this domain has revealed each subunit to be composed of 5 α -helices arranged in 'stalk' and 'head' subdomains [307]. CD81-LEL contains the E2 binding residues which form a hydrophobic ridge that can be mapped onto the head subdomain of CD81-LEL [5,245,257,308,309].

Upon attachment to cells, HCV is thought to translocate to tight junctions where the virus is internalised. One study showed that binding of recombinant E2 or E1E2 to CD81 was able to induce these relocalisation events by activation of Rho GTPase family members which are known to have a role in regulating the actin cytoskeleton [89,310]. This finding is supported by evidence that other tetraspanin proteins such as CD82 and CD151 are capable of activating signalling cascades for reorganisation of cytoskeletal proteins [311,312]. Whether this role of CD81 is truly representative of native events in polarised hepatocytes remains unclear but provides a mechanism by which receptors at the luminal surface as well as tight junction proteins may be involved in HCV entry.

Kinetic studies using an anti-CD81 MAb, JS-81, indicate that CD81 is likely to be involved in an early, but post-attachment stage of entry. The reported time for half maximal inhibition of entry occurs when the antibody is added 18 to 50 mins following initial binding of the virus at 4°C [7,8,300]. The variation in timing reported by groups may be due to differences in cell lines, and/or virus type used.

1.6.3 Scavenger Receptor Class B Type 1 (SR-BI)

SR-BI (also known as Cla1) is a 509 amino acid glycoprotein that contains two transmembrane domains which protrude into the cytoplasm, and a highly glycosylated large extracellular loop [313]. SR-BI has been described as a multi-ligand receptor, capable of binding lipoproteins including HDL, LDL and VLDL. SR-BI plays an important role in regulating cholesterol transport via HDL. This activity is considered bidirectional. For example, in the liver and steroidogenic tissues SR-BI mediates selective uptake of cholesteryl ester from lipoproteins, while in macrophages SR-BI mediates cholesterol efflux to HDL [314,315,316,317,318,319,320].

The function of SR-BI during HCV entry remains unclear. Several studies have demonstrated its role as an essential virus entry factor using siRNA knockdown and antibody inhibition studies [7,252,261]. The reliance of HCV on SR-BI during entry is somewhat genotype specific although all 6 HCV genotypes show reduced entry in response to siRNA knockdown of SR-BI [261]. Like CD81, it is predicted that SR-BI is required for an early but post-attachment stage in virus entry. Antibody directed to SR-BI can inhibit HCVcc entry when added 60 min after virus binding [7,321].

SR-BI was initially proposed to function in HCV entry by binding E2 and HVR1 of E2 has been identified as an important SR-BI binding determinant [6]. Soluble and HCVpp-incorporated E2 that lack HVR1 demonstrate impaired binding and entry into human hepatoma cells, respectively, while MAbs directed towards HVR1 also prevent E2 binding to cell surface SR-BI [6,252]. Despite these observations a direct interaction between SR-BI and virion incorporated

heterodimeric E1E2 has not been demonstrated. Furthermore, entry of HCVcc can still occur, although attenuated, when HVR1 is removed [274]. Therefore the physiological relevance of HVR-1 association with SR-BI remains unclear.

Natural SR-BI ligands including VLDL [322] and oxidised LDL [323], have been shown to significantly inhibit serum-derived HCV and HCVpp/cc cell entry via SR-BI, respectively. Given that HCVpp are not associated with lipoproteins this finding indicates that either the binding site for E2 on SR-BI is no longer available in the presence of oxidised LDL, or oxidised LDL alters the activity of cellular factors required for HCV entry. High density lipoprotein (HDL) is also a natural ligand of SR-BI and a recent publication indicated that distinct regions of SR-BI are involved in soluble E2 and HDL binding [321]. This would suggest that the two binding events are independent. HDL has been shown to enhance HCVpp and HCVcc entry [7,266]. A possible explanation for HDL-enhanced HCV entry is that HDL binding may up-regulate SR-BI activity, potentially resulting in increased cholesterol content in cellular membranes [324]. This is supported by one publication which has shown a reduction in HCV entry following cholesterol depletion [325].

Whether a direct association of HCV with SR-BI is required, or whether binding of SR-BI by HCV-associated lipoprotein stimulates entry, or even a combination of these events remains to be determined.

1.6.4 Claudin-1 and occludin

Claudin-1 and occludin have recently been identified as HCV entry factors and have been shown, together with CD81 and SR-BI, to be sufficient to allow several non-permissive cell lines including mouse NIH3T3 cells to support HCV entry [10].

Claudin-1 and occludin are components of tight junction complexes that are involved in cell-cell adhesion and maintenance of cell polarity [326]. Both proteins contain 4 membrane spanning regions and have two extracellular loops [327]. All

claudins (except claudin-12) have intracellular C-terminal PDZ-binding motifs that interact with PDZ domains in cytoplasmic scaffold proteins such as ZO-1, 2, and 3 amongst others [328]. It is thought that this function is essential for maintaining ordered arrangement of claudin proteins at tight junctions [329]. Occludin is predicted to play significant roles in cellular signalling with half of the C-terminal residues localised in the cytoplasm. This C-terminal region is important for interactions with the ZO family proteins as well as membrane trafficking protein VAP33 [330].

As has been observed for CD81 and SR-BI, siRNA knockdown of occludin and claudin-1 abrogates HCV entry [8,10]. Neither protein has been shown to bind directly to HCV glycoproteins, however the first extracellular loop of claudin-1 which contains a W-GLW-C-C motif (a defining characteristic of claudin family members) has been identified as a functional determinant in controlling HCV entry [8]. Two groups have shown that other claudin isoforms, 6 and 9, are also functional entry cofactors [9,331]. Sequence homology does not explain this redundancy in function, and it is therefore suggested that they may share a common three dimensional motif [331].

Interestingly, Ploss *et al.* (2009) found that murine forms of claudin-1 and SR-BI support HCVpp infection at least as well as the human proteins [10]. Murine claudin-1 and SR-BI demonstrate 90% and 80% identity with their respective human forms. This finding is consistent with a role for these proteins as entry cofactors rather than as direct binding partners for HCV envelope proteins.

There have been mixed reports regarding when claudin-1 is required in the entry cascade relative to CD81. The seminal study that identified claudin-1 as an HCV entry factor indicated a late involvement of this receptor, post-CD81 interactions [8]. However, in the absence of antibody directed towards claudin-1 the group engineered a FLAG tag into a claudin-1 construct to analyse neutralisation of HCV entry in claudin-1-negative cells transfected with claudin-1-FLAG. A more recent study, using antibody targeted towards native claudin-1 in Huh-7 hepatoma cells, indicated that CD81 and claudin-1 are likely to be involved

at a similar time during entry [300]. The group attributed the differences in timing to possible changes in claudin-1 trafficking due to introduction of the FLAG tag.

A publication by Harris *et al.* (2010) determined that claudin-1 could be detected in association with CD81 at the basolateral membrane of polarised hepatocytes whereas very little tight junction-localised claudin-1 was associated with CD81 [91,332]. In addition they found that CD81-claudin-1 association was mediated through the first extracellular loop of claudin-1 and that their association was essential for HCV entry [91]. The first extracellular loop also appeared to be important for mediating co-localisation of claudin-1 with occludin at tight junctions. It is possible that claudin-1 from this CD81-claudin-1 receptor complex is the functional form that facilitates HCV entry, rather than the tight junction form of the receptor.

Although no studies have been performed with anti-occludin antibodies to determine the timing of involvement of this receptor, one group has shown that siRNA knockdown of occludin still allows HCVcc attachment to Huh-7 cells despite abrogation of entry [90]. This suggests that like CD81, SR-BI and claudin-1, occludin is required for a post-binding stage in virus entry.

HCV enters the liver via the sinusoidal blood and therefore the virus will first encounter receptors expressed on the basal surface of hepatocytes. The possibility that both basolateral and tight junction localised proteins are required to mediate infection would suggest that HCV entry involves carefully coordinated events at both regions of the cell. A similar translocation event has been described for Coxsackievirus B. Coxsackievirus B first binds to its main receptor at the luminal surface of epithelial cells followed by transfer of the receptor–virus complex to tight junctions where it interacts with a second receptor in an occludin-dependent fashion to initiate virus uptake [333,334].

Further work is required in order to link the roles of these various receptors, to determine their temporal involvement as well as to verify the involvement of tight junction proteins in HCV entry. It is still possible that other critical entry factors are

yet to be identified which may be ubiquitously expressed in the cell types tested to date. Identification of these factors will be essential for understanding the molecular basis for HCV infection.

1.7 Virus-Cell Membrane Fusion

1.7.1 Structure and function of viral fusion proteins

In addition to defining cellular interactions, fusion proteins present on the surface of enveloped viruses are required to mediate merger of the viral and cellular membranes for delivery of the viral nucleocapsid into the target cell cytoplasm. All fusion proteins identified to date have two membrane interactive sequences including a C-terminal TMD that anchors the fusion protein to the virus membrane, and an N-terminal or internal hydrophobic fusion peptide. The fusion peptide is sequestered within the prefusion conformation but a virus-specific trigger activates conformational changes in the envelope protein complex that exposes the fusion peptide, projecting it towards the cellular membrane. This is followed by major conformational changes in the fusion protein complex such that the C-terminal membrane anchor of the fusion protein folds back towards the site of fusion peptide insertion forming a highly stabilised, elongated hairpin structure [56]. The energy that is released during these conformational changes is considered sufficient to mediate merger of the viral and cellular membranes.

Reorganisation of the virus-cell membranes during virus fusion occurs by a sequence of defined events. Firstly, contact of the fusion peptide with the cellular membrane is thought to cause a localised dehydration event that destabilises the outer leaflet of the viral and cellular membranes, resulting in lipid mixing (hemifusion). Formation and expansion of a fusion pore occurs as the fusion proteins adopt the stabilised hairpin conformation, apposing the viral and cellular membranes, as described above. Pore expansion ensues upon completion of these conformational changes which then allows delivery of the viral nucleocapsid into the cellular cytoplasm [93,335] (Figure 1-6).

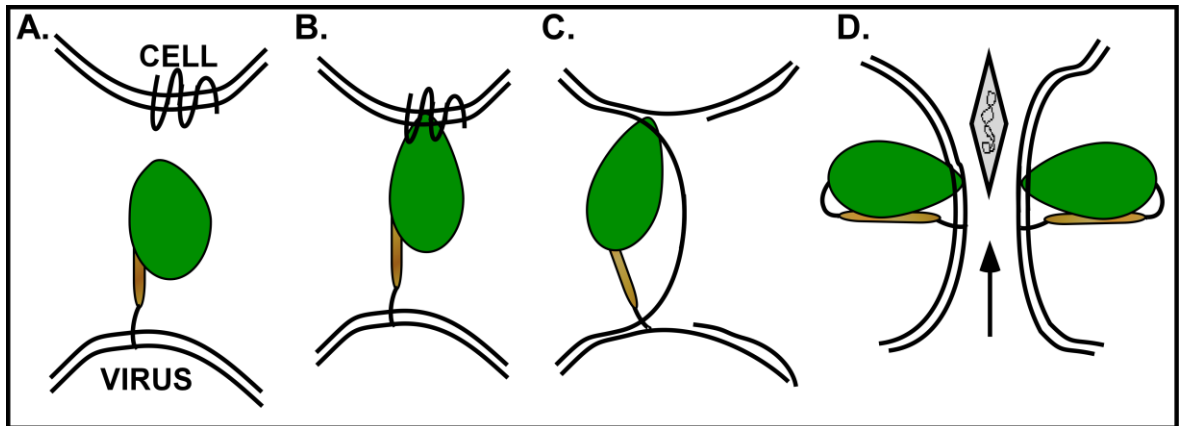


Figure 1-6. Virus-cell membrane fusion. A. Virus envelope glycoproteins mediate attachment to target cells. B. A specific trigger activates the fusion protein to insert its hydrophobic fusion peptide into the cellular membrane. C. Conformational rearrangements in the fusion protein draws the viral and cellular membranes into close proximity causing the outer leaflets of the lipid bilayers to merge. D. The lowest energy conformation of the fusion proteins is obtained and a fusion pore is formed through which the viral nucleocapsid (shown in grey) can pass. Note that a single fusion monomer is shown for simplicity.

Three dimensional structures of viral fusion proteins allow their classification into one of three distinct classes. Despite significant structural differences between fusion proteins from each class, the post fusion conformations all display a typical hairpin arrangement with the C-terminus of the protein located at the same end of the molecule as the membrane-inserted fusion loop.

Class I fusion proteins are predominantly α -helical and are arranged as trimers, projecting as spikes from the surface of the virus [56,336]. Fusion proteins in this class have a trimeric arrangement in both the pre and post fusion conformations. Influenza virus HA is an example of a well characterised class I fusion protein [337,338,339,340]. HA is expressed as an inactive precursor, H_0 , that is cleaved by host cell proteases into HA1, which has a receptor binding function, and the HA2 fusion protein. HA1 has a large globular fold while HA2 forms a long α -helical coiled-coil [340]. The hydrophobic fusion peptide is contained within the N-terminal residues of HA2 [289,339,341] (a hallmark of most

class I fusion proteins) and remains sequestered at the metastable trimer interface until fusion is activated by low pH-induced dissociation of the HA1 trimer [339]. Subsequent conformational changes in HA2 include extension of the central α -helical coiled coil region and insertion of the fusion peptide into the target cell membrane, such that HA2 is now embedded in both the viral and cellular membranes. This conformational state has been termed the pre-hairpin intermediate [342]. The C-terminal TMD then reorientates towards the membrane-inserted fusion peptide, allowing HA2 to adopt a low energy hairpin structure, referred to as the trimer of hairpins. This conformation is stabilised by the membrane proximal region of HA2 which packs into a groove within the N-terminal trimeric coiled coil [339].

Class II fusion proteins typically contain three sub-domains consisting predominantly of β -sheet secondary structure [343]; the central domain (I), domain III which is connected to the transmembrane region via the stem region, and domain II (schematically represented in Figure 1-7). In the prefusion state, class II fusion proteins may arrange as homodimers on the surface of the virus, as is the case for the flavivirus E glycoproteins [62,63], or as heterodimers with a partner envelope protein, as described for alphavirus E1 [344]. This arrangement sequesters the fusion peptide which is located within an internal sequence at the tip of domain II at the dimer interface. Cryo-EM and X-ray crystallography studies reveal that the class II fusion proteins of the flaviviruses lie flat on the viral surface, compared to the spike arrangement described for class I fusion proteins [62,63]. By contrast, the envelope proteins on the surface of the alphavirus chikungunya virus are arranged as protruding spikes [279,345].

The prefusion structures for class II fusion proteins from flaviviruses (TBEV [277] and dengue virus [346,347]) and alphaviruses (Semliki Forest virus [348,349] and chikungunya virus [279]) have been determined. These structures reveal a highly conserved fold across the three domains. Domain I forms the central domain that contains the N-terminus of the polypeptide. It is rich in β -sheet with an 'up and down' topology. Domain II extends from a connecting region between adjacent β -strands from domain I, and forms the "fusion domain". Domain III has

an immunoglobulin-like fold and is adjacent to the membrane proximal stem region [56].

Activation of the fusion potential of class II fusion proteins induces dissociation of the metastable envelope protein hetero- or homodimer, followed by homotrimerisation of the fusion protein. Cryo EM of dengue virus together with the post fusion crystal structures of the class II flaviviral glycoprotein E obtained at low pH have provided insight into the conformational changes of this fusion protein during low pH induced entry [62]. Mature dengue virus particles display 90 glycoprotein E dimers on the surface in an icosahedral arrangement, with three E monomers per icosahedral asymmetric unit. Low pH is thought to induce transition of glycoprotein E homodimers to a homotrimer arrangement, facilitating interdomain rotation of each glycoprotein E monomer. These events do not appear to alter the fold of the E sub-domains, but cause the C-terminus of the ectodomain to rotate $\sim 30\text{-}40$ Å towards the membrane-inserted N-terminal fusion peptide [350,351]. It is predicted that the stem region may pack into a channel formed by intersubunit contacts between domain II from trimeric glycoprotein E, that extends towards the fusion peptide. In fact, the stem region has been shown to promote trimerisation of glycoprotein E [280], consistent with a role in stabilising a fusion activated conformation of the glycoprotein.

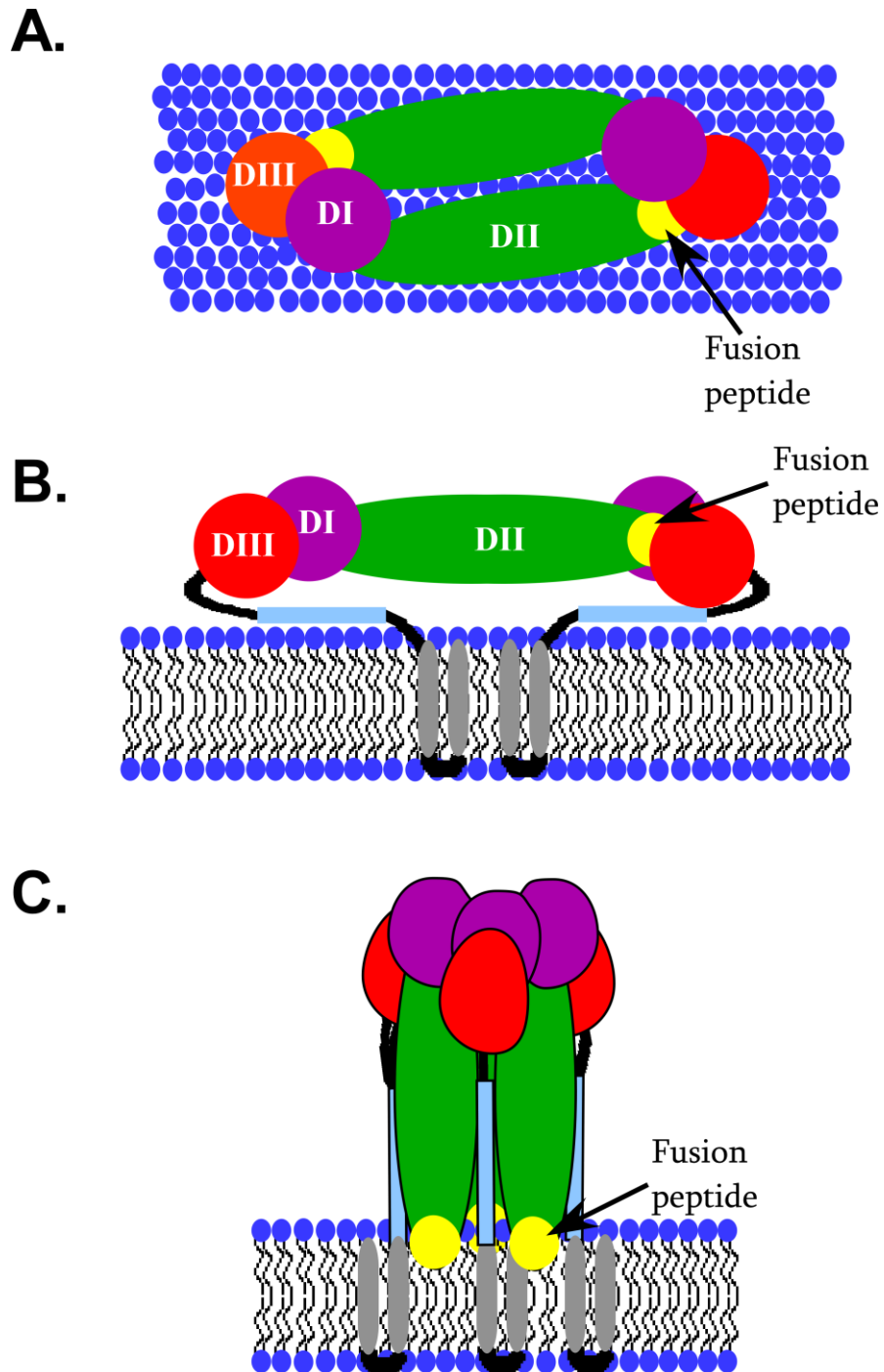


Figure 1-7. Schematic representation of a class II fusion protein pre and post fusion activation. A and B. Dengue virus glycoprotein E domain organisation and dimeric arrangement in the prefusion structure is shown as viewed from above (A) or from the side (B). The fusion peptide in yellow is sequestered at the dimer interface. The stem region is shown in light blue. The double transmembrane anchor is shown in grey. Polar head groups of the phospholipid bilayer are shown in royal blue. C. Fusion activated, hairpin structure of trimeric glycoprotein E. The fusion peptide (in yellow) is embedded in the membrane adjacent to the transmembrane anchor. The stem region (in light blue) is packed into the hydrophobic groove along domain II.

Class III fusion proteins contain features in common with class I and II fusion proteins [352]. Only a small number of fusion proteins have been assigned to this class and indeed vesicular stomatitis virus protein G (VSVg) is the only one for which the pre and post fusion conformations have been solved. VSVg is comprised of 5 domains and in both states the protein is arranged as a trimer [353,354]. The N-terminal residues of VSVg form domain IV. Extensions within this domain form domain III, which in turn contains an extension that forms domain II, which again contains an extension that forms domain I. Domain V is C-terminal to domain IV, adjacent to the transmembrane region. VSVg domains I, II and IV largely consist of β -sheet structure, reminiscent of class II fusion proteins. The predicted fusion peptide for VSVg is contained within an internal sequence of domain I (formed by 2 fusion loops), also similar to a class II fusion protein [353,355,356]. However, domain III of VSVg and other class III fusion proteins, has a long central α -helix with a trimeric coiled coil structure formed with helices from the other two protomers; a hallmark of class I fusion proteins.

In the prefusion structure, VSVg trimers appear as compact spikes with the fusion peptide (domain I) located near the virus membrane. Low pH activation induces an extremely large reorientation event whereby domain I dissociates from the C-terminus of the protomer and rotates 94° relative to domain II. The central helix of domain III is extended during these events, allowing stabilisation of the fusion activated conformation by intermolecular contacts mediated by an α -helical region in domain V. The resulting fusion activated form of VSVg appears as an extended hairpin conformation.

As discussed in section 1.5.3, it is predicted that HCV glycoprotein E2 may function as a class II fusion protein. Three dimensional structures of E1 and E2 pre and post fusion activation will be essential for validation of E2 as a class II fusion protein as well as for understanding how the glycoproteins function during entry.

1.7.2 Fusion activation triggers

Fusion proteins on the surface of enveloped viruses are expressed as inactive precursors such that the hydrophobic fusion peptide is sequestered. A specific trigger is required to release the fusion protein from this metastable conformation, exposing the fusion peptide for insertion into the target cell membrane. Consequently the fusion protein adopts a more stable fusion active conformation, mediating merger of the viral and target cell membranes as described above. Activation of fusion proteins prior to cellular attachment renders the virus inactive and thus delivery of the activation trigger must be carefully timed.

The trigger that induces these rearrangements is specific for each virus. Exposure of influenza virus to low pH is sufficient to induce irreversible conformational changes in the fusion protein HA, associated with fusion activation [78]. Avian sarcoma and leukosis retrovirus fusion activation requires priming of the fusion protein by virus-receptor binding followed by low pH exposure [357]. Ebola virus also requires exposure to low endosomal pH, however, the fusion proteins must additionally undergo cleavage by cathepsin B and/or L to induce activation [358]. Fusion activation of retroviruses murine leukaemia virus (MLV) and human T cell leukaemia virus type 1 (HTLV-1) requires reduction of a constraining disulfide bond between receptor binding glycoprotein SU, and the fusion protein TM, induced by a catalytic thiol within the glycoprotein complex [359,360].

For HCV, entry into hepatocytes is dependent on an initial attachment event with glycosaminoglycans [83,361] followed by cellular receptors CD81, SR-BI, claudin-1, 6 or 9 and occludin [5,6,8,9,10,252,331]. RNA knockdown of clathrin heavy chain or treatment of cells with agents which raise the endosomal pH is sufficient to inhibit HCV entry indicating the virus undergoes clathrin mediated endocytosis following receptor engagement [92]. However, HCV displays acid-resistance indicating that exposure to low pH is insufficient to induce fusion activation [11]. Furthermore, low pH does not efficiently induce virus entry at the plasma membrane of cells treated with the endosomal neutralising agent,

bafilomycin [92]. Together, these findings indicate that a series of stepwise events is likely to be required in order to prime the HCV fusion proteins for activation upon endocytic uptake.

1.8 Hypotheses and Aims

The HCV glycoproteins E1 and E2 operate as a heterodimer to facilitate HCV fusion and entry. Both covalently associated and non-covalently associated heterodimers have been described on the surface of virions. Recent evidence suggests that all 18 Cys residues are involved in 9 intramolecular disulfide bonds in monomeric E2 [273]. However, direct examination of HCVcc particles reveals that E1 and E2 may exist as multimers indicative of intermolecular disulfide bonding arrangements [137]. Therefore, the oxidation state of E1 and E2 on functional heterodimers remains unclear.

Our examination of 389 E1 sequences deposited in the Los Alamos database reveals the presence of a conserved C²²⁶V/LPC motif in E1, similar to the CXXC motif observed in thioredoxin domains. Thioredoxin family proteins regulate disulfide bonding arrangements. The N-terminal cysteine is typically in a reduced state and forms mixed disulfides with target proteins that are resolved by the second cysteine, leaving the target protein in a reduced state and free to adopt its lowest energy conformation.

Regulation of the oxidation state of retroviruses MLV and HTLV-1 has been shown to be essential in the formation of functional envelope protein complexes and in initiating fusion activation of these viruses [359,360]. In these cases, the receptor binding protein SU contains a CXXC motif that forms a labile disulfide with a free thiol group in the TM fusion protein. Receptor binding and calcium displacement triggers activation of the CXXC motif that reduces the labile disulfide, allowing the TM protein to mediate membrane fusion.

It is hypothesised that the oxidation state of E1 and E2 is an important determinant of virus entry competence and that the C²²⁶V/LPC motif in E1 is critical for the formation of functional E1E2 heterodimers. It is further hypothesised that regulation of disulfide bonding rearrangement within E1 and/or E2 is one of the fusion activation triggers for HCV entry.

The aims for this study are to:

1. Investigate the oxidation state of E1E2 in HCVpp and HCVcc during virus entry.
2. Investigate the role of the C²²⁶V/LPC motif in E1E2 assembly and virus entry.
3. Express recombinant E1 to examine the domain organisation and determine whether E1 has reducing activity *in vitro*.

Chapter 2 – Materials and Methods

2.1 Construction of pE1E2H77c Encoding HCV Envelope Glycoproteins

Construction of pE1E2H77c has been described previously [3]. Briefly, this construct is based on the cytomegalovirus (CMV) immediate early promoter-driven expression vector pCDNA4HisMax (Invitrogen, California, USA). The regions encoding E1 (191-383) and E2 (384-746) from the full-length infectious clone pCV-H77c (genotype 1a) were cloned into *EcoRI* and *XbaI* restriction sites within the multiple cloning site of pCDNA4HisMax (Invitrogen, California, USA). This construct was used to express wild-type E1E2 and as a template for site directed mutagenesis within E1E2.

In vitro mutagenesis of the pE1E2H77c vector was carried out using standard overlap extension PCR (see section 2.6.2). The sequence of E1E2 was confirmed using Big Dye terminator chemistry (see section 2.6.4; Applied Biosystems, California, USA) and analysed using ClustalX software.

2.2 Construction of Full Length HCV Vector pJC1FLAG2(p7-NS-GLUC2A)

The vector pJC1FLAG2(p7-NS-GLUC2A), was a kind gift from Charles Rice (Rockefeller Institute, New York, USA). pJC1FLAG2(p7-NS-GLUC2A) comprises the structural region (core-p7) of HCV-J6 (genotype 2a) and the non-structural region (NS2A-NS5B) of JFH1 (genotype 2a) [362]. The plasmid encodes a FLAG epitope tag at the N-terminus of E2 and gaussia luciferase which is secreted from infected or transfected cells. This vector was used to produce wild-type virus and as a template for site-directed mutagenesis of E1E2. *In vitro* mutagenesis was performed using the QuikChange II Site-Directed Mutagenesis Kit (Stratagene, California, USA; see section 2.6.3). The sequences of E1E2 were confirmed using Big Dye terminator chemistry (Applied Biosystems, California, USA; see section

2.6.4) and analysed using ClustalX software. In some instances a subfragment encoding the E1E2 region was subcloned into wild-type pJC1FLAG2(p7-NS-GLUC2A) via unique restriction sites *EcoRI* and *BsiWI*.

2.3 Construction of pMBP-E1

Construction of the modified maltose binding protein (MBP) expression vector has been described previously [363]. Briefly, this vector is based on pMAL-c2 (New England Biolabs, Ipswich, USA) encoding *Escherichia coli* (*E. coli*) MBP. This vector was modified to encode a rigid tri-alanine linker sequence for production of chimeric MBP proteins. E1 from pE1E2H77c was amplified with primers containing flanking 5'-*NotI* and 3'-*PstI* restriction sites (See Table 2-1). Glycoprotein E1 amplicons with C-terminal extensions of the ectodomain were ligated into the template vector following digestion with *NotI* and *PstI* restriction enzymes.

The sequence of E1 inserts was confirmed using Big Dye terminator chemistry (see section 2.6.4; Applied Biosystems, California, USA) and analysed using ClustalX software.

Table 2-1. pMBP-E1 primers. Restriction sites are underlined, stop-codons are in bold.

Construct	Sense primer	Anti-sense primer
pMBP-E1 ₁₉₁₋₂₅₉	5'-cgcg <u>cgccgc</u> cctaccaagtgcgcaattcctcg	5' gcctgcag tt aacgtcgaagctgcgttgt
pMBP-E1 ₁₉₁₋₃₂₉	As above	5'-cgctgcag tt acgtaggggaccagttcatcat
pMBP-E1 ₁₉₁₋₃₄₀	As above	5'-cgctgcag tt agatccggagcagctgagctac
pMBP-E1 ₁₉₁₋₃₅₁	As above	5'-cgctgcag tt aagcaccagcgatcatgtccat

2.4 Construction of pcE1myc

Construction of the pcE1myc plasmid is based on the pcE2₆₆₁myc expression vector which directs the expression of soluble E2₆₆₁ RBD of the H77c isolate [245]. This construct incorporates an N-terminal tissue plasminogen activator leader sequence which translocates the E2₆₆₁ RBD protein into the lumen

of the endoplasmic reticulum. Briefly, E1 from pE1E2H77c was amplified with primers containing a flanking 5'-*NheI* restriction site, a 3'-*XbaI* restriction site and a 3' myc epitope tag [364] (see Table 2-2). Glycoprotein E1 amplicons with C-terminal extensions were ligated into the template vector following digestion with *NheI* and *XbaI* restriction enzymes. The sequence of E1 inserts was confirmed using Big Dye terminator chemistry (see section 2.6.4; Applied Biosystems, California, USA) and analysed using ClustalX software.

Table 2-2. pcE1myc primers. Restriction sites underlined, stop-codons in bold, myc tag in capital letters.

Construct	Sense primer	Anti-sense primer
pcE1myc ₁₉₁₋₂₅₉	5'- cgcgctagctaccaagtgcgcaatt cctcg	5'- cgctctag atta CAGATCCTCTTCTGAGATGAGTTT TTGTTCAGTACTacgtcgaagctgcgttggtggg
pcE1myc ₁₉₁₋₃₂₉	As above	5'- cgctctag atta CAGATCCTCTTCTGAGATGAGTTT TTGTTCAGTACTcgtaggggaccagttcatcat
pcE1myc ₁₉₁₋₃₄₀	As above	5'- cgctctag atta CAGATCCTCTTCTGAGATGAGTTT TTGTTCAGTACTgatccggagcagctgagctac
pcE1myc ₁₉₁₋₃₅₁	As above	5'- cgctctag atta CAGATCCTCTTCTGAGATGAGTTT TTGTTCAGTACTagcaccagcgatcatgtccat

2.5 Additional Plasmids

The HIV-1 luciferase reporter vector pNL4-3.LUC.R⁻E⁻ was obtained from Dr. N. Landau through the NIH AIDS Research and Reference Reagent Program [365].

Plasmid pHEF-VSVg encoding VSVg was obtained from Dr. Lung-Ji Chang through the NIH AIDS Research and Reference Reagent Program [366].

Plasmid pET-32a(+) encoding bacterial thioredoxin and a C-terminal 6 x His tag was purchased from Novagen (Merck, Darmstadt, Germany).

2.6 Cloning Procedures

2.6.1 Restriction digestion of DNA

All restriction enzymes used for DNA digestion were used according to the manufacturer's instructions. Restriction enzymes used in this project include: *Bam*HI, *Bsi*WI, *Eco*RI, *Nhe*I, *Not*I, *Pst*I and *Xba*I (New England Biolabs, Ipswich, USA).

2.6.2 Site directed mutagenesis by overlap extension PCR

Overlap extension mutagenesis was used to introduce single site mutations within the plasmid pE1E2H77c. In the first round of PCR, a fragment 5' to the site of mutagenesis (PCR 1) was obtained using a positive sense primer complimentary to the N-terminus of E1, incorporating an *Eco*RI restriction site (underlined); 5'- ggtggaattctggcaacagggaaaccttctgg. The antisense primer was complimentary to a region of DNA 21 nucleotides in length directly 5' to the site of mutagenesis (see Table 2-3). The 3' fragment was amplified (PCR 2) using a positive sense primer 54 nucleotides in length which incorporated the mutation to be introduced and overlapped with the antisense primer from PCR 1 (see Table 2-3). The antisense primer in PCR 2 was complimentary to the C-terminus of E2 and incorporated an *Xba*I restriction site and a stop codon (5'- ggctctagattacgctccgcttgggatat).

PCR reactions 1 and 2 contained 100 nM primer (sense and antisense), 100 pg pE1E2H77c template DNA, 250 nM dNTPs, 1 x Expand High Fidelity Buffer (containing 15 mM MgCl₂; Roche, Indianapolis, USA) and 3.5 U Expand High Fidelity enzyme (Roche, Indianapolis, USA). For cycle conditions see Table 2-4.

PCR reactions 1 and 2 were purified using UltraClean[®] PCR Clean-Up Kit (Mo Bio, Carlsbad, USA) as per the manufacturer's instructions, with 1 µl of each

reaction forming the template DNA for PCR 3. The positive sense primer complimentary to the N-terminus of E1 and anti-sense primer complimentary to the C-terminus of E2 used are described above. dNTPs, buffer and enzyme were used as described for PCRs 1 and 2.

PCR products containing the entire E1E2 sequence (1.7 kb) produced by PCR 3 were isolated by agarose gel purification using UltraClean[®] GelSpin[®] DNA Extraction Kit (Mo Bio, Carlsbad, USA) as per the manufacturer's instructions.

Purified PCR products and pE1E2H77c (wild-type) vector were digested sequentially with *EcoRI* and *XbaI*. Digested pE1E2H77c was treated with alkaline phosphatase (Roche, Indianapolis, USA) according to the manufacturer's instructions. Digested PCR products and digested, de-phosphorylated pE1E2H77c were isolated by agarose gel purification using UltraClean[®] GelSpin[®] DNA Extraction Kit (Mo Bio, Carlsbad, USA) as per the manufacturer's instructions. PCR products containing the mutant E1E2 were ligated into the digested and de-phosphorylated pE1E2H77c at a ratio of 10:1 using T4 DNA Ligase (0.1 U; Roche, Indianapolis, USA) in 1 x T4 DNA Ligase buffer (Roche, Indianapolis, USA), overnight at 4°C.

Ligation reactions were precipitated by addition of a 1/10th volume of 3 M sodium acetate (pH 5.2), 2.5 volumes of 100% ethanol and 3 µl tRNA (precipitation aid) at -80°C for 30 min. DNA was pelleted at 13 000 rpm in a microfuge at 4°C for 15 min. DNA pellets were washed twice with 70% ethanol, re-suspended in 5 µl H₂O then transformed by electroporation into electrocompetent DH10β *E. coli* (see section 2.6.7).

Colonies obtained were screened for the presence of DNA encoding E1E2 by mini-prep (see section 2.6.8) and digestion with *EcoRI* and *XbaI*. Site directed mutagenesis was confirmed by sequencing the E1E2 region using Big Dye terminator chemistry (see section 2.6.4; Applied Biosystems, California, USA) and analysis using ClustalX software.

Table 2-3. Primers used for site directed mutagenesis of pE1E2H77c. Mutation is shown in capital letters.

Construct	Sense primer	Anti-sense primer
pE1E2H77c -AVPC	5'- gccatcctgcacactccggggGCTgtccttgcgttcgagggtaac gcctcg	5'-ccccggagtgtgcaggatggc
pE1E2H77c -CVPA	5'- gccatcctgcacactccgggggtgtgcctGCCgttcgagggtaac gcctcg	As above
pE1E2H77c -AVPA	5'- gccatcctgcacactccggggGCTgtcctGCCgttcgagggta acgcctcg	As above
pE1E2H77c -CMPC	5'- gccatcctgcacactccgggggtATGccttgcgttcgagggtaacg cctcg	As above
pE1E2H77c -CLPC	5'- gccatcctgcacactccgggggtCTCccttgcgttcgagggtaacg cctcg	As above
pE1E2H77c -CIPC	5'- gccatcctgcacactccgggggtATCccttgcgttcgagggtaacg cctcg	As above
pE1E2H77c -CAPC	5'- gccatcctgcacactccgggggtGCCccttgcgttcgagggtaac gcctcg	As above
pE1E2H77c -CEPC	5'- gccatcctgcacactccgggggtGAGccttgcgttcgagggtaac gcctcg	As above
pE1E2H77c -CVAC	5'- gccatcctgcacactccgggggtgtGCGtgcgttcgagggtaac gcctcg	As above

Table 2-4. PCR cycle conditions for reactions 1, 2 and 3 of overlap extension PCR.

PCR	Temperature	Time	Number of cycles
PCR 1 + 2	95°C	5 min	1
	92°C	30 sec	30
	55°C	30 sec	
	72°C	2 min	
	72°C	10 min	1
PCR 3	95°C	5 min	1
	92°C	30 sec	30
	55°C	30 sec	
	72°C	4 min	
	72°C	10 min	1

2.6.3 Site directed mutagenesis by QuikChange II Site-Directed Mutagenesis Kit

Site directed mutagenesis of pJC1FLAG2(p7-NS-GLUC2A) was performed using Quikchange XL II mutagenesis kit (Stratagene, California, USA) according to the manufacturer's instructions. DNA was transformed into XL10-Gold® Ultracompetent Cells (Stratagene, California, USA). Primers are described below (mutation in capital letters).

Table 2-5. Quikchange primers used for site directed mutagenesis of pJC1FLAG2(p7-NS-GLUC2A). Mutation is shown in capital letters.

Construct	Sense primer	Anti-sense primer
pJC1FLAG2(p7-NS-GLUC2A)-AVPC	5'-ccacgtccccgggGCCgtcccgtgcgag	5'-ctcgcacgggacGGCccccggggacgtgg
pJC1FLAG2(p7-NS-GLUC2A)-CVPA	5'-gggtgcggtcccGCCgagaaagtggg	5'-ccccactttctcGGCcgggacgcaccc
pJC1FLAG2(p7-NS-GLUC2A)-CMPC	5'-cacgtccccgggtgcATGccgtgcgagaaagtg	5'-cactttctgcacggCATgcacccggggacgtg
pJC1FLAG2(p7-NS-GLUC2A)-CAPC	5'-cacgtccccgggtgcGCCccgtgcgagaaagtg	5'-cactttctgcacggGGCgcacccggggacgtg
pJC1FLAG2(p7-NS-GLUC2A)-CEPC	5'-cacgtccccgggtgcGAGccgtgcgagaaagtg	5'-cactttctgcacggCTCgcacccggggacgtg

2.6.4 DNA cycle sequencing

DNA isolated by miniprep (see section 2.6.8) was sequenced using BigDye Terminator chemistry (Applied Biosystems, California, USA). Each 20 µl reaction was set up with 400 ng of DNA, 1 µl BigDye Premix (v3.1), 1x BigDye Terminator Reaction Buffer and 166 nM sequencing primers spanning E1 and E2. PCR cycle conditions are shown in Table 2-6.

Reactions were precipitated by addition of 3 µl 3 M sodium acetate pH 5.2, 62.5 µl 100% ethanol, addition of H₂O to 100 µl, and incubation for 15 min at room temperature. Precipitated DNA was pelleted at 13 000 rpm in a microfuge for 30 min, then washed once with 70% ethanol. Samples were air dried then stored at 4°C and protected from the light until analysis by 3730S Genetic Analyser (Applied Biosystems, California, USA).

Table 2-6. BigDye Terminator cycle sequencing conditions.

Temperature	Time	Number of cycles
96°C	1 min	1
96°C	10 sec	30
50°C	5 sec	
60°C	4 min	

2.6.5 Agarose gel electrophoresis of DNA

Agarose gels (0.8%) were prepared in TAE buffer (40 mM Tris-acetate, 1 mM EDTA). SYBR[®] Safe Gel Stain (Invitrogen, California, USA) was added to molten agarose and DNA visualized under ultra-violet light.

2.6.6 Preparation of competent cells

Electrocompetent cells were prepared by growing a single colony of DH10 β *E. coli* in 10 ml of Luria Bertani broth (LB; 10 g tryptone, 5 g yeast extract, 10 g NaCl per litre) broth overnight at 37°C. Fourteen hours later 1 L of LB broth was inoculated with the 10 ml overnight culture and incubated with shaking until an OD₆₀₀ of 0.6 was reached. The culture was chilled on ice for 30 min and then pelleted at 5 000 xg for 15 min.

Pellets were washed twice in cold, sterile H₂O then once in cold, sterile 10% glycerol. Cells were resuspended in 3 ml cold 10% glycerol then snap frozen in 40 μ l aliquots. Cells were stored at -80°C.

2.6.7 Plasmid transformation into competent cells

Transformation of plasmids produced by Quikchange XL II mutagenesis kit (Stratagene, California, USA) were carried out in heat shock XL10-Gold[®] Ultracompetent Cells (Stratagene, California, USA) according to the manufacturer's instructions. All other transformations were carried out in DH10 β *E. coli* prepared as described above using standard electroporation techniques

[367]. Transformants were grown on LB agar containing selective antibiotics ampicillin (100 µg/ml) or kanamycin (50 µg/ml).

2.6.8 Small scale plasmid purification (mini-prep)

All small scale plasmid preparations were carried out using UltraClean® 6 Minute Mini Prep Kit (Mo Bio, Carlsbad, USA) according to the manufacturer's instructions.

2.6.9 Large scale plasmid purification (midi-prep)

All large scale plasmid preparations were carried out using Plasmid Midi Kit or Plasmid Maxi Kit (QIAGEN, Hilden, Germany) according to the manufacturer's instructions.

2.7 RNA Transcription

Wild type and mutated HCV RNA was transcribed *in vitro* from *Xba*I-linearised pJC1FLAG2(p7-NS-GLUC2A) DNA using Ampliscribe™ T7 High Yield Transcription Kits (Epicentre Biotechnologies, Wisconsin, USA) for 4 h according to the manufacturer's instructions. Reactions were treated with 1 U of DNase for 30 min at 37°C to remove template DNA. RNA was purified, either by standard phenol/chloroform extraction and ethanol precipitation [367], or using the RNeasy Mini Kit (QIAGEN, Hilden, Germany). Purified RNA was stored at -80°C.

2.7.1 RNA gel electrophoresis

All RNA gel electrophoresis was performed under reducing conditions. Five-hundred mg of agarose was dissolved in 36 ml of nuclease-free H₂O then cooled to 60°C. Five ml of 10X MOPS running buffer (0.4M MOPS, pH 7.0, 0.1M sodium acetate, 10 mM EDTA), 18 ml 37% formaldehyde (12.3 M) and 1X SYBR® Safe Gel Stain (Invitrogen, California, USA) were added to the molten agarose. RNA samples were heated to 60°C with 1X Gel Loading Buffer II (Ambion, Texas, USA) for 10 min prior to electrophoresis followed by visualisation under ultra-violet light.

2.7.2 RNA quantification by quantitative reverse transcriptase PCR (qRT-PCR)

In order to normalise RNA concentrations for transfection and production of mutant and wild-type HCVcc, qRT-PCR was performed using TaqMan[®] One-Step RT-PCR Master Mix Reagents Kit (Applied Biosystems, California, USA). This kit allows reverse transcription of viral RNA to cDNA followed by amplification in a single reaction. The kit employs FAM[™] dye-labeled TaqMan probe technology (Applied Biosystems, California, USA) with the custom FAM[™] probe complementary to a conserved region of core (5'-ctgcggaaccggtgagtacac) in between the binding sites of sense and anti-sense primers. Displacement of this probe as amplification of the cDNA occurs gives rise to a fluorescent signal which can be followed in real time. Primers to conserved regions of the core gene were used; 5'-cgggagagccatagtg (sense) and 5'-agtaccacaaggccttgc (anti-sense).

Briefly, duplicate RNA samples were diluted 10^4 and 10^5 in nuclease free H₂O. Ten μ l of each sample was added to a master mix containing 1X AmpliTaq Gold[®] DNA Polymerase mix (containing AmpliTaq Gold[®] DNA Polymerase, dNTPs with dUTP, and optimized buffer components; Applied Biosystems, California, USA), 1X reverse transcriptase enzyme mix (containing MultiScribe[™] Reverse Transcriptase and RNase Inhibitor; Applied Biosystems, California, USA), 200 nM sense and anti-sense primers, 150 nM FAM[™] probe, and nuclease free H₂O to 25 μ l. PCR reactions were performed on an Mx3000P[™] Real-Time PCR System (Stratagene, California, USA). Cycle conditions are shown in Table 2-7. RNA concentrations were normalised to the sample containing the lowest concentration of RNA prior to transfection of Huh-7.5 cells (see section 2.9.2).

Table 2-7. Cycle conditions for quantitative real-time RT PCR.

Temperature	Time	Number of cycles
48°C	30 min	1
95°C	8 min 30 sec	1
95°C	15 sec	40
62°C	1 min	

2.8 Antibodies

Monoclonal antibodies (MAb) A4, H53 and H52 [131,197] were a kind gift from Dr. Jean Dubuisson (Institut Pasteur de Lille, Lille, France). Monoclonal antibodies CBH 4D, CBH 7 and CBH 11 [94,368] were a kind gift from Professor Steven Fong (Stanford University School of Medicine, Stanford, USA).

GP1 is polyclonal serum raised to the H77c E2₆₆₁His protein in guinea pigs.

MAb 24 is a neutralising MAb raised in mice against E2₆₆₁His protein. It recognises a linear epitope (residues 411-428) adjacent to HVR1.

Immunoglobulin G (IgG14) was purified from the plasma of HIV-1 infected individuals using protein G sepharose (Amersham Pharmacia Biotech, Buckinghamshire, UK). The anti-HIV-1 capsid MAb 183 was obtained from the AIDS Research and Reference Reagent Program [369,370].

Anti-FLAG M2 is a commercial MAb available from Sigma (St Louis, USA).

MAb 9E10 which recognises a linear epitope within human c-Myc was purified from the cell line MYC 1-9E10.2 using protein G sepharose (Amersham Pharmacia Biotech Buckinghamshire, UK).

2.9 Cell Lines and Transient Transfections

All cell lines were maintained in a Thermo Direct Heat CO₂ Incubator at 37°C with 5% CO₂.

Human embryonic kidney 293T (HEK 293T), Chinese hamster ovary K1 (CHO-K1), Lec-8 and Human hepatoma-7 (Huh-7) cells were maintained in Dulbecco's minimal essential medium (DMEM; Invitrogen, California, USA) with

10% fetal calf serum and 2 mM L-glutamine (DMF10). Human hepatoma-7.5 (Huh-7.5) cells were a kind gift from Professor Charles Rice. These cells were maintained in DMF10 supplemented with 0.1 mM nonessential amino acids (DMF10NEA). Antibiotics gentamycin (80 µg/ml) and minocycline (1 µg/ml) were added to DMF10 and DMF10NEA to limit contamination events.

2.9.1 FuGene-6 DNA transfection

HEK 293T cells were seeded in 6 well plates (Nunc, Roskilde, Denmark) either 5 or 18 h prior to transfection (cell densities and seeding times are specified for each experiment). Optimem (Invitrogen, California, USA) and FuGene-6 (Roche, Indianapolis, USA) were used at room temperature. Optimem (97 µl) was mixed with 3 µl of FuGene-6 (per µg DNA) and incubated for 5 min at room temperature. The Optimem-FuGene-6 mix was added to DNA for 15 min then added dropwise to HEK 293T cells.

2.9.2 DMRIE-C RNA transfection

Huh-7.5 cells were seeded at 350 000 cells/well in 6 well plates (Nunc, Roskilde, Denmark) 18 h prior to transfection in antibiotic-free DMF10NEA. Transfection mix consisting of 1 ml Optimem, 8 µl of DMRIE-C reagent (Invitrogen, California, USA) and 6 µg of RNA were prepared in polystyrene tubes. Cells were washed once with Optimem followed by addition of the transfection mix. Four h post-transfection the medium was removed and replaced with DMF10NEA. Seventy two h later, virus in the tissue culture supernatant was filtered (0.45 µm) and stored at -80°C until further use.

For HCVcc used in infectivity assays in the presence of 4-(N-Maleimido)benzyl- α -trimethylammonium iodide (M135; Toronto Research Chemicals Inc., Ontario, Canada), fresh Optimem was added to cells 4 h post-transfection. Seventy-two h later virus in the tissue culture supernatant was filtered (0.45 µm) and buffer exchanged via ultrafiltration (MWCO 100 kDa; Amicon, Massachusetts, USA) into TN-Ca²⁺ (14 mM Tris, 12 mM HEPES, 150 mM NaCl,

1.8 mM Ca²⁺, pH 6.8) in order to diminish sulfhydryl containing contaminants. Virus was stored at -80°C until further use.

2.10 Protein Analysis

2.10.1 Sodium dodecyl sulphate polyacrylamide gel electrophoresis (SDS-PAGE)

Proteins isolated from transformed bacteria, transiently expressed in HEK 293T, CHO-K1 or Lec-8 cells. or isolated from HCVpp, were subjected to SDS-PAGE for visualisation. Cell or viral lysates or purified protein were denatured at 95°C for 5 min in 2.5X reducing or non-reducing sample buffer (sample buffer for tris-glycine gels: 30 mM tris, 5% glycerol, 2.5% SDS, 0.03% bromophenol blue; sample buffer for tricine gels: 150 mM tris pH 7, 3% SDS, 30% glycerol, 0.05% Coomassie G-250). For reducing gels, 3% or 6% β-mercaptoethanol was added to each sample (tris-glycine and tricine respectively). Boiled samples and a prestained broad range marker (Biorad; California, USA) were then loaded onto either a 10-15% gradient tris-glycine gel, a 10% tricine gel or a 10-16% gradient tricine gel and run in an Apollo vertical electrophoresis device (CLP, California, USA) at 120 V for 2 h.

For radiolabelled samples, gels were dried on to filter paper using a heated vacuum drier for 1 h followed by phosphorimage analysis.

For Coomassie stained gels, gels were immediately stained with Coomassie blue [0.1% (w/v) Coomassie brilliant blue R-250, 5% glacial acetic acid (v/v), 50% methanol (v/v)] for 18 h, followed by sequential washes with destain solution (10% methanol and 10% acetic acid) until the gel background was clear. Destained protein gels were scanned on an Odyssey Infrared Imaging System at 700 nm (LI-COR).

For Western blotting, proteins were transferred using an Apollo tank electroblotter (CLP, California, USA) onto nitrocellulose membrane (0.22 μM, Amersham Biosciences, Buckinghamshire, UK) in transfer buffer [20 mM tris-HCl,

200 mM glycine, 20% (v/v) methanol] at 100 V for 1 h at 4°C. The membrane was rinsed in phosphate buffered saline (PBS) and blocked in 1x PBS + 5% skim milk for 1 h to prevent non-specific binding. Primary antibody dilutions were prepared in 1x PBS + 0.05% Tween-20 (PBST) + 2.5% skim milk and incubated with the membrane for 1 h with rocking. After four 5 min washes with PBST, membranes were incubated with Alexa Fluor 680 goat anti-mouse (Invitrogen, California, USA) antibody diluted 1:2000 in PBST + 2.5% skim milk. Excess secondary antibody was removed by four 5 min washes with PBST and the blot imaged using an Odyssey Infrared Imaging System at 700 nm (LI-COR).

2.10.2 Radio-immunoprecipitation (RIP)

Radioimmunoprecipitations (RIP) were performed as previously described [3]. For analysis of intracellular E1E2 or E1-myc, HEK 293T cells were seeded at 500 000 cells/well in 6 well plates 18 h prior to transfection with 2 ug DNA using FuGene-6 (see section 2.9.1). Cells were starved in methionine and cysteine-deficient DMF10 (MP Biomedicals, California, USA) for 30 min followed by labeling with 150 µCi Trans-³⁵S-label in methionine and cysteine-deficient DMF10 for 15 mins, 30 mins or 4 h, as indicated. Cells were chased in DMF10 (times specified for each reaction).

For analysis of HCVpp, HEK 293T cells were seeded at 350 000 cells/well in 6 well plates 18 h prior to co-transfection with wild type, mutant pE1E2H77c or cDNA4 empty vector and pNL4-3.LUC.R⁺, using FuGene-6 (see section 2.9.1). Thirty h post-transfection cells were labeled with 75 µCi Trans-³⁵S-label in methionine and cysteine-deficient DMF10 for 16h. Tissue culture fluid was clarified by filtration (0.45 µm) then radiolabeled viruses were pelleted by centrifugation at 14 000 xg for 2 h at 4°C.

Radiolabeled virions or cell lysates were lysed in RIP lysis buffer (0.6 M KCl, 0.05 M tris pH 7.4, 1 mM EDTA, 0.02% sodium azide, 1% triton X-100) and cleared overnight at 4°C with BSA-sepharose in the presence of MAb H53, MAb H52, MAb 24, MAb A4, polyclonal GP1, MAb 183 or IgG14. Antibody-bound

proteins were precipitated by protein G-sepharose (Amersham Pharmacia Biotech, Buckinghamshire, UK) for 1 h at room temperature, prior to SDS-PAGE and phosphorimage analysis (see section 2.10.1).

In assays where glycoproteins were treated with sulfhydryl alkylating agent *N*-Ethylmaleimide (NEM; Sigma, St Louis, USA) prior to lysis, HCVpp were produced and radiolabelled with Trans-³⁵S-label as described above. HCVpp were pelleted by centrifugation at 14 000 xg for 2 h at 4°C then incubated in PBS containing 5 mM NEM for 10 min at room temperature. Particles were then lysed in NP-40 buffer (50 mM tris, pH 7.5, 150 mM NaCl, 2 mM EDTA, 1% NP-40) containing 5 mM NEM. Immunoprecipitations were performed as described above.

2.10.3 Deglycosylation of mammalian expressed, secreted proteins

CHO-K1 or Lec-8 cells were seeded at 500 000 cells/well in a 6 well plate. Five h later, cells were transfected with 2 µg pcE1myc constructs using FuGene-6 (see section 2.9.1). Twenty-four h post transfection cells were radiolabelled with 150 µCi Trans-³⁵S-label/well as described in section 2.10.2. Cells were chased in DMF10 for 18 h. Cellular supernatants were filtered (0.45 µm) and added to 1x RIP lysis buffer. Samples were cleared for 1 h at room temperature with BSA-sepharose in the presence of MAb A4. Antibody-bound proteins were precipitated by protein G-sepharose (Amersham Pharmacia Biotech, Buckinghamshire, UK) for 1 h at room temperature. Deglycosylation assays using Endo H (New England Biolabs, North Dakota, USA) and PNGase F (New England Biolabs, North Dakota, USA) were performed under reducing conditions according to the manufacturer's instructions. Following deglycosylation, protein from each sample was precipitated by standard methanol/chloroform precipitation [367], prior to resuspension in 2.5 X tricine sample buffer. Proteins were run on 10-16% tricine SDS-PAGE and phosphorimaged (see section 2.10.1).

2.10.4 Biotinylation of E1E2

HEK 293T cells were seeded at 500 000 cells/well in a 6 well plate. Five h later cells were co-transfected with 1 µg of wild type, mutant pE1E2H77c or cDNA4 empty vector along with 1 µg of pNL4-3.LUC.R⁻E⁻ using FuGene-6 (see section 2.9.1). Seventy-two h post-transfection culture supernatants were filtered (0.45 µm). HCVpp were pelleted by ultracentrifugation (SW 41 rotor, 25 000 rpm, 4°C, 2 h) over a 25% sucrose cushion. Pelleted particles were resuspended in 1.25 mM EZ-Link Maleimide-PEG2-Biotin (Thermo Scientific, Massachusetts, USA) or Sulfo-NHS-LC-Biotin (Thermo Scientific, Massachusetts, USA) and incubated at room temperature for 30 min. Reactions were quenched with 100 mM cysteine or glycine, respectively, for 30 min at room temperature. Particles were pelleted by centrifugation (14 000 xg, 2 h, 4°C) then lysed in Western lysis buffer (1 % triton X-100, 1 mM EDTA, 0.02 % sodium azide, in PBS). For reduced samples, 100 mM DTT was added to particle lysates. A fraction of sample was then diluted in RIP lysis buffer and applied to High Capacity Streptavidin Agarose Resin (Thermo Scientific, Massachusetts, USA) to isolate biotinylated proteins. Samples were run on reducing or non-reducing SDS-PAGE and Western blotted with MAbs H52, A4 and 183 (see section 2.10.1).

The expression and purification of a chimera composed of maltose-binding protein linked to CD81 large extracellular loop residues 113-201 (MBP-LEL¹¹³⁻²⁰¹) has been described previously [245]. In maleimide biotinylation assays where HCVpp were pre-bound to CD81, 500 µg wild type or F186S mutant MBP-LEL¹¹³⁻²⁰¹ [245] were added to particles and incubated at room temperature for 1 h prior to ultracentrifugation and labeling as described above. Alternatively, HCVpp were pre-bound to heparin sodium salt (from porcine intestinal mucosa, 1mg/ml; Sigma, St Louis, USA) for 1 h at room temperature prior to ultracentrifugation and labeling.

2.10.5 Solid phase E1E2-CD81 binding assay

Maxisorb enzyme linked immunosorbent assay plates (Nunc, Roskilde, Denmark) were coated with 5 µg/ml of dimeric MBP-LEL¹¹³⁻²⁰¹ in PBS at 4°C

overnight, followed by blocking of unoccupied sites with bovine serum albumin (10 mg/ml in PBS) for 1 h. The plates were washed four times with PBST. Radiolabelled HCVpp were produced as described in section 2.10.2 and pelleted from tissue culture medium by centrifugation at 14 000 xg for 2 h. The virions were lysed in RIP lysis buffer and a fraction of each lysate subjected to H53-immunoprecipitation, non-reducing SDS-PAGE and phosphorimaging (see sections 2.10.1 and 2.10.2). The E2 content of each lysate was determined by densitometry. Viral lysates were normalized according to E2 content then applied to MBP-LEL¹¹³⁻²⁰¹ coated plates, serially diluted and incubated at room temperature for 2 h. After washing, bound E2 was detected with MAb H53 and rabbit-anti-mouse immunoglobulin-horse radish peroxidase conjugate (Dako, California, USA). The plates were developed with tetramethylbenzidine substrate according to the manufacturer's recommendations (Sigma, St Louis, USA). Plates were read at 450 nm and the background absorbance at 620 nm subtracted.

In assays where M135 treated HCVpp were used, HCVpp were produced and partially purified as described in section 2.10.4. HCVpp were incubated with 0-5 mM M135 in TN-Ca²⁺ for 30 min at room temperature prior to quenching with 100 mM cysteine for 30 min. Particles were pelleted by centrifugation (14 000 xg, 2 h, 4°C) then lysed in Western lysis buffer for SDS-PAGE analysis. A fraction of each sample was further diluted in RIP lysis buffer and applied to MBP-LEL¹¹³⁻²⁰¹ coated plates as described above.

2.11 E1E2-Pseudotyped HIV-1 Particle Entry Assay

Pseudotyped particle (pp) entry assays were performed as described previously [3]. Briefly, HEK 293T cells were seeded at 350 000 cells/well in 6 well plates (Nunc, Roskilde, Denmark). Eighteen h later cells were co-transfected with 1 µg of wild type pE1E2H77c, mutant pE1E2H77c, pHEF-VSVg, or cDNA4 empty vector along with 1 µg of pNL4-3.LUC.R⁻E⁻ using FuGene-6 (see section 2.9.1). Seventy-two h post-transfection culture supernatants were filtered (0.45µm) and added to Huh-7 or Huh-7.5 cell monolayers for 4 h. Cells were then washed with PBS and fresh DMF10 (Huh-7) or DMF10NEA (Huh-7.5) added. Luciferase activity

in the cell lysates was measured 72 h later with a Fluostar (BMG Lab Technologies, Offenburg, Germany) fitted with luminescence optics, using the Firefly luciferase reagent system (Promega, Wisconsin, USA).

For HCVpp infectivity assays performed in the presence of sulfhydryl alkylating agent M135 (Toronto Research Chemicals Inc., Ontario, Canada), HCVpp were produced as described above. Seventy-two h post-transfection culture supernatants were filtered (0.45 μm) then clarified by ultracentrifugation (SW 41 rotor, 10 000 rpm, 4°C, 10 min). To diminish sulfhydryl containing contaminants particles were pelleted (SW 41 rotor, 16 000 rpm, 4°C, 2 h) then resuspended in TN-Ca²⁺. Partially purified HCVpp were alkylated with 0 to 5 mM M135 for 50 min at 37°C. Reactions were quenched by addition of DMF20NEA. Alkylated virus was applied to cells at 37°C for 2 h. Cells were washed once with TN-Ca²⁺ and fresh DMF10NEA added.

For assays where alkylation was performed after virus was bound to cells, HCVpp were produced and partially purified as above then bound to cells for 2 h at 4°C. Unbound virus was removed and cells were washed once with TN-Ca²⁺ prior to addition of 0 to 5 mM M135 in TN-Ca²⁺. Alkylation was performed for 50 min at 37°C. Cells were washed once with TN-Ca²⁺ then fresh DMF10NEA added. For both alkylation assays luciferase activity in the cell lysates was assayed 72 h later as described above.

For assays where HCVpp were pre-incubated with heparin sodium salt, HCVpp were produced as above. Seventy-two h post-transfection culture supernatants were filtered (0.45 μm) then directly incubated with 1 mg/ml of heparin sodium salt (from porcine intestinal mucosa; Sigma, St Louis, USA) for 1 h at room temperature prior to incubation with Huh-7.5 cells for 4 h at 37°C. Luciferase activity in the cell lysates was assayed 72 h later as described above.

2.12 HCVcc Quantification

2.12.1 HCVcc TCID₅₀/ml

The 50% Tissue Culture Infectious Dose (TCID₅₀) is the dilution of virus that infects 50% of replicating cells. This was calculated for wild-type pJC1FLAG2(p7-NS-GLUC2A) virus stocks. Huh-7.5 cells were seeded at 6 000 cells/well in a 96 well format (Nunc, Roskilde, Denmark). Eighteen h later 10 fold serial dilutions of HCVcc were prepared from 10¹ to 10¹¹ and added to 6 replicate wells. An uninfected control row was also included. Four h post infection the virus was removed and fresh DMF10NEA added.

Seventy-two h later media was removed and cells washed twice with PBS. Cells were fixed with 100% methanol at -20°C overnight then washed once with PBS prior to permeabilisation with PBS containing 0.1% tween-20. To prevent non-specific antibody binding, cells were blocked with 2% horse serum in PBS for 1 h at room temperature. To block endogenous peroxidase activity cells were treated with 3% H₂O₂ in PBS for 5 min. Cells were washed once with PBS and once with PBST. Cellular infection was detected by anti-Flag M2 MAb (Invitrogen, California, USA) diluted in PBST for 1 h at room temperature. Cells were washed once with PBS and once with PBST then primary antibody binding was detected using Impress peroxidase conjugated anti-mouse Ig (Vector Laboratories, California, USA) for 1 h at room temperature and developed using 3-3'-diaminobenzidine tetrahydrochloride (DAB; Sigma, St Louis, USA) at the recommended concentration for 5 min at room temperature. Cells were washed once with PBS and once with PBST then stored in PBS for visualization. Wells were scored for positive staining and the TCID₅₀/ml determined using the Reed and Muench Calculator [371].

2.12.2 Core ELISA assay

Because many of the mutant HCVcc viruses produced were not entry competent it was not possible to normalise virus levels for infection assays using TCID₅₀. Therefore the concentrations of virus produced from transfected Huh-7.5

cells were determined by quantifying core protein levels using the ORTHO[®] HCV Antigen ELISA Test Kit (In Vitro Diagnostics, Tokyo, Japan) according to the manufacturer's instructions.

2.13 HCVcc Infection

Huh-7.5 cells were seeded at 30 000 cells/well in a 48 well plate format (Nunc, Roskilde, Denmark). Twenty-four h later virus stocks of wild-type pJC1FLAG2(p7-NS-GLUC2A) and mutant pJC1FLAG2(p7-NS-GLUC2A) were adjusted to 218 fmol core/L (the lowest concentration of core detected) and incubated with Huh-7.5 cell monolayers for 4 h at 37°C. Cells were washed once with PBS then 300 µl of DMF10NEA per well was added. Luciferase activity in the tissue culture supernatant (associated with virus release) was assayed 72 h later using the Renilla luciferase kit (Promega, Wisconsin, USA) and quantified on a Fluostar Optima fitted with luminescence optics (BMG Lab Technologies, Offenburg, Germany).

For HCVcc infectivity assays performed in the presence of sulfhydryl alkylating agent M135 (Toronto Research Chemicals Inc., Ontario, Canada), partially purified HCVcc was diluted to 1210 TCID₅₀/ml in TN-Ca²⁺ then alkylated with 0 to 1 mM M135, quenched and applied to cells as described for HCVpp. Luciferase activity in the tissue culture supernatant was assayed 72 h later using the Renilla luciferase kit (Promega, WI, USA) and quantified on a Fluostar Optima fitted with luminescence optics (BMG LABTECH, Offenburg, Germany). For assays where alkylation was performed after virus was bound to cells, partially purified HCVcc (1210 TCID₅₀/ml) was bound to Huh-7.5 cells at 4°C for 2 h. Unbound virus was washed off and 0 to 5 mM M135 in TN-Ca²⁺ was added to cell-bound virus for 50 min at 37°C. Cells were washed and fresh DMF10NEA added. Luciferase activity in the tissue culture supernatant was assayed 72 h later as described above.

For assays where DTT was added to alkylated HCVcc, cell free virus was alkylated as described above, prior to cellular binding. Virus was then applied

directly to Huh-7.5 cells for 2 h at 4°C. Unbound virus was washed off and DTT in TN-Ca²⁺ was added to cells for 1 h at 37°C. Luciferase activity in cell culture supernatants were measured 72 h later as described above.

2.14 Huh-7.5 Viability Assays

To determine toxicity effects of M135 and DTT reagents on Huh-7.5 cells, a trypan blue exclusion assay was employed. Cells were seeded at 30 000 cells/well in a 48 well plate format. Twenty-four h later cells were incubated with 0 to 5 mM M135 for 2 h at 37°C, washed once with TN-Ca²⁺ and fresh DMF10NEA added. Alternatively, cells were incubated with 0 to 10 mM DTT for 1 h at 37°C, followed by washing and addition of fresh DMF10NEA. Seventy-two h later cells were washed and removed from the plates by trypsin-versene, resuspended in DMF10NEA and stained with trypan blue. Cells were examined for trypan blue exclusion and the total number of viable cells/well was determined using a haemocytometer.

2.15 Bacterial Protein Expression

A single colony of *E. coli* strain BL21(DE3) transformed with pMBP-E1 was grown for 16 h in 15 ml of terrific broth (TB; 12 g tryptone, 24 g yeast extract, 4 ml glycerol, 17 mM KH₂PO₄, 72 mM K₂HPO₄ per litre) at 37°C with shaking, and used to inoculate 1.5 L of TB the following day. This culture was grown to an OD₆₀₀ of 1.8, and protein expression induced by addition of 0.2 mM isopropyl-β-D-thiogalactopyranoside (IPTG) for 5 h.

Bacterial cells were pelleted at 5 000 xg for 15 min then washed twice in ice-cold PBS. Bacterial pellets were snap frozen in liquid nitrogen and stored at -80°C overnight.

To harvest proteins from the soluble fraction, bacterial pellets were resuspended in S-buffer (0.1 M Tris, 0.3 M NaCl, 1 mM EDTA, 0.02% sodium

azide, pH 8) for MBP-tagged proteins, or His protein binding buffer (20 mM Na_3PO_4 , 500 mM NaCl, 5 mM imidazole, 0.02% sodium azide, pH 7.4) for His-tagged proteins, containing protease inhibitors phenylmethanesulfonylfluoride (PMSF; 1 mM) and A-proteinase inhibitor (5 $\mu\text{g}/\text{ml}$). Bacterial pellets were sonicated five times for 1 min on ice using a Branson Sonifier 250 (output control: 6; Duty cycle: 60%) then clarified for 1 h at 20 000 xg, 4°C.

2.15.1 Small scale purification of MBP tagged proteins

For small scale purifications of MBP tagged proteins, 1 ml of clarified supernatant from sonicated bacteria was added to 25 μl of amylose agarose slurry (New England Biolabs, Ipswich, USA) equilibrated in S-buffer. Samples were incubated with mixing for 1 h at room temperature. Beads were washed 3 times with S-buffer, then once with PBS to remove excess salt. Protein was eluted from beads by addition of sample buffer followed by boiling for 10 min then examined by Western blotting and/or Coomassie stained SDS-PAGE (see section 2.10.1).

2.15.2 Large scale purification of MBP-tagged proteins

MBP-fusion proteins were affinity purified over an amylose agarose column (New England Biolabs, Ipswich, USA) equilibrated in S-buffer as recommended by the manufacturer. Proteins were additionally purified by gel-filtration chromatography using a Superdex 75 (HiLoad 16/60) or Superdex 200 (HiLoad 26/60) column equilibrated in S-buffer followed by visualisation by SDS-PAGE and Western blotting and/or Coomassie staining (see section 2.10.1).

2.15.3 Large scale purification of His-tagged proteins

His-tagged proteins were affinity purified over a Profinity IMAC nickel agarose column (Bio-Rad, California, USA) equilibrated in His protein binding Buffer, as recommended by the manufacturer. Five hundred mM imidazole in His protein binding buffer was used for elution of His-tagged proteins from the resin. Proteins were additionally purified by gel-filtration chromatography using a

Superdex 75 (HiLoad 16/60) equilibrated in His protein binding buffer followed by visualisation by SDS-PAGE and Western blotting and/or Coomassie staining (see section 2.10.1).

2.16 Limited Proteolysis of MBP-E1₂₅₉

Resistance to cleavage by chymotrypsin provides an indication of secondary structure in a substrate protein. To determine the resistance of MBP-E1₂₅₉ to proteolysis, purified protein was incubated with increasing concentrations of chymotrypsin. Briefly, chymotrypsin was added to 7 µg of MBP-E1₂₅₉ in a total of 14 µl 100 mM ammonium bicarbonate pH 8 and incubated at 37°C for 10 min. The digest was stopped by addition of 10 mM PMSF. Samples were run on 10-16% tricine SDS-PAGE then stained with Coomassie as described in section 2.10.1. For samples subjected to mass spectrometry analysis, reactions were quenched with 0.1% trifluoroacetic acid instead of protease inhibitor.

2.17 Insulin Reduction Assay

To test the redox activity of recombinantly expressed E1, an insulin reduction assay was employed [372]. Briefly, a 10 mg/ml stock of insulin (Sigma, St Louis, USA) was prepared by dissolving insulin in 50 mM tris-HCl pH 7.5. The pH was adjusted to 3 with 1 M HCl to dissolve the insulin completely then rapidly titrated back to pH 7.5 with 1 M NaOH.

Protein samples were assayed at 4 µM and 8 µM concentrations. Protein was reduced by addition of 20 mM DTT to purified protein. The reaction was started by addition of 0.1 M sodium phosphate pH 7.4, 1 mM EDTA pH 8 and 1 mg/ml insulin. Reduction of insulin was detected by formation of a precipitate measured spectrophotometrically at 650 nm for 30 min.

Chapter 3 – Oxidation State of HCV Envelope Glycoproteins E1 and E2

3.1 Introduction

The structure and stability of a protein can be strongly influenced by the presence of cysteine (Cys) residues. A pair of Cys residues with a distance of $< 5 \text{ \AA}$ between the α -carbon atoms may be joined by a disulfide bond assuming angular limitations are met. Cys residues that do not meet the necessary constraints to disulfide bond with another Cys may be free in a reduced state. Disulfide bonds define conformational constraints of a protein while free Cys residues may provide a protein with redox activity directing disulfide reduction or isomerisation events in a target protein. The oxidation state of fusion proteins present on the surface of enveloped viruses can influence conformational changes associated with fusion activation [359,360,373,374,375,376]. For example, a free sulfhydryl group within the receptor binding envelope protein from retroviruses MLV and HTLV-1 has been shown to catalyse a disulfide reduction event within the glycoprotein complex that is essential for virus entry [359,360].

In heterologous expression systems HCV envelope glycoproteins E1 and E2 exist as both non-covalent and disulfide linked heterodimers. Conformation dependent, but non-neutralising antibody directed towards E2 (MAb H53) immunoprecipitates predominantly non-covalent forms of E1E2 heterodimers from retroviral pseudotype particles (Supplementary Figure 3-1A). However, when the same precipitations are performed with a neutralising MAb directed towards a linear epitope in E2 (MAb 24), high molecular weight disulfide linked forms of the glycoproteins are predominantly detected with little non-covalently associated E1 and E2 evident (Supplementary Figure 3-1B). From recombinant expression studies and studies performed using retroviral particles incorporating E1 and E2 (HCVpp), the non-covalent heterodimeric form of E1E2 has long been assumed to represent the functional species incorporated into virus particles [3,131,138,197,232,243]. Recently the first analysis of E1 and E2 from infectious

cell culture derived HCV was reported [137]. The group observed that intracellular forms of the glycoproteins largely assembled as non-covalently associated heterodimers. However, once incorporated into infectious particles, although some non-covalently linked E1 and E2 was evident, the majority of E1 and E2 appeared to form high molecular weight disulfide linked complexes. E1 and E2 contain 8 and 18 highly conserved Cys residues, respectively, therefore this would suggest that free sulfhydryl groups are likely to be maintained in the virion incorporated form of the glycoproteins.

Several groups have examined the oxidation state of recombinantly expressed, soluble E2 [273,283,377]. In each instance it was reported that this form of E2 is likely to be completely oxidised. Krey *et al.* (2010) expressed the entire ectodomain of E2 (E2e) and using trypsin digestion and mass spectrometry, mapped the disulfide bonding arrangement within a monomeric form of E2e [273]. The study reported that E2e is completely oxidised. The location of cysteines involved in 7 of 8 possible disulfide bonds in E2e was determined and although the final disulfide bond (Cys597 and Cys620) was not conclusively identified, it was assumed to form. This would appear to contradict the observation that full length glycoproteins are disulfide linked in mature virus particles. However, it should be noted that Krey *et al.* (2010) excluded higher molecular weight forms of E2e from their studies. There are no reports on the oxidation state of E1 or full length virion incorporated E2, nor is it clear whether non-covalently associated E1E2 or disulfide linked E1E2 represents the functional form of the glycoprotein complex. The aim of this chapter was to determine the oxidation state of full length heterodimeric E1 and E2 on infectious virus particles and to determine the significance of the glycoprotein oxidation state in virus entry.

3.2 Results

3.2.1 E1E2 contain free sulfhydryl groups that are essential for HCV entry

The significance of the redox state of E1 and E2 in virus entry was investigated in the context of full length, replication competent cell culture derived

virus which incorporates a luciferase reporter gene, JC1FLAG2(p7-NS-GLUC2) (HCVcc; genotype 2a) [362] as well as retroviral pseudotyped particles bearing E1E2 from the prototype strain H77c (HCVpp; genotype 1a) [3].

To examine whether the redox state of E1 and E2 is a determinant in virus entry, partially purified HCVcc and HCVpp were treated with increasing concentrations of the membrane impermeable sulfhydryl alkylating agent 4-(N-Maleimido)benzyl- α -trimethylammonium iodide (M135). The reactions were quenched by addition of DMF20NEA and alkylated virus particles were then applied to Huh-7.5 cells for 2 h at 37°C. Seventy-two h post infection the level of virus entry was quantified by measuring luciferase activity in the tissue culture supernatant (HCVcc) or cell lysate (HCVpp).

Reaction of HCVcc or HCVpp with M135 resulted in a dose dependent reduction in virus entry (Figure 3-1A and B, respectively). For HCVcc a significant decrease in entry was observed when treated with 0.2, 0.5 and 1 mM M135 ($p < 0.05$, Student's *t*-test) compared to untreated virus controls. Complete inhibition of HCVcc entry occurred at 0.5 and 1 mM M135. Similar results were obtained in the HCVpp system although virions appeared to be more resistant to M135 alkylation. Entry of HCVpp was significantly reduced when treated with 0.5, 1, 2 and 5 mM M135 ($p < 0.05$, Student's *t*-test). Entry was reduced by approximately 80% following treatment with 5 mM M135.

Vesicular stomatitis virus (VSV) is a member of the enveloped *Rhabdoviridae* family. VSV envelope protein G (VSVg) provides the fusion activity for the virus, undergoing extensive structural reorganisation to adopt a typical fusion-activated hairpin conformation upon exposure to low pH. VSVg contains 12 Cys residues engaged in 6 disulfide bonds which are evident in both the pre and post fusion structures of VSVg [353,354]. Consistent with the absence of free thiol groups, pseudotype particles bearing VSVg (VSVg pp) remained unaffected following incubation with up to 5 mM M135 (Figure 3-1B) indicating that inhibition of HCVpp and HCVcc is specific. The embedded Western blot probed with MAb

183 for HIV-1 structural protein p24 confirms that similar amounts of pseudotype particles were introduced into the HCVpp and VSVg pp reactions.

When HCVcc was titrated into the alkylation reaction (1 mM M135) it was found that high concentrations of virus overcame the inhibitory effect of M135 indicating that when M135 is saturated with excess virus the unalkylated virus in the reaction remains entry competent (Figure 3-1C). In this assay the HCVcc-M135 mix was added directly to Huh-7.5 cells without quenching. Importantly, this shows that M135 is specifically reacting with viral proteins and the inhibition effect is not due to alkylation of a cellular factor.

To confirm that the inhibitory effect of M135 on virus entry was not due to cellular toxicity, Huh-7.5 cells were incubated with increasing concentrations of M135 for 2 h at 37°C. Seventy-two h later cell viability was determined by trypan blue staining of the cells. It was found that incubation of Huh-7.5 cells with up to 5 mM M135 had no effect on cell survival (Figure 3-1D). This indicates that entry inhibition of HCVcc after incubation with up to 1 mM M135, and HCVpp with up to 5 mM M135 is due to specific modification of the virus rather than cellular toxicity.

CD81 is an essential attachment factor required for HCV infection into liver cells [5]. Direct binding between E2 and CD81 has been demonstrated by many groups [95,247,254,255,256,273]. To determine whether M135 alkylation of HCV glycoproteins has affected the ability of virus to engage the CD81 receptor, a direct CD81 binding assay was used. This assay employs recombinant dimeric CD81 consisting of the large extracellular loop (LEL) of CD81 (residues 113-201) N-terminally fused to maltose binding protein (MBP-LEL¹¹³⁻²⁰¹). This construct has been used extensively to characterise CD81-E2 interactions [95,245,246,247,259,378], demonstrates binding to virion incorporated E2 [247,286], and is thought to mimic the native form of CD81 by interacting with claudin-1 [91].

Due to the low titre of HCVcc produced, CD81 binding analyses were performed with HCVpp only. It was found that incubation of partially purified

HCVpp with up to 5 mM M135 had no effect on the ability of HCVpp-derived E2 to bind MBP-LEL¹¹³⁻²⁰¹ (Figure 3-1E). Addition of an equivalent concentration of particles to the binding assay was confirmed by Western blot analysis using MAb directed towards E1, E2 and HIV-1 structural protein p24 (A4, H52 and 183 respectively; Figure 3-1F). This indicates that abrogation of HCV entry following incubation with M135 is not likely to be due to an inability of alkylated virus to bind CD81. Furthermore, M135 alkylation of E2 does not appear to significantly alter the structure of E2 with respect to the formation of the CD81 binding region.

Together, these results demonstrate that free sulfhydryl groups are present on the envelope glycoproteins of both HCVcc and HCVpp infectious virions, and these free sulfhydryl groups are essential for virus entry.

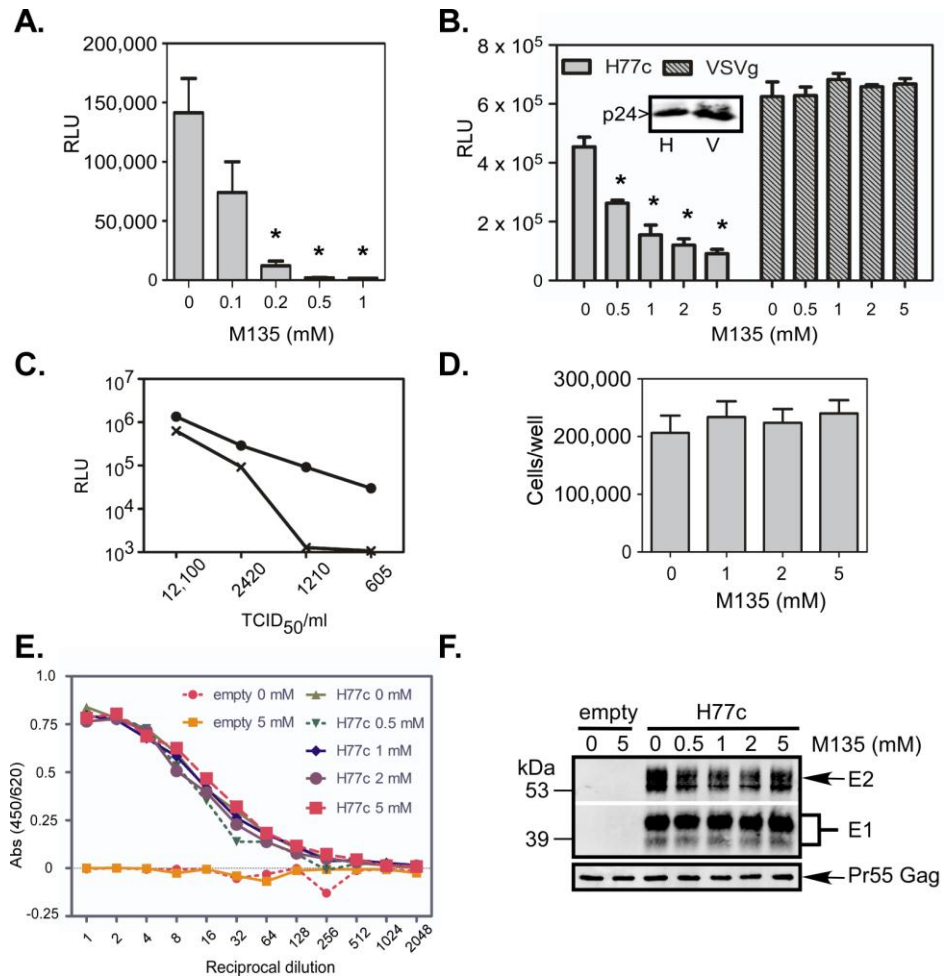


Figure 3-1. HCV entry is dependent on the presence of free sulfhydryl groups. A and B. Partially purified HCVcc (A) HCVpp and VSVg pp (B) were alkylated with M135. Reactions were quenched then virus was added to Huh-7.5 cells. Luciferase activity (RLU) was measured 72 h later. Data are the mean and standard error of 4 (A) or 3 (B) independent experiments each consisting of six (A) or four (B) replicates. Asterisks indicate significantly different entry activity relative to untreated virus ($p < 0.05$, Student's t -test). Similar levels of HCVpp (H) and VSVg pp (V) input virus was confirmed by Western blot analysis using MAb 183 directed towards HIV-1 capsid protein p24 (B, inset). C. Increasing concentrations of HCVcc were incubated with 0 (●) or 1 mM M135 (×) and directly added to cells. Luciferase activity (RLU) in the culture supernatant was measured 72 h later. Data shown are a representative assay with each point the average of quadruplet wells. D. Huh-7.5 cells were incubated with increasing concentrations of M135 for 2 h at 37°C. Cell viability was determined 72 h later by trypan blue staining. E. The ability of E1E2 incorporated into HCVpp (H77c) to bind CD81 following M135 alkylation was determined by a direct binding immunoassay using recombinant CD81 MBP-LEL¹¹³⁻²⁰¹ (representative assay). F. Equivalent input of E1, E2 and HIV-1 structural protein pr55 Gag were determined by Western blot for each sample applied to the binding assay (probed with MAbs A4, H52 and 183 respectively).

3.2.2 Free sulfhydryl groups are present on HCVpp incorporated forms of E1 and E2

The low virus titre produced by the HCVcc system prevents extensive biochemical analyses of glycoproteins derived from replication competent virus. Therefore, experiments to visualise free sulfhydryl groups on E1 and E2 were performed in the context HCVpp. The HCV glycoproteins present on retroviral particles have been extensively characterised, and both HCVpp and HCVcc are known to utilise the same cellular receptors in virus entry and mediate entry in a pH dependent manner [3,10,243,295,303]. Furthermore, free sulfhydryl groups were deemed to be essential for both HCVcc and HCVpp entry in the previous section.

HCVpp were partially purified through a 25% sucrose cushion then labelled with membrane impermeable sulfhydryl biotinylating agent, EZ-Link Maleimide-PEG2-Biotin (maleimide-biotin). As a control, HCVpp were also labelled with the amine biotinylating agent Sulfo-NHS-LC-Biotin (NHS-biotin). Partially purified HCVpp were lysed followed by reduction with 100 mM dithiothreitol (DTT) to separate heterodimeric forms of E1E2. Biotinylated proteins were isolated by high capacity streptavidin agarose resin and analysed under reducing conditions on SDS-PAGE.

Streptavidin-precipitated biotinylated forms of both E1 and E2 were detected in separate Western blots using monoclonal antibodies directed towards E1 (MAb A4), and E2 (MAb H52) [131,197] (Figure 3-2A). To confirm equal input of particles expressing equivalent amounts of E1 and E2 in each reaction, Western blot analysis of HCVpp lysate prior to streptavidin agarose precipitation was performed using monoclonal antibodies directed towards HIV-1 structural protein p24 (MAb 183), E1 (MAb A4) and E2 (MAb H52) (Figure 3-2A, lower panel).

The results demonstrate that free sulfhydryl groups can be detected in both E1 and E2 in mature HCVpp. To verify that maleimide-biotin was reacting specifically with sulfhydryl groups, HCVpp were pre-incubated with M135 prior to

biotinylation. It was found that incubation with M135 inhibited labelling of E1 and E2 with maleimide-biotin, while NHS-labelling of E1 and E2 remained unaffected (Figure 3-2A). Quantitation of biotinylated glycoproteins by densitometry showed that pre-incubation of particles with increasing concentrations of M135 reduced maleimide-biotin labelling of E2 (Figure 3-2B, crosses) and E1 (Figure 3-2C, crosses) by 86% and 83%, respectively, when compared to E2 and E1 labelled in the absence of M135. Pre-incubation of virions with M135 did not decrease the amount of glycoprotein E2 labelled with amine reactive NHS-biotin (Figure 3-2B, circles). For E1, a 19% decrease in the amount of E1 labelled with NHS-biotin was observed for HCVpp pre-incubated with 500 nM M135. However, this change is not likely to be significant as there was no dose dependent effect (Figure 3-2C, circles). These data indicate that biotinylation events occur specifically at the respective reactive groups in substrate proteins and demonstrate that both E1 and E2 contain free sulfhydryl groups when incorporated into mature HCVpp.

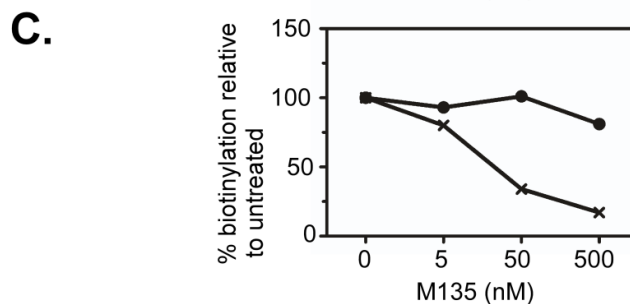
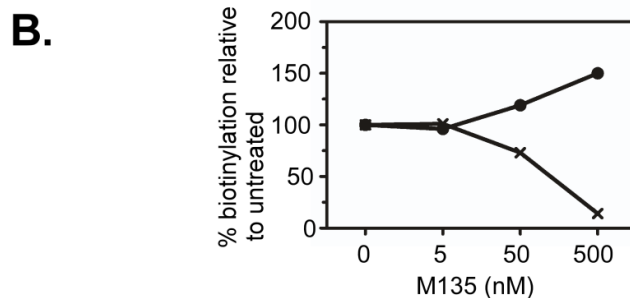
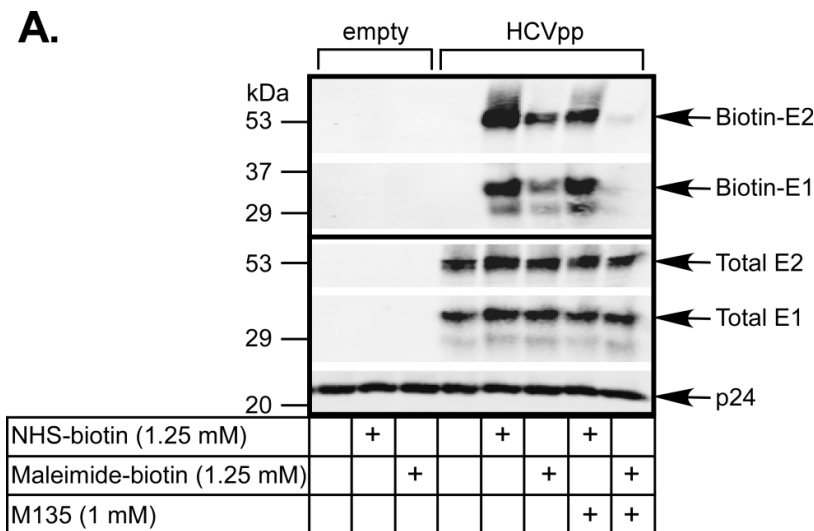


Figure 3-2. Free sulfhydryl groups are present on both E1 and E2 in mature virus particles. A. Partially purified HCVpp or no envelope control particles (empty) were labelled with maleimide-biotin or NHS-biotin. Particles were lysed and reduced by addition of DTT prior to capture of biotinylated proteins by streptavidin agarose. For M135 treated samples, partially purified HCVpp were incubated with 1 mM M135 followed by labelling with maleimide-biotin or NHS-biotin. Samples were run on reducing SDS-PAGE and examined in Western blotting with anti-E2 and anti-E1 MAbs H52 and A4, respectively. Blots were imaged using an Odyssey Infrared Imaging System at 680 nm (LI-COR). Molecular weight markers are shown to the left. Equivalent input of E1, E2 and HIV-1 capsid protein p24 were determined by Western blot (probed with MAbs A4, H52 and 183, respectively) for each sample prior to streptavidin agarose pull-down. B and C. Quantification of Western blot analyses of E2 (B) and E1 (C) labelled by maleimide-biotin (×) or NHS-biotin (●) following incubation with 5-500 nM M135 (representative assay).

3.2.3 E1 and E2 are not linked via a labile disulfide bond

Both HCVpp and HCVcc comprise high molecular weight disulfide linked forms of E1E2 (represented by E1/E2) in addition to non-covalently associated forms of E1E2 (see Supplementary Figure 3-1A and B) [3,131,137,243]. It is not clear which oligomer represents the functional form. In addition, it has been reported that extraction of viral proteins by detergent lysis can disrupt labile disulfide bonds if free thiol groups are not first stabilised by alkylation [360].

To examine whether E1 and E2 are linked via a labile disulfide bond, HCVpp were produced in HEK 293T cells. Thirty h post-transfection cells were labeled with ³⁵S-Met/Cys in methionine and cysteine-deficient DMF10 for 16 h. Radiolabelled HCVpp were pelleted by centrifugation then incubated in PBS containing sulfhydryl alkylating agent *N*-Ethylmaleimide (NEM; 5 mM) prior to lysis (also in the presence of 5 mM NEM). Particle lysates were immunoprecipitated with a neutralising MAb directed towards a linear epitope in E2 (MAb 24) then run on reducing or non-reducing SDS-PAGE and phosphorimaged.

Extraction of glycoproteins from HCVpp in the presence or absence of NEM did not appear to alter the amount of monomeric or high molecular weight forms of E1 and E2 precipitated by MAb 24 as would be expected if they were linked through a labile disulfide bond (Figure 3-3). This suggests that the mixture of covalent and non-covalent forms of E1 and E2 detected in HCVpp is real and not an artefact arising from disulfide reduction during lysis. Therefore, it is not likely that mature, virion incorporated forms of E1 and E2 are linked via a labile disulfide bond.

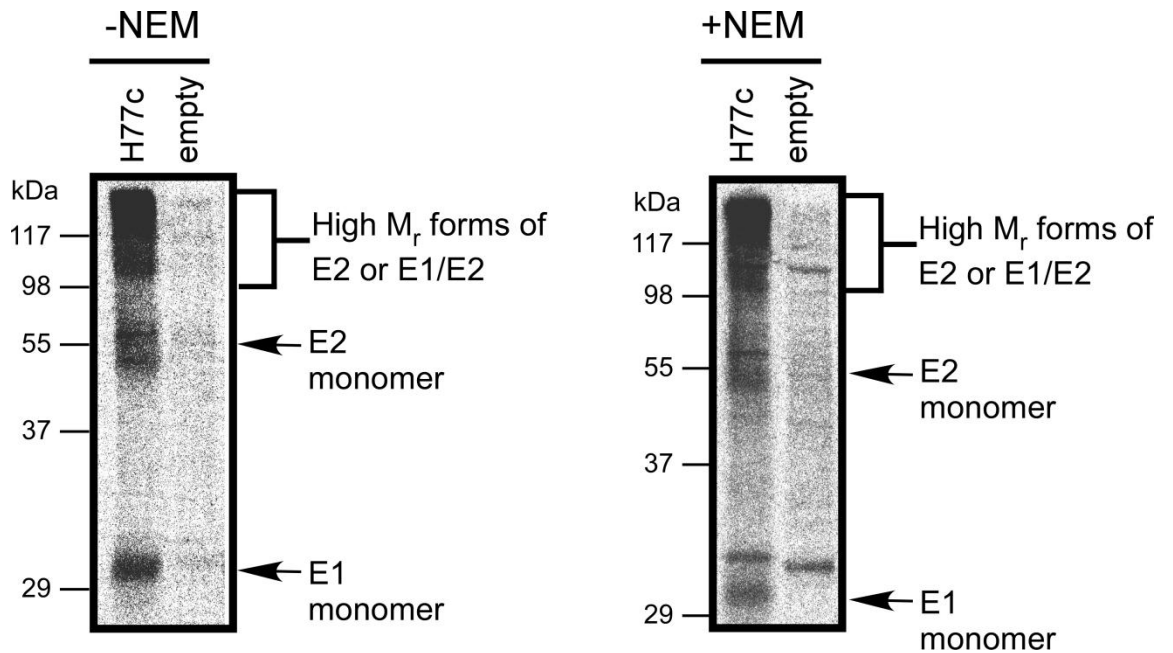


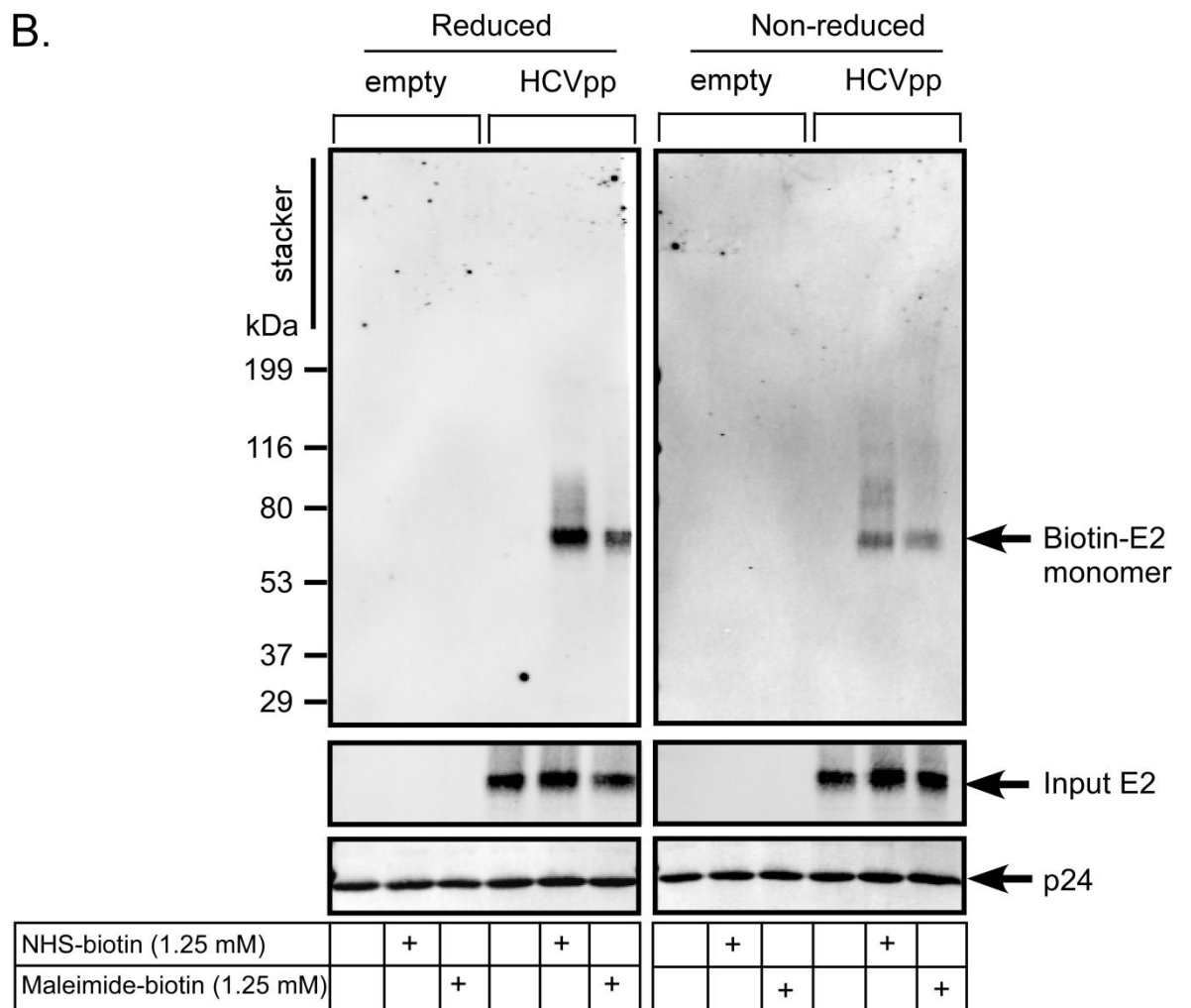
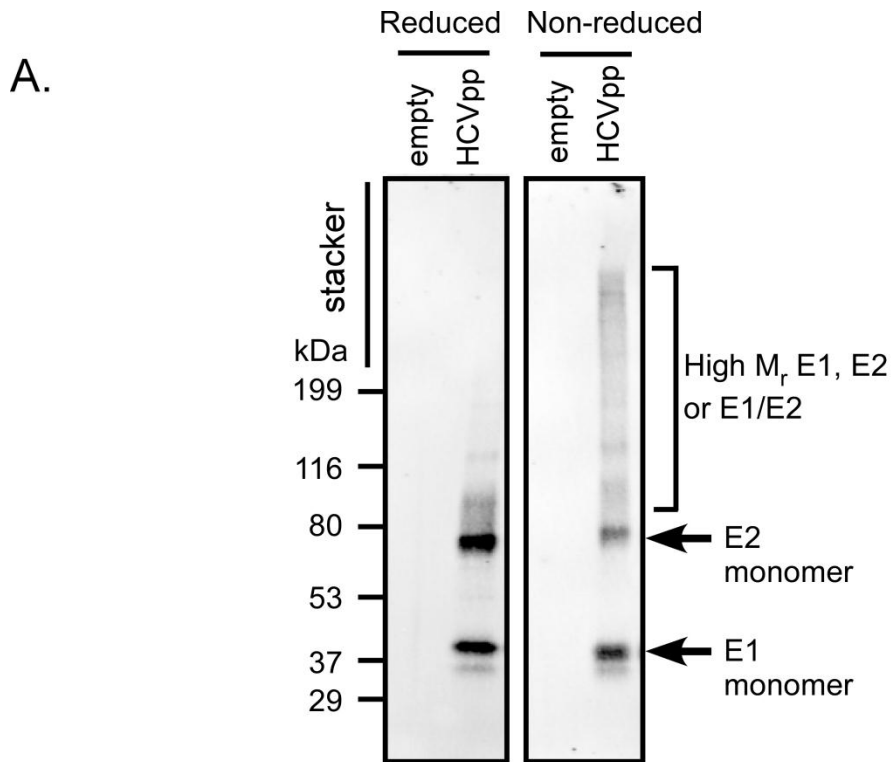
Figure 3-3. E1 and E2 are not linked via a labile disulfide bond. HCVpp produced in HEK 293T cells were metabolically labelled with ^{35}S -Met/Cys. HCVpp were pelleted by centrifugation then lysed in the presence or absence of NEM. Immunoprecipitations were performed using a neutralising MAb directed towards a linear epitope in E2 (MAb 24). Samples were run on non-reducing SDS-PAGE and phosphorimaged. Molecular markers are shown to the left of the gels.

3.2.4 Non-covalent E1 and E2 contain free sulfhydryl groups in mature HCVpp

The study of Krey *et al.* (2010) reported that monomeric soluble E2 lacking its transmembrane domain, and not associated with E1, has nine disulfide bonds and suggests that no free sulfhydryl groups are available. We therefore investigated which heterodimeric form of E1E2 contains free sulfhydryl groups. HCVpp were labelled with NHS-biotin or maleimide-biotin then subjected to streptavidin agarose pull down in the presence (reduced) or absence (non-reduced) of DTT. Reduced samples were run on SDS-PAGE under reducing conditions while non-reduced samples were run under non-reducing conditions, followed by Western blot analysis with H52 and A4. Equivalent input of E1, E2 and p24 was determined as described in section 3.2.2 (run under reducing conditions).

When run under non-reducing conditions, non-biotinylated E1 and E2 from HCVpp appear mostly in a non-covalent form. However, a smear of high molecular weight forms of the glycoproteins is evident (Figure 3-4A). This laddering is lost when the samples are run under reducing conditions.

Maleimide-biotin reacted with free sulfhydryl groups present in both virion incorporated disulfide-linked forms (reduced) and non disulfide linked forms (non-reduced) of E2 and E1 (Figure 3-4B and C, respectively). It is important to note that since heterodimerisation is maintained between E1 and E2 when subjected to streptavidin agarose pull down in the absence of DTT, it is not possible to determine which glycoprotein (E1 or E2, or both E1 and E2) has reacted with biotin as one will coprecipitate the other. Although it remains unclear which heterodimeric form is the functional form, these results indicate that there is at least one free sulfhydryl group maintained on non-covalent E1E2 heterodimers and at least one free sulfhydryl group on both E1 and E2 in high molecular weight forms of the glycoproteins.



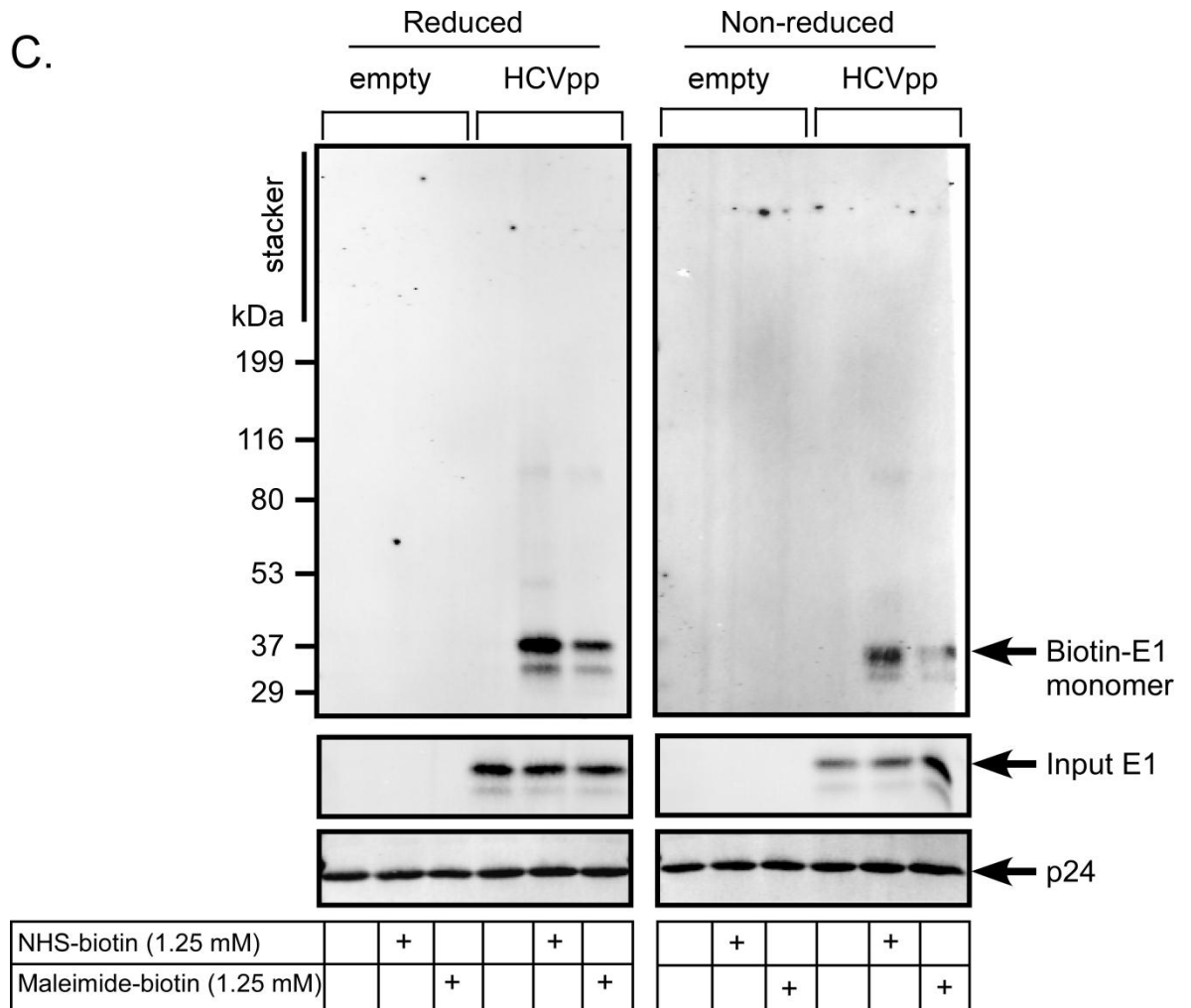


Figure 3-4. Non-covalent and multimeric oligomers of HCVpp incorporated E1 and E2 contain free sulfhydryl groups. A. Lysed HCVpp or no envelope control particles (empty) were run under reducing or non-reducing conditions and Western blotted with monoclonal antibodies towards E1 and E2 (A4 and H52, respectively). B and C. Partially purified HCVpp were labelled with maleimide-biotin or NHS-biotin and subjected to streptavidin precipitation in the presence (reduced) or absence (non-reduced) of DTT. Biotinylated proteins were run under reducing or non-reducing conditions and probed for E2 using MAb H52 (B) or E1 with MAb A4 (C). Equivalent input of E1, E2 and HIV-1 capsid protein p24 were determined by Western blot (probed with MAbs A4, H52 and 183 respectively) for each sample prior to streptavidin agarose pull-down. Blots were imaged by LI-COR. Molecular weight markers are shown to the left.

3.2.5 HCVpp but not HCVcc remains sensitive to M135 labelling following attachment to cells

To examine whether a change in oxidation state occurs in the HCV envelope glycoproteins after cellular attachment, partially purified HCVcc or HCVpp were bound to Huh-7.5 cells at 4°C for 2 h to allow virus binding to cells but not internalisation. M135 was then added and the temperature raised to 37°C to allow entry events to proceed.

Addition of M135 to cell bound HCVcc had no effect on virus entry indicating an absence of free cysteine residues available for alkylation (Figure 3-5A). In contrast, entry of cell-bound HCVpp was significantly reduced when treated with 2 or 5 mM M135, with a 61% reduction in entry observed for virus treated with 5 mM M135 compared to untreated virus ($p < 0.05$, Student's *t*-test) (Figure 3-5B). Entry of cell-bound VSVg pp remained unaffected by treatment with M135 indicating that inhibition of HCVpp entry is specific. The embedded Western blot probed with MAb 183 directed towards HIV-1 structural protein p24 demonstrates that similar amount of particles were introduced into the HCVpp and VSVg pp reactions.

HCVcc sulfhydryl alkylation experiments indicate that prior to cellular attachment surface glycoproteins on mature virus particles contain at least one free cysteine residue essential for entry. However, after receptor attachment reduced cysteine residues are no longer available for alkylation. Such a result is consistent with a change in oxidation state of the glycoproteins from a reduced state to an oxidised state. Given that HCVpp entry is reduced by 61% when M135 is added following cellular attachment, this would suggest that the envelope glycoproteins still contain available free sulfhydryl groups that are required for entry. Furthermore, this finding indicates that 5 mM M135 is sufficient to induce a specific effect on virus bound to cells. It is possible that HCVpp surface glycoproteins may undergo a change in oxidation state following events that occur at 37°C, compared to glycoproteins expressed on HCVcc that appear to become oxidised at 4°C.

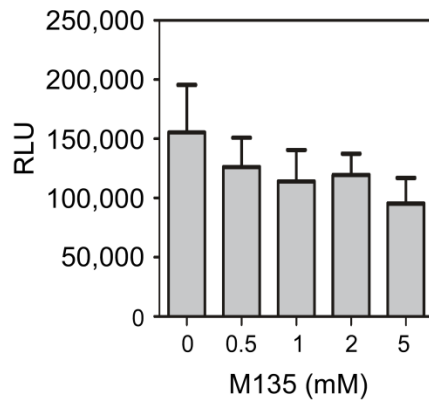
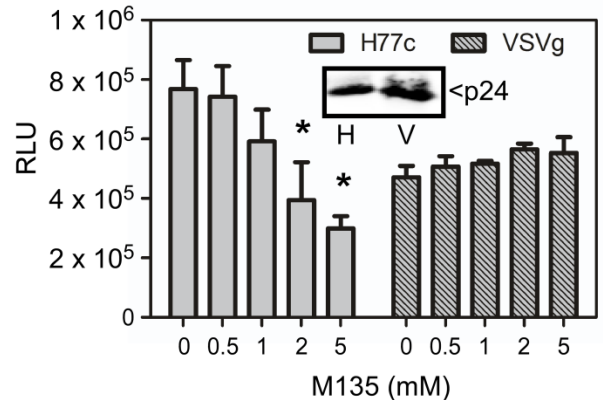
A.**B.**

Figure 3-5. HCVpp but not HCVcc remains sensitive to M135 labelling following attachment to cells. HCVcc (A), HCVpp or VSVg pp (B) were bound to Huh-7.5 cells for 2 h at 4°C prior to addition of M135 for 50 min at 37°C. Luciferase activity (RLU) was determined 72 h later. Data are the mean and standard error of 4 (A) or 3 (B) independent experiments each consisting of six (A) or four (B) replicates. (B) Asterisks indicate significantly different entry activity relative to untreated virus ($p < 0.05$, Student's *t*-test). Equivalent input of HCVpp and VSVg pp was confirmed by Western blot using MAb 183 directed towards HIV-1 capsid protein p24.

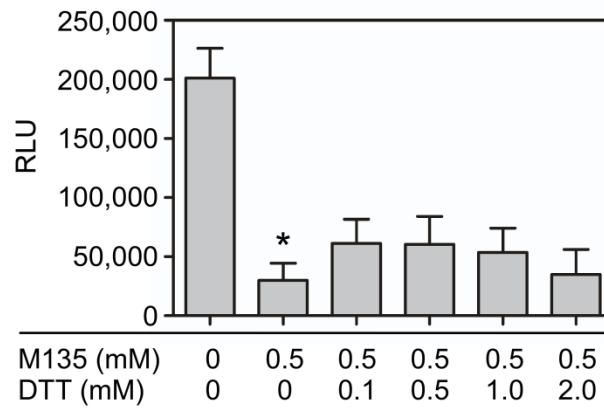
3.2.6 DTT does not rescue entry of alkylated virus

The finding that free thiol groups are available for alkylation on HCVcc prior to, but not following cellular attachment, indicates the glycoproteins may undergo a change in redox state following receptor engagement. If free thiol groups in E1 and/or E2 are acting as redox regulators catalysing isomerisation of disulfide bonds within the glycoproteins during HCV entry it is likely that alkylation of these residues by M135 induces an entry incompetent, isomerisation arrested state. It was therefore tested whether the infectivity of M135-treated virus could be restored after attachment to cells by replacing the reducing activity of the alkylated thiols with exogenous reducing agent. Alkylated HCVcc was added to Huh-7.5 cells at 4°C for 2 h. Excess virus was washed off and DTT was added to the cells at increasing concentrations for 1 h at 37°C. Luciferase activity in the cell culture supernatant was determined 72 h post infection. It was found that addition of DTT did not significantly restore entry of alkylated HCVcc (Figure 3-6A).

To ensure that DTT did not have a toxic effect on Huh-7.5 cells, cells were incubated with increasing concentrations of DTT for 1 h at 37°C. Seventy-two hours later cell viability was determined by trypan blue staining. It was found that there was no significant difference in cell viability following incubation with 2 mM DTT compared to the untreated control (Figure 3-6B, $p=0.10$, Student's *t*-test). However, cell viability following incubation with 10 mM DTT was calculated to be 43% compared to untreated cells indicating that this concentration of DTT is toxic.

This finding suggests that exogenous reducing agents cannot rescue the isomerisation-arrested state of E1 and/or E2 induced by M135 alkylation of HCVcc. Such a result is consistent with an isomerisation event occurring within the glycoproteins whereby M135-alkylated sulfhydryl groups are required to participate in new disulfide bonds at fusion activation.

A.



B.

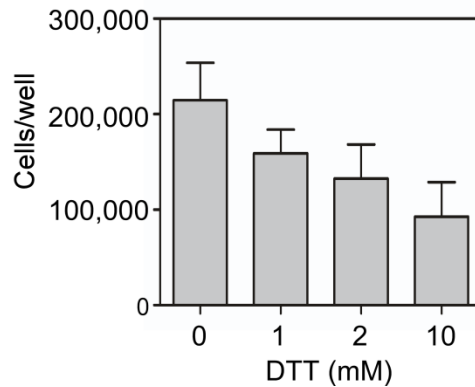


Figure 3-6. DTT treatment of alkylated HCVcc does not rescue HCVcc entry. A. M135 alkylated HCVcc were bound to cells for 2 h at 4°C, followed by incubation with DTT at 37°C. Luciferase activity (RLU) in the tissue culture supernatant was assayed 72 h later. Data shown are the mean and standard error of 4 independent experiments each performed with 6 replicates. Asterisks indicate significantly different entry activity to untreated HCVcc ($p < 0.05$, Student's *t*-test). B. Huh-7.5 cells were incubated with increasing concentrations of DTT for 1 h at 37°C. Cell viability was determined 72 h later by trypan blue staining. Data are the mean and standard error of 3 independent experiments each performed with 4 replicates.

3.2.7 Characterisation of free sulfhydryls in E1 and E2 post CD81 binding

HCVcc glycoproteins appear to transition from a reduced to oxidised state immediately following cellular binding, therefore receptor engagement is likely to trigger these events. CD81 represents a possible candidate as it is known to be involved in an early stage of entry and has been shown by several groups to directly interact with E2 [5,247,254,255,256]. Recombinantly expressed dimeric CD81 (MBP-LEL¹¹³⁻²⁰¹) was shown to specifically bind HCVpp-derived E2 in a direct binding assay in Figure 3-1E.

To investigate the effect of receptor binding on the oxidation state of E1 and E2, HCVpp were incubated with MBP-LEL¹¹³⁻²⁰¹ or the mutant MBP-LEL¹¹³⁻²⁰¹F186S that shows reduced binding to E2 [245], prior to labelling with maleimide- or NHS-biotin.

It was found that pre-incubation of HCVpp with MBP-LEL¹¹³⁻²⁰¹ did not significantly alter the amount of E1 or E2 labelled with either maleimide- or NHS-biotin (Figure 3-7 and Table 3-1). To confirm equal input of particles expressing equivalent amounts of E1 and E2 in each reaction, Western blot analysis of HCVpp lysate prior to streptavidin agarose precipitation was performed using monoclonal antibodies directed towards HIV-1 pr55 Gag (MAb 183), E1 (MAb A4) and E2 (MAb H52) (Figure 3-7, lower panel).

This result suggests that either there is no net change in the number of free sulfhydryl groups in E1 or E2 after CD81 binding, or that CD81 binding is not sufficient to induce a change in the oxidation state of the HCV glycoproteins and that other HCV entry receptors are required to trigger this event.

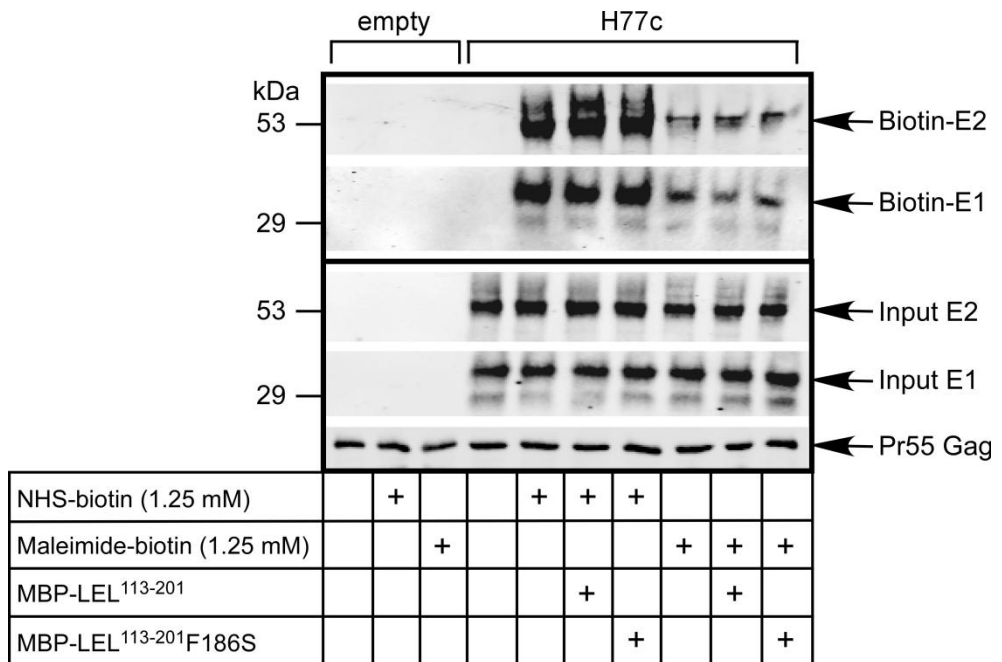


Figure 3-7. E1 and E2 contain free sulfhydryl groups post CD81 binding. HCVpp were incubated with dimeric MBP-LEL¹¹³⁻²⁰¹ or mutant MBP-LEL¹¹³⁻²⁰¹F186S prior to purification and labelling with maleimide- or NHS-biotin. Particles were lysed and reduced by addition of DTT prior to streptavidin capture of biotinylated proteins. Samples were run on reducing SDS-PAGE and Western blotted with anti-E2 and anti-E1 MAbs (H52 and A4, respectively). Blots were imaged by LI-COR. Molecular weight markers are shown to the left. Equivalent input of E1, E2 and HIV-1 Gag was determined by Western blot (probed with MAbs A4, H52 and 183 respectively) for each sample prior to streptavidin agarose pull-down.

Table 3-1. Quantification of free sulfhydryl groups in E1 and E2 post CD81 binding.

Ratio of Maleimide-biotin and NHS-biotin labelling was calculated for E1 and E2 \pm CD81 MBP-LEL¹¹³⁻²⁰¹ or CD81 MBP-LEL¹¹³⁻²⁰¹F186S by densitometry from 3 independent experiments (mean \pm standard error).

	E2 biotinylation (– CD81:+ CD81)	E1 biotinylation (– CD81:+ CD81)
NHS-biotin	1	1
NHS-biotin + MBP-LEL ¹¹³⁻²⁰¹	0.69 \pm 0.05	0.91 \pm 0.11
NHS-biotin + MBP-LEL ¹¹³⁻²⁰¹ F186S	1.22 \pm 0.40	1.21 \pm 0.15
Maleimide-biotin	1	1
Maleimide-biotin + MBP-LEL ¹¹³⁻²⁰¹	0.96 \pm 0.04	1.08 \pm 0.32
Maleimide-biotin + MBP-LEL ¹¹³⁻²⁰¹ F186S	1.37 \pm 0.36	1.39 \pm 0.37

3.2.8 Characterisation of free sulfhydryls in E1 and E2 post heparin binding

It has been proposed that CD81 is involved in an early, but post-attachment stage of HCV entry as antibody directed towards CD81 can block infection when added 18 to 50 mins following cellular binding of the virus at 4°C [7,8,300]. It is possible that an earlier attachment factor triggers the apparent oxidation changes in E1 and/or E2.

Several factors have been described that promote HCV-cellular attachment. Here, the effect of heparan sulfate on HCV glycoprotein oxidation was examined. Addition of soluble heparin (a homolog of highly sulfated heparan sulfate) or highly sulfated heparan sulphate itself to virus at the time of infection has been shown by multiple groups to inhibit HCVcc and HCVpp entry [7,84,299,300].

To determine whether heparin binding induces a change in HCV glycoprotein oxidation, HCVpp were incubated with heparin sodium salt prior to purification and labelling with maleimide- or NHS-biotin.

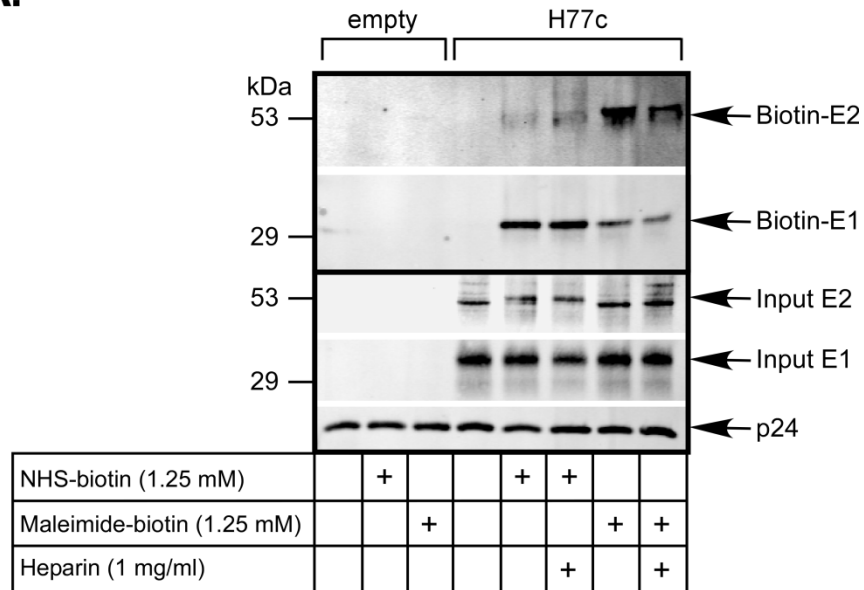
It was found that there was no clear difference in the amount of E1 and E2 detected by maleimide- and NHS-biotin following pre-incubation of HCVpp with heparin (Figure 3-8A). Equal input of particles into each reaction was confirmed by Western blot analysis of a fraction of each HCVpp lysate prior to streptavidin precipitation as described above (Figure 3-8A, lower panel).

To confirm that this form of heparin is capable of binding HCVpp, an infection assay was performed with HCVpp pre-incubated with heparin. HCVpp produced in HEK 293T cells were incubated with heparin sodium salt for 1 h at room temperature. The HCVpp-heparin mix was then added directly to Huh-7.5 cells for 4 h at 37°C. Luciferase activity in the cell lysate was determined 72 h post infection.

It was found that incubation of HCVpp with heparin sodium salt reduced HCVpp entry in a dose dependent manner. When HCVpp were incubated with 1 mg/ml of heparin, entry was reduced by 88% compared to untreated control particles (Figure 3-8B). This finding demonstrates that this form of heparin is able to bind HCVpp and prevent virus entry into Huh-7.5 cells.

Together, these results suggest that heparin binding to HCVpp, in this context, is not sufficient to induce a change in the oxidation state of the HCV glycoproteins.

A.



B.

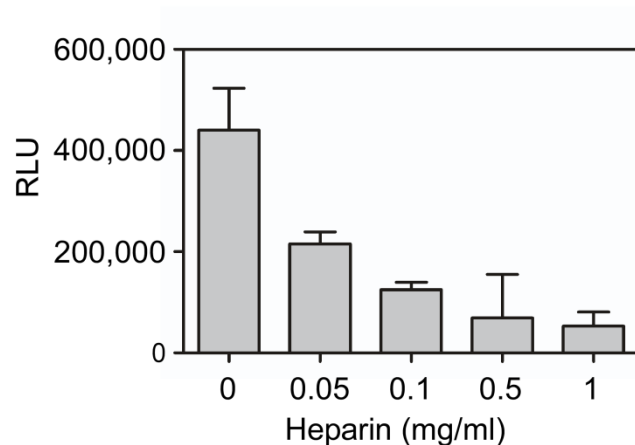


Figure 3-8. E1 and E2 contain free sulfhydryl groups post heparin binding. A. HCVpp were incubated with heparin then partially purified and labelled with maleimide- or NHS-biotin. Particles were lysed and reduced by addition of DTT prior to streptavidin capture of biotinylated proteins. Samples were run on reducing SDS-PAGE and Western blotted with anti-E2 and anti-E1 MAbs (H52 and A4, respectively). Molecular weight markers are shown to the left. Equivalent input of E1, E2 and HIV-1 capsid p24 was determined by Western blot (probed with MAbs A4, H52 and 183 respectively) for each sample prior to streptavidin agarose pull-down. Blots were imaged by LI-COR B. HCVpp were incubated with heparin sodium salt then directly applied to Huh-7.5 cells. Infection was determined by luciferase activity (RLU) in the cell lysate 72 h later. Data are the mean and standard deviation of 4 replicate wells (representative assay).

3.3 Discussion and Conclusions

This project examined for the first time, the oxidation state of full length heterodimeric, virion incorporated E1 and E2. The results demonstrate that virion incorporated forms of both E1 and E2 maintain at least one free sulfhydryl group each. In addition, chemical blockade of these free sulfhydryl groups abrogates virus entry in a dose dependent manner indicating that these free sulfhydryls play an essential role in virus entry.

Previous investigations into the redox state of the HCV glycoproteins have been carried out using recombinantly expressed, soluble forms of E2 (E2e) lacking the E2 TMD and E1 [273,377]. Krey *et al.* (2010) reported that monomeric E2e is completely oxidised [273]. There have been reports that E1 and E2 may influence the folding of each other [231,232,234], therefore the group expressed E2e as a polyprotein in fusion with full length E1 in an attempt to ensure the correct folding of E2e. However, in the absence of the E2 TMD (membrane anchor, ER retention signal and major E1E2 heterodimerisation determinant) it is likely that E2e would be rapidly trafficked from the ER and targeted for secretion. In this case native E1E2 associations are unlikely to be retained thereby preventing any influence of E1 on the folding of E2 outside the ER.

In another study, Fenouillet *et al.* (2008) also expressed a recombinant form of E2e then used a sulfhydryl biotinylating agent, 3-(N-maleimidylpropionyl) biocytin to quantitate the number of free sulfhydryl groups. The group concluded that E2e contained <0.5 free sulfhydryl groups per E2e molecule and that all 18 Cys residues were engaged in 9 disulfide bonds. Alternatively, this finding may suggest a mixture of reduced and oxidised forms of E2e were present and the results reflect an average oxidation state.

Here, full length E1 and E2 were coexpressed and native forms of the intact heterodimeric glycoproteins as found in infectious viral particles were examined. Free sulfhydryls were identified in E1 and E2 and were found to play an essential role in virus entry, indicating that free sulfhydryl groups are maintained on a

functionally relevant form of the glycoproteins. This appears to be a conserved feature of HCV as entry of both genotype 2a (HCVcc) and genotype 1a (HCVpp) viruses were inhibited when free sulfhydryl groups were blocked. It is possible that non-covalent E2e represents an alternative conformational state of E2 such as a fusion intermediate or an endpoint of the fusion reaction.

The investigation by Fenouillet *et al.* (2008) reported that HCVpp and HCVcc infectivity is not affected by sulfhydryl alkylating agents [377]. However, the group did not describe depletion of sulfhydryl containing contaminants prior to labelling, which was found to be essential in this study in order to achieve specific labelling of E1E2 thiol groups. In addition, it was shown here that increasing the ratio of HCVcc:M135 above 1210 TCID₅₀/ml reduced the effectiveness of M135, presumably by saturating the sulfhydryl reactive agent. M135 at 1 mM was sufficient to inhibit HCVcc entry only when virus titres below 1210 TCID₅₀/ml were used. It is possible that the amount of virus used in the study by Fenouillet *et al.* (2008) was saturating and did not allow the effect of alkylating agents to be detected. As the virus concentration was not stated it is not possible to determine if this was the case.

Understanding the higher order arrangements of E1 and E2 on the surface of HCV particles is essential for determining how the glycoproteins function during virus entry. A cell culture system for growing replication competent HCV has been made available only recently, therefore many studies on full length E1 and E2 have been carried out in the context of HCVpp. In HCVpp, the majority of glycoprotein incorporated into HCVpp is non-covalent E1E2 heterodimer with high molecular weight forms also evident. However, the apparent predominant oligomeric form of E1E2 detected in a protein preparation derived from HCVpp is highly dependent on the MAb used in detection (Supplementary Figure 3-1A and B). A recent publication demonstrated Western blot analysis of E1E2 from cell culture derived virus for the first time and reported that cell free HCVcc contains only a small amount of non-covalent heterodimer with the majority forming a smear of high molecular weight disulfide linked oligomers [137]. These high molecular weight forms could be immunoprecipitated by conformation sensitive

monoclonal antibodies and were shown to selectively bind human CD81, indicating that they represent functional forms of the glycoproteins. However, it is important to note that these studies were performed under standard SDS-PAGE conditions. Although the group stated that the same oligomeric forms were observed even when samples were heated to just 37°C prior to SDS-PAGE, further studies are required to confirm these results by native PAGE. This would allow analyses of protein oligomerisation without boiling and in the absence of denaturing agents within the gel such as sodium dodecyl sulfate (SDS) which may influence disulfide bonding arrangements. Labelling of free sulfhydryl groups prior to glycoprotein extraction is also essential to ensure disulfide bond isomerisation events do not occur during sample preparation. Furthermore, to ensure antibody bias is not occurring in Western blot and/or immunoprecipitation reactions characterisation of the oligomeric state of E1E2 in HCVcc should be performed using other neutralising monoclonal and polyclonal antibodies. In this study attempts to visualise biotinylated forms of HCVcc-derived E1 and E2 by Western blot failed as it was not possible to isolate HCVcc at a sufficient concentration.

While it remains unclear which oligomer represents the functional form in infectious virus, it was found here that free sulfhydryl groups are functionally relevant and can be detected on E1E2 in both non-covalent and high molecular weight forms of the glycoproteins in HCVpp. Given that both glycoproteins contain an even number of conserved cysteine residues there are several scenarios that could result in reduced cysteines being maintained. Firstly, E1 and E2 could be disulfide linked to each other, leaving one free sulfhydryl group present on each glycoprotein. Secondly, E1 and E2 may form disulfide linked homodimers, again resulting in one free sulfhydryl group being maintained. This would further require associations between E1 and E2 homodimers given that E1 and E2 can be co-precipitated. A third possibility is that non-covalent E1E2 heterodimers comprise the functional form with each glycoprotein containing 2 free cysteine residues. Identification of the functional oligomer is required in order to determine which of these situations occurs on the surface of the virus. The possibility that a combination of covalent and non-covalently linked forms of E1 and E2 are required to comprise a functional virus should not be excluded.

Free sulfhydryl groups are significant not only because they influence the structure of a protein, but also because in redox active proteins such as thioredoxin, reduced cysteines demonstrate catalytic activity capable of reducing existing disulfide bonds [379]. As discussed in Chapter 1, receptor binding envelope protein SU from retroviruses MLV and HTLV-1 contains a free, redox active thiol that reduces a constraining disulfide bond linking SU and fusion protein TM. Receptor binding by SU activates the catalytic thiol which reduces the linking disulfide, triggering fusion activation of TM [359,360]. The redox activity of the free thiol in SU is essential for virus infectivity.

Investigations into the mechanism controlling thiol isomerisation in the MLV and HTLV-1 glycoproteins have shown that the catalytic thiol is contained within a highly conserved CXXC thiol isomerisation motif in SU. The C-terminal cysteine residue in the motif is disulfide linked to a CX₆CC motif within TM. Alkylation of the active thiol in SU inhibits entry. However, entry can be restored by chemical reducing agents that can replace the activity of the blocked catalytic thiol. This would suggest that fusion activation requires disulfide reduction only, with no new structurally significant disulfides forming during fusion activation.

Disulfide reduction has also been described as an essential component of HIV glycoprotein fusion activation [374,375,376]. Azimi *et al.* (2010) demonstrated that reduction of a disulfide bond formed between Cys296 and Cys331 in variable loop 3 of receptor binding protein gp120 is catalysed by cell surface thioredoxin. The group found that binding of gp120 to chemokine receptor CD4 enhanced reduction and proposed that this activity may promote subsequent co-receptor selection [373].

For HCV, although free thiol group(s) are essential for mediating virus entry, these are unlikely to be located on a protein other than the viral glycoproteins as incubation reactions containing M135 and HCVcc/pp were quenched with Cys containing DMF20NEA prior to addition of the virus to cells. This would prevent any active M135 from reacting with cellular components. Furthermore, when an excess of HCVcc was added to the alkylation reaction then applied directly to Huh-

7.5 cells without quenching, it was found that the virus remained largely entry competent. This finding demonstrates that the Huh-7.5 cells were still able to support infection events for the unalkylated virus in the reaction.

For HCVcc, alkylation of free thiol groups within E1E2 resulted in abrogation of entry only when alkylation was performed prior to virus attachment to cells. The inability to block entry after cell-binding indicates a loss of availability of free sulfhydryl groups. Such a finding is consistent with a transition from a reduced to oxidised state occurring in the glycoproteins upon attachment to cells. The finding that entry of M135-alkylated HCVcc could not be rescued by addition of exogenous DTT is further consistent with a disulfide isomerisation reaction, whereby the alkylated sulfhydryl groups are required to participate in new disulfide bonds during the entry process. Together, these results suggest that free thiol groups in HCV operate in a manner distinct to that previously identified for the retroviruses.

Interestingly it was found that HCVpp remained somewhat sensitive to sulfhydryl alkylation immediately following cellular attachment. In contrast to HCVcc which are thought to occur by budding events from the ER [129,130], HCVpp are produced by budding of retroviral particles from the cell surface membrane which incorporates a portion of cell surface localised E1 and E2 [3]. It is therefore likely that the arrangement of E1 and E2 on the surface of HCVpp will be similar to HIV-1 where 8-10 glycoprotein trimers are evident per virus particle [380]. This is in contrast to the native HCVcc glycoprotein arrangement which is predicted to be similar to flaviviruses [60,61] where a lattice of highly ordered glycoproteins is evident [62,63]. These organisational differences in E1 and E2 may cause conformational changes that occur during entry to take place more rapidly in HCVcc than HCVpp. Alternatively, it is possible that glycoprotein recruitment to the site of receptor attachment is required for HCVpp during virus entry as has been described for HIV-1 [381]. Given that relocalisation of glycoproteins through the viral membrane will not occur at 4°C, the finding that HCVpp remain sensitive to M135 immediately following cellular attachment while HCVcc do not, may be due to a delay in recruitment and subsequent

conformational changes in HCVpp glycoproteins. As such, resistance to M135 may occur later for HCVpp than HCVcc. Future experiments may include time course analyses of HCVpp-M135 sensitivity. Performing these experiments side by side with MAbs directed towards the HCV receptors may provide an insight in to the sequence of events required to mediate conformational changes in the viral glycoproteins during virus entry.

Differences in the glycoprotein arrangement on HCVcc and HCVpp may explain the finding that HCVcc appeared to be more sensitive to M135 alkylation than HCVpp prior to cellular attachment. The finding that HCVcc entry was abrogated by treatment with just 1 mM M135 compared to 5 mM M135 for HCVpp may additionally be due to differing concentrations of virus-associated protein in the two systems. It is not impossible to normalise virus concentrations between HCVpp and HCVcc systems as HCVpp consist of retroviral particles displaying HCV envelope proteins and do not contain HCV RNA. Furthermore, the envelope proteins from HCVcc and HCVpp used in these assays are different genotypes preventing normalisation of virus concentrations by Western blotting. In this case, HCVpp assays may have been performed using a higher concentration of virus than HCVcc. This would potentially mean that there are more titratable groups present to consume excess M135 on HCVpp. Alternatively, the decreased sensitivity of HCVpp to M135 prior to cellular binding may be attributed to conformational differences between genotype 2a (HCVcc) and genotype 1a (HCVpp) viruses. Both genotypes appear to require free sulfhydryl groups to mediate entry. However, it is possible that in HCVpp these residues are not as accessible to alkylation.

HCVpp and HCVcc also differ significantly in lipoprotein association. While serum derived virus and HCVcc are well recognised to associate with lipoprotein, HCVpp are produced in a non-VLDL producing cell line and therefore virus is free. It is possible that HCVcc-associated lipoprotein may occlude free sulfhydryl groups following cellular attachment preventing alkylation events. Given that cell-free HCVcc is also associated with lipoprotein, yet remains sensitive to M135, this does not seem a likely explanation.

At which stage the free thiol group(s) are required during HCV entry is unclear. HCV entry into hepatocytes requires the presence of receptors CD81 [5], scavenger receptor B1 (SR-B1) [6,7] and tight junction proteins claudin-1, 6 or 9 [8,9] and occludin [10] as well as initial attachment factors that may include LDL receptor (LDLr) [80,81], heparan sulfate, [82,83,84,85], lectin receptor L-SIGN [86] and the asialoglycoprotein receptor (ASGP-R) [88]. Following attachment, HCV undergoes clathrin mediated endocytosis and membrane fusion within the early endosome [92,382]. Formation of new disulfides would not occur in the low pH of the endosome therefore it is likely that an isomerisation event would occur during the early stages of entry. This is consistent with the finding that HCVcc is no longer sensitive to M135 immediately following cellular binding. This project investigated CD81 and heparin as potential activation triggers for thiol isomerisation. However, no net change in the number of free sulfhydryl groups could be detected in E1 or E2 post binding. To determine whether an isomerisation reaction has occurred would require analysis of the glycoproteins by mass spectrometry to determine whether different sulfhydryl groups are being labelled by the maleimide-biotin after receptor binding. The observation that HCVcc is no longer sensitive to M135 following cellular attachment indicates that an isomerisation event resulting in complete oxidation of the glycoproteins has occurred, which is not the case following CD81 or heparin binding only.

Given that HCVcc-M135 insensitivity occurs immediately following cellular attachment, this would suggest that a change in oxidation state has been triggered by association of the viral glycoproteins with an attachment factor involved in a very early stage of entry. Antibody directed towards CD81, SR-B1 and claudin-1 receptors can inhibit HCV entry when added to cells 18-60 mins after virus attachment to cells [7,8,300,321]. As such, these receptors are unlikely to be catalysts for activating the free thiol group(s) in HCV consistent with the finding that CD81 does not affect the oxidation state of E1 or E2. By contrast, data suggests that heparan sulfate proteoglycans are likely to be involved in an early virus attachment stage, as HCVcc/pp entry can be inhibited by soluble heparan sulfate homologs only if these factors are present at the time of virus addition to cells [7,84,299,300]. The finding that HCVpp-heparin binding does not alter the

availability of Cys residues for maleimide-biotin reaction in E1 or E2 indicates that heparin alone is not able to induce a change in glycoprotein oxidation. It is possible that another attachment factor is responsible for triggering the change in oxidation state. Alternatively, these factors may need to be present in their native, full length forms in a cellular context. Indeed it is possible that a combination of binding events may be required to induce glycoprotein oxidation.

To thoroughly examine the changes in glycoprotein oxidation in the context of HCVcc and HCVpp, a more efficient, high titre virus system is required. Thiol labelling of HCVpp and HCVcc following cellular binding and subsequent whole cell lysis was attempted in this study. However, sufficient HCVcc could not be obtained for analysis by Western blot even following large scale concentration of virus. Furthermore, specific binding of HCVpp to Huh-7.5 cells could not be achieved (data not shown). No-envelope control particles and HCVpp were found to bind Huh-7.5 cells equally well. Ultimately, validation of the oxidation and/or conformational changes that occur during HCV entry will require crystal structures of the viral glycoproteins in pre and post fusion conformations.

Tscherne *et al.* (2005) reported that HCVcc demonstrates resistance to acid, suggesting that exposure to low pH alone is not sufficient to induce the irreversible conformational changes usually associated with glycoprotein fusion activation [11]. The group also observed that endosomal neutralisation by the H⁺ pump inhibitor bafilomycin A1 followed by immediate exposure of the cells to low pH was not sufficient to induce fusion of HCV at the plasma membrane as is the case for other viruses that undergo fusion within endosomes such as avian sarcoma and leukosis virus [357]. However, when HCVcc were bound to bafilomycin A1 treated Huh-7.5 cells then treated with low pH buffer after 1 h incubation at 37°C, significant, albeit low levels, of infection could be detected. This suggests that a specific sequence of events must occur at the plasma membrane during HCV entry in order to induce fusion activation of the glycoproteins. It is possible that disulfide rearrangements within E1 and E2 must occur upon attachment to cells in order to allow downstream associations with

other receptors, and/or to prime the glycoproteins to undergo the conformational changes associated with fusion activation once exposed to low pH.

HCV together with pestiviruses and flaviviruses comprise the *Flaviviridae* family. While there have been no reports of thiol isomerisation within flaviviruses, there is evidence for thiol isomerisation occurring during virus entry for the more closely related pestivirus, bovine viral diarrhoea virus (BVDV) [383]. BVDV expresses 3 envelope glycoproteins on its surface including E^{rms}, E1 and E2. These form complex arrangements of disulfide linked homo- and heterodimers [384,385,386,387]. Krey *et al.* (2005) confirmed the entry route of BVDV via clathrin dependent endocytosis but found that exposure of the virus to low pH was not sufficient to inactivate the virus, as is observed for HCV [383]. When BVDV was exposed to reducing agent DTT followed by low pH, significant inactivation of the virus was observed. The group concluded that destabilisation of the disulfides was required to prime the glycoproteins for fusion activation at low pH. It is noteworthy that it is not possible to tell from these data whether inactivation of the virus is due to induction of fusion activation or a result of destabilisation of structurally critical disulfide bonds. However, it is interesting that fusion at the plasma membrane could be induced at low levels for BVDV when cells were treated with the endosomal neutralising agent bafilomycin A1, followed by low pH exposure and addition of 10 mM DTT. This effect was not observed in the absence of DTT, and suggests that disulfide bond destabilisation is an essential component of entry for BVDV. It is possible that a similar mechanism to HCV is in place here, and maybe a time course assay whereby BVDV is exposed to low pH at various times following attachment to bafilomycin A1 treated cells, may induce more efficient entry. Thiol reduction or isomerisation within the envelope glycoproteins requires the presence of a catalytic thiol, therefore it should be possible to induce disulfide destabilisation within the BVDV envelope glycoprotein complexes in the absence of DTT – with either the virus or a cellular thioredoxin family protein providing the catalytic thiol. In any case, the results still suggest that BVDV envelope glycoproteins require destabilisation of disulfide bonds prior to fusion activation. It is possible that BVDV and HCV may have co-evolved a disulfide bond

reduction and/or isomerisation priming step as an essential component of the entry cascade prior to fusion activation at low pH.

Like the retroviruses MLV and HTLV-1 which undergo thiol reduction during fusion activation, HCV also contains a highly conserved CXXC motif within the envelope glycoprotein complex. This motif forms the active site of redox active thioredoxin proteins and has been shown to provide the active thiol which catalyses reduction/isomerisation of disulfide bonds in target proteins [379]. In HCV this motif is located near the N-terminus of E1 and its role in HCV entry will be the focus of investigations in the next chapter.

This project has identified the presence of functionally significant free thiol groups on both E1 and E2 glycoproteins incorporated into virus particles. The results obtained are consistent with an isomerisation reaction occurring within the glycoproteins at an early stage in entry. In addition, it appears that the free thiol groups function using a mechanism distinct to that previously identified for retroviruses. In the following chapter, the role of the E1 CXXC motif in assembly and virus entry will be explored.

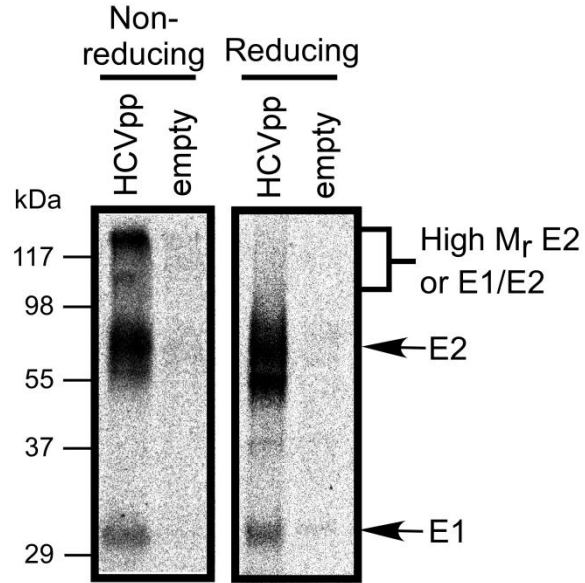
3.4 Supplementary Data

To investigate antibody bias towards various oligomeric forms of heterodimeric E1E2, HCVpp displaying E1E2 from prototype strain H77c were produced in HEK 293T cells. Thirty h post-transfection cells were labeled with 75 μ Ci Trans-³⁵S-label in methionine and cysteine-deficient DMF10 for 16h. Radiolabeled virus was pelleted by centrifugation then lysed and immunoprecipitated with MAbs directed towards E2 (conformation sensitive, non-neutralising H53 or neutralising MAb 24 that binds a linear epitope) and protein G-sepharose, prior to SDS-PAGE and phosphorimage analysis.

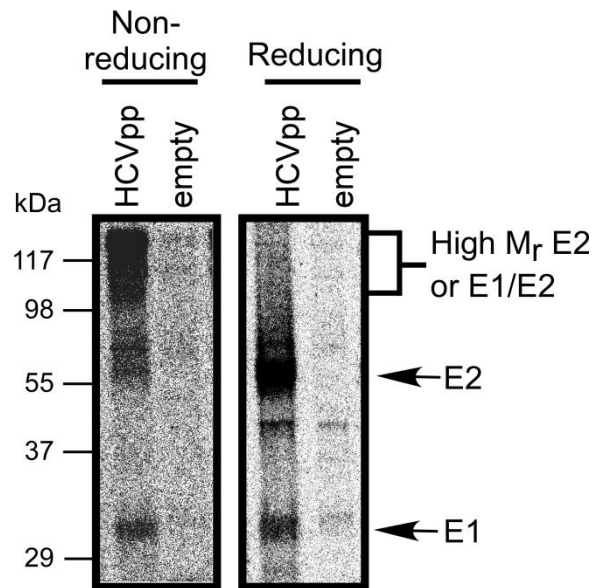
Immunoprecipitation of HCVpp-derived heterodimeric E1 and E2 using MAb H53 reveals that E2 containing the H53 conformational epitope largely exists as a non-covalently associated heterodimer with E1 when run under non-reducing conditions (Supplementary Figure 3-1A). The band of high molecular weight protein disappears when the same samples are run under reducing conditions indicating that these high molecular weight species are likely to be disulfide linked forms of E2 or E1E2. By contrast, immunoprecipitations carried out using non-conformational, neutralising MAb 24 show the majority of the protein is high molecular weight forms (non-reducing; Supplementary Figure 3-1B). When the samples are run under reducing conditions these high molecular weight forms are no longer evident, but the bands of non-covalent E2 and E1 are significantly enhanced, indicating that these high molecular weight forms are disulfide linked E2 or E1E2.

These immunoprecipitations were performed on the same preparations of HCVpp therefore this finding suggests that although a variety of oligomeric forms of the glycoproteins are present in a single preparation, some forms are more readily detected than others by particular MAbs.

A.



B.



Supplementary Figure 3-1. Immunoprecipitation of E1E2 from HCVpp using conformation sensitive and neutralising MAb directed towards E2. HCVpp were metabolically labelled with ^{35}S -Met/Cys prior to lysis followed by immunoprecipitation with conformation sensitive, non-neutralising anti-E2 MAb H53 (A) or neutralising MAb 24 that binds a linear epitope (B). Proteins were separated by non-reducing or reducing SDS-PAGE as indicated and phosphorimaged. The positions of molecular weight markers are shown to the left of the gel.

Chapter 4 – Characterisation of a Conserved CXXC Thiol-Disulfide Exchange Motif in E1

4.1 Introduction

Thioredoxin family proteins such as protein disulfide isomerase (PDI) regulate protein folding by catalysing changes in the disulfide bonding arrangement of target proteins. For most thioredoxin family proteins this redox activity is regulated by a characteristic CXXC motif located at the protein's active site. The N-terminal cysteine in this motif typically has a lower pK_a that allows its deprotonation at physiological pH [388]. When this Cys is in a reduced state, deprotonation induces the active thiol to randomly form mixed disulfides with a target protein. Resolution of the mixed disulfide by the second Cys in the motif leaves the target protein reduced and the CXXC motif oxidised in an intramolecular disulfide bond. Once reduced, the target protein can adopt its native disulfide bonding arrangement allowing the lowest energy conformation to be obtained.

PDI and other redox active proteins provide an essential control point during protein biosynthesis in the endoplasmic reticulum, catalysing the refolding of misfolded proteins (for review see [389]). In the context of virus entry, the viral envelope glycoproteins of MLV and HTLV-1 contain a conserved CXXC motif which catalyses disulfide bond reduction within the envelope glycoprotein complex in order to induce the conformational changes required for fusion of viral and target cell membranes [359,360].

In Chapter 3 free cysteine residues were identified in virion incorporated E1 and E2 that were essential for HCV entry. Furthermore, it was determined that the HCVcc glycoproteins appear to undergo a change in oxidation upon cellular attachment consistent with a disulfide isomerisation reaction. To determine whether E1 or E2 contain a CXXC motif that may regulate the oxidation state of

the HCV glycoproteins, sequence analysis of E1 and E2 from the 6 HCV genotypes was performed. Alignment of 389 non-redundant E1 sequences identified the presence of a highly conserved C²²⁶V/LPC thioresoxin-like motif [390] located near the N-terminus of E1 (Figure 4-1). In all but genotype 6 the motif sequence is CVPC.

In order to determine the significance of the E1 C²²⁶V/LPC motif, its function during glycoprotein biosynthesis and virus entry was examined. Note that because genotype 1a and 2a constructs have been used for all experiments this motif will be referred to as C²²⁶VPC for simplicity.

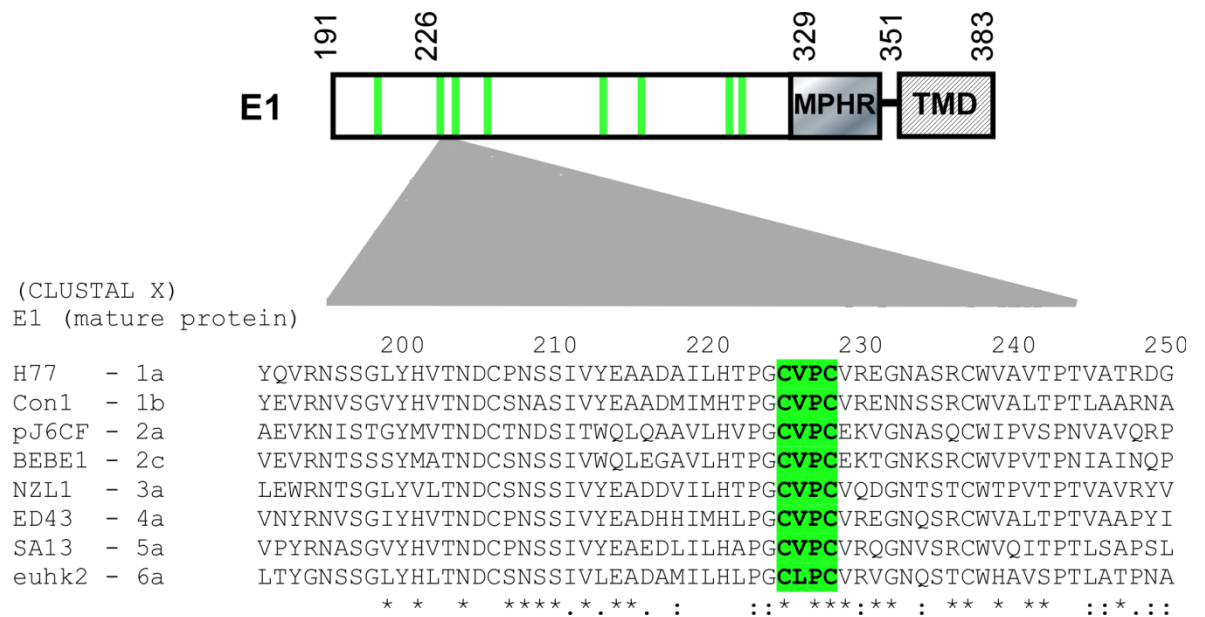


Figure 4-1. Schematic representation of E1 and Clustal X alignment of prototype strains representative of each HCV genotype. H77c (AF011751) 1a, Con-1 (AJ238799) 1b, pJ6CF (AF1770363) 2a, BEBE1 (D50409) 2c, NZL1 (D17763) 3a, ED43 (Y11604) 4a, SA13 (AF064490) 5a and euhk2 (Y12083) 6a. Residues that are identical (*), conserved (:), or similar (.) across the genotypes are indicated. The highly conserved C²²⁶V/LPC motif is located near the N-terminus of E1 and is highlighted in green in the alignment. Schematic representation of E1 shows the conserved MPHR in grey shading, the TMD in grey hatching, and conserved cysteine residues are represented by vertical green lines.

4.2 Results - Role of C²²⁶VPC Cys Residues in Glycoprotein Biosynthesis and Virus Entry

To assess the role of the C²²⁶VPC motif in glycoprotein biosynthesis and virus entry, site directed mutagenesis was performed in the context of the prototype strain H77c using the CMV promoter driven E1E2 expression vector, pE1E2H77c [3]. Each cysteine within the motif was replaced with alanine to remove the disulfide bonding activity at this position. This was done for each Cys residue individually and in combination; C226A (AVPC), C229A (CVPA) and C226A/C229A (AVPA).

4.2.1 Expression of E1 and E2 containing C²²⁶VPC Cys to Ala mutations

To determine the effect of cysteine mutagenesis on E1 and E2 expression, cell lysates of transfected HEK 293T cells were analysed. Cells transfected with pE1E2H77c were lysed 24 h post-transfection and lysates run directly on reducing SDS-PAGE. Western blot analysis was performed with non-conformation dependent MAbs directed towards E1 (A4) and E2 (H52) to determine E1 and E2 expression levels. The results show that by 24 h post transfection, total E1 and E2 expression in the cell lysate is similar for CVPC-wt, AVPC and CVPA (Figure 4-2). This suggests that mutation of Cys226 and Cys229 in E1 does not significantly affect the total E1 or E2 produced at the level of cell lysate. When both Cys residues were mutated in combination (AVPA) the total level of E1 in the cell lysate appeared slightly reduced compared to CVPC-wt. This suggests that when E1 contains the AVPA mutations the protein may undergo some level of degradation probably due to misfolding and removal by the proteasome. E2 expression remained normal for each mutant.

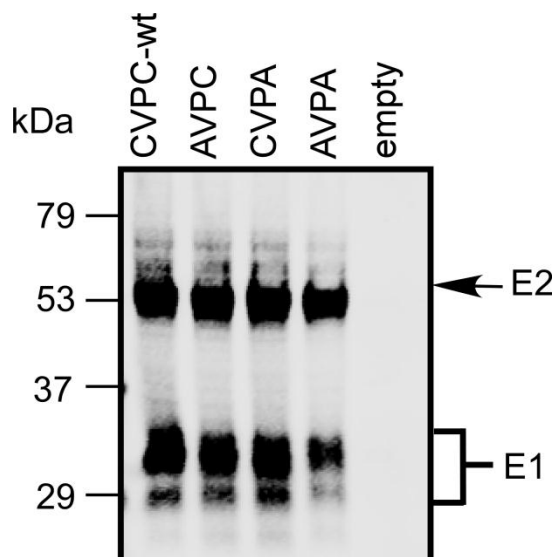


Figure 4-2. Expression of E1 and E2 containing C²²⁶VPC Cys to Ala mutations. HEK 293T cells transfected with pE1E2H77c were lysed 24 h post transfection and lysates subjected to reducing SDS-PAGE. E1 and E2 expression was detected by non-conformational MAbs A4 and H52 respectively. Blots were imaged using an Odyssey Infrared Imaging System at 680 nm (LI-COR). Positions of the molecular weight markers are shown to the left of the gel.

4.2.2 Heterodimerisation of E1E2 containing E1 Cys to Ala mutations

To assess whether mutagenesis of the C²²⁶VPC Cys residues to Ala affected formation of E1E2 heterodimers, HEK 293T cells were transfected with pE1E2H77c and radiolabelled with ³⁵S-Met/Cys for 30 min prior to lysis of cells. MAb H53, directed towards a conformational epitope in E2, was used to immunoprecipitate E2 and any associated E1. Mutagenesis of each of the Cys residues within the C²²⁶VPC motif, individually or in combination, resulted in a complete loss of non-covalent heterodimerisation between E1 and E2 (Figure 4-3). It should be noted that high molecular weight forms of E2 or E1E2 oligomers (represented as E1/E2) were observed for both wild type and mutant forms. This suggests that mutagenesis of Cys226 or Cys229 causes a folding defect, at least in monomeric E1, such that it fails to properly associate with E2. Alternatively it is possible that the conformation of E2 outside the H53 epitope has been altered in such a way that E2 is no longer able to form heterodimers with mutant E1.

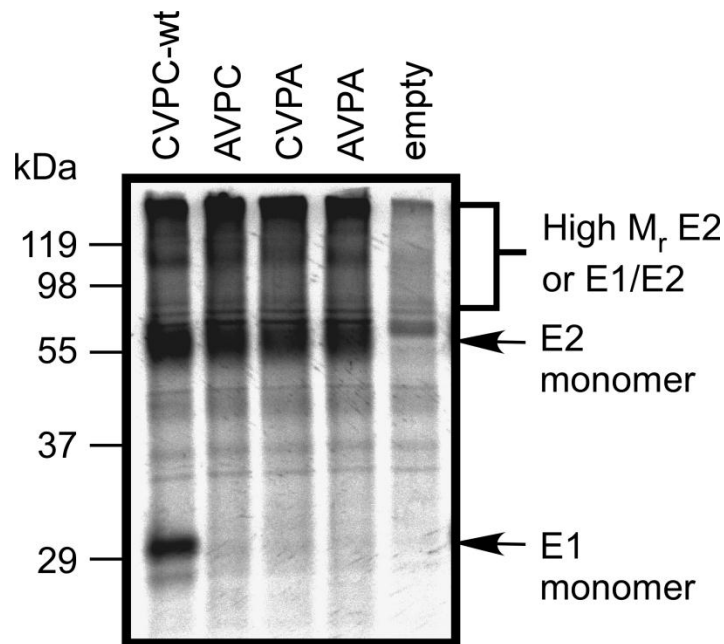


Figure 4-3. Heterodimerisation of E1E2 containing C²²⁶VPC Cys to Ala mutations. HEK 293T cells transfected with pE1E2H77c were metabolically labelled with ³⁵S-Met/Cys prior to cell lysis. Immunoprecipitation was performed with conformation sensitive anti-E2 MAb H53 followed by separation of the proteins by non-reducing SDS-PAGE and phosphorimaging. The positions of molecular weight markers are shown to the left of the gel.

4.2.3 HCVpp incorporation of conformational and non-conformational E1E2 for E1 Cys to Ala mutants

To determine the effect of mutagenesis of the C²²⁶VPC cysteine residues on E1E2 maturation and incorporation into virions, HCVpp produced in HEK 293T cells and were metabolically labelled with ³⁵S-Met/Cys prior to lysis. The ability of mutant E1E2 from HCVpp to form non-covalent heterodimers was assessed by immunoprecipitation using conformation-sensitive anti-E2 MAb H53 or non-conformational anti-E2 polyclonal antibody GP1. Samples were subjected to non-reducing (Figure 4-4A and B) or reducing (Figure 4-4C) SDS-PAGE followed by phosphorimaging.

Immunoprecipitation by H53 detected monomeric E2 from each mutant at similar levels to CVPC-wt. However, E1 was not co-precipitated with E2 from AVPC, CVPA or double cysteine mutant AVPA, indicating a loss of H53 reactive non-covalently associated heterodimers (Figure 4-4A). The same result was

obtained when HCVpp were lysed in the presence of cysteine reactive NEM (data not shown). This finding reflects the earlier result which demonstrated a loss of intracellular non-covalently associated heterodimers for these mutants. To ensure equivalent amounts of HCVpp were assayed for each construct, HIV-1 capsid protein p24 was immunoprecipitated by a MAb directed towards p24 (MAb 183, Figure 4-4A lower panel).

To determine whether alternative conformational forms of heterodimeric E1E2 were incorporated into HCVpp, immunoprecipitations were performed using non-conformational polyclonal anti-E2 antibody GP1. By using polyclonal serum all forms of E2 incorporated into HCVpp should be precipitated without conformational bias, allowing examination of the total E2 glycoprotein expressed on HCVpp for each mutant. When run under non-reducing conditions E2 precipitated by GP1 was detected at wild-type levels for each of the cysteine mutants. However, non-covalent heterodimerisation was absent in all cases (Figure 4-4B). This indicates that mutagenesis of either or both of the Cys residues within the C²²⁶VPC motif prevents formation of non-covalently associated E1E2 heterodimers.

To determine whether covalent forms of heterodimeric E1E2 were incorporated into mature HCVpp, E1E2 immunoprecipitated by GP1 were run under reducing conditions. While equivalent amounts of E2 were detected in mature HCVpp for each mutant, only very low levels of E1 were co-precipitated (Figure 4-4C). Equal input of HCVpp was confirmed by HIV-1 capsid protein p24 immunoprecipitation as described above (Figure 4-4B, lower panel). This suggests that mutagenesis of Cys226 or Cys229 causes a folding defect in E1 such that it fails to properly associate with E2 and mature through the secretory pathway for incorporation into HCVpp. Or, as suggested above, it is possible that the conformation of E1 may have been altered in such a way that it is no longer able to heterodimerise efficiently with E2. The absence of E1 when run under reducing conditions indicates that the high molecular weight forms detected when the mutants were run under non-reducing conditions are likely to be largely comprised of disulfide linked E2.

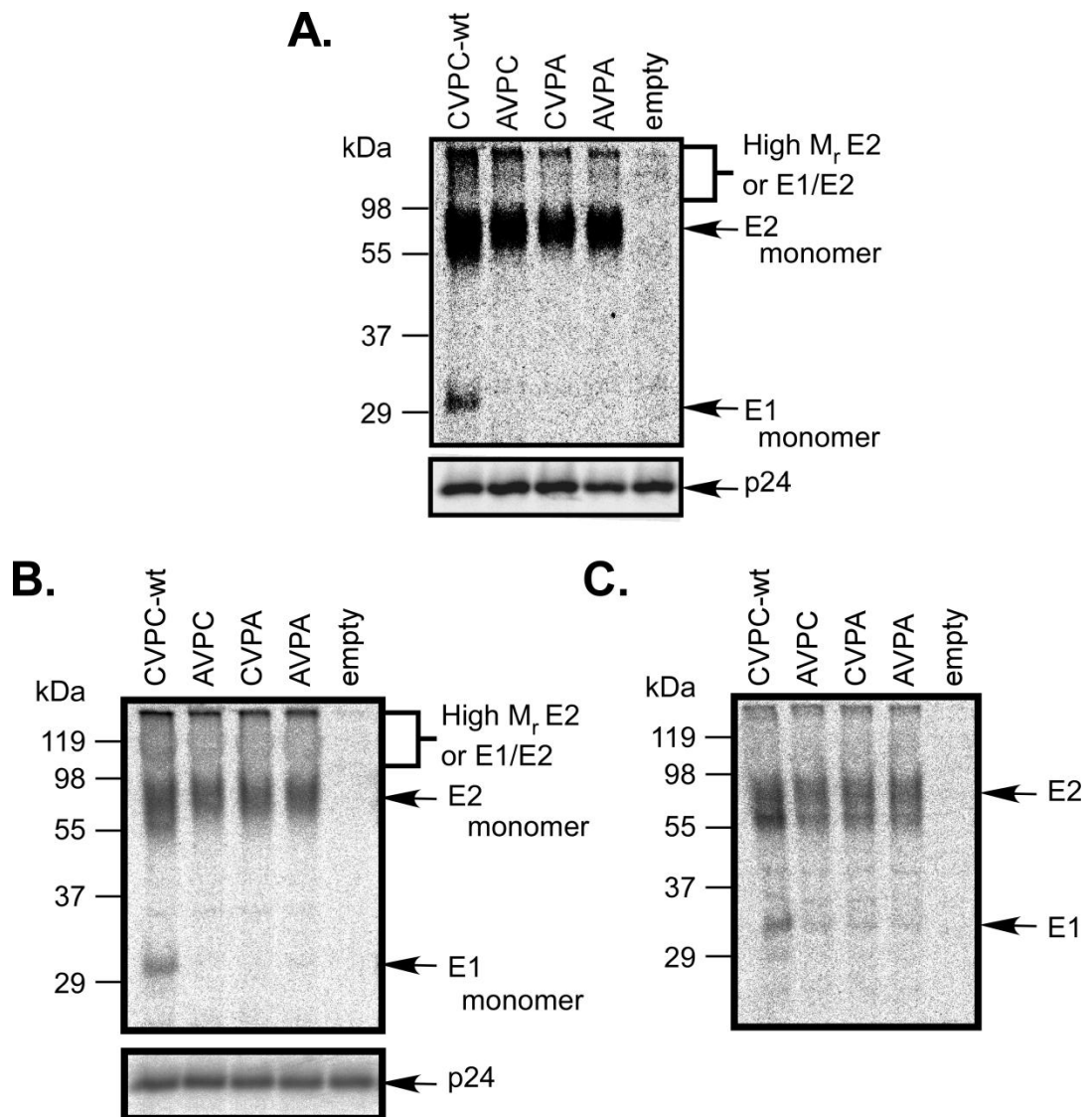


Figure 4-4. HCVpp incorporation of conformational and non-conformational E1E2 containing C²²⁶VPC Cys to Ala mutations. HCVpp were metabolically labelled with ³⁵S-Met/Cys prior to lysis followed by immunoprecipitation with conformation sensitive anti-E2 MAb H53 (A) or non-conformation sensitive polyclonal anti-E2 antibody GP1 (B). Proteins were separated by non-reducing (A and B) or reducing (C) SDS-PAGE and phosphorimaged. The positions of molecular weight markers are shown to the left of the gel. Incorporation of HIV-1 capsid protein p24 into each HCVpp mutant was determined by immunoprecipitation with MAb 183. For B, samples were split after E2 immunoprecipitation therefore a single MAb 183 immunoprecipitation was performed.

4.2.4 Expression of E1 and E2 containing C²²⁶VPC Cys to Ser mutations

In order to more closely examine the requirement of the C²²⁶VPC Cys residues in E1 and E2 biosynthesis, each cysteine was replaced with serine in the context of pE1E2H77c, producing mutants C226S (SVPC) and C229S (CVPS). Replacement of Cys with Ser retains the length of the carbon side chain while the hydroxyl group on the Ser side chain promotes hydrogen bond formation in place of the native disulfide bond activity provided by Cys. As such, serine is more likely to facilitate native intermolecular interactions than alanine substitution.

To investigate the effect of C²²⁶VPC Cys to Ser mutagenesis on E1 and E2 expression, HEK 293T cells were transfected with CVPC-wt and mutant pE1E2H77c. Twenty-four h post transfection cell lysates were run directly on SDS-PAGE and analysed by Western blot. Detection of E1 and E2 using non-conformational MAbs A4 and H52, respectively, determined equal levels of glycoprotein expression in SVPC and CVPS mutants compared to CVPC-wt (Figure 4-5). This suggests that replacement of Cys with Ser at these positions allows normal intracellular expression of E1 and E2.

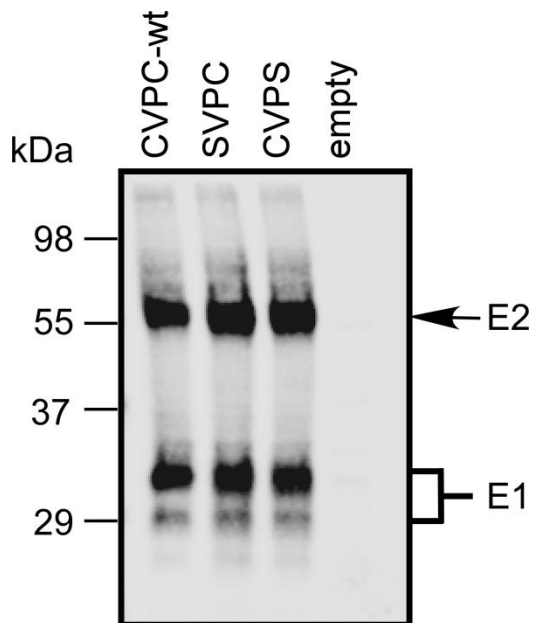


Figure 4-5. Expression of E1 and E2 containing C²²⁶VPC Cys to Ser mutations. HEK 293T cells transfected with pE1E2H77c were lysed 24 h post transfection and lysates subjected to reducing SDS-PAGE. E1 and E2 expression was detected by non-conformational MAbs A4 and H52, respectively. Blots were imaged by LI-COR. Positions of the molecular weight markers are shown to the left of the gel.

4.2.5 Heterodimerisation of E1E2 containing C²²⁶VPC Cys to Ser mutations

To determine whether introduction of Ser at Cys226 or Cys229 affected the ability of E1 and E2 to form non-covalent heterodimers, HEK 293T cells transfected with pE1E2H77c were radiolabelled with ³⁵S-Met/Cys for 30 min followed by chase in DMF10 and cell lysis. Conformation sensitive MAb H53 was used to immunoprecipitate E2 and any associated E1.

Despite Western blot analysis indicating WT levels of E1 and E2 expression for both SVPC and CVPS, no E1 was co-precipitated with H53-reactive E2 for either mutant (Figure 4-6). This indicates that similar to the Cys to Ala mutations, replacement of C²²⁶VPC Cys residues with Ser alters the fold of E1E2 in such a way that native heterodimerisation is abolished. The observation that WT levels of E2 were precipitated by conformational MAb H53 for each mutant indicates that this epitope has formed correctly despite the absence of non-covalently associated E1.

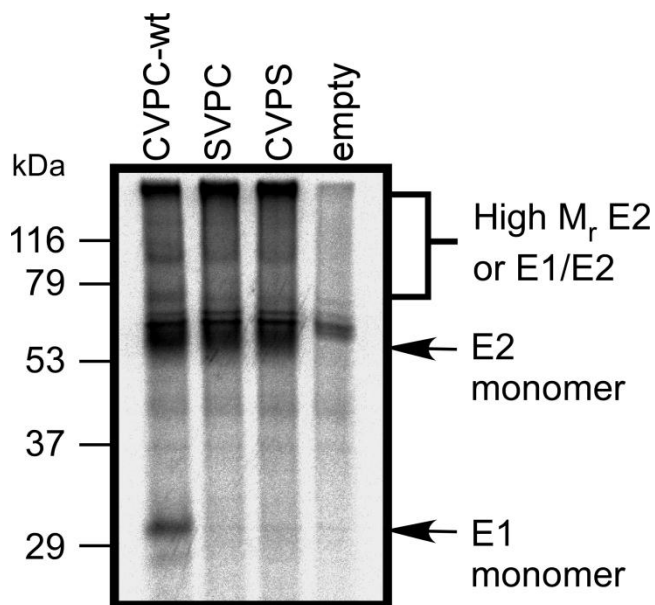


Figure 4-6. Heterodimerisation of E1E2 containing C²²⁶VPC Cys to Ser mutations. HEK 293T cells transfected with pE1E2H77c were metabolically labelled with ³⁵S-Met/Cys prior to cell lysis. Immunoprecipitation was performed with conformation sensitive anti-E2 MAb H53 followed by separation of the proteins by non-reducing SDS-PAGE and phosphorimaging. The positions of molecular weight markers are shown to the left of the gel.

4.2.6 HCVpp incorporation of conformational E1E2 containing Cys to Ser mutations

To determine whether the loss of non-covalent E1E2 heterodimers in transfected cell lysates observed for the C²²⁶VPC Cys to Ser mutants reflected the incorporation of E1 and E2 into virus particles, HCVpp were metabolically labelled with ³⁵S-Met/Cys prior to lysis. The ability of mutant E1E2 from HCVpp to form non-covalent heterodimers was assessed by immunoprecipitation using conformation-sensitive anti-E2 MAb H53.

It was found that replacement of either Cys within the C²²⁶VPC motif with Ser resulted in a loss of non-covalent H53-reactive heterodimeric E1E2 (Figure 4-7). This result is consistent with what was observed for the Cys to Ala mutants and indicates that the hydrogen bonding activity provided by Ser is not sufficient to allow formation of non-covalent E1E2 heterodimers. As such, these data indicate a

strict requirement for the Cys residues within the C²²⁶VPC motif for correct E1E2 biosynthesis.

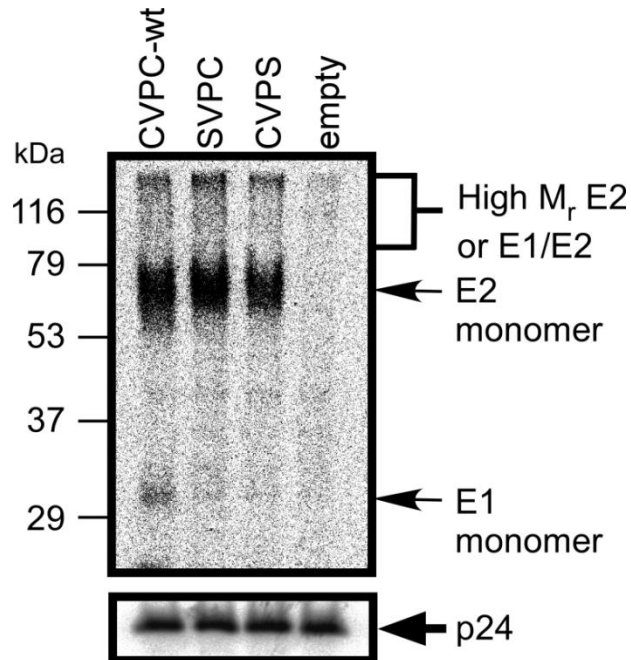


Figure 4-7. HCVpp incorporation of conformational E1E2 containing C²²⁶VPC Cys to Ser mutations. HCVpp were metabolically labelled with ³⁵S-Met/Cys prior to lysis followed by immunoprecipitation with conformation sensitive anti-E2 MAb H53. Proteins were separated by non-reducing SDS-PAGE and phosphorimaged. The positions of molecular weight markers are shown to the left of the gel. Incorporation of HIV-1 capsid protein p24 into each HCVpp mutant was determined by immunoprecipitation with MAb 183.

4.2.7 Pulse chase analysis of AVPC and CVPA mutants

In order to examine the effect of Cys226 and Cys229 in E1E2 biosynthesis, pulse chase analysis was performed on AVPC and CVPA mutants. HEK 293T cells transfected with pE1E2H77c were metabolically labelled with ³⁵S-Met/Cys for 15 min followed by chase in DMF10 for the indicated time (maximum chase time 20 h). Cell lysates were subjected to immunoprecipitation with MAb H52 which recognises a linear epitope in E2, conformational anti-E2 MAb H53, or MAb A4 which recognises a linear epitope in E1 (Figure 4-8A, B and C respectively). MAb

9E10 which recognises a linear epitope within human c-Myc protein, was used as an irrelevant MAb to immunoprecipitate the longest chase time for each construct.

Immunoprecipitation was performed with MAb H52 to visualise total intracellular E2 at each chase time. For CVPC-wt and mutants AVPC and CVPA, monomeric forms of glycoprotein E2 and E1, but not E1E2 heterodimers, were immunoprecipitated with MAb H52 and A4, respectively, following the 15 min pulse. Equivalent amounts of E2 and E1 were detected in the pulse period for CVPC-wt, AVPC and CVPA mutants indicating comparable cellular transfection and expression levels.

For CVPC-wt, a decrease in the amount of monomeric E2 immunoprecipitated with H52 was observed over the 20 h chase period. By contrast, the amount of non-covalently associated E1 co-precipitated with E2 using MAb H52 steadily increased over the 20 h chase period. High molecular weight forms of CVPC-wt E2 or E1 associated with E2 (represented as E1/E2) were detected in the pulse but steadily decreased in intensity during the chase period. Non-covalently associated CVPC-wt E1E2 heterodimers were also detected with conformation sensitive MAb H53 following 1 h chase. The levels remained constant throughout the chase period to 8 h with a decrease observed at 20 h indicative of degradation. It is important to note that a protein species migrates just above monomeric E2 and is immunoprecipitated with the irrelevant antibody 9E10. This species should be excluded from the interpretation of these results.

MAb A4 specific to E1 was found to immunoprecipitate monomeric CVPC-wt E1 in the pulse period as well as high molecular weight forms of E1 or E1/E2, including a species that migrates at ~ 70kDa. This band is only precipitated by anti-E1 MAb A4 and is likely to represent dimeric E1 as the band is no longer evident when samples are run under reducing conditions (data not shown). At least three distinct molecular mass forms of monomeric E1 were detected in the pulse period. These are likely to be various glycoforms as they migrate similarly on reducing SDS-PAGE (as observed in Figure 4-2). The amount of high molecular weight E1 or E1/E2 steadily decreased during the chase period.

The formation of non-covalently associated E1E2 heterodimers was severely impaired in the mutant AVPC. Non-covalently associated E1 was not co-precipitated with E2 from this mutant using MAbs H52 or H53 at any time point (Figure 4-8A and B). Instead, large amounts of high molecular weight oligomers of E2 or E1/E2 were precipitated during the pulse period and these were maintained throughout the chase period up to 8 h detected by H52 and A4. At 20 h chase, the amount of high molecular weight material detected with H52, H53 and A4 decreased, indicative of degradation. Despite this accumulation of aggregate forms from the AVPC mutant, monomeric E2 appeared at similar levels to CVPC-wt throughout the chase for both H52 and H53 immunoprecipitations.

The defects in E1E2 folding did not appear to be as severe for mutant CVPA as compared to mutant AVPC, but the formation of E1E2 heterodimers was not similar to wild-type. Non-covalently associated E1 was co-precipitated with E2 using MAb H52 with small amounts detected in the pulse period, increasing following 1 h chase and maintained throughout the chase period. Given that no non-covalent heterodimerisation was detected for CVPA E1E2 incorporated into HCVpp when immunoprecipitated with polyclonal serum GP1 directed towards E2 (Figure 4-4 B and C), it is unlikely that this heterodimeric form matures into virions. This is supported by the absence of non-covalent heterodimers detected with conformation sensitive MAb H53. Instead, E2 alone was detected with H53 up to 8 h. Levels declined after 20 h chase, suggestive of degradation and consistent with what was observed for CVPC-wt. Using MAb A4 specific to E1, three glycoforms of monomeric E1 were detected in the pulse and maintained throughout the chase period. In addition, high molecular weight forms of E1 or E1/E2 were immunoprecipitated with A4 in the pulse and chase periods.

These results suggest that the mutation AVPC alters E1E2 biosynthesis such that covalently associated E1 and disulfide linked forms of E1 associated with E2 are stabilised and prevent the formation of non-covalently associated E1E2 heterodimers. Mutant CVPA causes a similar biosynthetic defect but does not appear to be as severe, as a non-covalent form of E1E2 is detected with a conformation insensitive antibody. However, non-covalent heterodimer cannot be

detected with a conformation sensitive antibody and is not incorporated into HCVpp suggesting it has a severe folding defect. It is possible that mutagenesis of the Cys residues within the C²²⁶VPC motif traps the glycoproteins in high molecular weight disulfide linked folding intermediates possibly mediated by the single remaining Cys within the C²²⁶VPC motif.

These results show that mutagenesis of Cys226 and Cys229 within the C²²⁶VPC motif induces folding defects that prevent formation of non-covalent E1E2 heterodimers.

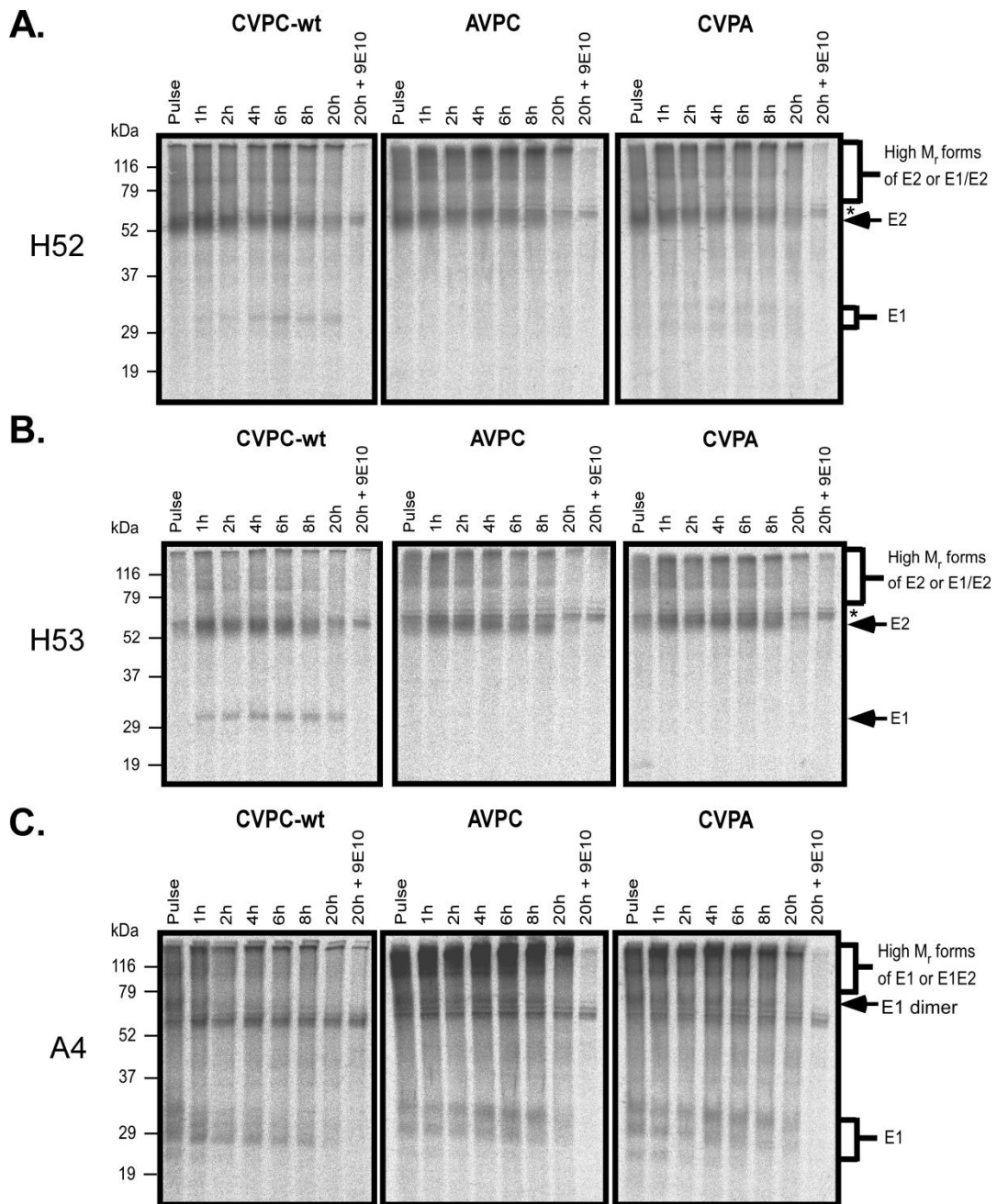


Figure 4-8. Pulse chase analysis of CVPC-wt, AVPC and CVPA mutants. HEK 293T cells were transfected with pE1E2H77c. Twenty four h post transfection cellular proteins were metabolically labelled with ^{35}S -Met/Cys for 15 min. Cells were lysed at the indicated time points then immunoprecipitated using non-conformation sensitive anti-E2 MAb H52 (A), conformation sensitive anti-E2 MAb H53 (B), or non-conformation sensitive anti-E1 MAb A4 (C). Immunoprecipitation of the 20 h chase with irrelevant MAb 9E10 is included for each construct. Samples were run on non-reducing SDS-PAGE and phosphorimaged. Molecular markers are shown to the left of the gels. Asterisks represent non-specific bands.

4.2.8 Pulse chase analysis of AVPA mutant

The high molecular weight forms of E1E2 detected for AVPC and CVPA mutants in Figure 4-8 suggest that mutation of either Cys residue traps E1 and/or E2 in a disulfide linked state. To determine whether these disulfide bonds occur via the single (free) remaining Cys residue in the C²²⁶VPC motif in each mutant, pulse chase analysis of the double Cys to Ala mutant (AVPA) was performed. HEK 293T cells transfected with pE1E2H77c were metabolically labelled with ³⁵S-Met/Cys for 15 min and chased in DMF10 as described in section 4.2.7.

Immunoprecipitation of the cell lysate by MAbs H52 or A4 that recognise linear epitopes in E2 and E1, respectively, detected similar levels of monomeric E2 and monomeric E1 at the pulse and throughout the chase for CVPC-wt and AVPA (Figure 4-9A and C). However, unlike AVPC or CVPA where large amounts of high molecular weight forms of intracellular E1, E1/E2 or E2 were detected, high molecular weight forms of E1, E1/E2 or E2 were not evident for AVPA and was in fact comparable to CVPC-wt. Similar to the CVPA mutant, a low level of non-covalent E1E2 heterodimer could be detected for AVPA from 1 h chase onwards.

When immunoprecipitations were performed using conformation sensitive anti-E2 MAb H53, E2 was detected at the same level for AVPA as CVPC-wt at the pulse and throughout the chase (Figure 4-9B). However, only very low levels of non-covalent E1E2 heterodimers were detected indicating that the heterodimer observed by H52 immunoprecipitation were largely of an alternative conformation.

Importantly, immunoprecipitations of AVPA-transfected cell lysates performed with anti-E1 MAb A4 demonstrated no difference in high molecular weight forms of E1 or E1/E2 at the pulse or throughout the chase compared to CVPC-wt (Figure 4-9C). This finding indicates that the high molecular weight forms observed in immunoprecipitations for AVPC and CVPA mutants are likely to be disulfide linked forms of the glycoproteins mediated through the single remaining Cys in the motif. This finding demonstrates that both Cys residues are required for the correct formation of non-covalently associated E1 and E2.

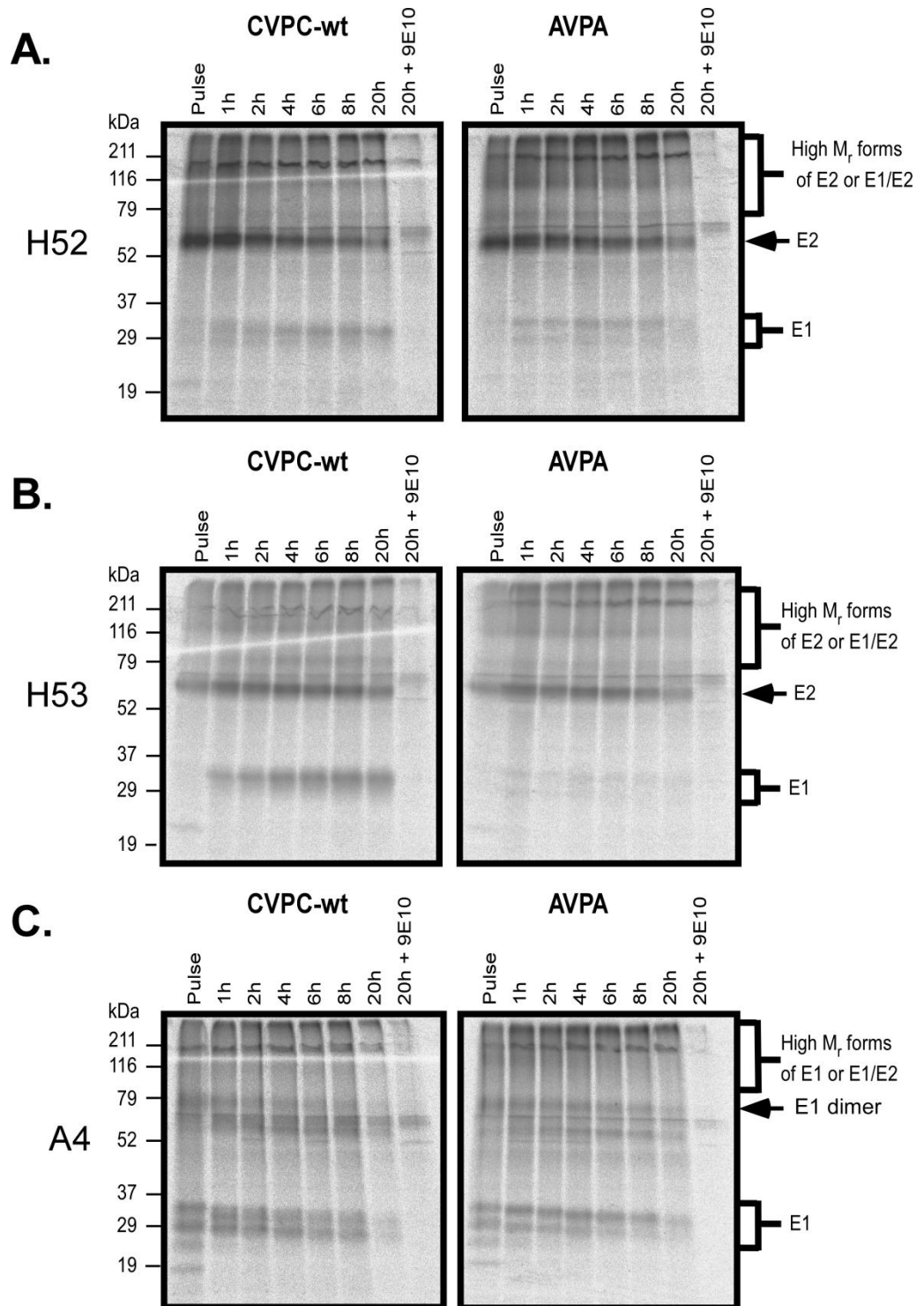


Figure 4-9. Pulse chase analysis of CVPC-wt and AVPA mutant. HEK 293T cells were transfected with pE1E2H77c. Twenty four h post transfection cellular proteins were metabolically labelled with ^{35}S -Met/Cys for 15 min. Cells were lysed at the indicated time points then immunoprecipitated using MAb H52 that recognises a linear epitope in E2 (A), conformation sensitive anti-E2 MAb H53 (B), or MAb A4 that recognises a linear epitope in E1 (C). Immunoprecipitation of the 20 h chase with irrelevant MAb 9E10 is included for each construct. Samples were run on non-reducing SDS-PAGE and phosphorimaged. Molecular markers are shown to the left.

4.2.9 CD81 binding by C²²⁶VPC Cys to Ala mutants

The tetraspanin CD81 is an essential attachment factor required for HCV infection of liver cells [5]. E2 contains the CD81 binding site which has been mapped to 4 discontinuous sequences present in two separate subdomains [95,247,254,255,256,273]. These are thought to be brought together by the tertiary fold of the protein. Therefore, the ability of E2 to bind CD81 provides information about the conformational integrity of E2. It has been suggested that E1 may influence the folding of E2 during biosynthesis [234]. To determine whether the E1 folding defective cysteine mutants AVPC, CVPA and AVPA induce folding defects in E2, a direct CD81 binding assay was used. This assay employs recombinant dimeric CD81 (MBP-LEL¹¹³⁻²⁰¹) which was described in Chapter 3.

To determine whether the E1 cysteine mutants had altered the conformation of the CD81 binding site in E2, radiolabelled wild-type and mutant HCVpp were produced as described in section 4.2.3. The amount of HCVpp-incorporated E2 precipitated by conformation-sensitive MAb H53 was determined by densitometry analysis. Equivalent amounts of E2 from HCVpp lysates were applied to solid-phase MBP-LEL¹¹³⁻²⁰¹ and serially diluted. Binding was detected by H53 and horseradish peroxidase-conjugated rabbit anti-mouse immunoglobulin.

The results demonstrate that the dilution of HCVpp required to achieve 50% binding to CD81 was similar for E2 from each C²²⁶VPC cysteine mutant compared to CVPC-wt (Figure 4-10). This suggests that while Cys226 and Cys229 are essential for E1 biosynthesis and heterodimerisation, the mutations do not influence the formation of the CD81 binding site on E2. However, each Cys mutant showed a slight but significant reduction in the total amount of E2 bound to CD81 ($p < 0.05$, Student's *t*-test). This result is consistent with a change in E1E2 stoichiometry whereby changes in glycoprotein oligomerisation have caused a reduction in the total amount of E2 capable of binding to CD81. This is reflected in the pulse chase analyses of AVPC and CVPA mutants where an increase in high molecular weight forms of the glycoproteins was evident. Although there was no

apparent increase in disulfide linked glycoproteins for AVPA, this mutant was still heterodimerisation defective indicating a change in the fold of the glycoproteins.

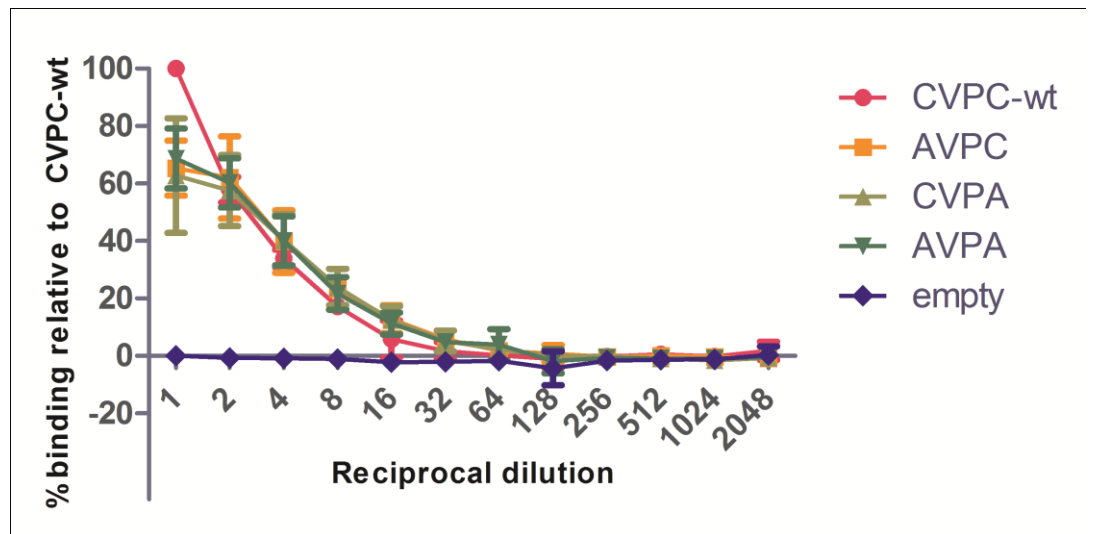


Figure 4-10. Solid phase E2-CD81 binding assay for Cys to Ala mutants. The ability of E1E2 from HCVpp to bind CD81 relative to CVPC-wt was determined in a direct binding immunoassay using recombinant CD81 MBP-LEL¹¹³⁻²⁰¹. Background binding of HCVpp lacking envelope (empty) is shown. Data shown are the mean and standard error of 4 independent experiments.

4.2.10 Entry competence of C²²⁶VPC cysteine mutants

The above result demonstrates that E2 expressed in the presence of E1 containing CVPA, AVPC or AVPA mutations largely retains the ability to bind CD81. Entry competence of the C²²⁶VPC Cys mutants was assessed by applying HCVpp to Huh-7 cells. Luciferase activity in cell lysates was determined 72 h later. As expected, the loss of heterodimerisation induced by mutation of the Cys residues within the C²²⁶VPC motif to either Ala or Ser led to a complete loss in viral entry competence of HCVpp ($p < 0.01$, for Cys to Ala mutants, Students' *t* test) (Figure 4-11A and B).

Due to the low virus titre produced by full length replication competent virus (HCVcc) it was not possible to perform biochemical analyses on the E1E2

glycoproteins from HCVcc. However, to determine whether the entry phenotypes observed in HCVpp were representative of those in full length virus, mutations were introduced into the genotype 2a JC1FLAG2(p7-NS-GLUC2A) construct. Cell-free virus obtained from Huh-7.5 cells transfected with *in vitro* transcribed wild-type and mutant RNA, was quantified by Ortho HCV Antigen ELISA Test kit (In Vitro Diagnostics, Tokyo, Japan). The concentration of HCV structural protein core was used to normalise virus levels prior to infection (Table 4-1). Equivalent amounts of HCVcc were applied to Huh-7.5 cells and entry levels were determined by measuring luciferase activity in the cell culture supernatant 72 h post-infection. Genotype 2a HCVcc with mutations AVPC, CVPA, SVPC or CVPS failed to infect Huh-7.5 cells and gave luciferase counts similar to the replication incompetent NS5B mutant GND [115] consistent with entry abrogation observed for these mutants in HCVpp (Figure 4-11C and D).

To determine whether the mutations affected virus replication, CVPC-wt and mutant RNAs were normalised by real time RT-PCR amplification of a conserved region of core, prior to transfection of Huh-7.5 cells. Transfected cells were lysed 24 h later and luciferase activity in the cell lysate measured. It was found that replication of each Cys to Ala mutant was comparable to CVPC-wt (Table 4-1).

These results demonstrate that the Cys residues in the C²²⁶VPC motif are strictly required for the formation of a functional E1E2 heterodimer.

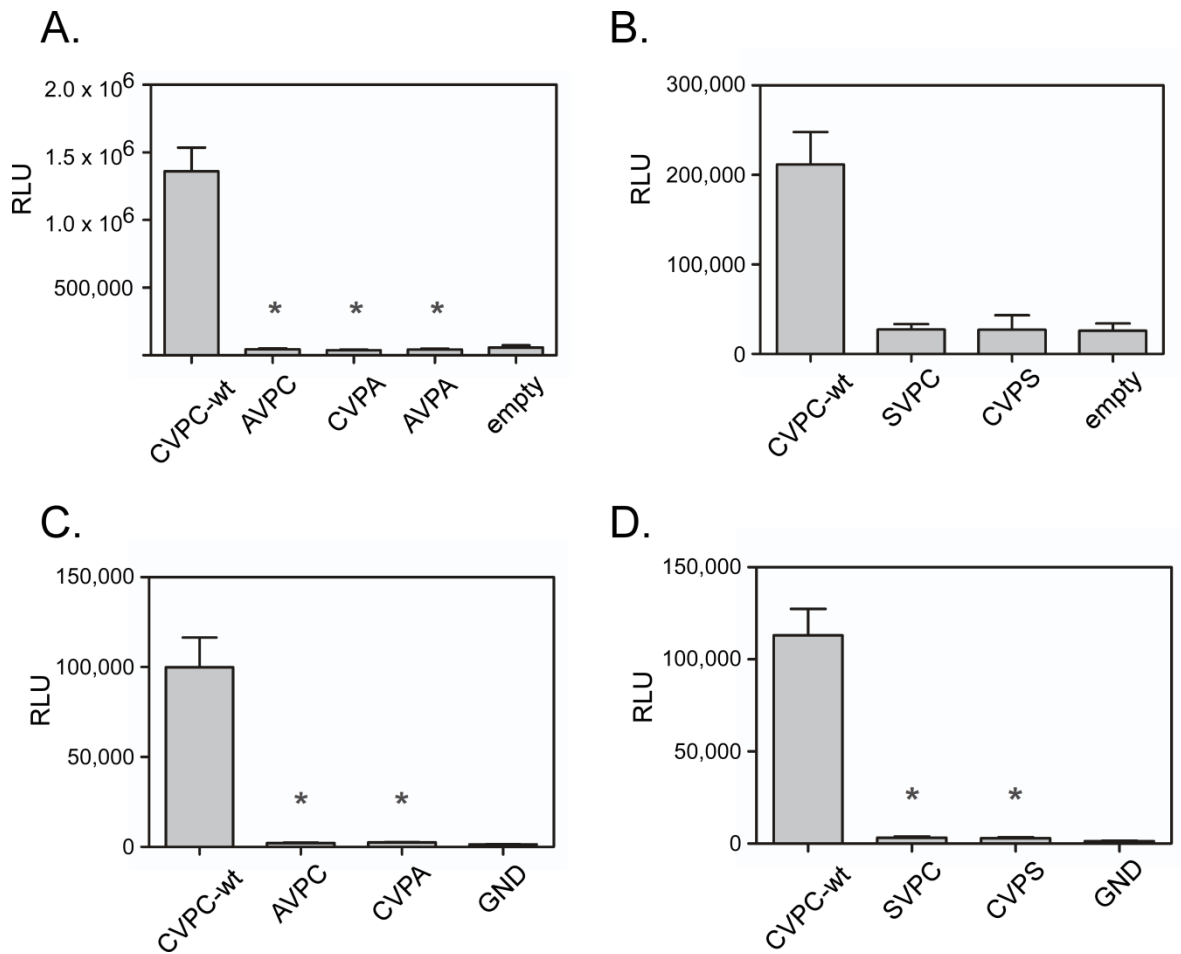


Figure 4-11. Effect of cysteine mutagenesis on HCVpp and HCVcc entry. A and B. Single cycle entry of CVPC-wt HCVpp and HCVpp containing Cys to Ala (A) or Cys to Ser (B) mutations in E1 were determined by luciferase activity (RLU) in the cell lysate 72 h post Huh-7 infection. Background entry of HCVpp lacking envelope (empty) is shown. C and D. Infectivity of genotype 2a full length virus JC1FLAG2(p7-NS-GLUC2A) containing Cys to Ala (C) or Cys to Ser mutations (D) was determined by addition of equivalent amounts of cell free virus to Huh-7.5 cells. Luciferase activity (RLU) in the cell culture supernatant was determined 72 h post-infection. Replication incompetent mutant GND shows the background level of entry. Data are the mean and standard error of 4 (A, C and D) or 2 (B) independent experiments performed in quadruplet. Asterisks indicate mutants with significantly different entry levels relative to CVPC-wt ($p < 0.05$, Student's *t*-test).

Table 4-1. Replication rate and concentration of structural protein core in HCVcc CVPC-wt and Cys mutant viruses. Replication rates of each mutant relative to CVPC-wt were determined by luciferase activity in the cell lysate of transfected cells 24 h post transfection. Quantification of structural protein core in virus stocks is shown as determined by ORTHO® HCV Antigen ELISA Test Kit (In Vito Diagnostics, Tokyo, Japan).

Mutant	Replication rate relative to CVPC-wt	Core (fmol/L)
CVPC-wt	100%	853
AVPC	84%	691
CVPA	70%	893
SVPC	[Not done]	994
CVPS	[Not done]	2 000
GND	2%	[Not done]

4.3 Results - Role of C²²⁶VPC Val, Pro Dipeptide in Glycoprotein Biosynthesis and Virus Entry

Since mutagenesis of the conserved cysteine residues within the C²²⁶VPC motif prevented formation of a functional E1E2 heterodimer, it was not possible to use these mutants to investigate the role of this motif in virus entry. In redox active proteins, the pK_a of the internal dipeptide within the CXXC motif contributes to the redox potential of the motif by influencing the pK_a of the catalytic thiol [391,392,393]. Furthermore, the structure of the dipeptide residues determines the position and accessibility of the thiol active cysteine to the target protein [394]. Compared to cysteine mutagenesis, mutagenesis of the dipeptide residues may allow subtle modification of C²²⁶VPC motif activity without necessarily abrogating it altogether. Introduction of mutations that allow normal biosynthesis of the E1E2 glycoproteins would then allow examination of the role of this motif in virus entry.

Mutagenesis of dipeptide residues Val227 and Pro228 was performed in the context of the prototype strain H77c using the CMV promoter driven E1E2 expression vector, pE1E2H77c. A series of mutations were introduced at Val227

and Pro228 that modified the structure and/or the pK_a of the residues. Mutagenesis of Val227 to Met, Leu, Ile or Ala (CMPC, CLPC, CIPC and CAPC, respectively) retained the neutral charge at this position while altering the size and length of the carbon side chain. Substitution of Val227 with Glu (CEPC) was performed to provide the motif with a negative charge at physiological pH, thereby altering the local environment (and potentially the pK_a) of the C²²⁶VPC Cys residues. Proline is considered a helix breaking residue, inducing kinks in helical regions of approximately 26° [281]. To investigate the significance of this residue in the C²²⁶VPC motif, Pro228 was mutated to the helix inducing residue, alanine (CVAC).

4.3.1 Western blot analysis of Val227, Pro228 mutants

To determine the effect of Val, Pro dipeptide mutagenesis on E1 and E2 expression, Western blot analysis was performed on HEK 293T cells transfected with pE1E2H77c. Cells were lysed 48 h post transfection and lysates run on reducing SDS-PAGE. Blots were probed with anti-E1 and anti-E2 MAbs, A4 and H52, that recognise linear epitopes in E1 and E2, respectively. Visualisation of the blots shows that mutants CMPC, CLPC, CIPC and CAPC show normal levels of E1 and E2 expression (Figure 4-12). However, CVAC and to a lesser degree, CEPC, show slightly reduced levels of E1. This indicates that mutations that alter the charge of the C²²⁶VPC motif (CEPC) or alter the structure of the motif (CVAC) result in a decrease in E1 protein expression, or possibly its degradation upon expression. In all cases E2 was expressed at WT levels suggesting that the reduced level of E1 observed for CEPC and CVAC mutants has not affected the amount of E2 produced. Importantly, subtle mutations at Val227 that have retained the neutral charge but changed the length of the carbon side chain at this position, allowed WT levels of E1 and E2 expression.

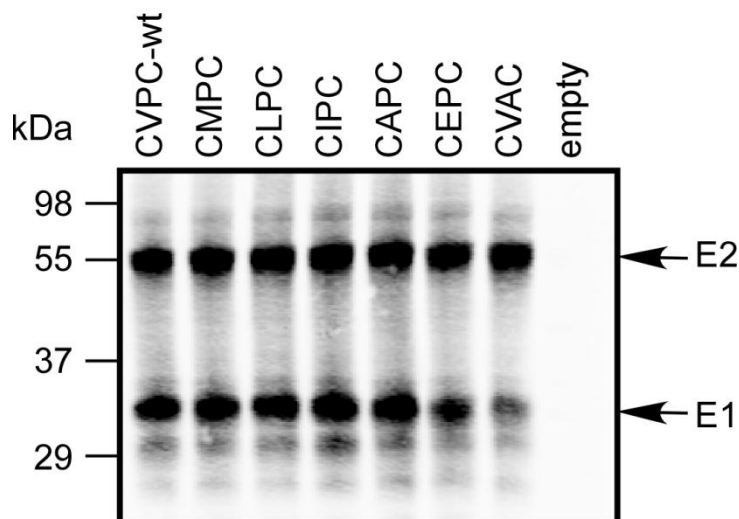


Figure 4-12. Western blot analysis of Val227, Pro228 mutants. HEK 293T cells transfected with pE1E2H77c were lysed 48 h post transfection and lysates were subjected to reducing SDS-PAGE. Expression of E1 and E2 was detected by MAbs A4 and H52 that recognise linear epitopes in E1 and E2, respectively. Blots were imaged by LI-COR. Molecular weight markers are shown to the left of the gel.

4.3.2 Expression of E1E2 heterodimers from Val, Pro mutants

To investigate the effect of Val and Pro mutagenesis on E1E2 heterodimerisation, HEK 293T cells transfected with pE1E2H77c were radiolabelled with ^{35}S -Met/Cys for 30 min followed by chase in DMF10 and cell lysis. Conformation sensitive MAb H53 was used to immunoprecipitate E2 and any associated E1. Samples were run on non-reducing SDS-PAGE and phosphorimaged. It was found that all mutant forms of E1 were able to form non-covalent heterodimers with E2 (Figure 4-13). CAPC, CEPC and CVAC mutants showed slightly reduced levels of E1 co-precipitated with E2. However, non-covalent E1 containing mutations V227M, L or I, co-precipitated with E2 at similar levels to CVPC-wt. This suggests that the ability of E1 and E2 to heterodimerise has been retained for each of these mutants.

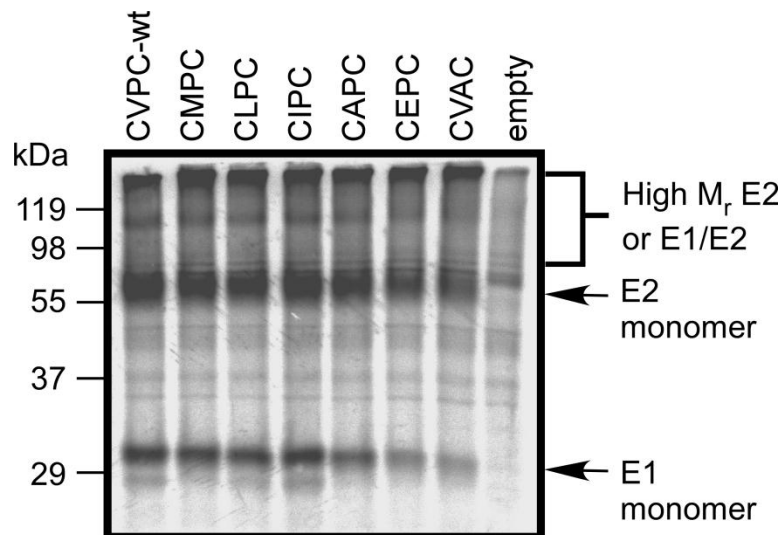


Figure 4-13. Analysis of E1E2 heterodimerisation of Val, Pro mutant E1E2 in HEK 293T cell lysates. HEK 293T cells transfected with pE1E2H77c were metabolically labelled with ^{35}S -Met/Cys prior to cell lysis. Immunoprecipitation was performed with conformation sensitive anti-E2 MAb H53 followed by separation of the proteins by non-reducing SDS-PAGE and phosphorimaging. The positions of molecular weight markers are shown to the left of the gel.

4.3.3 HCVpp incorporation of conformational E1E2 from Val, Pro mutants

To determine whether Val or Pro mutagenesis affects maturation and incorporation of E1E2 into HCVpp, wild-type and mutant HCVpp produced in HEK 293T cells were metabolically labelled with ^{35}S -Met/Cys prior to lysis. HCVpp incorporation of non-covalent E1 and E2 heterodimers was analysed for each mutant by immunoprecipitation using conformational anti-E2 MAb H53.

Introduction of an acidic residue at Val227 (CEPC) largely abrogated incorporation of H53-reactive non-covalent E1E2 heterodimer into HCVpp (Figure 4-14A). This was also the case when Pro228 was mutated to Ala, indicating that these mutations caused structural defects preventing E1E2 heterodimerisation. However, it was found that conservative mutations at Val227 that retained the hydrophobicity at this position (M, L, I or A) allowed incorporation of E1E2 heterodimers into mature HCVpp. Quantitative analysis of E1 and E2 from 4 independent experiments showed that level of E1 incorporation relative to E2 varied for each mutant. This was calculated by dividing the amount of non-

covalent E1 by the amount of non-covalent E2 detected in HCVpp for each mutant. For Val227 mutants, it was found that E1E2 heterodimerisation consistently followed the order CVPC-wt>M=L>A>E. The P228A mutant did not have detectable levels of E1 incorporation (Figure 4-14B). Equivalent input of HCVpp for each immunoprecipitation reaction was confirmed by MAb 183 precipitation of HIV-1 capsid p24 (Figure 4-14A, lower panel).

This finding demonstrates that mutagenesis of Val227 to Met, Iso or Leu allows incorporation of high levels of non-covalent, conformational, heterodimeric E1 and E2 into mature HCVpp. Therefore, these mutations introduced into the E1 C²²⁶VPC motif are not likely to induce severe biosynthetic defects in the HCV envelope glycoproteins.

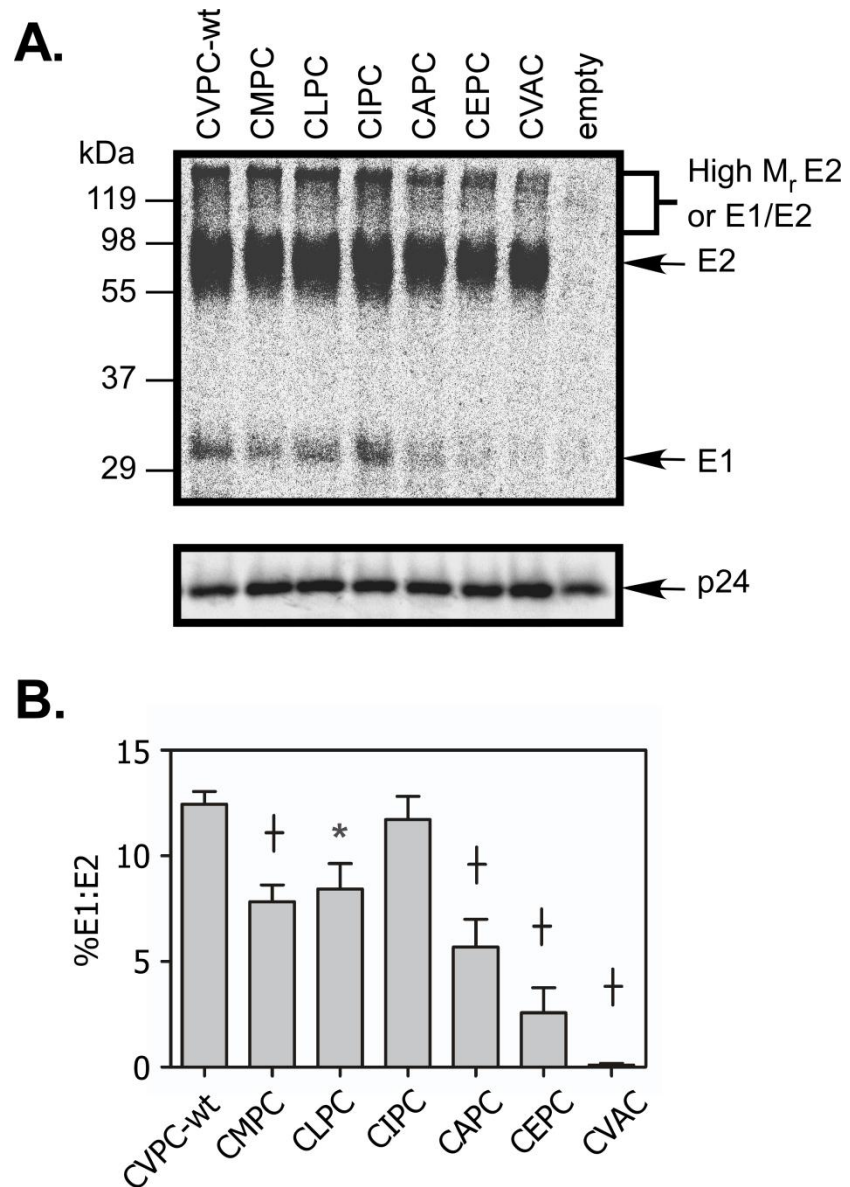


Figure 4-14. Characterisation of conformational E1E2 incorporation into mature HCVpp for V227, P228 mutants. A. Incorporation of non-covalently associated wild-type (CVPC-wt) and mutant E1E2 heterodimers into HCVpp was determined by metabolically labelling HCVpp with ³⁵S-Met/Cys and immunoprecipitation with conformation sensitive anti-E2 MAb H53. Proteins were separated by non-reducing SDS-PAGE and phosphorimaged. The positions of molecular weight markers are shown to the left. Incorporation of HIV-1 capsid protein p24 into each HCVpp mutant was determined by immunoprecipitation with MAb 183 (bottom panel). B. Quantification of E1 incorporation into HCVpp relative to E2 was determined for each mutant by densitometry. Data shown are the mean and standard error from 4 independent experiments. Asterisks and crosses represent E1 incorporation that is significantly lower than CVPC-wt ($p < 0.05$ and $p < 0.01$, respectively, Student's *t*-test).

4.3.4 HCVpp incorporation of total E1E2 from Val, Pro mutants

To compare the total amount of heterodimeric E1E2 incorporated into viral particles for each mutant, HCVpp were radiolabelled with ^{35}S -Met/Cys prior to lysis. Particle lysates were then subjected to immunoprecipitation by polyclonal anti-E2 antibody GP1. When run under non-reducing conditions, non-covalent E1E2 heterodimer incorporation appeared identical to that seen by conformational anti-E2 precipitation for each construct (Figure 4-15A). This was also the case when the samples were run under reducing conditions (Figure 4-15B). Notably, CEPC and CVAC still showed reduced levels of E1 suggesting these mutations may induce a conformational change in E1 or E2 that precludes HCVpp incorporation of non-covalent heterodimers.

Together, these results demonstrate that Pro228 and a hydrophobic residue at Val227 are essential for normal glycoprotein biosynthesis. Importantly, they show that substitution of Val227 with isoleucine allows WT levels of E1E2 incorporation while CMPC and CLPC mutants demonstrate only slightly lower levels of non-covalent E1E2 heterodimerisation compared to CVPC-wt. Therefore in the absence of obvious biosynthetic defects, these mutants represent good candidates for assessing the role of the C²²⁶VPC motif in virus entry.

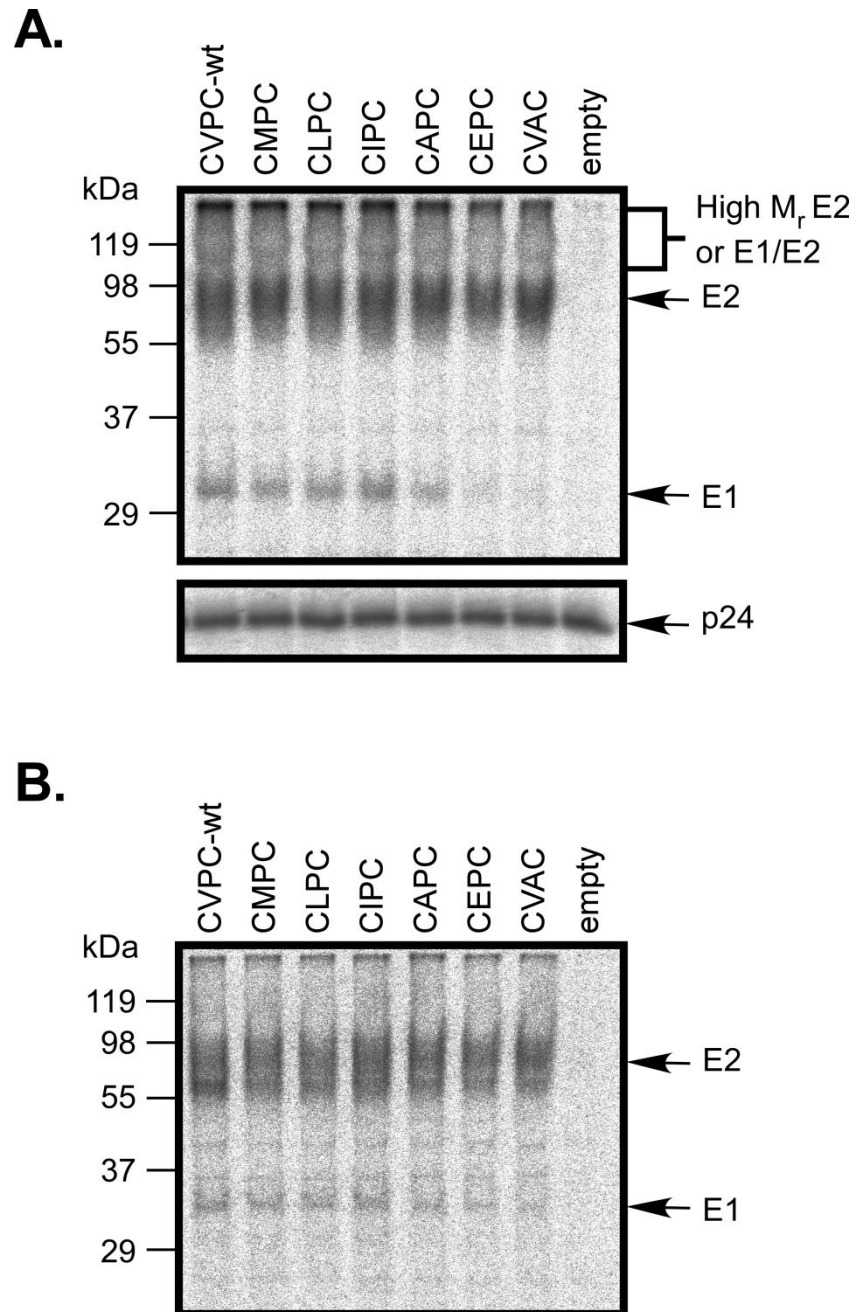


Figure 4-15. Characterisation of total E1E2 incorporation into mature HCVpp for V227, P228 mutants. A and B. HCVpp were prepared and radiolabelled with ^{35}S -Met/Cys prior to lysis. Immunoprecipitation was performed using polyclonal anti-E2 antibody GP1. Proteins were separated by non-reducing (A) or reducing (B) SDS-PAGE and phosphorimaged. The positions of molecular weight markers are shown to the left. Incorporation of HIV-1 capsid protein p24 into each HCVpp mutant was determined by immunoprecipitation with MAb 183 (A, bottom panel). Note that samples were split after E2-immunoprecipitation therefore a single MAb 183 immunoprecipitation was performed.

4.3.5 CD81 binding by Val227, Pro228 mutants

In order to identify a role for the C²²⁶VPC motif in virus entry it is important to first determine whether the mutations introduced have affected formation of important conformational regions in the glycoproteins such as the E2 CD81 binding site. Therefore, dipeptide mutants were assessed for CD81 binding by direct binding immunoassay as described in section 4.2.9. HCVpp normalised for E2 input were serially diluted across immobilised MBP-LEL¹¹³⁻²⁰¹. E2 binding was detected by H53 and horseradish peroxidase-conjugated rabbit anti-mouse immunoglobulin.

Across 4 independent experiments it was found that the dilution of HCVpp required to achieve 50% binding to CD81 was similar for each mutant compared to CVPC-wt, indicating that the mutations in E1 have not affected formation of the CD81 binding site in E2 (Figure 4-16). However, like the Cys mutants, a slight but significant decrease in the total E2 bound to CD81 was evident for mutants CMPC, CAPC, CEPC and CVAC ($p < 0.05$, Student's *t*-test). As described above, this effect may be indicative of a change in binding stoichiometry. It is possible that mutations within the C²²⁶VPC dipeptide may have altered the proportion of non-covalent and high molecular weight forms of E1E2 incorporated into HCVpp for these mutants. This hypothesis is supported by the significant variation in heterodimeric non-covalent E1E2 incorporation into HCVpp for each mutant, despite the presence of similar levels of non-covalent E2 (Figure 4-14 and Figure 4-15). This would suggest that the arrangement of the glycoproteins on the surface of these mutant viruses may be different. In spite of this, CD81 binding by CLPC and CIPC mutants was observed at WT levels indicating that these mutants appear to allow normal maturation of E1 and E2 into HCVpp, with no detectable perturbations to the CD81 binding site in E2. As such, CLPC and CIPC provide good candidates for analysing the role of the C²²⁶VPC motif in virus entry.

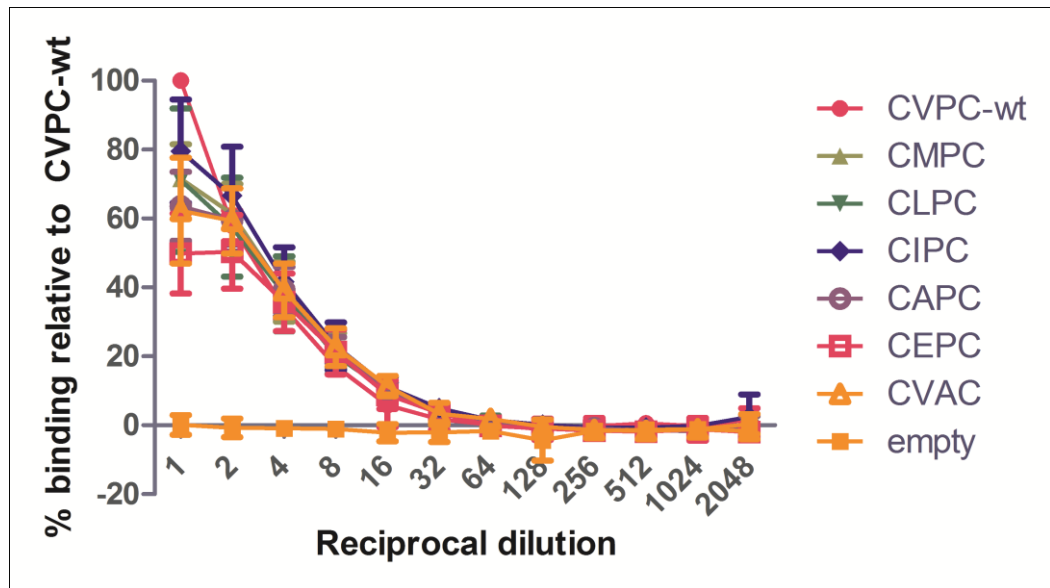


Figure 4-16. Solid phase E2-CD81 binding assay for Val227, Pro228 mutants. The ability of E1E2 from HCVpp to bind CD81 relative to CVPC-wt was determined in a direct binding immunoassay using recombinant CD81 MBP-LEL¹¹³⁻²⁰¹ as described above. Data shown are the mean and standard error of 4 independent experiments.

4.3.6 Formation of immunologically distinct domains in C²²⁶VPC mutants

In 2004, Keck *et al.* identified three immunologically distinct domains in E2 (termed A, B and C) which contain conformational epitopes [94]. In the proposed E2 structure of Krey *et al.* (2010) the majority of the CD81 binding site on E2 occurs within domain I (B) while an additional CD81 binding determinant is located on domain III (C) [273].

The CD81 binding data suggests that domain B (I) and possibly C (III) is intact for all mutants. To further probe the conformation of domains A (II) and C (III) a selection of E1 C²²⁶VPC mutants were further screened for conformational defects in E2 induced by the E1 mutations. Immunoprecipitation of radiolabelled E1E2 from lysed HCVpp was carried out using conformation sensitive monoclonal antibodies directed against domains A and C [94,368,395].

Monoclonal antibodies CBH 4D (domain A) and CBH 7 (domain C) recognised E2 from CVPC-wt and mutants AVPC, CLPC and CEPC equally well

while control MAb CBH 11 did not detect E2 from any construct (Figure 4-17). Equivalent input of HCVpp into each immunoprecipitation reaction was determined by precipitation of HIV-1 structural protein p24 using MAb 183 (Figure 4-17, bottom panel). These results suggest that despite the heterodimerisation defects observed for AVPC and CEPC mutants, conformational epitopes on all three immunological domains are formed in E2. Given the absence of non-covalently associated E1 for AVPC and the low levels detected for CEPC, it is unlikely that non-covalent E1 is required for the acquisition of these domains in E2.

Using a range of anti-E2 MAbs directed towards different conformational epitopes, it appears that mutation of Val227 to leucine does not affect the folding of E2 or the ability of each of these conformers to heterodimerise with E1, confirming this mutant as a candidate for assessing the role of the C²²⁶VPC motif in virus entry. Although there is no equivalent panel of antibodies with which to probe conformational changes in E1, the ability of E1 to form a non-covalent heterodimer with E2 provides a stringent test for ensuring that the integrity of the E1 fold has been maintained.

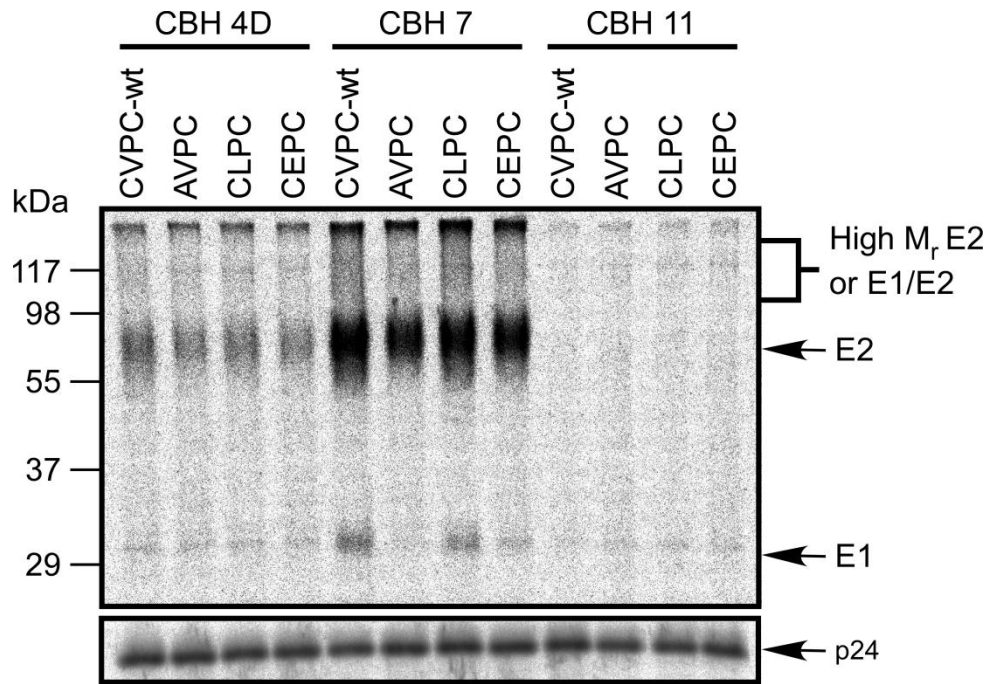


Figure 4-17. Characterisation of E1 and E2 incorporated into HCVpp by domain specific, conformational antibodies. HCVpp incorporation of non-covalently associated CVPC-wt and mutant E1E2 heterodimers was determined by metabolically labelling HCVpp with ^{35}S -Met/Cys prior to lysis, and immunoprecipitation with conformation sensitive MAbs against 2 immunologically distinct domains in E2. Non-reactive MAb CBH 11 was included as a control. Proteins were separated by non-reducing SDS-PAGE and phosphorimaged. The positions of molecular weight markers are shown to the left. Incorporation of HIV-1 capsid protein p24 into each HCVpp mutant was determined by immunoprecipitation with MAb 183 (bottom panel).

4.3.7 Entry competence of Val227 and Pro228 mutants

To determine whether mutagenesis of the C^{226}VPC internal dipeptide affects virus entry, each HCVpp mutant was subjected to a single cycle entry assay as described in section 4.2.10. All HCVpp mutants were found to enter at significantly lower levels than CVPC-wt (Figure 4-18A, $p < 0.05$, Student's *t*-test). For mutants that demonstrated little or no E1E2 heterodimerisation (CEPC and CVAC) entry was abrogated as expected. Interestingly, for V227 mutants where heterodimerisation was retained a range of entry competence was observed. Heterodimerisation competent mutants CMPC, CIPC and CAPC entered at 31%, 37% and 41%, respectively, compared to CVPC-wt. However, CLPC which

demonstrated normal E1E2 incorporation and heterodimerisation in HCVpp, normal CD81 binding and E2 domain formation, failed to mediate virus entry. This result suggests that the C²²⁶VPC motif is strictly and specifically required for maintaining entry competence of HCV.

A selection of mutations were introduced into the full length replication competent construct JC1FLAG2(p7-NS-GLUC2A) (HCVcc). These mutants were chosen based on the range of heterodimerisation phenotypes observed in HCVpp. Cell free virus obtained from Huh-7.5 cells transfected with *in vitro* transcribed wild-type and mutant JC1FLAG2(p7-NS-GLUC2A) RNA, was quantified by Ortho HCV Antigen ELISA Test kit (In Vitro Diagnostics, Tokyo Japan). The concentration of HCV structural protein core was used to normalise virus levels prior to infection. The replication rate for each mutant was also determined as described in section 4.2.10, and was found to be similar to CVPC-wt in each instance (Table 4-2).

Consistent with the observed effects in HCVpp, HCVcc virus encoding CEPC failed to enter and replicate in Huh-7.5 cells. By contrast, replication of HCVcc virus encoding CMPC was less attenuated compared to HCVpp, displaying a 30% reduction in infectivity, although this was not deemed to be a significant difference ($p=0.053$, Student's *t*-test) (Figure 4-18B). The CAPC mutant, which had a 60% reduction in HCVpp entry, was further attenuated in the HCVcc system; no entry and replication was observed. These results indicate that the highly conserved C²²⁶VPC motif is essential for virus entry in both genotype 1a (HCVpp) and genotype 2a (HCVcc) viruses.

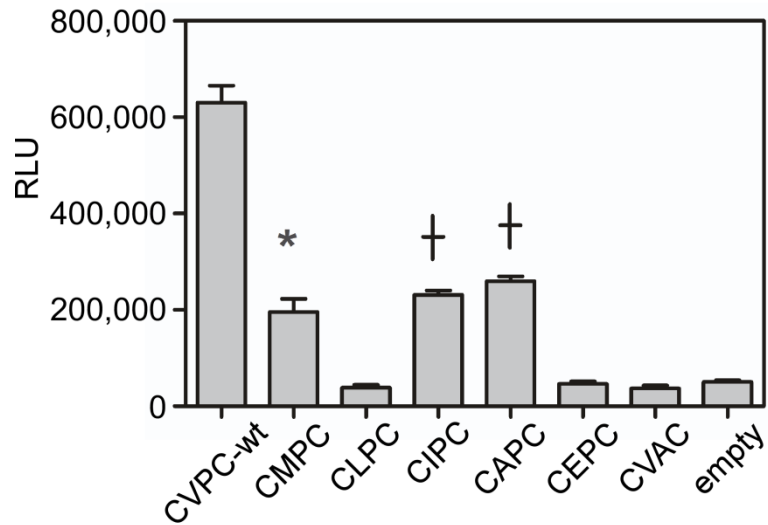
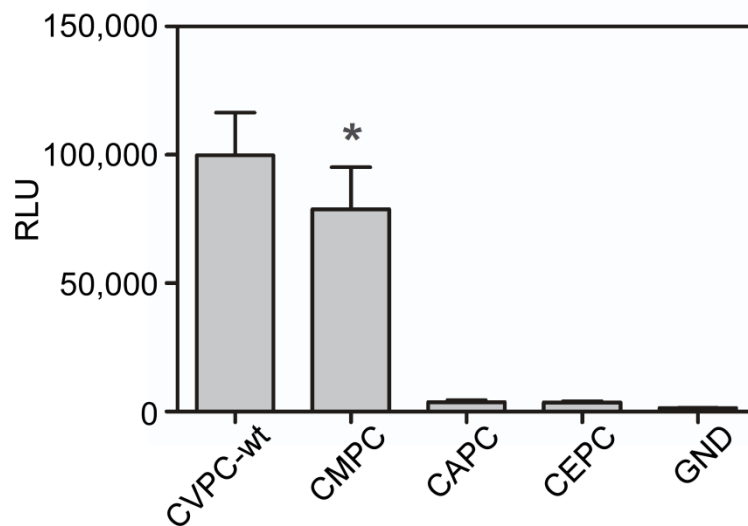
A.**B.**

Figure 4-18. Effect of Val, Pro mutagenesis on HCVpp and HCVcc entry. A. Single cycle entry of CVPC-wt HCVpp and HCVpp containing Val227 or Pro228 mutations in E1 were determined by luciferase activity (RLU) in the cell lysate 72 h post Huh-7 infection. Background entry of HCVpp lacking envelope (empty) is shown. B. Infectivity of genotype 2a HCVcc containing Val227 or Pro228 mutations was determined by addition of equivalent amounts of cell free virus to Huh-7.5 cells. Luciferase activity (RLU) in the cell culture supernatant was determined 72 h post-infection. Replication incompetent mutant GND shows the background level of entry. Data shown are the mean \pm standard error of 3 (A) or 4 (B) independent experiments performed in quadruplet. Asterisks and crosses indicate mutants with significantly different entry levels relative to empty (A) or GND (B) background controls ($p < 0.05$ and $p < 0.01$ respectively, Student's *t*-test).

Table 4-2. Replication rate and concentration of structural protein core in HCVcc CVPC-wt and Val227, Pro228 mutant viruses. Quantification of structural protein core used for normalisation of virus concentrations prior to infectivity assays is shown as determined by ORTHO® HCV Antigen ELISA Test Kit (In Vito Diagnostics, Tokyo, Japan). Replication rates of each mutant relative to CVPC-wt were determined by luciferase activity in the cell lysate of transfected cells 24 h post transfection.

Mutant	Core (fmol/L)	Replication rate relative to CVPC-wt
CVPC-wt	853	100%
CMPC	1413	87%
CAPC	852	115%
CEPC	218	139%
GND	[Not done]	2%

4.4 Results - Maleimide Biotinylation of Val227 Mutants

As described above, the internal dipeptide of a CXXC motif modulates the structure [394] and redox potential [396,397,398] of thioredoxin family proteins. The redox potential is largely pH dependent and has been shown to be related to the pK_a of the side chains of the dipeptide. In addition, other regions proximal to the motif in secondary structure can influence the pK_a of the N-terminal catalytic thiol with a reduction in pK_a corresponding to an increase in redox potential [388,391].

If the role of the C²²⁶VPC motif is to control disulfide bonding changes in E1 and/or E2, it is possible that the mutations introduced at Val227 have altered the redox potential of the motif. Mutation of Val227 to another uncharged residue such as Leu or Ile would not change the pK_a within the dipeptide but may induce localised structural changes that alter the redox potential of the catalytic thiol group as described above. If the redox potential has been altered then it is possible that the active site sulfhydryl groups would be in an inactive oxidised state in the pre-fusion form of E1E2. This would prevent the motif from catalysing reduction of existing disulfide bonds within the glycoprotein complex.

Two mutants, CIPC and CLPC, were investigated to determine whether introduction of these mutations altered the number of free sulfhydryl groups in pre-fusion E1 and/or E2 in the context of HCVpp. These mutants were selected because they both demonstrate apparently normal E1E2 biosynthesis and incorporation into HCVpp. In addition they both bind CD81 in a wild-type manner. However, each mutant demonstrates severely impaired entry. This suggests that despite normal biosynthesis, CIPC and CLPC cannot proceed past CD81 binding during virus entry.

HCVpp were partially purified through a sucrose cushion and labelled with maleimide-biotin or NHS-biotin as described in Chapter 3. For mutants CIPC and CLPC, E1 and E2 could be detected with both biotinyllating agents. Across an average of three experiments it was determined that maleimide-biotin labelling of E1 and E2 from each mutant was not significantly different to wild-type (Figure 4-19 and Table 4-3). Equivalent input of HCVpp expressing equal amounts of E1 and E2 was confirmed by Western blot analyses of lysed HCVpp prior to streptavidin agarose precipitation for CVPC-wt and each mutant (Figure 4-19, lower panel). These results suggest that CIPC and CLPC have the same pre fusion oxidation state as CVPC-wt E1 and E2. Given that these mutants appear to have a normal biosynthesis phenotype and are capable of binding CD81, it seems these mutants are blocked at a stage of entry, unable to undergo fusion activation. This result may indicate that mutation of the internal dipeptide residues alters the redox potential within the CXXC motif whereby the catalytic thiol group is no longer able to catalyse disulfide reduction/isomerisation required to facilitate conformational changes associated with fusion activation. Alternatively, although these mutants can still bind CD81, it is possible that CLPC and CIPC mutations block a conformational change at cellular binding that affects downstream events required for fusion activation.

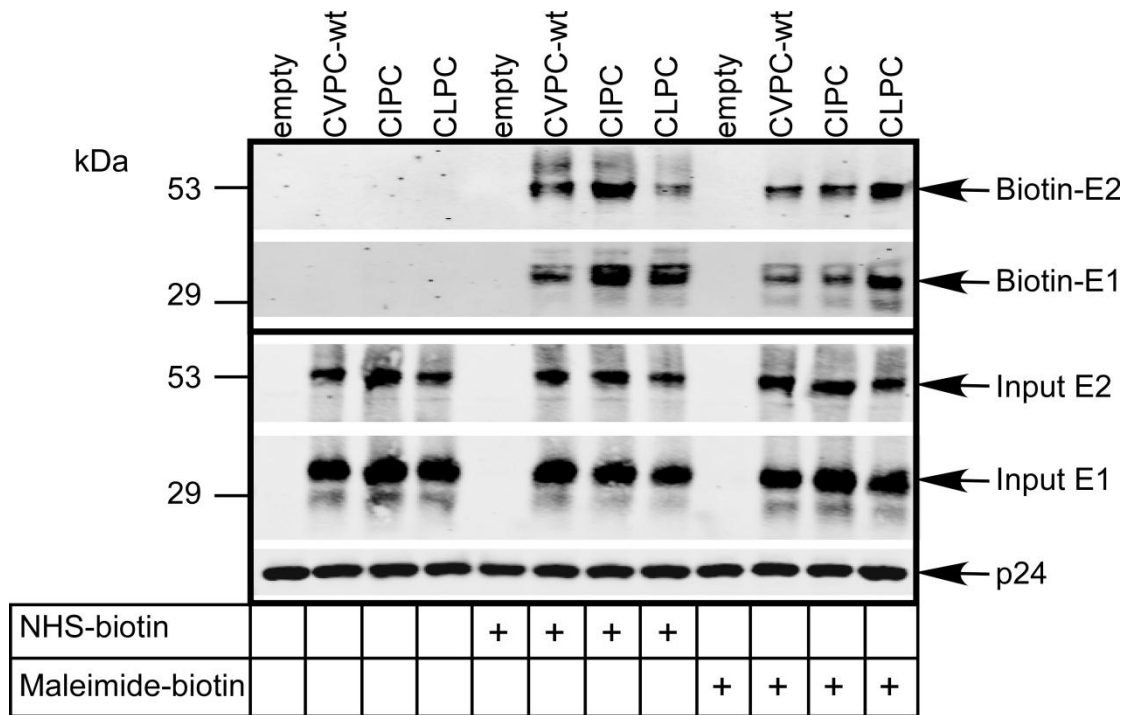


Figure 4-19. Characterisation of free sulfhydryl groups in E1 and E2 of Val227 mutants. Partially purified HCVpp expressing CVPC-wt, CIPC or CLPC mutant E1E2 or no envelope control (empty) were labelled with Maleimide-PEG2-Biotin (Maleimide-Biotin) or Sulfo-NHS-LC-Biotin (NHS-Biotin). Particles were lysed and reduced by addition of DTT prior to capture of biotinylated proteins by streptavidin agarose. Samples were run on reducing SDS-PAGE and examined in Western blotting with anti-E2 and anti-E1 MAbs H52 and A4, respectively. Blots were imaged by LI-COR. Molecular weight markers are shown to the left. Equivalent input of E1, E2 and HIV-1 capsid protein p24 were determined by Western blot (probed with MAbs A4, H52 and 183, respectively) for each sample prior to streptavidin agarose pull-down.

Table 4-3. Quantitative comparison of Maleimide-biotin labelling of E1 and E2 from V227I/L HCVpp. Ratio of NHS-biotin labelling relative to Maleimide-biotin labelling was calculated for CVPC-wt, CIPC and CLPC E1 and E2 by densitometry from 3 independent experiments. Data shown are the mean \pm standard error.

Mutant	E2	E1
CVPC-wt	2.50 \pm 0.77	1.55 \pm 0.45
CIPC	1.95 \pm 0.21	1.57 \pm 0.11
CLPC	1.78 \pm 0.48	1.63 \pm 0.44

4.5 Discussion and Conclusions

This investigation identified and characterised a highly conserved thioredoxin-like C²²⁶VPC motif in HCV envelope glycoprotein E1 and found that it is essential for both correct E1E2 biosynthesis and HCV entry. Mutagenesis of the cysteine residues within the C²²⁶VPC motif to either Ala or Ser caused biosynthetic defects, including a loss of non-covalent heterodimeric E1 and E2 in mature viral particles. Conservative mutations introduced at Val227 that retained the neutral charge at this position, allowed normal biosynthesis of E1 and E2 glycoproteins and mutant virus retained CD81 binding function. However, each of these valine mutants demonstrated severely impaired entry suggesting that this motif is additionally required to function during virus entry.

Thioredoxin family proteins are found in all living organisms. Although diverse in sequence these proteins typically have the common feature of a CXXC isomerisation motif [399]. Proteins from this family have been shown to demonstrate a range of functional activities including catalysing disulfide bond formation, reduction and isomerisation in target proteins, and therefore play an integral role in protein folding. The activity of these proteins is provided by a catalytic thiol, usually the N-terminal cysteine within the CXXC motif. When in a reduced state, deprotonation of this cysteine renders the thiol active, capable of attacking disulfide bonds in a target protein. Resolution of this mixed disulfide by the second Cys in the CXXC motif leaves the motif oxidised in an intermediary intramolecular disulfide bond, while the target protein is left reduced. Without the constraints of the original disulfide bonding arrangement, the target protein then refolds to adopt its lowest energy conformation.

Redox active proteins have been described in many cellular locations including, but not limited to, the bacterial cytosol [379] and periplasmic space [400], the endoplasmic reticulum of mammalian cells (for example PDI [401]), and on the surface of cells [402]. In addition, as described in Chapter 3, the receptor binding glycoprotein from MLV and HTLV-1 viruses has been shown to contain a CXXC motif that controls the redox status and fusion activation of their viral

envelope glycoproteins [359,360], demonstrating a role for CXXC motifs in virus entry. Thus redox active proteins have a great propensity to adapt their functionality to specific roles.

In 2005, Brazzoli *et al.* showed association of un-oxidised forms of HCV glycoprotein E2 (folding intermediates) with oxidised forms of E1 at early stages of biosynthesis and proposed that E1 may act as a chaperone assisting the folding of E2 [234]. While this was not directly assessed in this project, an interesting finding from the pulse chase analyses of the C²²⁶VPC single cysteine mutants was the apparent accumulation of high molecular weight species identified by each immunoprecipitation reaction. These may represent trapped folding intermediates unable to resolve intermolecular disulfide linkages, or possibly glycoprotein aggregates resulting from aberrantly formed disulfide bonds. Given that the high molecular weight forms were detected when precipitated by MAbs directed towards linear epitopes in E1 and E2, (H52 and A4, respectively), the oligomeric forms may consist of E1, E2 or disulfide linked E1E2. The involvement of the C²²⁶VPC Cys residues in modulating formation of the disulfide linked multimers is supported by the finding that these forms did not accumulate when both Cys residues within the motif were removed (AVPA). Therefore, one apparent role of the C²²⁶VPC motif is to regulate the folding of a functional non-covalent E1E2 heterodimer.

Although these data indicate that the E1 C²²⁶VPC motif is required for formation of a functional heterodimer there have been many publications demonstrating expression of the E2 ectodomain in a soluble form independently of E1. This form of E2 (E2₆₆₁ RBD) is recognised by conformational, neutralising antibody and is capable of binding CD81 and SR-BI receptors [5,6,246,403]. The results from this mutagenesis study suggest that E1 is not likely to be required for the folding of a receptor-binding competent form of E2 consistent with these reports. Although substitution of either or both Cys residues with alanine prevented incorporation of non-covalently associated E1 into mature HCVpp, conformational epitopes on E2 recognised by MAb H53 and receptor CD81 were retained in the virion incorporated forms of E2. In addition, analysis of the AVPC mutant using

domain specific conformational MAbs directed toward two further immunological domains in E2₆₆₁ RBD suggests these too are formed correctly. These data indicate that non-covalent E2-associated E1 is not required to maintain the three immunologically distinct domains in E2₆₆₁ RBD. However, given that HCV is not functional in the absence of E1 it is not possible to determine whether E2 present in virions without E1 is truly representative of pre fusion heterodimeric virion incorporated E2. The available conformation-sensitive antibodies are directed towards the receptor binding domain (RBD) of E2 and do not probe the membrane MPHR that is located between the RBD and the TMD. The MPHR is an important heterodimerisation determinant and its structural integrity is essential for HCV infectivity [95]. It is predicted that the E2 MPHR may be functionally analogous to the stem region in flavivirus glycoprotein E which provides important hydrophobic contacts stabilising the prM-E heterodimer at neutral pH as well as promoting trimer formation during fusion activation at low pH [280]. Therefore alteration to this region of HCV E2 is likely to be detrimental to virus function. Although the exact role of HCV glycoprotein E1 during biosynthesis and entry remains unclear, one possibility is that it is required to maintain the metastable conformation of pre fusion E2. It is possible that here, in the absence of virion incorporated E1, the structure of E2 has been altered outside of the RBD, for example within the MPHR, rendering the virus inactive.

In contrast to the effects of cysteine mutagenesis, some conservative mutations were tolerated at Val227 within the C²²⁶VPC motif without interfering with E1E2 heterodimerisation. Interestingly, all mutations tested reduced entry competence, indicating that this motif plays an essential role during virus entry. Mutants CLPC and CIPC were found to bind recombinant CD81 at WT levels which may indicate that the block in entry occurs at a stage after viral attachment to CD81. Alternatively, these mutants may be unable to undergo conformational changes following virus attachment required to initiate downstream events for fusion activation. Together, these results indicate that in addition to the requirement for the E1 C²²⁶VPC motif during glycoprotein biosynthesis, this motif is required during virus entry, possibly as a redox regulator.

The strict conservation of the dipeptide residues within the C²²⁶VPC motif is in contrast to what has been observed for numerous bacterial thioredoxin family proteins. The internal dipeptide in CXXC containing proteins has been implicated with controlling the redox potential [392,393] as well as determining how the protein positions the active thiol groups for substrate association [394]. Numerous studies have investigated substitution of the dipeptide between oxidoreductases. Substitution significantly alters the activity of the mutated protein and at times it will adopt the redox activity of the protein from which the dipeptide was derived [396,397,398].

The apparent lack of redundancy in the HCV E1 C²²⁶VPC motif may reflect specific protein-protein interactions required by the virus during the entry cascade. In contrast to many ER chaperones where a general role in facilitating protein folding is required, viral proteins are likely to develop specific roles over time in order to maintain a minimal genome while maximising viral replication and efficient infectivity. Although mutations CMPC, CLPC, CIPC and CAPC would not alter the charge of the dipeptide, it is possible that the minor structural changes introduced by lengthening or shortening of the amino acid side chain, may alter the local environment of the catalytic thiol, thus changing its pK_a. Given that the pK_a of a catalytically active thiol is directly related to its redox potential [388,391] it is possible that even these minor changes to the C²²⁶VPC motif could render it inactive. This is supported by the observation that mutations CMPC and CAPC had varying effects on the entry capacity of genotype 1a (HCVpp) virus compared to genotype 2a virus (HCVcc). In HCVpp, CMPC entered at 31% of CVPC-wt and CAPC entered at 41%, whereas in HCVcc CMPC entry was not significantly different to CVPC-wt and CAPC was not entry competent at all. While the redox potential of the tetrapeptide motif in isolation would be the same in each case, it is likely that due to sequence differences between the genotypes in the regions surrounding the motif, mutations would affect the secondary structure of E1 from each HCV strain differently. Therefore it is possible that the pK_a of the active thiol is now different in the two motifs.

In addition, thiol acidity is not considered the only factor that can influence the redox potential of the motif, as the difference in reduction potentials between bacterial thioredoxin (Trx; highly reducing) and DsbA (more oxidising) cannot be accounted for simply by thiol pK_a values. These studies suggest that the structure of the dipeptide and surrounding sequence can additionally influence the redox potential of the catalytic thiol in a pH independent manner. Although no single pH-independent factor can explain the redox differences between DsbA and Trx, factors such as the angle required for a disulfide bond to form and local van der Waals forces are thought to contribute. A high resolution structure of E1 or E1E2 is required in order to understand how the mutations at Val227 have affected the secondary structure of the protein.

Recently, the complete structure of the envelope glycoprotein complex from the alphavirus, chikungunya virus was reported [279]. Chikungunya virus has three envelope glycoproteins including E1, E2 and E3. Glycoproteins E2 and E3 are derived from furin cleavage of a p62 precursor. E2 is responsible for receptor binding while E1 represents a class II fusion protein, as has been described for other alphaviruses [343]. The fold of E2 consists entirely of β -sheet and belongs to the immunoglobulin (Ig) superfamily. It consists of three Ig domains termed A, B and C from the N- to C-termini. Domain A has an Ig structure analogous to domain III from class II fusion proteins. Within this domain are 2 insertions including a β -hairpin that is stabilized by two disulfide bonds, each involving a cysteine from a C¹⁹XXC thioredoxin-like motif that is conserved across the alphaviruses. The precursor glycoprotein p62 contains 9 disulfide pairs, including 6 pairs (12 cysteine residues) within E2 domains A, B and C. It has been suggested that the clustered arrangement of these disulfide pairs is compatible with disulfide reshuffling during folding of the p62-E1 heterodimer in the ER. This may be directly catalysed by the E2 CXXC motif, or may be regulated by other ER resident PDI proteins during folding. The close association of E2 domain A and E1 domain II suggests that these events would likely affect heterodimer conformation. Furthermore, the observation that the CXXC Cys residues are in an oxidised state in this structure indicates that the motif is not redox active in the mature form of the protein, consistent with a functional role for the motif during glycoprotein biosynthesis.

Interestingly, this finding demonstrates the conservation of a CXXC motif in envelope glycoproteins partnered with a predicted class II fusion protein, from distantly related alphaviruses and hepaciviruses.

From Chapter 3 it is tempting to infer that the free sulfhydryl group(s) identified in HCV glycoprotein E1 are located within the C²²⁶VPC motif. If the C²²⁶VPC motif does function at fusion activation, then it would be expected that the thiol active Cys within the motif is reduced in mature particles prior to cellular attachment in order for it to catalyse reduction of existing disulfides within the glycoprotein complex. However, in the absence of detailed biochemical analyses of E1 and E2 this remains unclear. To determine the location of the free sulfhydryl groups, mass spectrometry analyses of sulfhydryl alkylated glycoproteins from highly purified cell free HCVcc is required. Such experiments are complicated by the low titre produced by replication competent virus, as well as extensive glycosylation and apparent oligomeric heterogeneity of the glycoproteins expressed on particles [137]. Future experiments to determine the oxidation state of this motif in pre and post fusion forms of the virus will be essential to determine a role for this motif in regulation of disulfide isomerisation as a component of fusion activation.

The results from this mutagenesis study indicate that the C²²⁶VPC motif is required at both glycoprotein biosynthesis and fusion activation. As yet, it remains unclear whether a catalytic thiol within this motif is required at either or both stages. As described above, catalysing disulfide bond reduction or isomerisation requires a reduced Cys residue which ultimately transitions to an oxidised state forming an intramolecular disulfide bond with the second active site cysteine of the CXXC motif. In order for the motif to be active again, the intramolecular disulfide bond must be broken and the sulfhydryl groups recycled back to a reduced state. In the case of thioredoxin, a second enzyme thioredoxin reductase carries out this reaction. As proposed above, it is possible that the C²²⁶VPC motif functions to regulate glycoprotein folding, which would be consistent with the apparent role of the E2 CXXC motif from chikungunya virus [279]. However, there have been no reports of associations with reductases for HCV glycoproteins as would be

required for the motif to function again at fusion activation. There have been several publications regarding the associations of E1 and E2 with lectin chaperone calnexin [231,232,234]. Rather than providing catalytic thiols, lectin chaperones act by retaining unfolded or misfolded proteins in the ER by non-specific association with carbohydrate of N-linked glycoproteins and unfolded regions of proteins. This retention of glycoproteins in the ER increases the chance of degradation of the protein by the proteasome. Many mutations introduced into the E1 C²²⁶VPC motif impaired glycoprotein heterodimerisation and therefore are likely to have induced a change in the fold of E1. Rather than providing redox activity, the C²²⁶VPC motif may exert a structural influence on E1 folding, required to prevent prolonged association of E1 with chaperones and permit correct biosynthesis of E1E2. The CXXC Cys residues may then remain reduced throughout glycoprotein maturation and provide catalytic activity to drive conformational changes in the glycoproteins during virus entry. This would be consistent with the Chapter 3 finding that regulation of the oxidation state of the viral glycoproteins is intrinsically controlled during virus entry.

In support of a role for the E1 C²²⁶VPC motif in regulating entry events, it was found that mutations could be introduced into the motif that allowed normal E1E2 biosynthesis but impaired virus entry. E1 mutants CLPC and CIPC demonstrated WT E1E2 heterodimerisation, formation of the conformational CD81 binding site and were found to contain the same number of free sulfhydryl groups in E1 and E2 compared to CVPC-wt in the pre fusion conformations of these proteins, yet both mutants demonstrated severely reduced entry competence. Together, these data indicate that the C²²⁶VPC motif is strictly required for the virus to mediate entry, possibly via catalysing the reduction/oxidation of thiol groups. The observation that these mutants were capable of binding recombinant CD81 may suggest that this motif functions at a post-CD81 stage in entry. However, in Chapter 3 it was found that although free sulfhydryl groups are required to function during entry, and an isomerisation event within the glycoproteins is likely to occur immediately upon cellular attachment, blocking of the free sulfhydryl groups did not preclude binding of HCVpp-derived E2 to CD81. This suggests that the free sulfhydryl groups are not required to mediate this

event. Instead, it is possible that following cellular attachment a conformational change is induced within the glycoproteins outside of the CD81 binding site that facilitates other downstream events required for virus entry. It is important to also acknowledge that there may be some conformational differences between MBP-LEL¹¹²⁻³⁰¹ and full length CD81 that may affect the findings described here [246,259].

Further biochemical analysis is required to directly implicate the C²²⁶VPC motif with providing redox activity that drives the disulfide isomerisation events described in Chapter 3. For example, identification of differences in glycoprotein oxidation following cellular attachment for CVPC-wt virus compared to CIPC and CLPC mutants. The next chapter will investigate recombinant expression systems for E1 and examine whether E1 demonstrates classical thioredoxin redox activity *in vitro*.

5 Chapter 5 – Expression of Recombinant E1 for Redox Activity Assays

5.1 Introduction

In Chapter 3 it was determined that free sulfhydryl groups in HCV envelope glycoproteins E1 and E2 are essential for virus infection, while Chapter 4 identified a highly conserved CXXC thiol-disulfide exchange motif in E1. Characterisation of this motif demonstrated that it is required for correct biosynthesis of the HCV glycoproteins as well as during virus entry. It was not possible to determine whether the CXXC motif is directly responsible for regulating the free thiol groups in E1 and E2. However, many proteins that are predicted to provide redox activity *in vivo* can be shown to catalyse disulfide reduction using *in vitro* assays (for review see [399]).

To further study biochemical and structural properties of the HCV envelope proteins, a soluble, recombinant form is required which preserves the native conformation. There have been many investigations into the expression of E1 and E2 both as independent proteins and in co-expression systems. To date there has been no crystal structure reported for E1 or E2. There have been NMR structures of peptides representing a membrane proximal heptad repeat region of E1 (residues 314–342) [287] as well as the N-terminal region of the E1 TMD (residues 350-370) [236]. While both these regions show strong helical characteristics, in the absence of any other structural information for E1 it is unknown how these helices fit into the domain structure and organisation of the glycoprotein complex.

Both E1 and E2 contain membrane anchors that mediate retention of the glycoproteins in the ER [102,133,208,209]. An additional sequence in the juxtamembrane region of E1 (residues 290-333) has also been shown to mediate ER retention [211]. Therefore in order to obtain a soluble form of the glycoproteins

it is expected that these C-terminal sequences will need to be removed at minimum.

Michalak *et al.* (1997) used a recombinant vaccinia expression system to investigate the effect of C-terminal deletions on E1 and E2 secretion from mammalian cells [210]. The group found that E1 must be C-terminally truncated at residue 311 to achieve efficient secretion. E2 was secreted when truncated at residues 661 or 715, although only the 661 form was determined to be correctly folded. The group found that when E1₁₉₁₋₃₁₁ was expressed in isolation the protein was aggregated and proposed that E2 may be required to facilitate correct folding of E2.

A more recent report by Tello *et al.* (2010) demonstrated baculovirus co-expression and secretion of E1₁₉₁₋₃₄₁ and E2₃₈₄₋₆₆₁ [242]. The group reported that the protein had a high propensity to heterodimerise and associate into higher order arrangements despite lacking their TMDs (an important heterodimerisation determinant) [236,237,238]. Far-UV CD analysis and fluorescence spectroscopy of associated E1 and E2 was consistent with that of protein containing three-dimensional structure, and conformation sensitive antibody directed towards E2 immunoprecipitated non-covalent and disulfide linked variants of the protein. It should be noted that these high molecular weight forms may be artefacts resulting from boiling and aggregation of samples prior to SDS-PAGE and may not represent true higher order conformers. Although E1 did not appear to form aggregates in this co-expression system the group were unable to confirm the structural integrity of the protein due to a lack of conformation sensitive MAbs directed towards E1. It is important to note that this study is in contrast to several previous reports that demonstrate both the E1 and E2 TMDs are essential for heterodimerisation, where mutagenesis of residues within the TMDs, or truncation of either the E1 or E2 TMD abrogates E1E2 association [208,210,236,237,238].

In another study, Hussy *et al.* (1997) compared the reactivity of HCV-positive sera with un-glycosylated bacterially expressed E1 and E2 and glycosylated, baculovirus expressed forms of the glycoproteins [404]. The results

showed that bacterially expressed E1 (residues 191-309 and 191-334) was well recognised by patient sera while glycosylated forms of E1 were only recognised by a small proportion of sera. The group concluded that glycosylation is not required for folding of E1. However, it is not known whether patient sera is likely to contain conformational antibody directed towards E1 therefore variations in sera reactivity do not necessarily represent folding differences between these recombinant forms of E1 and may rather be due to glycan exclusion of epitopes in baculovirus expressed E1E2.

A comparison of E1 ectodomain (residues 191-326) expression in yeast and mammalian cells was performed by Lorent *et al.* (2008) [405]. The group performed extensive biochemical analysis including Fourier transform infrared (FTIR) spectroscopy and far-UV CD quantitation of the secondary structure of monomeric E1, and found no significant difference in the spectras produced by mammalian and yeast expressed forms of the protein. The immune reactivity of yeast and mammalian derived E1 was examined using sera from chronically HCV-infected persons. Comparable reactivity was observed for each protein. However, as described above, this is not necessarily indicative of protein conformation. Some differences in glycosylation were observed with yeast derived protein demonstrating heterogeneity in the use of potential N-linked glycosylation sites compared to more complete glycosylation in mammalian expressed E1. Without conformation sensitive MAb directed towards E1 it is unclear whether this is likely to have affected the conformation of the protein.

These studies indicate that while the E1 ectodomain has a great propensity to aggregate, it is possible to obtain a soluble, non-aggregated form of E1 using E1E2 co-expression systems based in mammalian or insect cells [210,242]. Evidence for soluble E1 expression in the absence of E2 is also available in a variety of systems including bacterial, insect, yeast and mammalian cells [404,405]. In each case, E1 was C-terminally truncated at least to residue 341. E1 contains several highly hydrophobic regions including a short membrane proximal heptad repeat (MPHR; residues 330–347) and a conserved membrane interactive region (residues 276–286) [285,286]. In the studies discussed above each

construct lacked the TMD and all, or much of the MPHR to aid solubility. A major limitation of these studies has been a lack of conformational monoclonal antibodies and functional assays for E1. Therefore it remains unknown whether these recombinant forms of E1 represent what is expressed on the surface of virus particles.

Although E1 is required to function as a heterodimer with E2 to facilitate virus entry, its role is yet to be determined. Development of a recombinant expression system for the ectodomain of E1 would provide opportunities for investigating domain structure to allow comparison with other viral protein paradigms. Pertinent to this study, recombinantly expressed E1 could also be used in functional assays to analyse potential enzymatic roles of the protein such as redox activity. In this chapter, a variety of expression systems were explored in order to produce a soluble form of E1 with which to test redox activity using *in vitro* thioredoxin activity assays.

5.2 Results - Bacterial Expression of E1

Escherichia coli (*E.coli*) is one of the most widely used systems for expression of recombinant protein due to the high yields produced. To investigate expression of soluble E1 in bacteria various C-terminal extensions of the E1 ectodomain (prototype strain H77c) were introduced into a pMAL-c2-based vector encoding an N-terminal maltose binding protein tag (MBP). An MBP tag was selected to aid in solubilisation and purification of the protein. In addition a rigid Ala-Ala-Ala linker was engineered into the vector between the MBP tag and the E1 sequence. This was done to promote independent folding and localisation of the two proteins.

Three lengths of the E1 ectodomain were introduced based on the location of various hydrophobic sequences (schematically represented in Figure 5-1). While it would be ideal to express the entire ectodomain of E1, previous studies indicate that removal of C-terminal membrane proximal sequences may promote the expression of soluble protein. To examine this hypothesis, sequential C-

terminal truncations of the E1 ectodomain were performed, terminating at residues 351, 340 and 329.

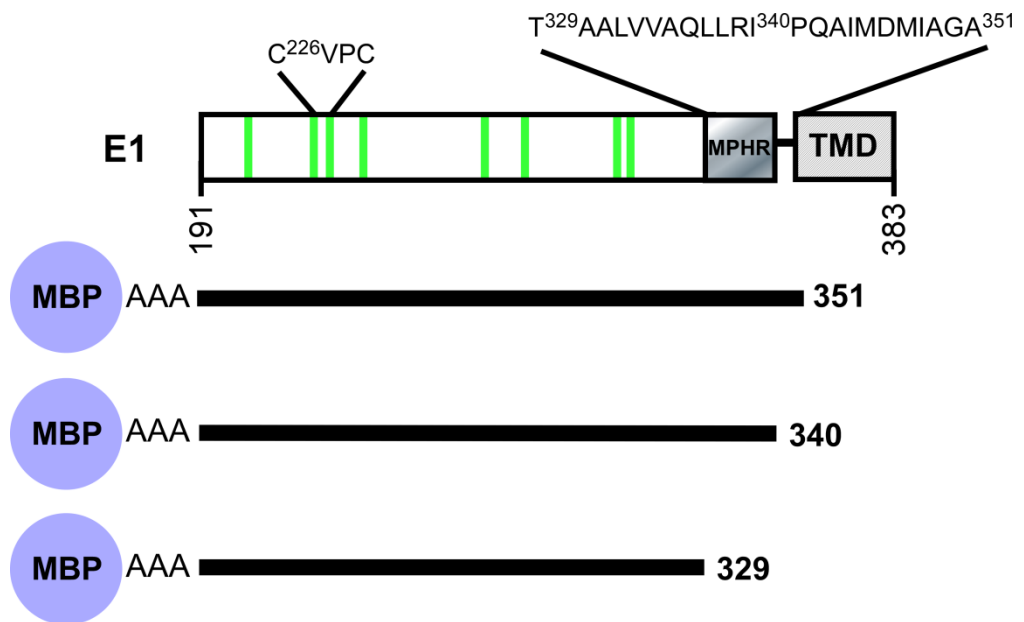


Figure 5-1. Schematic representation of various E1 ectodomain lengths expressed as MBP-tagged proteins in *E. coli*. Conserved cysteine residues are shown as green vertical lines. Location of the thioredoxin-like motif is indicated near the N-terminus of E1. The MPHR and the TMD are labelled in grey. The enhanced sequence between the MPHR and TMD show the residues at each truncation site.

5.2.1 Small scale expression of MBP-E1 proteins

E. coli strain BL21(DE3) was transformed with pMBP-E1 and expression was induced with isopropyl- β -D-thiogalactopyranoside (IPTG) for 5 h. Bacteria were sonicated to release proteins then soluble and insoluble fractions were separated by centrifugation. Soluble fractions were either run directly on SDS-PAGE or subjected to purification by amylose resin precipitation prior to SDS-PAGE analysis. Insoluble fractions were loaded directly onto SDS-PAGE. All gels were run under reducing conditions in duplicate, and either stained with Coomassie blue or analysed by Western blot using MAb A4 which recognises amino acid residues 197-207 at the N-terminus of E1 [138].

Coomassie staining identified a significant band of protein at the expected molecular weight of the MBP-E1 constructs, at ~60kDa, both in the soluble and insoluble fractions (MBP-fp; Figure 5-2A). This band was greatly enhanced in the soluble fraction when the protein was precipitated by amylose resin prior to SDS-PAGE indicating the presence of the MBP tag. Western blots probed with anti-E1 MAb A4 confirmed expression of MBP-E1 from each of these constructs (Figure 5-2B). Interestingly, a ~50 kDa species was also detected in Western blots probed with A4 indicating the presence of a truncated form of MBP-E1 that retained the A4 epitope.

These results show that MBP-E1 incorporating any of the three lengths of ectodomain tested can be expressed in a soluble form in bacteria.

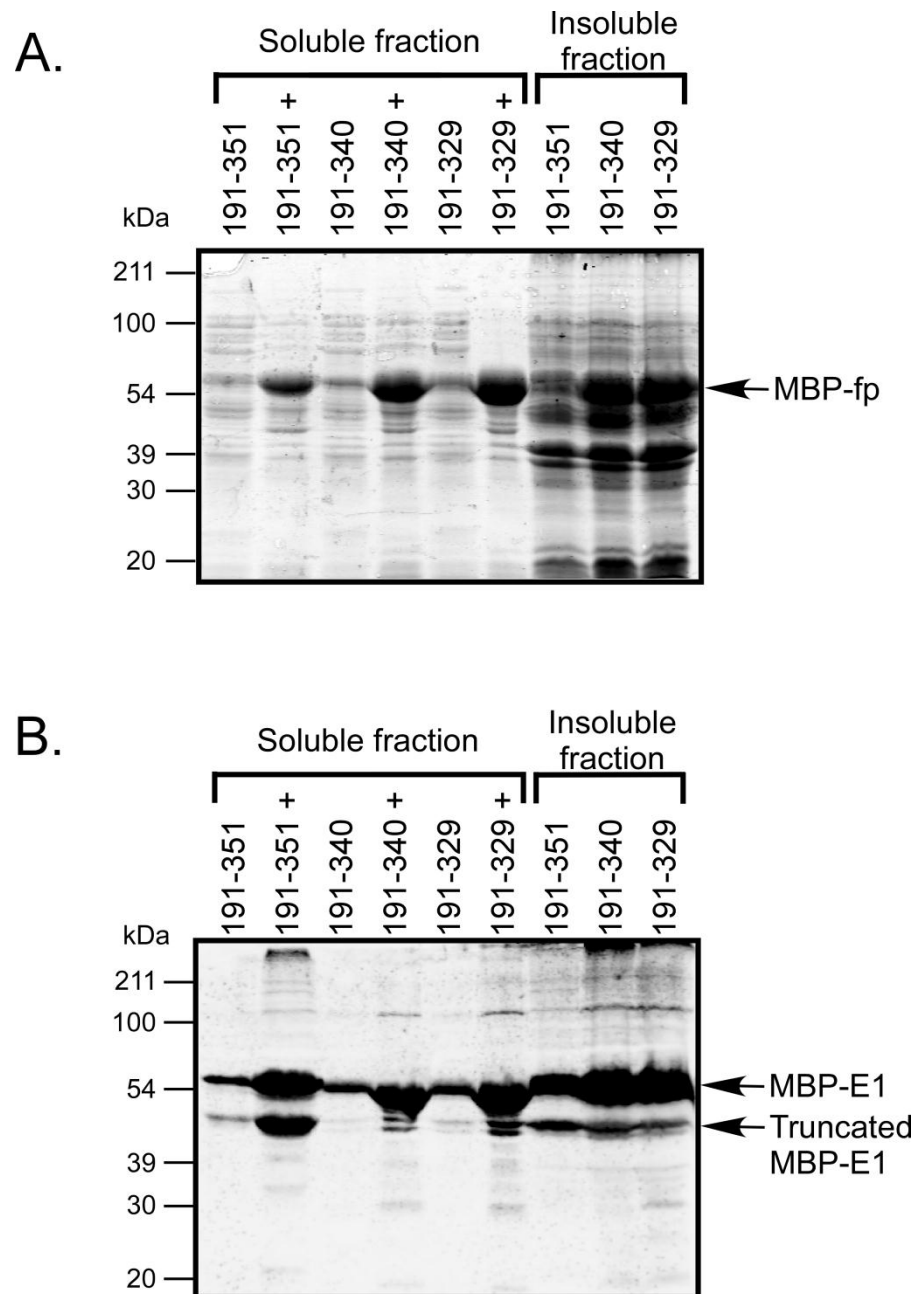


Figure 5-2. Small scale expression and purification of MBP-E1 constructs from *E. coli* strain BL21(DE3). Soluble fractions of *E. coli* cultures transformed with pMBP-E1 were loaded directly onto SDS-PAGE or subjected to amylose resin purification (indicated by +) prior to SDS-PAGE analysis. Insoluble fractions were run directly on SDS-PAGE. Samples were run under reducing conditions then either directly stained with Coomassie blue (A) or Western blotted with anti-E1 MAb A4 (B). Coomassie stained gels and Western blots were visualised by LI-COR. Molecular weight markers are shown to the left of the gels.

5.2.2 Large scale expression and purification of MBP-E1 proteins

To allow further biochemical analyses of each MBP-E1 protein species protein expression was up-scaled for each construct. Transformed *BL21(DE3)* were induced with IPTG as described in section 5.2.1 and soluble protein was released from the bacteria by sonication. MBP-tagged proteins were purified over amylose resin before separation of oligomeric forms by gel-filtration chromatography using a Superdex 200 (HiLoad 26/60) column. Eluent fractions were collected at 2 min intervals.

The majority of the MBP-tagged protein isolated from bacteria eluted in the void volume indicative of high molecular weight aggregate species (Figure 5-3). In addition, a 42 kDa species was eluted for each construct which corresponds in molecular mass to MBP alone. While there was no evidence for monomeric or higher order arrangements of MBP-E1 for any construct, a noticeable shoulder was evident on the 42 kDa peak fraction from each construct, indicative of a slightly larger species unresolved from the 42 kDa species.

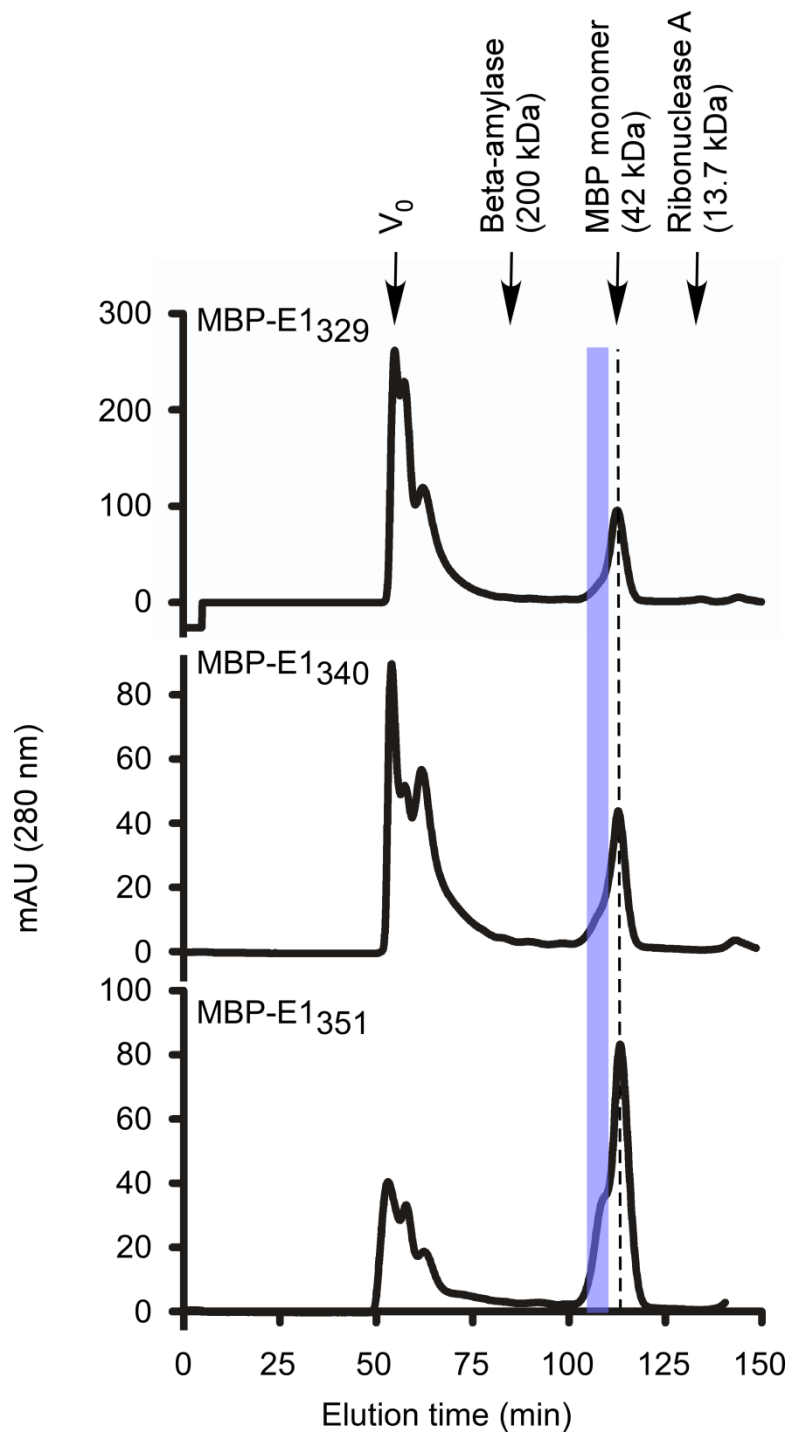


Figure 5-3. FPLC profiles of MBP-E1 proteins. BL21(DE3) *E. coli* transformed with pMBP-E1 were lysed by sonication following IPTG induction. MBP-tagged proteins were isolated by amylose resin then loaded onto a Superdex 200 (HiLoad 26/60) column. Fractions were collected at 2 min intervals for MBP-E1₃₂₉, MBP-E1₃₄₀ and MBP-E1₃₅₁. Blue shading indicates shoulder fractions unresolved from the 42 kDa MBP peak. Marker sizes and column void (V_0) are indicated above.

5.2.3 Analysis of MBP-E1₃₂₉ FPLC fractions

Each peak fraction collected from FPLC purification of the MBP-E1 constructs was analysed by Coomassie stained SDS-PAGE and Western blot, under reducing and non-reducing conditions.

Visualisation of MBP-E1₃₂₉ fractions 1-3 in Coomassie stained SDS-PAGE identified a protein band migrating at approximately 56 kDa under reducing conditions (Figure 5-4B, upper gel). This corresponds approximately to the expected size of MBP-E1₃₂₉. However, these fractions were eluted in the void of the column space indicating that the protein is present as high molecular weight aggregate. This was evident when the same protein fractions were run under non-reducing conditions. Fractions 1 and 2 appeared to contain aggregates too large to enter the gel as they were not detected by Western blot or Coomassie staining when run under non-reducing conditions. Western blot analysis of these fractions run under reducing conditions confirmed that the protein bands detected in fractions 1-3 contained E1 sequence as they were detected by anti-E1 MAb A4 (Figure 5-4, lower gel).

Fraction 5 is likely to represent a peak of MBP alone as MAb A4 which recognises residues at the very N-terminus of E1 did not detect protein from this peak. This protein ran as a single band at approximately 42 kDa which is the expected molecular weight for MBP.

Fraction 4 corresponds to the shoulder preceding the MBP peak fraction. When run under both reducing and non-reducing conditions on SDS-PAGE a single band appeared at approximately 50 kDa. This protein migrated higher than MBP (fraction 5), but lower than aggregate forms of MBP-E1₃₂₉ run under reducing conditions suggesting that perhaps this protein is a truncated form of MBP-E1₃₂₉. Indeed protein from fraction 4 was detected by MAb A4 indicating that a region of N-terminal E1 sequence has been expressed in fusion with MBP. Importantly it appears this fraction of protein is expressed in a non-covalently linked form

indicating that it is not forming disulfide linked aggregates as was observed in fractions 1-3.

These results suggest that expression of the E1 ectodomain residues 191-329 in fusion with MBP largely results in production of aggregated disulfide linked forms of protein indicating misfolding events. However, it seems that spontaneous cleavage of MBP-E1₃₂₉ by a bacterial protease produces a length of protein that is soluble and appears to form a monomeric domain of E1.

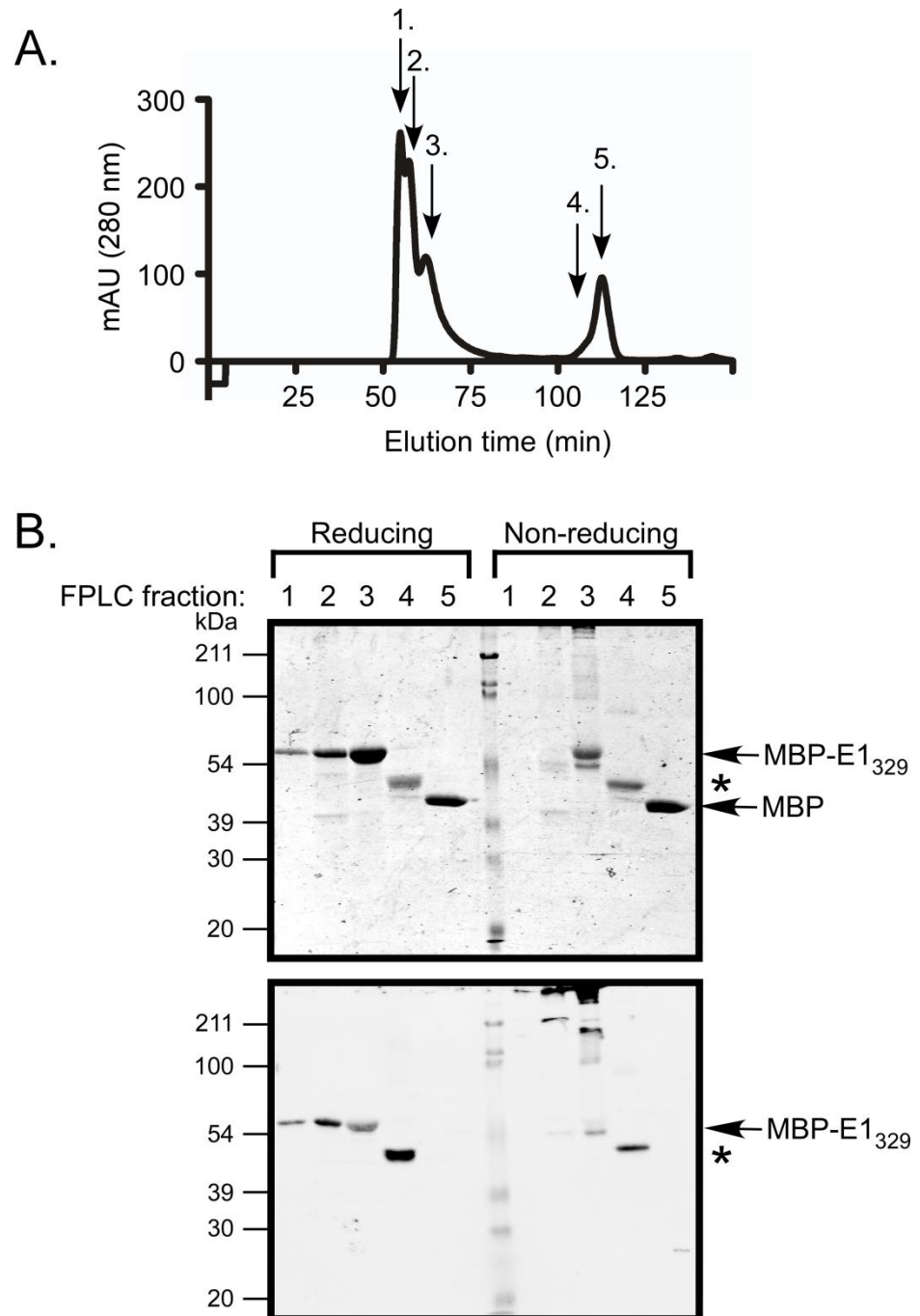


Figure 5-4. Purification of MBP-E1₃₂₉ and separation of oligomeric forms. A. Protein fractions were isolated by Superdex 200 (HiLoad 26/60) gel filtration chromatography of MBP-E1₃₂₉. B. Each fraction was run on SDS-PAGE under reducing or non-reducing conditions (lanes 1-5). Gels were either directly stained with Coomassie blue (upper gel) or probed with anti-E1 MAb A4 for Western blot analysis (lower gel). Coomassie stained gels and Western blots were visualised by LI-COR. Asterisks represent truncated forms of MBP-E1₃₂₉. Molecular weight markers are shown to the left of the gels.

5.2.4 Analysis of MBP-E1₃₄₀ FPLC fractions

Analysis of the MBP-E1₃₄₀ fractions isolated by FPLC revealed an identical profile to the MBP-E1₃₂₉ fractions, in both Coomassie blue stained SDS-PAGE and Western blot (Figure 5-5B, upper and lower gels, respectively). Fractions 1-3 eluted at a time consistent with high molecular weight aggregate forms of MBP-E1₃₄₀. Reducing Coomassie blue and Western blot analyses confirmed that the protein in these fractions corresponded to the approximate expected molecular weight of 57 kDa for MBP-E1₃₄₀. Fraction 5 contained MBP alone with no E1 sequence, running at approximately the expected molecular weight of 42 kDa, and not detected in Western blot by MAb A4.

Fraction 4 corresponds to the shoulder preceding the MBP peak fraction. When run under both reducing and non-reducing conditions on SDS-PAGE a single band appeared at approximately 50 kDa that was recognised by MAb A4. This protein migrated higher than MBP from fraction 5, but lower than reduced aggregate forms of MBP-E1₃₄₀.

These results suggest that expression of the E1 ectodomain residues 191-340 results in the majority of protein forming disulfide linked aggregate. Interestingly, a spontaneous cleavage event produced a truncation product of MBP-E1 at the same apparent molecular weight as identified in fraction 4 of MBP-E1₃₂₉ suggesting release of a common domain from each construct.

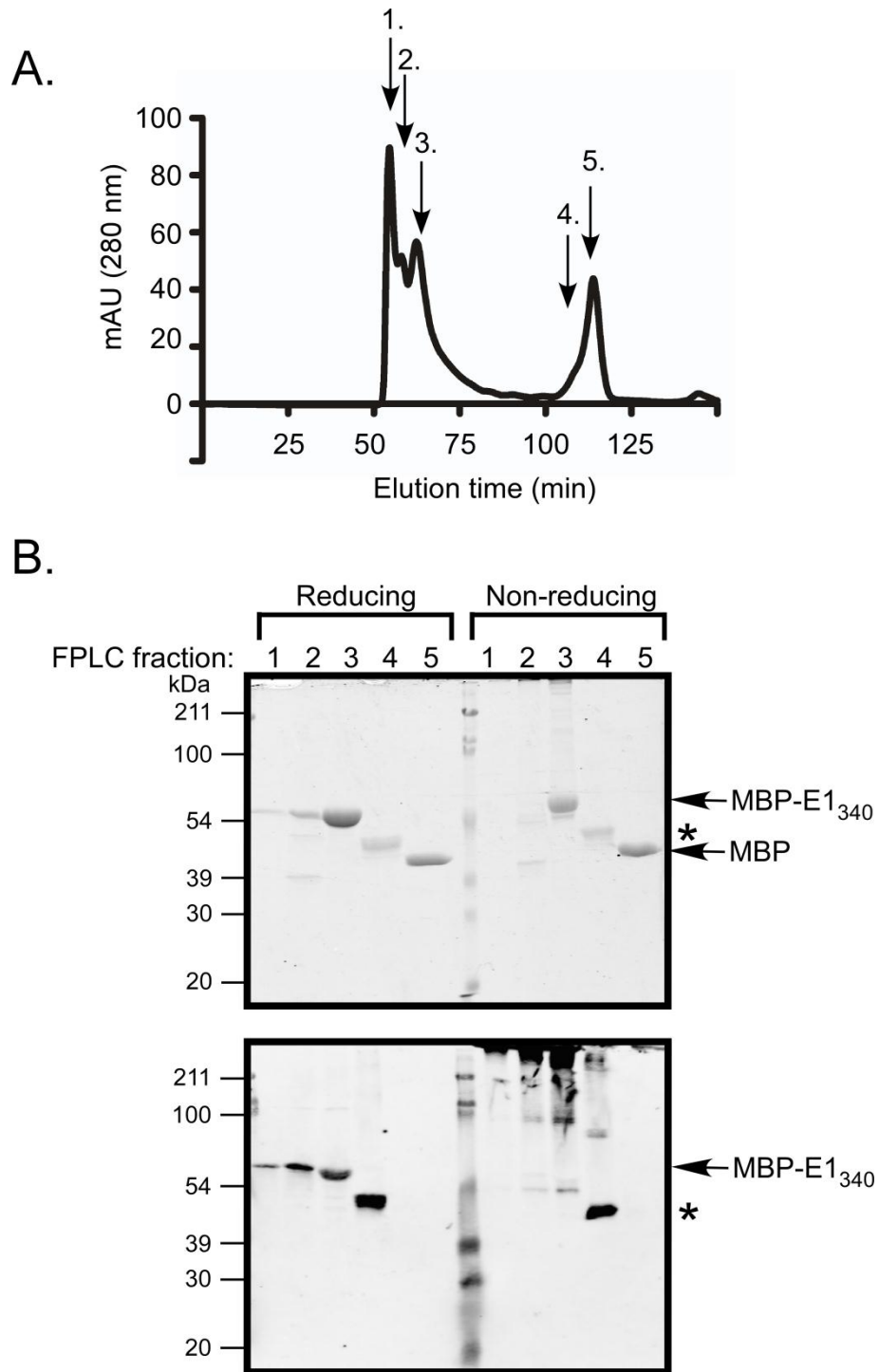


Figure 5-5. Purification of MBP-E1₃₄₀ and separation of oligomeric forms. A. Protein fractions were isolated by Superdex 200 (HiLoad 26/60) gel filtration chromatography of MBP-E1₃₄₀. B. Each fraction was run on SDS-PAGE under reducing or non-reducing conditions (lanes 1-5). Gels were either directly stained with Coomassie blue (upper gel) or probed with anti-E1 MAb A4 for Western blot analysis (lower gel). Coomassie stained gels and Western blots were visualised by LI-COR. Asterisks represent truncated forms of MBP-E1₃₄₀. Molecular weight markers are shown to the left of the gels.

5.2.5 Analysis of MBP-E1₃₅₁ FPLC fractions

Analysis of the FPLC profile from MBP-E1₃₅₁ indicated that the first three protein peaks eluted from the Superdex 200 (HiLoad 26/60) column at a time consistent with high molecular weight aggregate forms of the protein (Figure 5-6A). Reducing SDS-PAGE followed by Coomassie blue staining or Western blot analyses confirmed that the protein in these fractions contained E1 sequence and had the expected molecular weight for MBP-E1₃₅₁ of approximately 58 kDa (Figure 5-6B upper and lower gels, respectively). Fraction 5 appeared to contain MBP cleaved from E1 as this protein was not detected by anti-E1 MAb A4.

Fraction 4 corresponds to the shoulder preceding the MBP peak fraction, and ran as a single band at approximately 50 kDa under reducing and non-reducing conditions on SDS-PAGE. Although Western blot analysis showed this protein to contain the A4 epitope this is likely to be a truncated form of MBP-E1₃₅₁.

Together these results suggest that expression of the MBP-E1 ectodomain up to residues 329, 340 or 351 results in misfolding and aggregation. However, for each construct a proportion of protein appears to undergo spontaneous cleavage by a bacterial protease and does not become aggregated. This product is recognised by MAb A4 and is a soluble, monomeric fragment incorporating the N-terminal residues of E1.

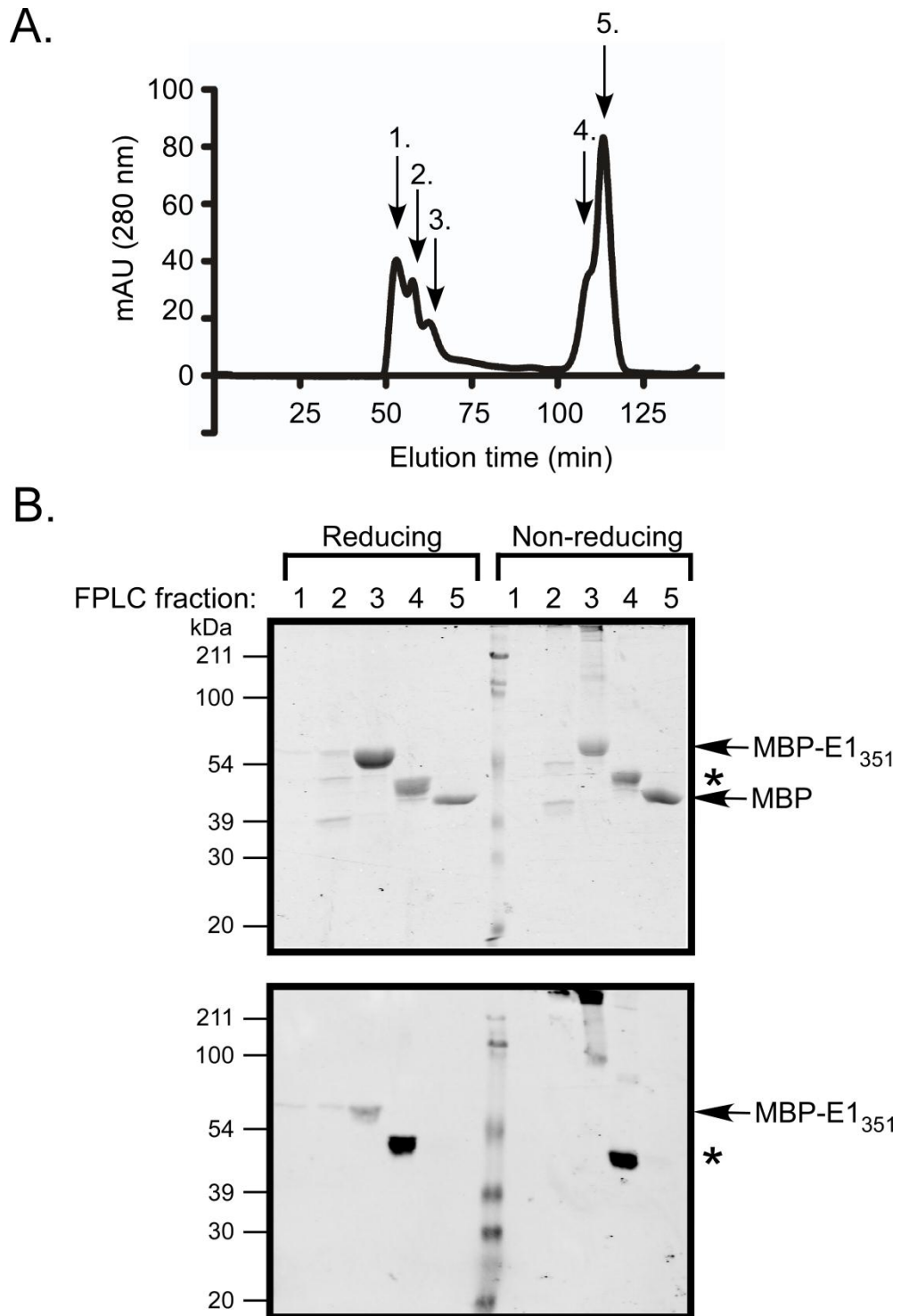


Figure 5-6. Purification of MBP-E1₃₅₁ and separation of oligomeric forms. A. Protein fractions were isolated by Superdex 200 (HiLoad 26/60) gel filtration chromatography of MBP-E1₃₅₁. B. Each fraction was run on SDS-PAGE under reducing or non-reducing conditions. Gels were either directly stained with Coomassie blue (upper gel) or probed with anti-E1 MAb A4 for Western blot analysis (lower gel). Coomassie stained gels and Western blots were visualised by LI-COR. Asterisks represent truncated forms of MBP-E1₃₅₁. Molecular weight markers are indicated to the left of the gels.

5.2.6 Identification of MBP-E1 truncation products

Attempts to express and purify E1 ectodomain residues in fusion with MBP in bacteria, largely resulted in the protein forming disulfide linked aggregates (fractions 1-3 for each construct, above). However, in each case an unresolved monomeric form of MBP-E1 was also isolated which appeared to contain a truncated E1 sequence (fraction 4 for each construct, above). It is possible that a co- or post-translational cleavage event at an N-terminal site(s) within E1 generates these truncated forms of MBP-E1.

To identify the C-terminus of MBP-E1 isolated from fraction 4 of MBP-E1₃₂₉, MBP-E1₃₄₀ and MBP-E1₃₅₁ mass spectrometry analysis was performed. Samples were reduced and alkylated by iodoacetamide (IAA) then digested with trypsin and analysed by matrix-assisted laser desorption/ionization time-of-flight/time-of-flight mass spectrometry (MALDI TOF/TOF) using an Ultraflex III MALDI-TOF/TOF mass spectrometer (Bruker Daltonics, Massachusetts, USA) with 2,5-dihydroxy benzoic acid as matrix.

It was found that fraction 4 from each construct contained peptides that mapped to all of MBP, and N-terminal residues of E1 including E1 residue Arg258 but not exceeding Arg259. Analysis of fraction 3 from each construct identified peptides that extended beyond Arg259 consistent with Western blot and Coomassie analyses which suggested this aggregate form of protein has a higher molecular mass than the MBP-E1 protein from fraction 4. A representative schematic of the peptide mapping result for MBP-E1₃₂₉ fractions 3 and 4 is shown in Figure 5-7.

The observation that MBP-E1₃₂₉, MBP-E1₃₄₀ and MBP-E1₃₅₁, are cleaved at a common site may indicate that E1 residues 191-259 form an independent sub-domain of E1.

Peptide assignment for MBP-E1₃₂₉ Peak 3:

MKIEEGK	LVIV	WINGDKGYNG	LAEVGK	KFEK	DTGIKVT	VEH	PDKLEEK	FPQ	VAATGDG	DPDI	IFWAHDR	FGG	YAQSGLL	AEI	TPDKAF	QDKL	YFFTWD	AVRY	
NGKLI	AYPIA	VEALSLI	YNK	DLLPNP	PKTW	EEIPAL	DKEL	KAKGK	SALMF	NLQEPY	FTWP	LIAADG	GYAF	KYENGKY	DIK	DVGVDN	NAGAK	AGLTFL	VLDLI
KNKHM	NADTD	YSIAE	AAFNK	GETAM	TINGP	WAWSN	IDTSK	VNYGV	TVLPT	FKGQPS	KPFV	GVLSA	GINAA	SPNKEL	AKEF	LENYLL	TDEG	LEAVNK	DKPL
GAVAL	KSYEE	ELAKD	PRIAA	TMENA	QKGEI	MPNIP	QMSAF	WYAVR	TAVIN	AASGR	QTUDA	ALAAA	QTNAA	AYQVR	NSSGL	YHVTN	DCPNS	SIVYEA	ADAI
220	230	240	250	260	270	280	290	300	310										
LHTPG	VPCV	REGNAS	R	CVV	AVTPT	VATRD	GKLP	TTQLR	R	HIDLL	VGSAT	LCSAL	V	VDL	CGSV	FLV	QGL	FTFSP	RRHWT
220																			
DMMMN																			

Peptide assignment for MBP-E1₃₂₉ Peak 4:

MKIEEGK	LVIV	WINGDKGYNG	LAEVGK	KFEK	DTGIKVT	VEH	PDKLEEK	FPQ	VAATGDG	DPDI	IFWAHDR	FGG	YAQSGLL	AEI	TPDKAF	QDKL	YFFTWD	AVRY	
NGKLI	AYPIA	VEALSLI	YNK	DLLPNP	PKTW	EEIPAL	DKEL	KAKGK	SALMF	NLQEPY	FTWP	LIAADG	GYAF	KYENGKY	DIK	DVGVDN	NAGAK	AGLTFL	VLDLI
KNKHM	NADTD	YSIAE	AAFNK	GETAM	TINGP	WAWSN	IDTSK	VNYGV	TVLPT	FKGQPS	KPFV	GVLSA	GINAA	SPNKEL	AKEF	LENYLL	TDEG	LEAVNK	DKPL
GAVAL	KSYEE	ELAKD	PRIAA	TMENA	QKGEI	MPNIP	QMSAF	WYAVR	TAVIN	AASGR	QTUDA	ALAAA	QTNAA	AYQVR	NSSGL	YHVTN	DCPNS	SIVYEA	ADAI
220	230	240	250	260	270	280	290	300	310										
LHTPG	VPCV	REGNAS	R	CVV	AVTPT	VATRD	GKLP	TTQLR	R	HIDLL	VGSAT	LCSAL	V	VDL	CGSV	FLV	QGL	FTFSP	RRHWT
220																			
DMMMN																			

Figure 5-7. Mass spectrometry analysis of MBP-E1₃₂₉ fractions 3 and 4. Fraction 3 and fraction 4 of MBP-E1₃₂₉ were alkylated with IAA then digested with trypsin. The mass of the peptide fragments was analysed by an Ultraflex III MALDI-tof/tof mass spectrometer using 2,5-dihydroxy benzoic acid as matrix. Peptide assignment was inferred from the observed molecular masses. Turquoise blocks indicate MBP sequence. Yellow blocks indicate E1 sequence with HCV polypeptide numbering indicated in black. Grey blocks indicate assigned peptide fragments matched to red sequences. Black sequences represent regions to which no peptide fragments could be assigned. The E1 C²²⁶VPC motif is boxed in blue.

5.2.7 Small scale expression of MBP-E1₂₅₉

To examine whether deletion of C-terminal residues beyond residue 259 result in the expression of monomeric MBP-E1, the pMBP-E1 construct was reengineered to incorporate E1 residues 191-259 for further analysis.

BL21(DE3) *E. coli* were transformed with pMBP-E1₂₅₉ and induced with IPTG. Proteins were released by sonication then soluble and insoluble fractions were separated by centrifugation. Soluble fractions were either run directly on SDS-PAGE or subjected to purification by amylose resin precipitation prior to SDS-PAGE analysis. Insoluble fractions were loaded directly onto SDS-PAGE.

Coomassie stained SDS-PAGE and Western blot analyses using MAb A4, identified a protein band that migrated near the 50 kDa molecular mass marker, similar to the expected molecular mass of ~48 kDa for MBP-E1₂₅₉ (Figure 5-8 upper and lower gels, respectively). This species was observed in both the soluble and insoluble fractions. Amylose agarose was successfully used to purify the 48 kDa species from the soluble fraction. Protein expression was therefore up-scaled in order to allow further biochemical analysis of MBP-E1₂₅₉.

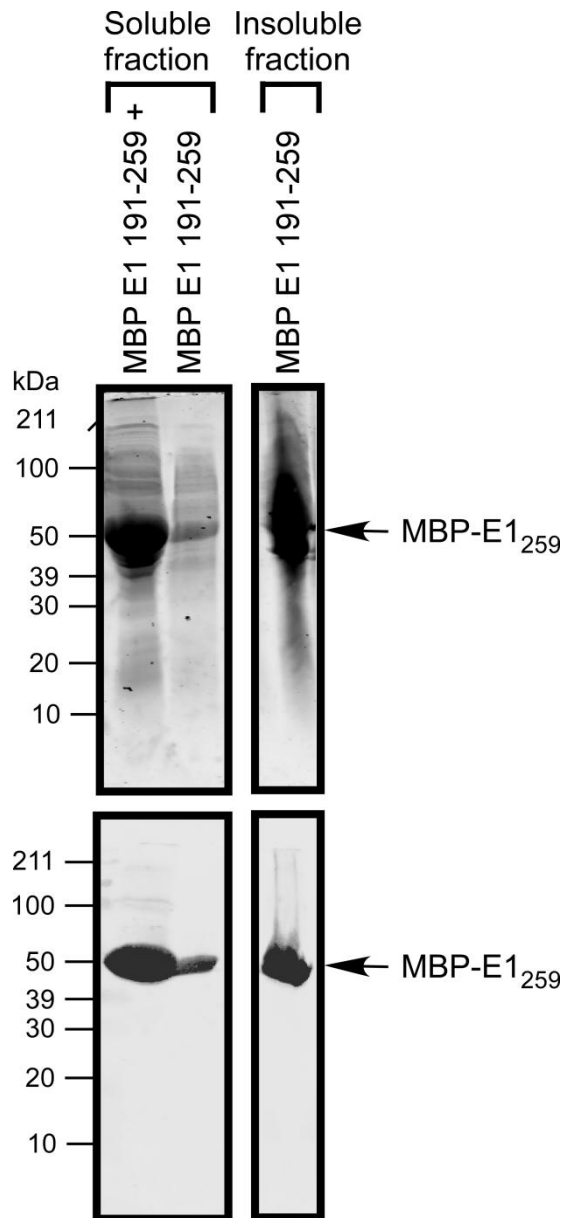


Figure 5-8. Expression and purification of MBP-E1₂₅₉. BL21(DE3) *E. coli* cultures transformed with pMBP-E1₂₅₉ were induced with IPTG. Bacteria were lysed by sonication and soluble and insoluble fractions separated by centrifugation. Soluble protein was either loaded directly onto SDS-PAGE or subjected to amylose agarose purification (indicated by +) prior to SDS-PAGE analysis. Samples were run under reducing conditions then either directly stained with Coomassie blue (upper gel) or probed with anti-E1 MAb A4 for Western blot analysis (lower gel). Coomassie stained gels and Western blots were visualised by LI-COR. Molecular weight markers are indicated to the left of the gels.

5.2.8 Large scale expression of MBP-E1₂₅₉

MBP-E1₂₅₉ was expressed in BL21(DE3) *E. coli* and released by sonication as described in section 5.2.1. The soluble protein fraction was subjected to affinity purification on an amylose agarose column before separation of oligomeric species by gel filtration using a Superdex 75 (HiLoad 16/60) column.

The gel filtration profile for MBP-E1₂₅₉ shows the majority of the protein to be present as a single oligomeric species with little high molecular weight aggregate observed (Figure 5-9A). This protein was eluted just prior to the expected time for MBP. Evaluation of the single peak by Coomassie stained SDS-PAGE showed that the protein ran as a distinct band of the expected molecular weight for MBP-E1₂₅₉ of ~48 kDa under both reducing and non-reducing conditions (Figure 5-9B). This indicates that removal of the region spanning residues 260 to 329 successfully prevents the formation of misfolded aggregates.

This result demonstrates that E1 residues 191-259 can be expressed in a soluble form in bacteria when produced as a fusion protein with MBP. The C²²⁶V/LPC thioredoxin-like motif is centrally located within the 191-259 residues therefore this may represent a stable domain and candidate protein for testing in a redox activity assay.

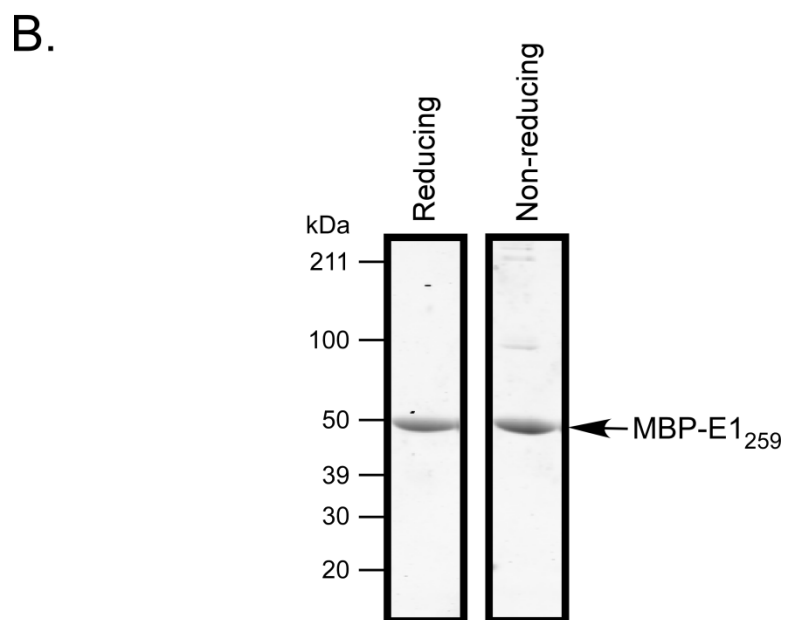
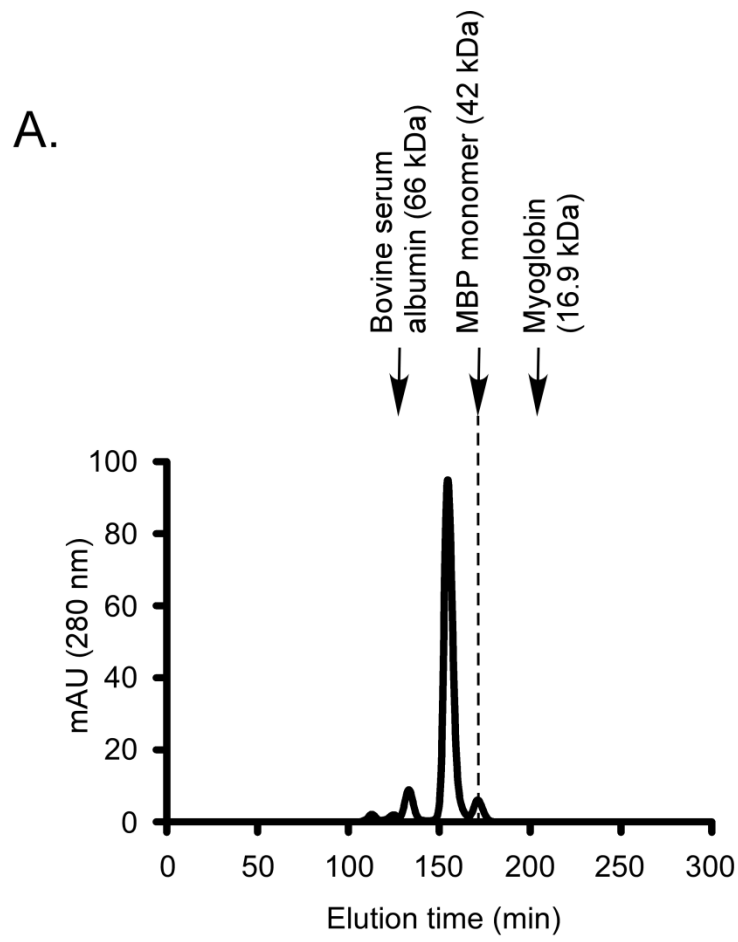


Figure 5-9. Purification of MBP-E1₂₅₉ and separation of oligomeric forms. A. Protein fractions of MBP-E1₂₅₉ were isolated by gel filtration using a Superdex 75 (HiLoad 16/60) column. B. Fractions were run on SDS-PAGE under reducing or non-reducing conditions. Gels were stained with Coomassie blue and visualised by LI-COR. Molecular weight markers are indicated at the left of the gel.

5.2.9 Limited proteolysis of MBP-E1₂₅₉

The availability of protease cleavage sites provides information about a protein's secondary structure. An unfolded region of protein will be highly susceptible to protease cleavage even at low protease concentrations, while a tightly folded region of protein is likely to shield potential recognition sites from digestion.

The protease chymotrypsin preferentially cleaves proteins at bulky aromatic residues including Trp, Tyr, Phe, while secondarily cleaving at small hydrophobic residues Leu, Met, Ala, Asp and Glu.

To determine whether MBP-E1₂₅₉ contains secondary structure, 7 µg of protein was digested with increasing amounts of chymotrypsin (w/w) and incubated at 37°C for 10 min. Samples were quenched with protease inhibitor phenylmethanesulfonylfluoride (PMSF) prior to running the samples on SDS-PAGE and staining with Coomassie blue. To identify the peptide fragments produced by chymotrypsin cleavage, samples digested at 1:40 and 1:5 (protease:protein) were subjected to analysis by mass spectrometry. For these samples, digestion reactions were quenched with 0.1% trifluoroacetic acid rather than PMSF to inactivate the protease.

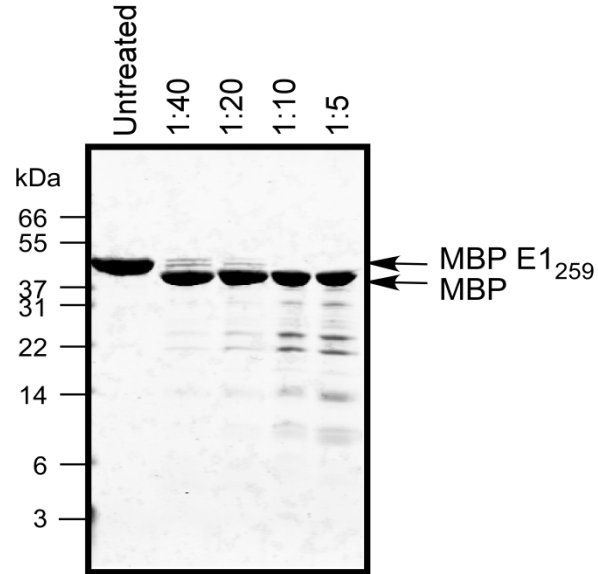
From the SDS-PAGE analysis it is apparent that as the concentration of chymotrypsin increases, MBP-E1₂₅₉ (represented by a single ~48 kDa band) diminishes, with the gradual emergence of a single band at ~42 kDa, expected to represent MBP alone (Figure 5-10A). The band at 42 kDa also reduces as the concentration of chymotrypsin increases, indicating some level of MBP cleavage.

Analyses of 1:40 and 1:5 MBP-E1₂₅₉ digestions were performed by MALDI TOF/TOF using an Ultraflex III MALDI-TOF/TOF mass spectrometer (Bruker Daltonics, Massachusetts, USA) with 2,5-dihydroxy benzoic acid as matrix. Four peptide fragments in each digest could be mapped to regions in E1. These had masses of 1790 Da, 1445 Da, 2653 Da and 1968/1970 Da (1:40 and 1:5 digests

respectively) (Figure 5-10B). Three of these peptide fragments were unambiguously assigned to E1 while the 1790 Da fragment could be assigned to an N-terminal region of E1 or a region in MBP. Each of the chymotrypsin cleavage sites occurred at an aromatic residue in E1.

There was no difference in the E1 peptide assignment between the 1:5 and 1:40 chymotrypsin digests indicating that low protease concentrations are sufficient to cleave E1 at the three aromatic residues Y201, Y214 and W239. Importantly, while the aromatic residues in the E1 sequence were readily cleaved, none of the secondary recognition sites (L, M, A, D or E) were cleaved by chymotrypsin even when the protein was exposed to high concentrations of protease. This suggests that these sites are shielded from digestion and indicates the presence of secondary structure in the protein. These results provide evidence that E1 residues 191-259 form a soluble domain when expressed in fusion with MBP and contains subdomains with secondary structure. This indicates that MBP-E1₂₅₉ represents a good candidate for testing in an *in vitro* redox activity assay.

A.



B.

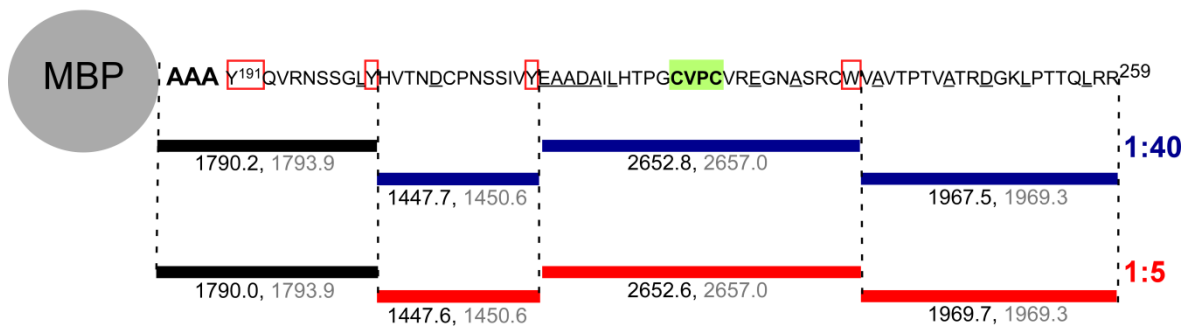


Figure 5-10. Analysis of MBP-E₁₂₅₉ by limited proteolysis. Purified MBP-E₁₂₅₉ was incubated with increasing concentrations of chymotrypsin prior to quenching. Proteolysed samples were either run on SDS-PAGE and visualised by Coomassie blue staining (A) or analysed by mass spectrometry (B). The mass of the peptide fragments was analysed by an Ultraflex III MALDI-tof/tof mass spectrometer using 2,5-dihydroxy benzoic acid as matrix. Peptide assignment was inferred from the observed molecular masses. Observed peptide masses are shown in Da in black while the predicted mass of each peptide is in grey. Fragments shown in blue were unambiguously mapped to E1 in the 1:40 digest while the red fragments were unambiguously mapped to E1 in the 1:5 digest. The molecular mass of the black fragments mapped to the designated region in E1 but could also be mapped to a predicted fragment in MBP. Aromatic residues in the E1 sequence are boxed in red, chymotrypsin secondary recognition sites are underlined and the C²²⁶VPC thioredoxin-like motif is highlighted in green.

5.2.10 Insulin reduction assay

To determine if the E1 C²²⁶V/LPC motif has the ability to regulate the oxidation state of the HCV envelope glycoprotein complex, the redox activity of the motif was measured using a classical thioredoxin assay. Thioredoxin is capable of reducing disulfide bonds across a broad range of substrates including insulin. Insulin consists of one α and one β chain linked by two disulfide bonds. Reduction of the disulfide bonds can be followed spectrophotometrically at 650 nm as the β chain precipitates [372].

Thioredoxin (Trx) containing a 6 x His C-terminal tag was expressed in BL21(DE3) *E. coli* and released by sonication as described for MBP-E1 proteins. The soluble protein fraction was subjected to affinity purification on a nickel agarose column before isolation of the monomeric species by gel filtration using a Superdex 75 (HiLoad 16/60) column.

To examine whether E1 demonstrates reducing activity, reduced MBP-E1₂₅₉ was added to insulin. Precipitation of insulin by 8 μ M Trx was complete by approximately 18 min, while the reaction took ~25 mins for 4 μ M Trx (Figure 5-11). No detectable precipitation of insulin occurred during the 30 min assay for MBP-E1₂₅₉, un-reactive MBP-CD81 or the water only control. This suggests that the E1 domain consisting of residues 191-259 are not able to catalyse reduction of insulin disulfide bonds *in vitro*.

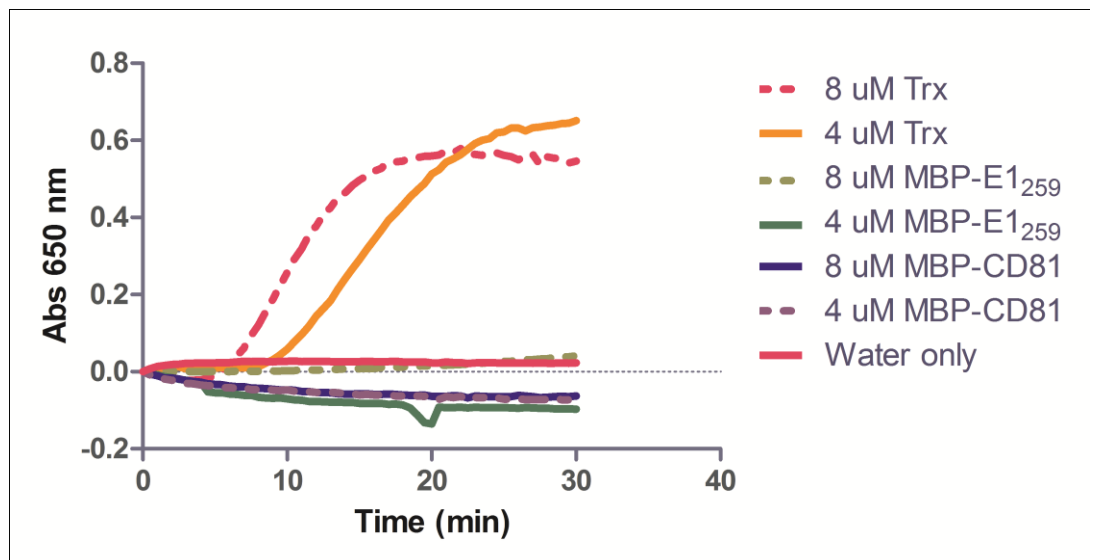


Figure 5-11. Insulin reducing activity of MBP-E1₂₅₉. Reduction of insulin disulfide bonds by thioredoxin, MBP-E1₂₅₉, negative control MBP-CD81 or water only, was measured spectrophotometrically by absorbance at 650 nm over 30 min using a Fluostar (BMG Lab Technologies). Data are from a representative experiment.

5.3 Results - Mammalian Expression of E1

5.3.1 Expression of E1-myc in HEK 293T cells

It was found that the maximum length of E1 that could be expressed in a soluble, non-aggregated form in bacteria was 68 residues (191-259). Thioredoxin consists of 105 amino acids and the fold is comprised of 5 β -sheets surrounded by 4 α -helices. A truncated form of human thioredoxin consisting of 80 amino acids does not demonstrate insulin reducing activity *in vitro* [406]. Therefore it is likely that E1₂₅₉ which includes just 68 residues is not long enough to constitute an active thioredoxin domain as it is lacking structural and functional elements. There are reports of redox active cysteines outside thioredoxin domains [407]. However, the results above show that the Cys residues contained in bacterially expressed E1₂₅₉ do not demonstrate insulin reducing activity. It is possible that the absence of ectodomain glycosylation has altered the structure and/or activity of E1, therefore expression of longer, glycosylated forms of the E1 ectodomain was investigated using a mammalian expression system.

Sequential C-terminal extensions of the E1 ectodomain were introduced into a pcDNA-based vector, terminating at residues 351, 340, 329 and 259. This vector incorporates a C-terminal myc epitope tag to facilitate detection and an N-terminal tissue plasminogen activator leader sequence to promote protein translocation into the ER lumen [246].

To examine expression and secretion of the E1 ectodomain in mammalian cells, pcDNA-E1-transfected HEK 293T cells were radiolabelled with ³⁵S-Met/Cys for 30 min then chased in fresh DMF10 for 4 h. Culture supernatants were subjected to immunoprecipitation with anti-E1 MAb A4 followed by SDS-PAGE analyses under non-reducing and reducing conditions and phosphorimaging (Figure 5-12A and B, respectively).

When run under non-reducing conditions, a single band was detected for the longest form of the ectodomain, E1₃₅₁myc, at approximately 70 kDa (Figure 5-12A). No protein was immunoprecipitated from the cellular supernatant for the E1₃₄₀myc construct. This suggests that E1₃₄₀myc is not maturing through the secretory pathway, possibly due to misfolding and degradation upon expression. Two bands were detected for E1₃₂₉myc at ~40 and 80 kDa. These are likely to represent monomeric and disulfide linked forms of E1 given that when run under reducing conditions the 80 kDa form is no longer evident (Figure 5-12B). For E1₂₅₉myc, a diffuse band was detected at approximately 40 kDa when run under both reducing and non-reducing conditions. These results demonstrate that E1₃₅₁myc, E1₃₂₉myc and E1₂₅₉myc can all be efficiently expressed and secreted from mammalian cells. Interestingly, each of the proteins is detected at a much higher than expected molecular weight. For instance, the amino acid backbone of E1₁₉₁₋₂₅₉ is expected to be ~8 kDa. The average molecular mass of glycan added per sequon is approximately 1687 Da for high-mannose sugar and between 2181 and 2663 Da for hybrid/complex type glycan depending on the modification. Taking into account the three N-linked glycosylation sites incorporated into this length of E1 the observed molecular mass of ~40 kDa is very large. It is possible that when the ectodomain of E1 is expressed in mammalian cells in the absence

of E2, E1 is more exposed for glycosylation resulting in production of hyperglycosylated protein.

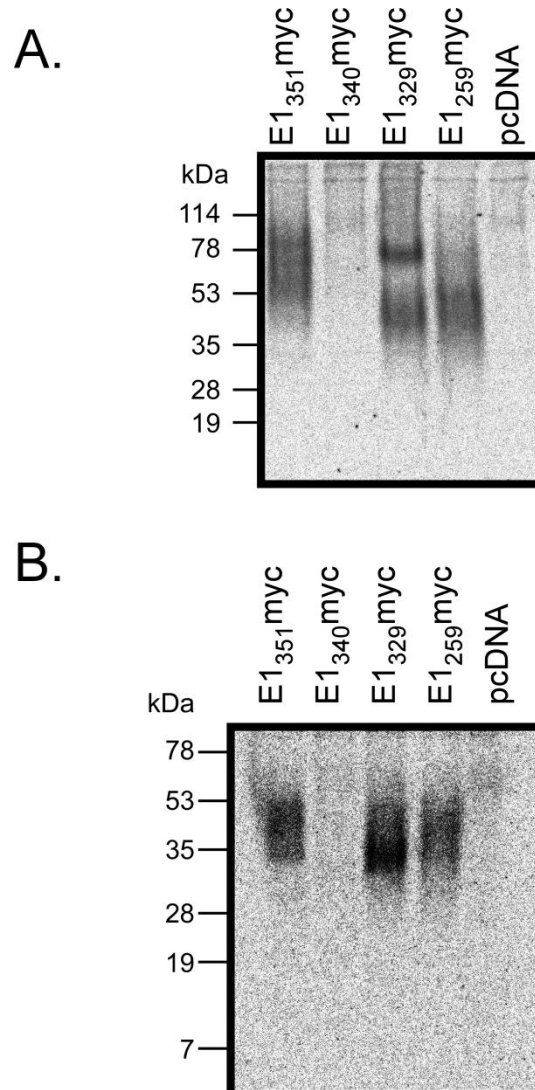


Figure 5-12. Expression of E1-myc in HEK 293T cells. HEK 293T cells transfected with pcE1myc were radiolabelled with ³⁵S-Met/Cys prior to immunoprecipitation of culture supernatant with anti-E1 MAb A4. Samples were run under reducing (A) or non-reducing (B) conditions on SDS-PAGE then phosphorimaged.

5.3.2 Expression of E1-myc in CHO-K1 and Lec-8 cells

To further investigate the observed hyperglycosylation effect for E1 expressed in HEK 293T cells, the pcE1myc constructs were transfected into CHO-

K1 derived cell line Lec-8. Lec-8 cells produce lectin resistant proteins that demonstrate reduced levels of carbohydrate modification [408].

Expression and secretion of each E1myc construct in CHO-K1 and Lec-8 cells was compared to determine if expression in the glycosylation defective Lec-8 cells reduced the extent of carbohydrate attachment. CHO-K1 and Lec-8 cells transfected with pcE1myc were radiolabelled with ³⁵S-Met/Cys for 30 min followed by chase in DMF10 for 4 h. Culture supernatants were examined for the presence of secreted forms of E1 by anti-E1 MAb A4 immunoprecipitation.

In contrast to expression in HEK 293T cells, E1₃₅₁myc was not detected in the culture supernatant of either CHO-K1 or Lec-8 cells by anti-E1 immunoprecipitation indicating that this length of E1 is likely to remain trapped in the ER of these cells or possibly degraded upon expression (Figure 5-13). E1₃₄₀myc was not detected in CHO-K1 or Lec-8 cells consistent with earlier observations. However, E1₃₂₉myc and E1₂₅₉myc were efficiently secreted from both CHO-K1 and Lec-8 cells. In CHO-K1 cells these bands appeared quite diffuse at ~35 and ~30 kDa respectively. In Lec-8 cells, the majority of E1₃₂₉myc migrated at ~35 kDa with a small proportion migrating at ~20 kDa. E1₂₅₉myc was detected at ~20 kDa. This result shows that E1₃₂₉myc can be expressed in a secreted form in a variety of mammalian cell lines. In addition, these results show that E1₃₂₉ is not likely to be hyperglycosylated given that it runs at approximately the same molecular weight in HEK 293T cells, CHO-K1 cells and Lec-8 cells. However, expression of this protein in Lec-8 cells appears to result in more homogenous glycosylation as indicated by a sharper band of protein. This may be advantageous for downstream biochemical analysis of the protein. It should be noted that for E1₃₂₉myc a fraction of protein immunoprecipitated by MAb A4 is evident at approximately the same molecular weight as E1₂₅₉myc. This may represent a cleavage product of E1₃₂₉myc.

E1₂₅₉myc was expressed in a soluble secreted form in the three mammalian cell lines tested. When expressed in HEK 293T and CHO-K1 cells E1₂₅₉myc was

found to be ~10-15 kDa larger than when produced in Lec-8 cells indicative of hyperglycosylation.

These results indicate that E1 residues 191-259 and 191-329 can be expressed and efficiently secreted from mammalian cells.

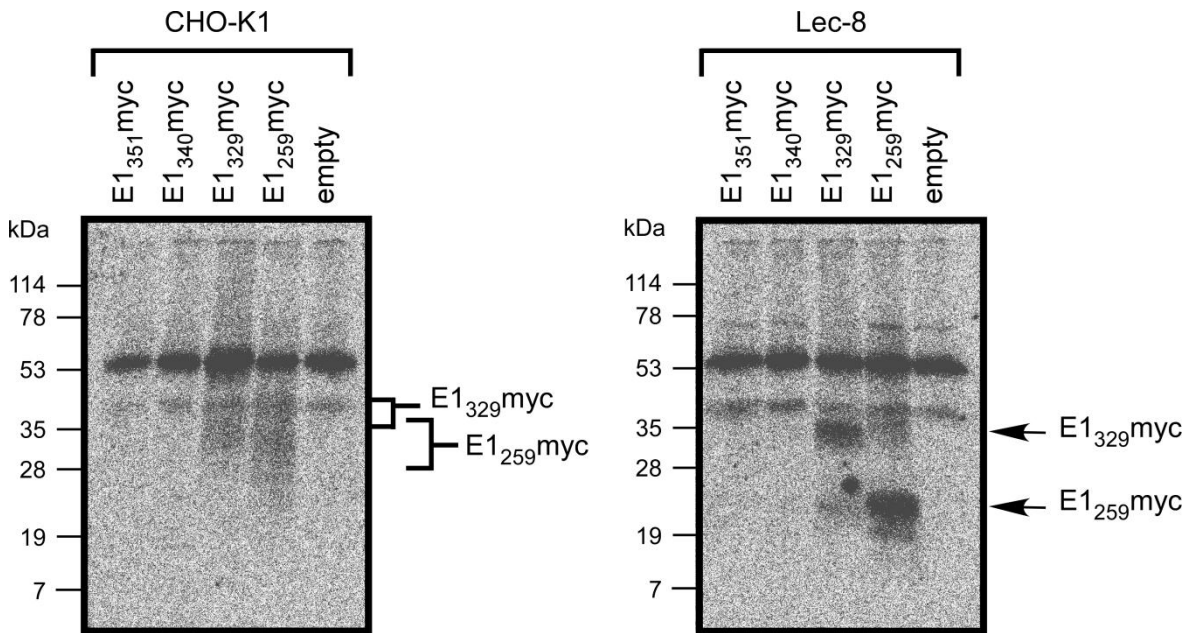


Figure 5-13. Expression of E1-myc in CHO-K1 cells and Lec-8 cells. Cells transfected with pcE1myc were radiolabelled with ^{35}S -Met/Cys prior to immunoprecipitation of culture supernatant with anti-E1 MAb A4. Samples were run under non-reducing conditions on SDS-PAGE then phosphorimaged. Molecular weight markers are indicated to the left of the gels.

5.3.3 Deglycosylation of E1-myc expressed in CHO-K1 and Lec-8 cells

Analysis of the glycans on surface expressed forms of E1 and E2 that are incorporated into HCVpp has shown that E2 contains complex/hybrid type glycan modifications, consistent with trafficking through the *trans*-Golgi network, while E1 contains high-mannose glycans, indicative of modification within the ER or *cis*-Golgi only [3]. It has therefore been suggested that E2 may shield E1 from carbohydrate modification enzymes during maturation through the secretory pathway. This is consistent with a recent examination of HCVcc-incorporated

glycoproteins which indicated that virion-incorporated E1 contains mostly high-mannose glycans [137].

It has been reported that expression of E1 in the absence of E2 can affect the efficiency of E1 glycosylation [221,409]. Glycosylation can directly alter HCV glycoprotein folding and virus function [218,227]. Therefore, the glycan modification on E1₃₂₉myc and E1₂₅₉myc expressed in CHO-K1 and Lec-8 cells was examined.

CHO-K1 and Lec-8 cells transfected with pcE1myc were radiolabelled with ³⁵S-Met/Cys for 4 h then chased in DMF10 for 18 h. Culture supernatants were immunoprecipitated with anti-E1 MAb A4 then treated with PNGase F or Endo H glycosidases. Endo H specifically cleaves high-mannose type and some hybrid glycans, while PNGase F cleaves both high-mannose and complex type glycans.

E1₂₅₉myc secreted from CHO-K1 and Lec-8 cells was found to be insensitive to Endo H digestion, suggesting that this form of E1 contains complex/hybrid type glycans (Figure 5-14A and B). The predicted molecular mass of E1₂₅₉myc with no glycan modification is 8.7 kDa. Treatment of E1₂₅₉myc with PNGase F yielded a protein approximately corresponding to the predicted backbone molecular weight, suggesting that the additional molecular mass associated with E1₂₅₉myc is accounted for by the N-linked complex/hybrid carbohydrates.

E1₃₂₉myc expressed in CHO-K1 and Lec-8 cells showed some sensitivity to Endo H with a proportion of protein running at ~ 9 kDa. When treated with PNGase F, the majority of protein shifted from ~30 kDa (untreated E1₃₂₉myc) to ~9 kDa. For CHO-K1 expressed E1₃₂₉myc, a small amount of protein was also evident at approximately 16 kDa. The predicted molecular mass for the unmodified E1₃₂₉myc peptide sequence is 16.4 kDa. This finding suggests that a proportion of E1₃₂₉myc is subject to proteolytic cleavage within the E1₃₂₉myc sequence generating a polypeptide of ~9 kDa, with a small amount of protein escaping protease digestion.

Together, these data indicate that in the absence of E2, E1₂₅₉myc and E1₃₂₉myc expressed in CHO-K1 and Lec-8 cells are modified by glucosyl hydrolase/transferase enzymes in the *trans*-Golgi network and that E1₃₂₉myc is subject to a post-translational proteolytic cleavage event.

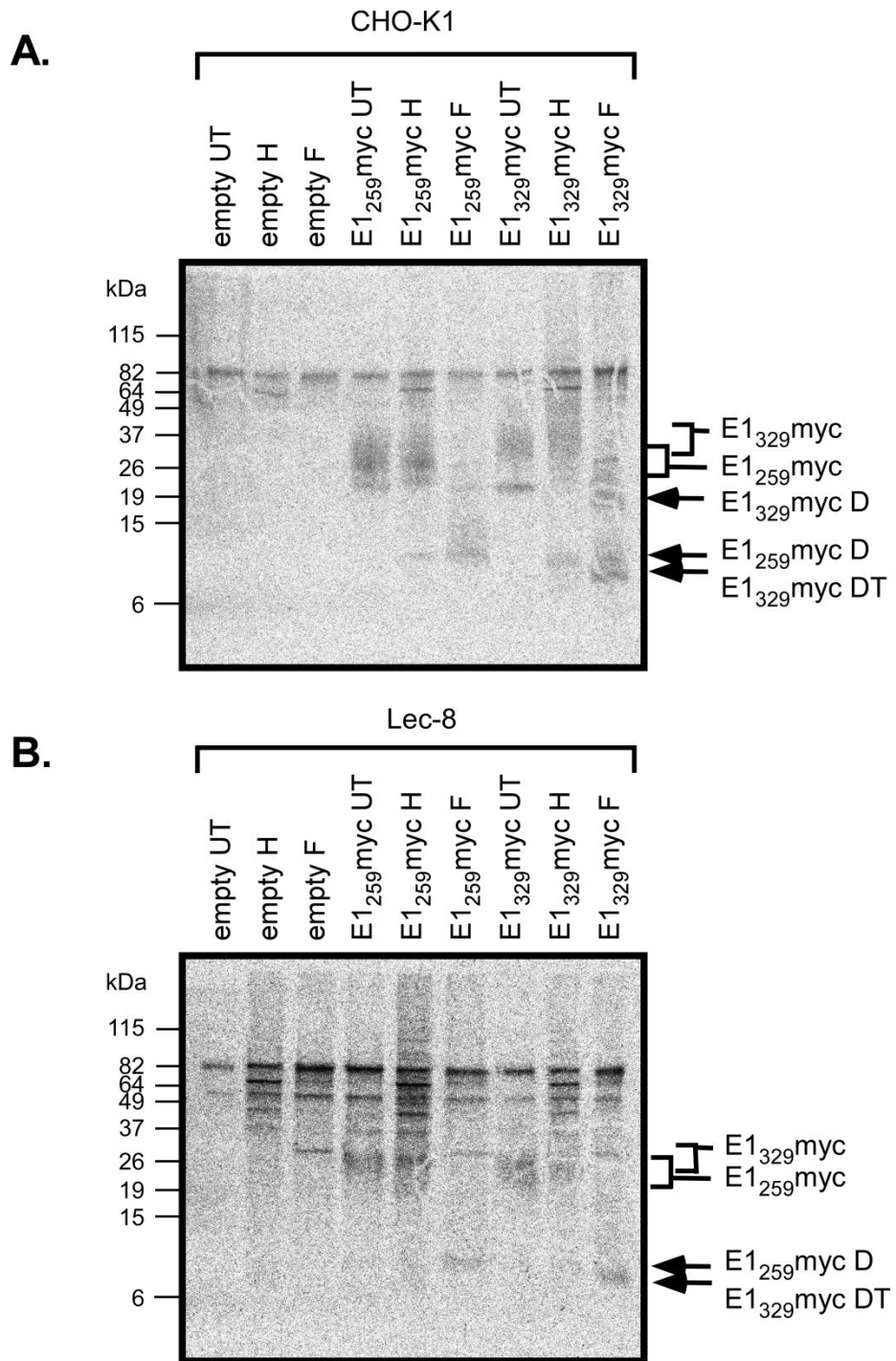


Figure 5-14. Deglycosylation of E1myc proteins expressed in CHO-K1 and Lec-8 cells. Cells transfected with pcE1myc were radiolabelled with ³⁵S-Met/Cys prior to immunoprecipitation of culture supernatant with anti-E1 MAb A4. Samples were treated with Endo H (H), PNGase F (F) or left untreated (UT), then run under non-reducing conditions on SDS-PAGE and phosphorimaged. Molecular weight markers are indicated to the left of the gels. Deglycosylated forms of the proteins are indicated (D), and a truncated product of deglycosylated E1₃₂₉myc is indicated (DT).

5.4 Discussion and Conclusions

In this chapter a variety of expression systems were investigated for production of a soluble, recombinant form of the E1 ectodomain. It was found that residues 191-259 could be expressed in a soluble form in both bacteria and mammalian cells. This is likely to represent a structured domain of E1 given that MBP-E1₂₅₉ demonstrates resistance to chymotrypsin digestion. Extension of the E1 ectodomain beyond residue 259 appeared to result in a proteolytic event in a proportion of E1 protein expressed, both in bacterial and mammalian systems, releasing a truncated form of the protein. This may suggest that E1 residues 191-259 fold to form a domain, independent of other E1 and E2 sequences. It is possible that when expressed in the absence of the E1 TMD, extension of the E1 ectodomain sequence beyond residue 259 may allow folding of residues 191-259 as an independent domain, although the extended sequence may remain unstructured and susceptible to proteolytic cleavage.

Analysis of MBP-E1₂₅₉ indicates that the protein contains secondary structure. However, it is not clear what these structural elements are or whether this form of E1 is similar to E1 that is incorporated into virus particles. Examination of MBP-E1₂₅₉ by techniques such as circular dichroism (CD) or by Fourier transform infrared (FTIR) spectroscopy could provide insight into the β -sheet and α -helical content of this protein. The MBP tag contributes significantly to the total molecular weight of MBP-E1₂₅₉. The structure of MBP is known. Therefore, these known structural elements could be assigned to MBP. It may then be possible to subtract these elements from the MBP-E1₂₅₉ analysis to determine the structural characteristics of E1. Alternatively, a protease cleavage site could be engineered into the MBP-E1₂₅₉ construct to allow removal of the tag after protein purification. By reducing the size of the protein this would also allow structural analysis of E1₂₅₉ by NMR. However, this may compromise E1 solubility. It may also be possible to purify and deglycosylate E1₂₅₉myc to allow analysis of mammalian expressed E1 ectodomain residues 191-259, using these described techniques.

Another limiting factor for evaluation of the structure of recombinantly expressed E1 is the lack of reported conformational antibodies directed towards E1. Comparison of structural epitopes in recombinantly expressed forms of E1 with virion-incorporated E1 could provide insight into the relevance of these forms of the E1 ectodomain.

It has been shown that recombinantly expressed forms of the E2 ectodomain can be used to block HCVcc entry when incubated with hepatocytes prior to addition of infectious virus. [273,283]. E2 has been shown to bind directly to HCV receptor CD81 [2,244,245] and also possibly SR-BI [6,248] and glycosaminoglycans [83,84]. Therefore, inhibition of infection presumably occurs by recombinant E2 occupying free receptor binding sites, preventing attachment of infectious virus. For E1, no receptor binding capacity has been described. However, for alphaviruses the fusion protein (E1) is maintained in a metastable conformation in the prefusion state by association with its partner protein, E2. Activation of the fusion potential of E1 causes dissociation of the heterodimers and rearrangement of E1 into a stabilised homotrimer [344]. It is possible that HCV glycoproteins will follow a similar rearrangement event, as described in section 1.7.1. In this case, addition of soluble recombinant E1 to an HCV infection assay may inhibit productive infection by binding to monomeric E2 during these dissociation and rearrangement events. If such an inhibition occurs following addition of recombinant E1, it would suggest the forms of E1 described here do in fact represent a functional form.

The findings from this study have been used to guide further projects including the development of a baculovirus expression system for soluble heterodimeric E1E2 (R Butcher and J Gu, unpublished). In this system the TMD's of E1 and E2 have been replaced with the soluble heterodimeric leucine zipper proteins jun and fos, respectively. Given that the TMDs of E1 and E2 are a major heterodimerisation determinant [95,236] this system may facilitate native glycoprotein associations while rendering the complex soluble. Furthermore, expression in insect cells allows ectodomain glycosylation to be retained, and by expressing both glycoproteins in *cis*, conformational defects due to potential

folding co-dependence are avoided. It has been found that a soluble, heterodimeric E1E2 complex can be expressed that consists of the entire ectodomain of E2 with *fos* replacing TMD residues 716-746, in association with E1 residues 191-329 C-terminally fused to *jun*. Together, these proteins can be secreted from insect cells as a soluble heterodimer that retains CD81 receptor binding functionality.

Interestingly, in this system E1₁₉₁₋₃₂₉*jun* can be expressed and purified without production of a cleavage product (data not shown). It may be that replacement of the E1 myc tag with the solubility tag *jun*, promotes folding and stability of the residues extending beyond E1 residue 259. Alternatively, co-expression of E1 with E2 may promote correct folding of E1. This construct will provide a useful tool for future investigations into E1E2 structure and functional activity.

The soluble domain of E1 residues 191-259 contains the highly conserved E1 C²²⁶V/LPC thiol-disulfide exchange motif. Structural analyses of the ectodomain of E1 may provide further insight into the function of this motif. The CXXC active site of many redox active proteins is contained within a thioredoxin domain. Well characterised *E. coli* thioredoxin is comprised of three parallel and two anti-parallel β -sheets surrounded by four α -helices [410]. This fold has also been described for many other thioredoxins including human and plant homologues. NMR structures demonstrating the thioredoxin active site CXXC motif in a reduced (human thioredoxin [411]) and oxidised state (thioredoxin from the eukaryotic green alga *Chlamydomonas reinhardtii* [412]) are shown in Figure 5-15. The structural features which enable a fold to be classed as a classical thioredoxin fold is more minimal, consisting of a four-stranded β -sheet and three flanking α -helices. This fold has been identified in the structure of 5 classes of protein that demonstrate a variety of redox functions, including thioredoxin [410,413], glutaredoxin [414,415,416,417], glutathione S-transferase [418,419,420,421], DsbA [422] and glutathione peroxidase [423] (for review of the thioredoxin fold see [390]).

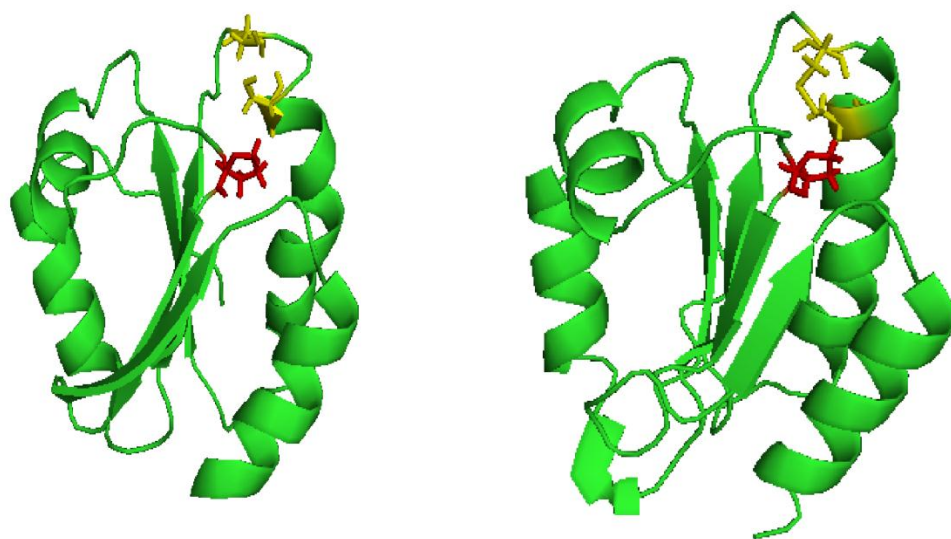


Figure 5-15. NMR structures of thioredoxin in reduced and oxidised forms. Reduced thioredoxin is shown to the left and oxidised thioredoxin is shown to the right. Cys residues of the CXXC motif are shown in yellow. The active site *cis*-Pro is shown in red. Derived from the coordinates 3TRX (reduced) and 1TOF (oxidized) and drawn in SwissProt.

An alternative way to evaluate the structural relevance of recombinantly expressed E1 may be to use a functional assay. Protein disulfide isomerase (PDI) is a member of the thioredoxin superfamily and is abundantly expressed in the ER of eukaryotic cells. It was first described in 1963 as a protein capable of assisting the refolding of ribonuclease [424]. There are now at least 19 published PDI family members classified by their ER localisation motif and the presence of at least one thioredoxin-like domain [399]. Not all of these PDIs contain a classical CXXC thioredoxin active site motif and as such do not demonstrate significant oxidoreductase activity by *in vitro* analyses (for example the non-catalytic human PDI, PDILT [425]). However, all PDIs identified that contain a CXXC motif have been able to catalyse disulfide exchange *in vitro* (see for example [426,427,428]). MBP-E1₂₅₉ did not demonstrate activity in an *in vitro* insulin reduction assay as described above possibly because the 68 residues expressed are not likely to be sufficient to represent a functional thioredoxin domain, typically 105 amino acids in length. It is important to note that catalytic thiols can still be active without being contained within a thioredoxin fold [407]. For example, a thioredoxin fold has not been described for MLV and HTLV-1 viral envelope protein SU, which contains a

catalytic thiol within a CXXC motif [359,360]. Therefore while HCV glycoprotein E1 may have evolved to contain a thioredoxin fold, this is not a requirement in order for E1 to demonstrate redox activity. Considering this, the truncated length of E1₂₅₉ will not necessarily restrict the redox activity of the C²²⁶V/LPC motif.

An insulin reduction assay has proved to be an efficient way to determine if a protein of interest demonstrates reducing activity (see [428,429,430] for example). Although, this is not necessarily a measure of the redox activity of a protein as it does not consider oxidising or isomerisation activity. Conventional assays used to determine if a protein demonstrates these activities are ribonuclease A (RNase A) oxidation and isomerisation assays [431]. RNase A has 8 cysteine residues which form four intramolecular disulfide bonds [432]. The oxidising ability of a protein can be measured by the rate of formation of the 4 disulfide bonds in unfolded RNase A. The subsequent activity of RNase A can be monitored spectrophotometrically by RNase A cleavage of a substrate such as cCMP. Alternatively, the isomerase activity of a protein can be determined by its ability to refold "scrambled" RNase A that has adopted mis-formed disulfide bonds. In order to restore the activity of scrambled RNase A, mis-formed disulfides must be broken followed by formation of the correct disulfides. It is possible that the HCV E1 C²²⁶V/LPC motif may demonstrate oxidation or isomerisation properties. However, without further insight into the role of the free sulfhydryl groups during E1E2 glycoprotein biosynthesis and/or virus entry this remains unclear. Despite the truncated length of MBP-E1₂₅₉ it is still possible that the CXXC motif will demonstrate redox activity as discussed above. Therefore, this protein represents a good candidate for testing in RNase A refolding assays in future experiments.

In addition to analysing redox activity of E1 it would be interesting to determine whether the E1 C²²⁶V/LPC motif is contained within a thioredoxin-like fold. This would be a novel find as this fold has not previously been reported for a viral envelope glycoprotein. Although the E1 sequence in MBP-E1₂₅₉ is not likely to be long enough to represent a complete thioredoxin domain, the residues may form a partial thioredoxin domain. The high quantity and purity of MBP-E1₂₅₉

produced make this a good candidate for crystallisation trials in order to gain structural insight into the fold of this domain.

As well as a CXXC motif, a highly conserved proline residue has been observed in 5 distinct classes of thioredoxin families proteins [390]. This proline is found in the less common *cis* conformation. Pro76 in bacterial thioredoxin is located in the *cis*-Pro loop formed between α -helix 2 and β -sheet 3, 44 residues upstream of the thiol active Cys. In this conformation proline is solvent exposed and has been shown to be critical for forming hydrogen bonds between thioredoxin-related protein glutaredoxin, and its substrate. Hence, the highly conserved *cis*-Pro is thought to form part of the substrate binding pocket. Without a crystal structure it is not possible to identify the presence of an equivalent *cis*-Pro in E1, although two candidate highly conserved proline residues may play a similar role including Pro244 and Pro294. Mutagenesis of these residues would determine their role in glycoprotein biosynthesis and/or virus entry and may provide supporting evidence for E1 as a thioredoxin-like protein.

Despite the fact that a complete thioredoxin fold is not required for a catalytic thiol to be active, sequences surrounding a CXXC motif can be essential for substrate interactions [394]. If truncation of the E1 sequence E1₂₅₉ has affected a substrate binding site(s) then this domain may not demonstrate activity in any *in vitro* assay. An alternative method for measuring the activity of a redox active protein has been described using a mammalian cell based intracellular assay. Such an assay would allow expression of full length glycosylated E1 avoiding potential conformation differences induced by expression of E1 in the absence of the glycoprotein TMD and partner protein E2. This assay has been described for Ero1-L α and Ero1-L β (hEROs) which help to regulate the redox state of the ER by selectively reducing the PDI CXXC motif after PDI has catalysed disulfide bond formation in a substrate protein [433]. The activity of hEROs can be monitored indirectly by measuring the rate of oxidative folding of immunoglobulin (Ig) subunit, J chain, in the ER of mammalian cells over-expressing either Ero1-L α or Ero1-L β . J chains are polymeric Ig subunits that are linked by three intra-chain disulfide bonds [434]. The formation of intrachain disulfide bonds is indicative of a folded

subunit which then exits the ER. Meanwhile unassembled J chains are retained in the ER leading to eventual degradation by the proteasome. J chain folding can be monitored by non-reducing SDS-PAGE analysis which shows the transition of reduced monomeric J chains to oxidised monomeric forms, followed by formation of dimeric and high molecular weight forms. PDI assists in the formation of the J chain disulfide bonds and hence by controlling the redox state of PDI, hEROs can contribute to the oxidative folding rate of proteins in the ER. This assay avoids the need for large amounts of recombinantly expressed protein and demonstrates an efficient way of monitoring redox regulation of an important ER factor, PDI.

Using an assay such as that described for the hEROs it can be determined whether E1 is capable of influencing the oxidative folding of proteins in the ER. To determine whether changes in redox activity are directly related to the E1 C²²⁶V/LPC motif, mutants described in Chapter 4 that were defective in folding and/or entry could be analysed.

Although a CXXC motif with apparent catalytic activity has been described for the receptor binding glycoprotein from HTLV-1 and MLV retroviruses, there have been no reports of *in vitro* thioredoxin activity for these proteins. It is possible that redox activity demonstrated by the viral CXXC motifs may be highly substrate specific. For example, HCV E1 may specifically provide redox activity to control folding of itself or E2 either during biosynthesis or during virus entry as discussed in Chapter 4. In this case it is unlikely that redox activity could be measured for E1 using the assays described above. More specialised assays that directly analyse changes in the oxidation state of E1 and/or E2 may need to be developed to determine whether the C²²⁶V/LPC motif demonstrates redox activity. For example, monitoring the availability of free thiol groups in E1 and E2 during biosynthesis and/or entry by the ability of a sulfhydryl-reactive fluorophore to bind the glycoproteins.

An important distinction between thioredoxin and HCV glycoprotein E1 is the presence of the membrane anchoring TMD in E1. Although most described redox active proteins exist in a soluble form, membrane bound thioredoxin-like

proteins have been described. An example is the TMX family which consists of four TMX family proteins each of which carries a TMD, an ER localisation sequence and a thioredoxin-like domain containing a CXXC motif (or SXXC for TMX2) [426,428,435,436]. Recently TMX4 was described as a membrane bound protein facing the lumen of the ER. A recombinant form of TMX4 was shown to have reductase activity, demonstrating reduction of disulfide bonds in insulin in a dose dependent manner *in vitro*. TMX4 can be co-precipitated with ER chaperone calnexin and thiol-oxidoreductase protein ERp57. Hence, TMX4 is predicted to form a complex with these proteins to aid productive folding of substrates in the ER [428]. This growing family of membrane bound thioredoxin-like proteins further demonstrates the diversity of proteins in which redox active thioredoxin domains are found and provides precedence for the functional relevance of a CXXC motif maintained in a membrane bound protein.

By investigating the effect of ectodomain length on E1 solubility, these results have provided further insight into the domain structure of E1 with residues 191-259 predicted to fold independently of other HCV envelope protein sequences. These results have been used to guide additional projects in the lab including development of a baulovirus expression system for soluble forms of the E1 and E2 ectodomains, as described above. This system, in conjunction with the soluble MBP-E1₂₅₉, E1₂₅₉myc and E1₃₂₉myc proteins described here, may be used to further evaluate the structure and function of the E1 and E2 glycoproteins in future studies.

Chapter 6 – General Conclusions

Despite the recent development of a full length, replication competent cell culture system for HCV, much of the basic biochemistry surrounding HCV envelope glycoprotein structure and function remains unclear.

This project examined for the first time the oxidation state of virion incorporated forms of HCV envelope glycoproteins E1 and E2. The findings demonstrate that at least one free thiol group is maintained on HCVpp-incorporated forms of each glycoprotein. Free thiol group(s) were shown to be essential for HCVcc and HCVpp virus entry. The observation that entry of alkylated HCVcc could not be rescued by addition of exogenous reducing agent, and that free thiol groups in HCVcc were no longer reactive to sulfhydryl alkylation following cellular binding, is consistent with the glycoproteins undergoing a disulfide isomerisation reaction following receptor engagement. This suggests that the free thiol groups in HCV E1E2 may catalyse a reaction distinct to that identified for the retroviruses MLV and HTLV-1 where a reduction event only is required to mediate virus entry [359,360].

A recent publication has suggested that HCVcc derived virus displays high molecular weight disulfide linked forms of E1 and E2 on its surface [137]. Given that both E1 and E2 contain an even number of conserved Cys residues this finding is consistent with the maintenance of at least one free thiol group on each glycoprotein. The authors suggested that intracellular E1E2 are non-covalently associated, indicating that HCV glycoproteins undergo a maturation step during egress whereby covalent linkages are formed. This is supported here by the finding that alanine mutagenesis of either Cys residue within a highly conserved E1 C²²⁶V/LPC thiol isomerisation motif results in accumulation of non-functional disulfide linked glycoprotein. This would suggest that the oligomeric arrangement of the glycoproteins must be carefully controlled during glycoprotein biosynthesis.

The HCV CXXC motif may function like a typical thioredoxin family domain, and regulate disulfide shuffling during glycoprotein biosynthesis in order to obtain a functionally active envelope complex. However, mutagenesis of the internal dipeptide residues of the HCV E1 C²²⁶V/LPC motif indicates the motif plays an essential role in virus entry. A role in regulating glycoprotein oxidation during virus entry would be consistent with the finding in Chapter 3 that the glycoproteins may undergo a disulfide rearrangement event following receptor binding. During biosynthesis the motif may instead provide structural constraints rather than acting as a redox catalyst.

Taken together, the data from this investigation suggest a model where prior to fusion activation disulfide linked E1 and E2 heterodimers contain at least one free thiol group each. This may include a catalytic thiol within the E1 CXXC motif (Figure 6-1). Following cellular binding, deprotonation of the catalytic thiol may occur causing the thiol to attack a disulfide bonded Cys within the glycoprotein complex, possibly in E2. If the E1 CXXC motif functions as a typical thioredoxin motif, then the mixed disulfide between the catalytic thiol and target Cys would be resolved by the second Cys in the CXXC motif. The reduced glycoproteins would then be able to form new disulfides to adopt a lower energy, oxidised conformation. This may leave the viral glycoproteins primed for fusion activation induced upon exposure to low pH.

In order to directly determine whether the C²²⁶V/LPC motif regulates disulfide rearrangement during virus entry an extensive proteomic analysis is required. Sulfhydryl alkylation of HCVcc incorporated glycoproteins followed by glycoprotein extraction and analysis by mass spectrometry is required in order to determine whether the C²²⁶V/LPC Cys residues are in the catalytically active, reduced state in the prefusion conformation. These experiments are limited by the low virus titre of the current HCVcc models. In addition, identification of the functional glycoprotein oligomer is required before relevant free thiol groups can be identified. In order to confirm whether changes in the oxidation state of E1 and E2 occur during virus entry, analyses of the glycoproteins following cellular attachment should be performed. It appears that neither cell free heparin nor

CD81 are individually sufficient to render the glycoproteins insensitive to sulfhydryl reactive agents, as observed following HCVcc attachment to cells. Instead, it is possible that the full length conformational form of these cellular factors, or a sequence of binding events is required to trigger disulfide oxidation in the HCV glycoproteins.

Viral envelope glycoproteins represent important antiviral targets. The HIV peptide Fuzeon (T-20) provides precedence for effective virus entry inhibitors, preventing HIV infection by binding to the N-trimer of envelope glycoprotein gp41 [437]. Furthermore, medically relevant thiol-reactive trivalent-arsenical agents that target free thiol groups have been shown to block HIV-1 entry via modification of cell-surface thioredoxin [376]. The C²²⁶V/LPC thioredoxin-like motif in E1 is highly conserved and is strictly required for HCV functionality therefore this region of E1 is likely to represent a good antiviral target. Furthermore, this study indicates that agents that manipulate the oxidation state of the HCV glycoproteins may act as potent entry inhibitors.

Development and optimisation of small molecules that specifically target and bind E1 and/or E2 will likely require a structural model of the glycoproteins. This project identified a stable domain of E1 that can be expressed at high levels in a non-aggregated form in bacteria, representing a good candidate for crystallisation studies. Structural information regarding this domain which incorporates the highly conserved, and functionally critical C²²⁶V/LPC motif, will provide an important tool for development of small molecule inhibitors that directly target E1.

This project is the first direct examination of the oxidation state of virion-incorporated forms of the HCV glycoproteins. The findings indicate that the oxidation state of E1 and E2 must be carefully regulated during glycoprotein biosynthesis and virus entry, and has identified critical regions of envelope glycoprotein E1 required for virus function.

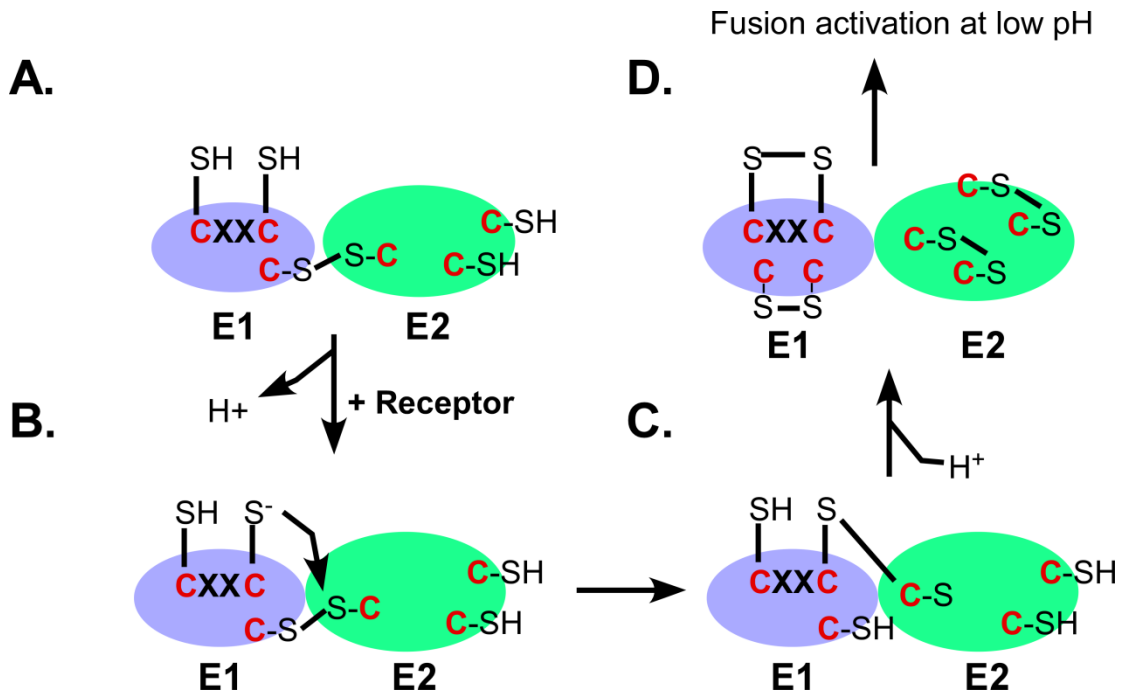


Figure 6-1. Schematic model demonstrating the predicated role of thiol isomerisation in fusion activation of HCV glycoproteins E1 and E2. A. Prior to fusion activation disulfide linked E1 and E2 heterodimers contain at least one free thiol group each. This may include a catalytic thiol within the E1 CXXC motif. B. Activation of the catalytic thiol by receptor engagement, for example, may activate the catalytic thiol to attack a disulfide bonded Cys, possibly in E2. C. Transient formation of a mixed disulfide between the catalytic thiol and target Cys is resolved by the second Cys in the CXXC motif. D. Reduced glycoproteins are able to reform new disulfides to adopt their lowest energy conformation, leaving the virus primed for final conformational changes induced upon exposure to low pH.

Chapter 7 - References

1. Group GBOHCW (2004) Global burden of disease (GBD) for hepatitis C. *J Clin Pharmacol* 44: 20-29.
2. Bartosch B, Dubuisson J, Cosset FL (2003) Infectious hepatitis C virus pseudo-particles containing functional E1-E2 envelope protein complexes. *J Exp Med* 197: 633-642.
3. Drummer HE, Maerz A, Pountourios P (2003) Cell surface expression of functional hepatitis C virus E1 and E2 glycoproteins. *FEBS Lett* 546: 385-390.
4. Matsuura Y, Tani H, Suzuki K, Kimura-Someya T, Suzuki R, et al. (2001) Characterization of pseudotype VSV possessing HCV envelope proteins. *Virology* 286: 263-275.
5. Pileri P, Uematsu Y, Campagnoli S, Galli G, Falugi F, et al. (1998) Binding of hepatitis C virus to CD81. *Science* 282: 938-941.
6. Scarselli E, Ansuini H, Cerino R, Roccasecca RM, Acali S, et al. (2002) The human scavenger receptor class B type I is a novel candidate receptor for the hepatitis C virus. *Embo J* 21: 5017-5025.
7. Zeisel MB, Koutsoudakis G, Schnober EK, Haberstroh A, Blum HE, et al. (2007) Scavenger receptor class B type I is a key host factor for hepatitis C virus infection required for an entry step closely linked to CD81. *Hepatology* 46: 1722-1731.
8. Evans MJ, von Hahn T, Tscherne DM, Syder AJ, Panis M, et al. (2007) Claudin-1 is a hepatitis C virus co-receptor required for a late step in entry. *Nature* 446: 801-805.
9. Zheng A, Yuan F, Li Y, Zhu F, Hou P, et al. (2007) Claudin-6 and claudin-9 function as additional coreceptors for hepatitis C virus. *J Virol* 81: 12465-12471.
10. Ploss A, Evans MJ, Gaysinskaya VA, Panis M, You H, et al. (2009) Human occludin is a hepatitis C virus entry factor required for infection of mouse cells. *Nature* 457: 882-886.
11. Tscherne DM, Jones CT, Evans MJ, Lindenbach BD, McKeating JA, et al. (2006) Time- and temperature-dependent activation of hepatitis C virus for low-pH-triggered entry. *J Virol* 80: 1734-1741.
12. Choo QL, Kuo G, Weiner AJ, Overby LR, Bradley DW, et al. (1989) Isolation of a cDNA clone derived from a blood-borne non-A, non-B viral hepatitis genome. *Science* 244: 359-362.
13. Kuo G, Choo QL, Alter HJ, Gitnick GL, Redeker AG, et al. (1989) An assay for circulating antibodies to a major etiologic virus of human non-A, non-B hepatitis. *Science* 244: 362-364.

14. Perz JF, Armstrong GL, Farrington LA, Hutin YJ, Bell BP (2006) The contributions of hepatitis B virus and hepatitis C virus infections to cirrhosis and primary liver cancer worldwide. *J Hepatol* 45: 529-538.
15. Frank C, Mohamed MK, Strickland GT, Lavanchy D, Arthur RR, et al. (2000) The role of parenteral antischistosomal therapy in the spread of hepatitis C virus in Egypt. *Lancet* 355: 887-891.
16. Shepard CW, Finelli L, Alter MJ (2005) Global epidemiology of hepatitis C virus infection. *Lancet Infect Dis* 5: 558-567.
17. Armstrong GL, Wasley A, Simard EP, McQuillan GM, Kuhnert WL, et al. (2006) The prevalence of hepatitis C virus infection in the United States, 1999 through 2002. *Ann Intern Med* 144: 705-714.
18. Hayashi J, Nakashima K, Yoshimura E, Hirata M, Maeda Y, et al. (1994) Detection of HCV RNA in subjects with antibody to hepatitis C virus among the general population of Fukuoka, Japan. *J Gastroenterol* 29: 147-151.
19. Ito S, Ito M, Cho MJ, Shimotohno K, Tajima K (1991) Massive sero-epidemiological survey of hepatitis C virus: clustering of carriers on the southwest coast of Tsushima, Japan. *Jpn J Cancer Res* 82: 1-3.
20. (1999) Prevalence of hepatitis C virus infection in the general population and patients with liver disease in China. *Hepatology Research* 14: 135-143.
21. Xia G-L, Liu C-B, Cao H-L, Bi S-L, Zhan M-Y, et al. (1996) Prevalence of hepatitis B and C virus infections in the general Chinese population. Results from a nationwide cross-sectional seroepidemiologic study of hepatitis A, B, C, D, and E virus infections in China, 1992. *International Hepatology Communications* 5: 62-73.
22. Bellentani S, Miglioli L, Masutti F, Saccoccio G, Tiribelli C (2000) Epidemiology of hepatitis C virus infection in Italy: the slowly unraveling mystery. *Microbes Infect* 2: 1757-1763.
23. Ishibashi M, Shinzawa H, Kuboki M, Tsuchida H, Takahashi T (1996) Prevalence of inhabitants with anti-hepatitis C virus antibody in an area following an acute hepatitis C epidemic: age-and area-related features. *J Epidemiol* 6: 1-7.
24. Sun CA, Chen HC, Lu SN, Chen CJ, Lu CF, et al. (2001) Persistent hyperendemicity of hepatitis C virus infection in Taiwan: the important role of iatrogenic risk factors. *J Med Virol* 65: 30-34.
25. Alter MJ (1997) Epidemiology of hepatitis C. *Hepatology* 26: 62S-65S.
26. Chiamonte M, Stroffolini T, Lorenzoni U, Minniti F, Conti S, et al. (1996) Risk factors in community-acquired chronic hepatitis C virus infection: a case-control study in Italy. *Journal of Hepatology* 24: 129-134.
27. (2010) HIV, viral hepatitis and sexually transmissible infections in Australia Annual Surveillance Report 2010. The University of New South Wales.
28. Hauri AM, Armstrong GL, Hutin YJ (2004) The global burden of disease attributable to contaminated injections given in health care settings. *Int J STD AIDS* 15: 7-16.

29. Miller FD, Abu-Raddad LJ (2010) Evidence of intense ongoing endemic transmission of hepatitis C virus in Egypt. *Proc Natl Acad Sci U S A* 107: 14757-14762.
30. Wise M, Bialek S, Finelli L, Bell BP, Sorvillo F (2008) Changing trends in hepatitis C-related mortality in the United States, 1995-2004. *Hepatology* 47: 1128-1135.
31. Chow JH, Chow, C. (2006) *The encyclopedia of hepatitis and other liver diseases*. New York: Facts on File Inc.
32. Seeff LB (1999) Natural history of hepatitis C. *Am J Med* 107: 10S-15S.
33. Farci P, Alter HJ, Wong D, Miller RH, Shih JW, et al. (1991) A long-term study of hepatitis C virus replication in non-A, non-B hepatitis. *N Engl J Med* 325: 98-104.
34. Major ME, Mihalik K, Fernandez J, Seidman J, Kleiner D, et al. (1999) Long-term follow-up of chimpanzees inoculated with the first infectious clone for hepatitis C virus. *J Virol* 73: 3317-3325.
35. Shimizu YK, Weiner AJ, Rosenblatt J, Wong DC, Shapiro M, et al. (1990) Early events in hepatitis C virus infection of chimpanzees. *Proc Natl Acad Sci U S A* 87: 6441-6444.
36. Thimme R, Oldach D, Chang KM, Steiger C, Ray SC, et al. (2001) Determinants of viral clearance and persistence during acute hepatitis C virus infection. *J Exp Med* 194: 1395-1406.
37. Shoukry NH, Cawthon AG, Walker CM (2004) Cell-mediated immunity and the outcome of hepatitis C virus infection. *Annu Rev Microbiol* 58: 391-424.
38. Hoofnagle JH (2002) Course and outcome of hepatitis C. *Hepatology* 36: S21-29.
39. Villano SA, Vlahov D, Nelson KE, Cohn S, Thomas DL (1999) Persistence of viremia and the importance of long-term follow-up after acute hepatitis C infection. *Hepatology* 29: 908-914.
40. Hoofnagle JH, Mullen KD, Jones DB, Rustgi V, Di Bisceglie A, et al. (1986) Treatment of chronic non-A,non-B hepatitis with recombinant human alpha interferon. A preliminary report. *N Engl J Med* 315: 1575-1578.
41. Di Bisceglie AM, Hoofnagle JH (2002) Optimal therapy of hepatitis C. *Hepatology* 36: S121-127.
42. McHutchison JG, Poynard T (1999) Combination therapy with interferon plus ribavirin for the initial treatment of chronic hepatitis C. *Semin Liver Dis* 19 Suppl 1: 57-65.
43. Glue P, Fang JW, Rouzier-Panis R, Raffanel C, Sabo R, et al. (2000) Pegylated interferon-alpha2b: pharmacokinetics, pharmacodynamics, safety, and preliminary efficacy data. *Hepatitis C Intervention Therapy Group. Clin Pharmacol Ther* 68: 556-567.
44. Pearlman BL (2004) Hepatitis C treatment update. *Am J Med* 117: 344-352.

45. Ghany MG, Strader DB, Thomas DL, Seeff LB (2009) Diagnosis, management, and treatment of hepatitis C: An update. *Hepatology* 49: 1335-1374.
46. Simmonds P, Holmes EC, Cha TA, Chan SW, McOmish F, et al. (1993) Classification of hepatitis C virus into six major genotypes and a series of subtypes by phylogenetic analysis of the NS-5 region. *J Gen Virol* 74 (Pt 11): 2391-2399.
47. Zeuzem S, Berg T, Moeller B, Hinrichsen H, Mauss S, et al. (2009) Expert opinion on the treatment of patients with chronic hepatitis C. *J Viral Hepat* 16: 75-90.
48. Afdahl N, Godofsky E, Dienstag J, Rustgi V, Schick L, et al. Final phase I/II trial results for NM283, a new polymerase inhibitor for hepatitis C: antiviral efficacy and tolerance in patients with HCV-1 infection, including previous interferon failures.; 2004; Boston, Massachusetts.
49. Jensen DM, Wedemeyer H, Jr RH, Ferenci P, Ma M-M, et al. High rates of early viral response, promising safety profile and lack of resistance-related breakthrough in HCV GT1/4 patients treated with RG7128 plus PegIFN alfa-2a (40KD)/RBV: Planned Week 12 interim analysis from the PROPEL study; 2010; Boston, MA.
50. Forestier N, Reesink HW, Weegink CJ, McNair L, Kieffer TL, et al. (2007) Antiviral activity of telaprevir (VX-950) and peginterferon alfa-2a in patients with hepatitis C. *Hepatology* 46: 640-648.
51. Reesink HW, Zeuzem S, Weegink CJ, Forestier N, van Vliet A, et al. (2006) Rapid decline of viral RNA in hepatitis C patients treated with VX-950: a phase Ib, placebo-controlled, randomized study. *Gastroenterology* 131: 997-1002.
52. Lindenbach BD, Thiel HJ, Rice CM (2007) *Fields Virology*; Knipe DM, Howley PM, editors. 3177 p.
53. Thiel HJ (2005) *Virus taxonomy*. 979-996 p.
54. Choo QL, Richman KH, Han JH, Berger K, Lee C, et al. (1991) Genetic organization and diversity of the hepatitis C virus. *Proc Natl Acad Sci U S A* 88: 2451-2455.
55. (2005) *Virus taxonomy* Fauquet CM, Mayo MA, Maniloff J, Desselberger U, Ball LA, editors. California, USA: Elsevier academic press.
56. Kielian M, Rey FA (2006) Virus membrane-fusion proteins: more than one way to make a hairpin. *Nat Rev Microbiol* 4: 67-76.
57. Wakita T, Pietschmann T, Kato T, Date T, Miyamoto M, et al. (2005) Production of infectious hepatitis C virus in tissue culture from a cloned viral genome. *Nat Med* 11: 791-796.
58. Kunkel M, Watowich SJ (2002) Conformational changes accompanying self-assembly of the hepatitis C virus core protein. *Virology* 294: 239-245.
59. Matsumoto M, Hwang SB, Jeng KS, Zhu N, Lai MM (1996) Homotypic interaction and multimerization of hepatitis C virus core protein. *Virology* 218: 43-51.

60. Bonnafous P, Perrault M, Le Bihan O, Bartosch B, Lavillette D, et al. (2010) Characterization of hepatitis C virus pseudoparticles by cryo-transmission electron microscopy using functionalized magnetic nanobeads. *J Gen Virol* 91: 1919-1930.
61. Yu X, Qiao M, Atanasov I, Hu Z, Kato T, et al. (2007) Cryo-electron microscopy and three-dimensional reconstructions of hepatitis C virus particles. *Virology* 367: 126-134.
62. Kuhn RJ, Zhang W, Rossmann MG, Pletnev SV, Corver J, et al. (2002) Structure of dengue virus: implications for flavivirus organization, maturation, and fusion. *Cell* 108: 717-725.
63. Mukhopadhyay S, Kim BS, Chipman PR, Rossmann MG, Kuhn RJ (2003) Structure of West Nile virus. *Science* 302: 248.
64. Bottcher C, Ludwig K, Herrmann A, van Heel M, Stark H (1999) Structure of influenza haemagglutinin at neutral and at fusogenic pH by electron cryo-microscopy. *FEBS Lett* 463: 255-259.
65. Roux KH, Taylor KA (2007) AIDS virus envelope spike structure. *Curr Opin Struct Biol* 17: 244-252.
66. Thomssen R, Bonk S, Propfe C, Heermann KH, Kochel HG, et al. (1992) Association of hepatitis C virus in human sera with beta-lipoprotein. *Med Microbiol Immunol* 181: 293-300.
67. Andre P, Komurian-Pradel F, Deforges S, Perret M, Berland JL, et al. (2002) Characterization of low- and very-low-density hepatitis C virus RNA-containing particles. *J Virol* 76: 6919-6928.
68. Nielsen SU, Bassendine MF, Burt AD, Martin C, Pumeechockchai W, et al. (2006) Association between hepatitis C virus and very-low-density lipoprotein (VLDL)/LDL analyzed in iodixanol density gradients. *J Virol* 80: 2418-2428.
69. Hijikata M, Shimizu YK, Kato H, Iwamoto A, Shih JW, et al. (1993) Equilibrium centrifugation studies of hepatitis C virus: evidence for circulating immune complexes. *J Virol* 67: 1953-1958.
70. Thomssen R, Bonk S, Thiele A (1993) Density heterogeneities of hepatitis C virus in human sera due to the binding of beta-lipoproteins and immunoglobulins. *Med Microbiol Immunol* 182: 329-334.
71. Gibbons GF, Islam K, Pease RJ (2000) Mobilisation of triacylglycerol stores. *Biochim Biophys Acta* 1483: 37-57.
72. Gibbons GF, Wiggins D, Brown AM, Hebbachi AM (2004) Synthesis and function of hepatic very-low-density lipoprotein. *Biochem Soc Trans* 32: 59-64.
73. Diaz O, Delers F, Maynard M, Demignot S, Zoulim F, et al. (2006) Preferential association of Hepatitis C virus with apolipoprotein B48-containing lipoproteins. *J Gen Virol* 87: 2983-2991.
74. Andreo U, Maillard P, Kalinina O, Walic M, Meurs E, et al. (2007) Lipoprotein lipase mediates hepatitis C virus (HCV) cell entry and inhibits HCV infection. *Cell Microbiol* 9: 2445-2456.

75. Owen DM, Huang H, Ye J, Gale M, Jr. (2009) Apolipoprotein E on hepatitis C virion facilitates infection through interaction with low-density lipoprotein receptor. *Virology* 394: 99-108.
76. Lamb RA, Paterson RG, Jardetzky TS (2006) Paramyxovirus membrane fusion: lessons from the F and HN atomic structures. *Virology* 344: 30-37.
77. Xu Y, Lou Z, Liu Y, Pang H, Tien P, et al. (2004) Crystal structure of severe acute respiratory syndrome coronavirus spike protein fusion core. *J Biol Chem* 279: 49414-49419.
78. Skehel JJ, Wiley DC (2000) Receptor binding and membrane fusion in virus entry: the influenza hemagglutinin. *Annu Rev Biochem* 69: 531-569.
79. Heinz FX, Allison SL (2000) Structures and mechanisms in flavivirus fusion. *Adv Virus Res* 55: 231-269.
80. Monazahian M, Bohme I, Bonk S, Koch A, Scholz C, et al. (1999) Low density lipoprotein receptor as a candidate receptor for hepatitis C virus. *J Med Virol* 57: 223-229.
81. Wunschmann S, Medh JD, Klinzmann D, Schmidt WN, Stapleton JT (2000) Characterization of hepatitis C virus (HCV) and HCV E2 interactions with CD81 and the low-density lipoprotein receptor. *J Virol* 74: 10055-10062.
82. Germi R, Crance JM, Garin D, Guimet J, Lortat-Jacob H, et al. (2002) Cellular glycosaminoglycans and low density lipoprotein receptor are involved in hepatitis C virus adsorption. *J Med Virol* 68: 206-215.
83. Barth H, Schafer C, Adah MI, Zhang F, Linhardt RJ, et al. (2003) Cellular binding of hepatitis C virus envelope glycoprotein E2 requires cell surface heparan sulfate. *J Biol Chem* 278: 41003-41012.
84. Barth H, Schnober EK, Zhang F, Linhardt RJ, Depla E, et al. (2006) Viral and cellular determinants of the hepatitis C virus envelope-heparan sulfate interaction. *J Virol* 80: 10579-10590.
85. Heo TH, Chang JH, Lee JW, Fong SK, Dubuisson J, et al. (2004) Incomplete humoral immunity against hepatitis C virus is linked with distinct recognition of putative multiple receptors by E2 envelope glycoprotein. *J Immunol* 173: 446-455.
86. Lozach PY, Lortat-Jacob H, de Lacroix de Lavalette A, Staropoli I, Fong S, et al. (2003) DC-SIGN and L-SIGN are high affinity binding receptors for hepatitis C virus glycoprotein E2. *J Biol Chem* 278: 20358-20366.
87. Pohlmann S, Zhang J, Baribaud F, Chen Z, Leslie GJ, et al. (2003) Hepatitis C virus glycoproteins interact with DC-SIGN and DC-SIGNR. *J Virol* 77: 4070-4080.
88. Saunier B, Triyatni M, Ulianich L, Maruvada P, Yen P, et al. (2003) Role of the asialoglycoprotein receptor in binding and entry of hepatitis C virus structural proteins in cultured human hepatocytes. *J Virol* 77: 546-559.
89. Brazzoli M, Bianchi A, Filippini S, Weiner A, Zhu Q, et al. (2008) CD81 is a central regulator of cellular events required for hepatitis C virus infection of human hepatocytes. *J Virol* 82: 8316-8329.

90. Benedicto I, Molina-Jimenez F, Bartosch B, Cosset FL, Lavillette D, et al. (2009) The tight junction-associated protein occludin is required for a postbinding step in hepatitis C virus entry and infection. *J Virol* 83: 8012-8020.
91. Harris HJ, Davis C, Mullins JG, Hu K, Goodall M, et al. (2010) Claudin association with CD81 defines hepatitis C virus entry. *J Biol Chem* 285: 21092-21102.
92. Blanchard E, Belouzard S, Goueslain L, Wakita T, Dubuisson J, et al. (2006) Hepatitis C virus entry depends on clathrin-mediated endocytosis. *J Virol* 80: 6964-6972.
93. Weissenhorn W, Hinz A, Gaudin Y (2007) Virus membrane fusion. *FEBS Lett* 581: 2150-2155.
94. Keck ZY, Op De Beeck A, Hadlock KG, Xia J, Li TK, et al. (2004) Hepatitis C virus E2 has three immunogenic domains containing conformational epitopes with distinct properties and biological functions. *J Virol* 78: 9224-9232.
95. Drummer HE, Pountourios P (2004) Hepatitis C virus glycoprotein E2 contains a membrane-proximal heptad repeat sequence that is essential for E1E2 glycoprotein heterodimerization and viral entry. *J Biol Chem* 279: 30066-30072.
96. Gamarnik AV, Andino R (1998) Switch from translation to RNA replication in a positive-stranded RNA virus. *Genes Dev* 12: 2293-2304.
97. Spahn CM, Kieft JS, Grassucci RA, Penczek PA, Zhou K, et al. (2001) Hepatitis C virus IRES RNA-induced changes in the conformation of the 40s ribosomal subunit. *Science* 291: 1959-1962.
98. Ji H, Fraser CS, Yu Y, Leary J, Doudna JA (2004) Coordinated assembly of human translation initiation complexes by the hepatitis C virus internal ribosome entry site RNA. *Proc Natl Acad Sci U S A* 101: 16990-16995.
99. Otto GA, Puglisi JD (2004) The pathway of HCV IRES-mediated translation initiation. *Cell* 119: 369-380.
100. Hijikata M, Kato N, Ootsuyama Y, Nakagawa M, Shimotohno K (1991) Gene mapping of the putative structural region of the hepatitis C virus genome by in vitro processing analysis. *Proc Natl Acad Sci U S A* 88: 5547-5551.
101. Cocquerel L, Duvet S, Meunier JC, Pillez A, Cacan R, et al. (1999) The transmembrane domain of hepatitis C virus glycoprotein E1 is a signal for static retention in the endoplasmic reticulum. *J Virol* 73: 2641-2649.
102. Cocquerel L, Meunier JC, Pillez A, Wychowski C, Dubuisson J (1998) A retention signal necessary and sufficient for endoplasmic reticulum localization maps to the transmembrane domain of hepatitis C virus glycoprotein E2. *J Virol* 72: 2183-2191.
103. Hijikata M, Mizushima H, Tanji Y, Komoda Y, Hirowatari Y, et al. (1993) Proteolytic processing and membrane association of putative nonstructural proteins of hepatitis C virus. *Proc Natl Acad Sci U S A* 90: 10773-10777.

104. Hijikata M, Mizushima H, Akagi T, Mori S, Kakiuchi N, et al. (1993) Two distinct proteinase activities required for the processing of a putative nonstructural precursor protein of hepatitis C virus. *J Virol* 67: 4665-4675.
105. Santolini E, Pacini L, Fipaldini C, Migliaccio G, Monica N (1995) The NS2 protein of hepatitis C virus is a transmembrane polypeptide. *J Virol* 69: 7461-7471.
106. Wolk B, Sansonno D, Krausslich HG, Dammacco F, Rice CM, et al. (2000) Subcellular localization, stability, and trans-cleavage competence of the hepatitis C virus NS3-NS4A complex expressed in tetracycline-regulated cell lines. *J Virol* 74: 2293-2304.
107. Lundin M, Monne M, Widell A, Von Heijne G, Persson MA (2003) Topology of the membrane-associated hepatitis C virus protein NS4B. *J Virol* 77: 5428-5438.
108. Brass V, Bieck E, Montserret R, Wolk B, Hellings JA, et al. (2002) An amino-terminal amphipathic alpha-helix mediates membrane association of the hepatitis C virus nonstructural protein 5A. *J Biol Chem* 277: 8130-8139.
109. Ivashkina N, Wolk B, Lohmann V, Bartenschlager R, Blum HE, et al. (2002) The hepatitis C virus RNA-dependent RNA polymerase membrane insertion sequence is a transmembrane segment. *J Virol* 76: 13088-13093.
110. Carrere-Kremer S, Montpellier-Pala C, Cocquerel L, Wychowski C, Penin F, et al. (2002) Subcellular localization and topology of the p7 polypeptide of hepatitis C virus. *J Virol* 76: 3720-3730.
111. Barba G, Harper F, Harada T, Kohara M, Goulinet S, et al. (1997) Hepatitis C virus core protein shows a cytoplasmic localization and associates to cellular lipid storage droplets. *Proc Natl Acad Sci U S A* 94: 1200-1205.
112. Boulant S, Montserret R, Hope RG, Ratinier M, Targett-Adams P, et al. (2006) Structural determinants that target the hepatitis C virus core protein to lipid droplets. *J Biol Chem* 281: 22236-22247.
113. Miyanari Y, Atsuzawa K, Usuda N, Watashi K, Hishiki T, et al. (2007) The lipid droplet is an important organelle for hepatitis C virus production. *Nat Cell Biol* 9: 1089-1097.
114. Lohmann V, Korner F, Koch J, Herian U, Theilmann L, et al. (1999) Replication of subgenomic hepatitis C virus RNAs in a hepatoma cell line. *Science* 285: 110-113.
115. Lindenbach BD, Evans MJ, Syder AJ, Wolk B, Tellinghuisen TL, et al. (2005) Complete replication of hepatitis C virus in cell culture. *Science* 309: 623-626.
116. Zhong J, Gastaminza P, Cheng G, Kapadia S, Kato T, et al. (2005) Robust hepatitis C virus infection in vitro. *Proc Natl Acad Sci U S A* 102: 9294-9299.
117. Behrens SE, Tomei L, De Francesco R (1996) Identification and properties of the RNA-dependent RNA polymerase of hepatitis C virus. *Embo J* 15: 12-22.

118. Friebe P, Lohmann V, Krieger N, Bartenschlager R (2001) Sequences in the 5' nontranslated region of hepatitis C virus required for RNA replication. *J Virol* 75: 12047-12057.
119. Yi M, Lemon SM (2003) 3' nontranslated RNA signals required for replication of hepatitis C virus RNA. *J Virol* 77: 3557-3568.
120. Friebe P, Bartenschlager R (2002) Genetic analysis of sequences in the 3' nontranslated region of hepatitis C virus that are important for RNA replication. *J Virol* 76: 5326-5338.
121. Yanagi M, St Claire M, Emerson SU, Purcell RH, Bukh J (1999) In vivo analysis of the 3' untranslated region of the hepatitis C virus after in vitro mutagenesis of an infectious cDNA clone. *Proc Natl Acad Sci U S A* 96: 2291-2295.
122. Kolykhalov AA, Mihalik K, Feinstone SM, Rice CM (2000) Hepatitis C virus-encoded enzymatic activities and conserved RNA elements in the 3' nontranslated region are essential for virus replication in vivo. *J Virol* 74: 2046-2051.
123. Egger D, Wolk B, Gosert R, Bianchi L, Blum HE, et al. (2002) Expression of hepatitis C virus proteins induces distinct membrane alterations including a candidate viral replication complex. *J Virol* 76: 5974-5984.
124. Gosert R, Egger D, Lohmann V, Bartenschlager R, Blum HE, et al. (2003) Identification of the hepatitis C virus RNA replication complex in Huh-7 cells harboring subgenomic replicons. *J Virol* 77: 5487-5492.
125. Salonen A, Ahola T, Kaariainen L (2005) Viral RNA replication in association with cellular membranes. *Curr Top Microbiol Immunol* 285: 139-173.
126. Mackenzie J (2005) Wrapping things up about virus RNA replication. *Traffic* 6: 967-977.
127. Moradpour D, Englert C, Wakita T, Wands JR (1996) Characterization of cell lines allowing tightly regulated expression of hepatitis C virus core protein. *Virology* 222: 51-63.
128. Martin S, Parton RG (2006) Lipid droplets: a unified view of a dynamic organelle. *Nat Rev Mol Cell Biol* 7: 373-378.
129. Murray CL, Jones CT, Rice CM (2008) Architects of assembly: roles of Flaviviridae non-structural proteins in virion morphogenesis. *Nat Rev Microbiol* 6: 699-708.
130. Roingard P, Hourieux C, Blanchard E, Brand D, Ait-Goughoulte M (2004) Hepatitis C virus ultrastructure and morphogenesis. *Biol Cell* 96: 103-108.
131. Deleersnyder V, Pillez A, Wychowski C, Blight K, Xu J, et al. (1997) Formation of native hepatitis C virus glycoprotein complexes. *J Virol* 71: 697-704.
132. Duvet S, Cocquerel L, Pillez A, Cacan R, Verbert A, et al. (1998) Hepatitis C virus glycoprotein complex localization in the endoplasmic reticulum involves a determinant for retention and not retrieval. *J Biol Chem* 273: 32088-32095.

133. Rouille Y, Helle F, Delgrange D, Roingeard P, Voisset C, et al. (2006) Subcellular localization of hepatitis C virus structural proteins in a cell culture system that efficiently replicates the virus. *J Virol* 80: 2832-2841.
134. Yu IM, Zhang W, Holdaway HA, Li L, Kostyuchenko VA, et al. (2008) Structure of the immature dengue virus at low pH primes proteolytic maturation. *Science* 319: 1834-1837.
135. Stadler K, Allison SL, Schalich J, Heinz FX (1997) Proteolytic activation of tick-borne encephalitis virus by furin. *J Virol* 71: 8475-8481.
136. Heinz FX, Stiasny K, Puschner-Auer G, Holzmann H, Allison SL, et al. (1994) Structural changes and functional control of the tick-borne encephalitis virus glycoprotein E by the heterodimeric association with protein prM. *Virology* 198: 109-117.
137. Vieyres G, Thomas X, Descamps V, Duverlie G, Patel AH, et al. (2010) Characterization of the Envelope Glycoproteins Associated with Infectious Hepatitis C Virus. *J Virol*.
138. Op De Beeck A, Voisset C, Bartosch B, Ciczora Y, Cocquerel L, et al. (2004) Characterization of functional hepatitis C virus envelope glycoproteins. *J Virol* 78: 2994-3002.
139. Huang H, Sun F, Owen DM, Li W, Chen Y, et al. (2007) Hepatitis C virus production by human hepatocytes dependent on assembly and secretion of very low-density lipoproteins. *Proc Natl Acad Sci U S A* 104: 5848-5853.
140. Gastaminza P, Cheng G, Wieland S, Zhong J, Liao W, et al. (2008) Cellular determinants of hepatitis C virus assembly, maturation, degradation, and secretion. *J Virol* 82: 2120-2129.
141. Blasirole DA, Davis RA, Attie AD (2007) The physiological and molecular regulation of lipoprotein assembly and secretion. *Mol Biosyst* 3: 608-619.
142. Gastaminza P, Kapadia SB, Chisari FV (2006) Differential biophysical properties of infectious intracellular and secreted hepatitis C virus particles. *J Virol* 80: 11074-11081.
143. Sakai A, Claire MS, Faulk K, Govindarajan S, Emerson SU, et al. (2003) The p7 polypeptide of hepatitis C virus is critical for infectivity and contains functionally important genotype-specific sequences. *Proc Natl Acad Sci U S A* 100: 11646-11651.
144. Steinmann E, Penin F, Kallis S, Patel AH, Bartenschlager R, et al. (2007) Hepatitis C virus p7 protein is crucial for assembly and release of infectious virions. *PLoS Pathog* 3: e103.
145. Griffin SD, Beales LP, Clarke DS, Worsfold O, Evans SD, et al. (2003) The p7 protein of hepatitis C virus forms an ion channel that is blocked by the antiviral drug, Amantadine. *FEBS Lett* 535: 34-38.
146. Pavlovic D, Neville DC, Argaud O, Blumberg B, Dwek RA, et al. (2003) The hepatitis C virus p7 protein forms an ion channel that is inhibited by long-alkyl-chain iminosugar derivatives. *Proc Natl Acad Sci U S A* 100: 6104-6108.

147. Steinmann E, Whitfield T, Kallis S, Dwek RA, Zitzmann N, et al. (2007) Antiviral effects of amantadine and iminosugar derivatives against hepatitis C virus. *Hepatology* 46: 330-338.
148. Griffin S, Stgelais C, Owsianka AM, Patel AH, Rowlands D, et al. (2008) Genotype-dependent sensitivity of hepatitis C virus to inhibitors of the p7 ion channel. *Hepatology* 48: 1779-1790.
149. Blight KJ, Kolykhalov AA, Rice CM (2000) Efficient initiation of HCV RNA replication in cell culture. *Science* 290: 1972-1974.
150. Jirasko V, Montserret R, Appel N, Janvier A, Eustachi L, et al. (2008) Structural and functional characterization of nonstructural protein 2 for its role in hepatitis C virus assembly. *J Biol Chem* 283: 28546-28562.
151. Ma Y, Anantpadma M, Timpe JM, Shanmugam S, Singh SM, et al. (2010) Hepatitis C Virus NS2 Protein Serves as a Scaffold for Virus Assembly by Interacting with both Structural and Nonstructural Proteins. *J Virol*.
152. Phan T, Beran RK, Peters C, Lorenz IC, Lindenbach BD (2009) Hepatitis C virus NS2 protein contributes to virus particle assembly via opposing epistatic interactions with the E1-E2 glycoprotein and NS3-NS4A enzyme complexes. *J Virol* 83: 8379-8395.
153. Stapleford KA, Lindenbach BD (2011) Hepatitis C virus NS2 coordinates virus particle assembly through physical interactions with the E1-E2 glycoprotein and NS3-NS4A enzyme complexes. *J Virol* 85: 1706-1717.
154. Lam AM, Frick DN (2006) Hepatitis C virus subgenomic replicon requires an active NS3 RNA helicase. *J Virol* 80: 404-411.
155. Grakoui A, McCourt DW, Wychowski C, Feinstone SM, Rice CM (1993) Characterization of the hepatitis C virus-encoded serine proteinase: determination of proteinase-dependent polyprotein cleavage sites. *J Virol* 67: 2832-2843.
156. Failla C, Tomei L, De Francesco R (1994) Both NS3 and NS4A are required for proteolytic processing of hepatitis C virus nonstructural proteins. *J Virol* 68: 3753-3760.
157. Frick DN, Rypma RS, Lam AM, Frenz CM (2004) Electrostatic analysis of the hepatitis C virus NS3 helicase reveals both active and allosteric site locations. *Nucleic Acids Res* 32: 5519-5528.
158. Gallinari P, Paolini C, Brennan D, Nardi C, Steinkuhler C, et al. (1999) Modulation of hepatitis C virus NS3 protease and helicase activities through the interaction with NS4A. *Biochemistry* 38: 5620-5632.
159. Suzich JA, Tamura JK, Palmer-Hill F, Warrenner P, Grakoui A, et al. (1993) Hepatitis C virus NS3 protein polynucleotide-stimulated nucleoside triphosphatase and comparison with the related pestivirus and flavivirus enzymes. *J Virol* 67: 6152-6158.
160. Piccininni S, Varaklioti A, Nardelli M, Dave B, Raney KD, et al. (2002) Modulation of the hepatitis C virus RNA-dependent RNA polymerase activity by the non-structural (NS) 3 helicase and the NS4B membrane protein. *J Biol Chem* 277: 45670-45679.

161. Foy E, Li K, Wang C, Sumpter R, Jr., Ikeda M, et al. (2003) Regulation of interferon regulatory factor-3 by the hepatitis C virus serine protease. *Science* 300: 1145-1148.
162. Li K, Foy E, Ferreon JC, Nakamura M, Ferreon AC, et al. (2005) Immune evasion by hepatitis C virus NS3/4A protease-mediated cleavage of the Toll-like receptor 3 adaptor protein TRIF. *Proc Natl Acad Sci U S A* 102: 2992-2997.
163. Hugle T, Fehrmann F, Bieck E, Kohara M, Krausslich HG, et al. (2001) The hepatitis C virus nonstructural protein 4B is an integral endoplasmic reticulum membrane protein. *Virology* 284: 70-81.
164. Jones DM, Patel AH, Targett-Adams P, McLauchlan J (2009) The hepatitis C virus NS4B protein can trans-complement viral RNA replication and modulates production of infectious virus. *J Virol* 83: 2163-2177.
165. Lindstrom H, Lundin M, Haggstrom S, Persson MA (2006) Mutations of the Hepatitis C virus protein NS4B on either side of the ER membrane affect the efficiency of subgenomic replicons. *Virus Res* 121: 169-178.
166. Blight KJ (2007) Allelic variation in the hepatitis C virus NS4B protein dramatically influences RNA replication. *J Virol* 81: 5724-5736.
167. Pfeifer U, Thomssen R, Legler K, Bottcher U, Gerlich W, et al. (1980) Experimental non-A, non-B hepatitis: four types of cytoplasmic alteration in hepatocytes of infected chimpanzees. *Virchows Arch B Cell Pathol Incl Mol Pathol* 33: 233-243.
168. Elazar M, Liu P, Rice CM, Glenn JS (2004) An N-terminal amphipathic helix in hepatitis C virus (HCV) NS4B mediates membrane association, correct localization of replication complex proteins, and HCV RNA replication. *J Virol* 78: 11393-11400.
169. Penin F, Brass V, Appel N, Ramboarina S, Montserret R, et al. (2004) Structure and function of the membrane anchor domain of hepatitis C virus nonstructural protein 5A. *J Biol Chem* 279: 40835-40843.
170. Tellinghuisen TL, Marcotrigiano J, Gorbalenya AE, Rice CM (2004) The NS5A protein of hepatitis C virus is a zinc metalloprotein. *J Biol Chem* 279: 48576-48587.
171. Gale MJ, Jr., Korth MJ, Tang NM, Tan SL, Hopkins DA, et al. (1997) Evidence that hepatitis C virus resistance to interferon is mediated through repression of the PKR protein kinase by the nonstructural 5A protein. *Virology* 230: 217-227.
172. Enomoto N, Sakuma I, Asahina Y, Kurosaki M, Murakami T, et al. (1995) Comparison of full-length sequences of interferon-sensitive and resistant hepatitis C virus 1b. Sensitivity to interferon is conferred by amino acid substitutions in the NS5A region. *J Clin Invest* 96: 224-230.
173. Enomoto N, Sakuma I, Asahina Y, Kurosaki M, Murakami T, et al. (1996) Mutations in the nonstructural protein 5A gene and response to interferon in patients with chronic hepatitis C virus 1b infection. *N Engl J Med* 334: 77-81.

174. Gale M, Jr., Foy EM (2005) Evasion of intracellular host defence by hepatitis C virus. *Nature* 436: 939-945.
175. Polyak SJ, Khabar KS, Paschal DM, Ezelle HJ, Duverlie G, et al. (2001) Hepatitis C virus nonstructural 5A protein induces interleukin-8, leading to partial inhibition of the interferon-induced antiviral response. *J Virol* 75: 6095-6106.
176. Shirota Y, Luo H, Qin W, Kaneko S, Yamashita T, et al. (2002) Hepatitis C virus (HCV) NS5A binds RNA-dependent RNA polymerase (RdRP) NS5B and modulates RNA-dependent RNA polymerase activity. *J Biol Chem* 277: 11149-11155.
177. Shimakami T, Hijikata M, Luo H, Ma YY, Kaneko S, et al. (2004) Effect of interaction between hepatitis C virus NS5A and NS5B on hepatitis C virus RNA replication with the hepatitis C virus replicon. *J Virol* 78: 2738-2748.
178. Reiss S, Rebhan I, Backes P, Romero-Brey I, Erfle H, et al. (2011) Recruitment and activation of a lipid kinase by hepatitis C virus NS5A is essential for integrity of the membranous replication compartment. *Cell Host Microbe* 9: 32-45.
179. Bressanelli S, Tomei L, Roussel A, Incitti I, Vitale RL, et al. (1999) Crystal structure of the RNA-dependent RNA polymerase of hepatitis C virus. *Proc Natl Acad Sci U S A* 96: 13034-13039.
180. Ago H, Adachi T, Yoshida A, Yamamoto M, Habuka N, et al. (1999) Crystal structure of the RNA-dependent RNA polymerase of hepatitis C virus. *Structure* 7: 1417-1426.
181. Ollis DL, Brick P, Hamlin R, Xuong NG, Steitz TA (1985) Structure of large fragment of *Escherichia coli* DNA polymerase I complexed with dTMP. *Nature* 313: 762-766.
182. Yamashita T, Kaneko S, Shirota Y, Qin W, Nomura T, et al. (1998) RNA-dependent RNA polymerase activity of the soluble recombinant hepatitis C virus NS5B protein truncated at the C-terminal region. *J Biol Chem* 273: 15479-15486.
183. Moradpour D, Brass V, Bieck E, Friebe P, Gosert R, et al. (2004) Membrane association of the RNA-dependent RNA polymerase is essential for hepatitis C virus RNA replication. *J Virol* 78: 13278-13284.
184. Walewski JL, Keller TR, Stump DD, Branch AD (2001) Evidence for a new hepatitis C virus antigen encoded in an overlapping reading frame. *RNA* 7: 710-721.
185. Cohen M, Bachmatov L, Ben-Ari Z, Rotman Y, Tur-Kaspa R, et al. (2007) Development of specific antibodies to an ARF protein in treated patients with chronic HCV infection. *Dig Dis Sci* 52: 2427-2432.
186. McMullan LK, Grakoui A, Evans MJ, Mihalik K, Puig M, et al. (2007) Evidence for a functional RNA element in the hepatitis C virus core gene. *Proc Natl Acad Sci U S A* 104: 2879-2884.

187. Shimoike T, Mimori S, Tani H, Matsuura Y, Miyamura T (1999) Interaction of hepatitis C virus core protein with viral sense RNA and suppression of its translation. *J Virol* 73: 9718-9725.
188. Santolini E, Migliaccio G, La Monica N (1994) Biosynthesis and biochemical properties of the hepatitis C virus core protein. *J Virol* 68: 3631-3641.
189. Tanaka Y, Shimoike T, Ishii K, Suzuki R, Suzuki T, et al. (2000) Selective binding of hepatitis C virus core protein to synthetic oligonucleotides corresponding to the 5' untranslated region of the viral genome. *Virology* 270: 229-236.
190. Ray RB, Lagging LM, Meyer K, Steele R, Ray R (1995) Transcriptional regulation of cellular and viral promoters by the hepatitis C virus core protein. *Virus Res* 37: 209-220.
191. Ray RB, Steele R, Meyer K, Ray R (1997) Transcriptional repression of p53 promoter by hepatitis C virus core protein. *J Biol Chem* 272: 10983-10986.
192. Bergqvist A, Rice CM (2001) Transcriptional activation of the interleukin-2 promoter by hepatitis C virus core protein. *J Virol* 75: 772-781.
193. Ray RB, Meyer K, Ray R (1996) Suppression of apoptotic cell death by hepatitis C virus core protein. *Virology* 226: 176-182.
194. Honda M, Kaneko S, Shimazaki T, Matsushita E, Kobayashi K, et al. (2000) Hepatitis C virus core protein induces apoptosis and impairs cell-cycle regulation in stably transformed Chinese hamster ovary cells. *Hepatology* 31: 1351-1359.
195. Lu W, Lo SY, Chen M, Wu K, Fung YK, et al. (1999) Activation of p53 tumor suppressor by hepatitis C virus core protein. *Virology* 264: 134-141.
196. Miller K, McArdle S, Gale MJ, Jr., Geller DA, Tenover B, et al. (2004) Effects of the hepatitis C virus core protein on innate cellular defense pathways. *J Interferon Cytokine Res* 24: 391-402.
197. Dubuisson J, Hsu HH, Cheung RC, Greenberg HB, Russell DG, et al. (1994) Formation and intracellular localization of hepatitis C virus envelope glycoprotein complexes expressed by recombinant vaccinia and Sindbis viruses. *J Virol* 68: 6147-6160.
198. Grakoui A, Wychowski C, Lin C, Feinstone SM, Rice CM (1993) Expression and identification of hepatitis C virus polyprotein cleavage products. *J Virol* 67: 1385-1395.
199. Lanford RE, Notvall L, Chavez D, White R, Frenzel G, et al. (1993) Analysis of hepatitis C virus capsid, E1, and E2/NS1 proteins expressed in insect cells. *Virology* 197: 225-235.
200. Ralston R, Thudium K, Berger K, Kuo C, Gervase B, et al. (1993) Characterization of hepatitis C virus envelope glycoprotein complexes expressed by recombinant vaccinia viruses. *J Virol* 67: 6753-6761.
201. Cocquerel L, Meunier JC, Op de Beeck A, Bonte D, Wychowski C, et al. (2001) Coexpression of hepatitis C virus envelope proteins E1 and E2 in cis improves the stability of membrane insertion of E2. *J Gen Virol* 82: 1629-1635.

202. Matsuura Y, Harada S, Suzuki R, Watanabe Y, Inoue Y, et al. (1992) Expression of processed envelope protein of hepatitis C virus in mammalian and insect cells. *J Virol* 66: 1425-1431.
203. Spaete RR, Alexander D, Rugroden ME, Choo QL, Berger K, et al. (1992) Characterization of the hepatitis C virus E2/NS1 gene product expressed in mammalian cells. *Virology* 188: 819-830.
204. Lo SY, Masiarz F, Hwang SB, Lai MM, Ou JH (1995) Differential subcellular localization of hepatitis C virus core gene products. *Virology* 213: 455-461.
205. Munro S, Pelham HR (1987) A C-terminal signal prevents secretion of luminal ER proteins. *Cell* 48: 899-907.
206. Nilsson T, Jackson M, Peterson PA (1989) Short cytoplasmic sequences serve as retention signals for transmembrane proteins in the endoplasmic reticulum. *Cell* 58: 707-718.
207. Nilsson T, Warren G (1994) Retention and retrieval in the endoplasmic reticulum and the Golgi apparatus. *Curr Opin Cell Biol* 6: 517-521.
208. Cocquerel L, Wychowski C, Minner F, Penin F, Dubuisson J (2000) Charged residues in the transmembrane domains of hepatitis C virus glycoproteins play a major role in the processing, subcellular localization, and assembly of these envelope proteins. *J Virol* 74: 3623-3633.
209. Flint M, McKeating JA (1999) The C-terminal region of the hepatitis C virus E1 glycoprotein confers localization within the endoplasmic reticulum. *J Gen Virol* 80 (Pt 8): 1943-1947.
210. Michalak JP, Wychowski C, Choukhi A, Meunier JC, Ung S, et al. (1997) Characterization of truncated forms of hepatitis C virus glycoproteins. *J Gen Virol* 78 (Pt 9): 2299-2306.
211. Mottola G, Jourdan N, Castaldo G, Malagolini N, Lahm A, et al. (2000) A new determinant of endoplasmic reticulum localization is contained in the juxtamembrane region of the ectodomain of hepatitis C virus glycoprotein E1. *J Biol Chem* 275: 24070-24079.
212. Strauss JH, Strauss EG (1994) The alphaviruses: gene expression, replication, and evolution. *Microbiol Rev* 58: 491-562.
213. Op De Beeck A, Molenkamp R, Caron M, Ben Younes A, Bredenbeek P, et al. (2003) Role of the transmembrane domains of prM and E proteins in the formation of yellow fever virus envelope. *J Virol* 77: 813-820.
214. Cocquerel L, Op de Beeck A, Lambot M, Roussel J, Delgrange D, et al. (2002) Topological changes in the transmembrane domains of hepatitis C virus envelope glycoproteins. *Embo J* 21: 2893-2902.
215. Kornfeld R, Kornfeld S (1985) Assembly of asparagine-linked oligosaccharides. *Annu Rev Biochem* 54: 631-664.
216. Gavel Y, von Heijne G (1990) Sequence differences between glycosylated and non-glycosylated Asn-X-Thr/Ser acceptor sites: implications for protein engineering. *Protein Eng* 3: 433-442.
217. Goffard A, Dubuisson J (2003) Glycosylation of hepatitis C virus envelope proteins. *Biochimie* 85: 295-301.

218. Meunier JC, Fournillier A, Choukhi A, Cahour A, Cocquerel L, et al. (1999) Analysis of the glycosylation sites of hepatitis C virus (HCV) glycoprotein E1 and the influence of E1 glycans on the formation of the HCV glycoprotein complex. *J Gen Virol* 80 (Pt 4): 887-896.
219. Fournillier Jacob A, Cahour A, Escriou N, Girad M, Wychowski C (1996) Processing of the E1 glycoprotein of hepatitis C virus expressed in mammalian cells. *J Gen Virol* 77 (Pt 5): 1055-1064.
220. Johnson AE, van Waes MA (1999) The translocon: a dynamic gateway at the ER membrane. *Annu Rev Cell Dev Biol* 15: 799-842.
221. Duvet S, Op De Beeck A, Cocquerel L, Wychowski C, Cacan R, et al. (2002) Glycosylation of the hepatitis C virus envelope protein E1 occurs posttranslationally in a mannosylphosphoryldolichol-deficient CHO mutant cell line. *Glycobiology* 12: 95-101.
222. Atkinson PH, Lee JT (1984) Co-translational excision of alpha-glucose and alpha-mannose in nascent vesicular stomatitis virus G protein. *J Cell Biol* 98: 2245-2249.
223. Helenius A, Aebi M (2001) Intracellular functions of N-linked glycans. *Science* 291: 2364-2369.
224. Sato K, Okamoto H, Aihara S, Hoshi Y, Tanaka T, et al. (1993) Demonstration of sugar moiety on the surface of hepatitis C virions recovered from the circulation of infected humans. *Virology* 196: 354-357.
225. Helle F, Goffard A, Morel V, Duverlie G, McKeating J, et al. (2007) The neutralizing activity of anti-hepatitis C virus antibodies is modulated by specific glycans on the E2 envelope protein. *J Virol* 81: 8101-8111.
226. Falkowska E, Kajumo F, Garcia E, Reinus J, Dragic T (2007) Hepatitis C virus envelope glycoprotein E2 glycans modulate entry, CD81 binding, and neutralization. *J Virol* 81: 8072-8079.
227. Slater-Handshy T, Droll DA, Fan X, Di Bisceglie AM, Chambers TJ (2004) HCV E2 glycoprotein: mutagenesis of N-linked glycosylation sites and its effects on E2 expression and processing. *Virology* 319: 36-48.
228. Imperiali B, O'Connor SE (1999) Effect of N-linked glycosylation on glycopeptide and glycoprotein structure. *Curr Opin Chem Biol* 3: 643-649.
229. Wormald MR, Dwek RA (1999) Glycoproteins: glycan presentation and protein-fold stability. *Structure* 7: R155-160.
230. Hebert DN, Garman SC, Molinari M (2005) The glycan code of the endoplasmic reticulum: asparagine-linked carbohydrates as protein maturation and quality-control tags. *Trends Cell Biol* 15: 364-370.
231. Choukhi A, Ung S, Wychowski C, Dubuisson J (1998) Involvement of endoplasmic reticulum chaperones in the folding of hepatitis C virus glycoproteins. *J Virol* 72: 3851-3858.
232. Dubuisson J, Rice CM (1996) Hepatitis C virus glycoprotein folding: disulfide bond formation and association with calnexin. *J Virol* 70: 778-786.

233. Merola M, Brazzoli M, Cocchiarella F, Heile JM, Helenius A, et al. (2001) Folding of hepatitis C virus E1 glycoprotein in a cell-free system. *J Virol* 75: 11205-11217.
234. Brazzoli M, Helenius A, Fong SK, Houghton M, Abrignani S, et al. (2005) Folding and dimerization of hepatitis C virus E1 and E2 glycoproteins in stably transfected CHO cells. *Virology* 332: 438-453.
235. Cudna RE, Dickson AJ (2003) Endoplasmic reticulum signaling as a determinant of recombinant protein expression. *Biotechnol Bioeng* 81: 56-65.
236. Op De Beeck A, Montserret R, Duvet S, Cocquerel L, Cacan R, et al. (2000) The transmembrane domains of hepatitis C virus envelope glycoproteins E1 and E2 play a major role in heterodimerization. *J Biol Chem* 275: 31428-31437.
237. Selby MJ, Glazer E, Masiarz F, Houghton M (1994) Complex processing and protein:protein interactions in the E2:NS2 region of HCV. *Virology* 204: 114-122.
238. Ciczora Y, Callens N, Penin F, Pecheur EI, Dubuisson J (2007) Transmembrane domains of hepatitis C virus envelope glycoproteins: residues involved in E1E2 heterodimerization and involvement of these domains in virus entry. *J Virol* 81: 2372-2381.
239. Russ WP, Engelman DM (2000) The GxxxG motif: a framework for transmembrane helix-helix association. *J Mol Biol* 296: 911-919.
240. Senes A, Engel DE, DeGrado WF (2004) Folding of helical membrane proteins: the role of polar, GxxxG-like and proline motifs. *Curr Opin Struct Biol* 14: 465-479.
241. Matsuura Y, Suzuki T, Suzuki R, Sato M, Aizaki H, et al. (1994) Processing of E1 and E2 glycoproteins of hepatitis C virus expressed in mammalian and insect cells. *Virology* 205: 141-150.
242. Tello D, Rodriguez-Rodriguez M, Yelamos B, Gomez-Gutierrez J, Ortega S, et al. (2010) Expression and structural properties of a chimeric protein based on the ectodomains of E1 and E2 hepatitis C virus envelope glycoproteins. *Protein Expr Purif* 71: 123-131.
243. Flint M, Logvinoff C, Rice CM, McKeating JA (2004) Characterization of infectious retroviral pseudotype particles bearing hepatitis C virus glycoproteins. *J Virol* 78: 6875-6882.
244. Flint M, Thomas JM, Maidens CM, Shotton C, Levy S, et al. (1999) Functional analysis of cell surface-expressed hepatitis C virus E2 glycoprotein. *J Virol* 73: 6782-6790.
245. Drummer HE, Wilson KA, Pountourios P (2002) Identification of the hepatitis C virus E2 glycoprotein binding site on the large extracellular loop of CD81. *J Virol* 76: 11143-11147.
246. McCaffrey K, Boo I, Pountourios P, Drummer HE (2007) Expression and characterization of a minimal hepatitis C virus glycoprotein E2 core domain that retains CD81 binding. *J Virol* 81: 9584-9590.

247. Drummer HE, Boo I, Maerz AL, Pountourios P (2006) A conserved Gly436-Trp-Leu-Ala-Gly-Leu-Phe-Tyr motif in hepatitis C virus glycoprotein E2 is a determinant of CD81 binding and viral entry. *J Virol* 80: 7844-7853.
248. Barth H, Cerino R, Arcuri M, Hoffmann M, Schurmann P, et al. (2005) Scavenger receptor class B type I and hepatitis C virus infection of primary tupaia hepatocytes. *J Virol* 79: 5774-5785.
249. Zhang J, Randall G, Higginbottom A, Monk P, Rice CM, et al. (2004) CD81 is required for hepatitis C virus glycoprotein-mediated viral infection. *J Virol* 78: 1448-1455.
250. Akazawa D, Date T, Morikawa K, Murayama A, Miyamoto M, et al. (2007) CD81 expression is important for the permissiveness of Huh7 cell clones for heterogeneous hepatitis C virus infection. *J Virol* 81: 5036-5045.
251. Molina S, Castet V, Pichard-Garcia L, Wychowski C, Meurs E, et al. (2008) Serum-derived hepatitis C virus infection of primary human hepatocytes is tetraspanin CD81 dependent. *J Virol* 82: 569-574.
252. Bartosch B, Vitelli A, Granier C, Goujon C, Dubuisson J, et al. (2003) Cell entry of hepatitis C virus requires a set of co-receptors that include the CD81 tetraspanin and the SR-B1 scavenger receptor. *J Biol Chem* 278: 41624-41630.
253. Cormier EG, Tsamis F, Kajumo F, Durso RJ, Gardner JP, et al. (2004) CD81 is an entry coreceptor for hepatitis C virus. *Proc Natl Acad Sci U S A* 101: 7270-7274.
254. Owsianka AM, Timms JM, Tarr AW, Brown RJ, Hickling TP, et al. (2006) Identification of conserved residues in the E2 envelope glycoprotein of the hepatitis C virus that are critical for CD81 binding. *J Virol* 80: 8695-8704.
255. Yagnik AT, Lahm A, Meola A, Roccasecca RM, Ercole BB, et al. (2000) A model for the hepatitis C virus envelope glycoprotein E2. *Proteins* 40: 355-366.
256. Roccasecca R, Ansuini H, Vitelli A, Meola A, Scarselli E, et al. (2003) Binding of the hepatitis C virus E2 glycoprotein to CD81 is strain specific and is modulated by a complex interplay between hypervariable regions 1 and 2. *J Virol* 77: 1856-1867.
257. Flint M, Maidens C, Loomis-Price LD, Shotton C, Dubuisson J, et al. (1999) Characterization of hepatitis C virus E2 glycoprotein interaction with a putative cellular receptor, CD81. *J Virol* 73: 6235-6244.
258. Shaw ML, McLauchlan J, Mills PR, Patel AH, McCrudden EA (2003) Characterisation of the differences between hepatitis C virus genotype 3 and 1 glycoproteins. *J Med Virol* 70: 361-372.
259. Drummer HE, Wilson KA, Pountourios P (2005) Determinants of CD81 dimerization and interaction with hepatitis C virus glycoprotein E2. *Biochem Biophys Res Commun* 328: 251-257.
260. McKeating JA, Zhang LQ, Logvinoff C, Flint M, Zhang J, et al. (2004) Diverse hepatitis C virus glycoproteins mediate viral infection in a CD81-dependent manner. *J Virol* 78: 8496-8505.

261. Lavillette D, Tarr AW, Voisset C, Donot P, Bartosch B, et al. (2005) Characterization of host-range and cell entry properties of the major genotypes and subtypes of hepatitis C virus. *Hepatology* 41: 265-274.
262. Farci P, Shimoda A, Coiana A, Diaz G, Peddis G, et al. (2000) The outcome of acute hepatitis C predicted by the evolution of the viral quasispecies. *Science* 288: 339-344.
263. Callens N, Ciczora Y, Bartosch B, Vu-Dac N, Cosset FL, et al. (2005) Basic residues in hypervariable region 1 of hepatitis C virus envelope glycoprotein e2 contribute to virus entry. *J Virol* 79: 15331-15341.
264. Penin F, Combet C, Germanidis G, Frainais PO, Deleage G, et al. (2001) Conservation of the conformation and positive charges of hepatitis C virus E2 envelope glycoprotein hypervariable region 1 points to a role in cell attachment. *J Virol* 75: 5703-5710.
265. Bartosch B, Verney G, Dreux M, Donot P, Morice Y, et al. (2005) An interplay between hypervariable region 1 of the hepatitis C virus E2 glycoprotein, the scavenger receptor BI, and high-density lipoprotein promotes both enhancement of infection and protection against neutralizing antibodies. *J Virol* 79: 8217-8229.
266. Voisset C, Callens N, Blanchard E, Op De Beeck A, Dubuisson J, et al. (2005) High density lipoproteins facilitate hepatitis C virus entry through the scavenger receptor class B type I. *J Biol Chem* 280: 7793-7799.
267. Kato N, Ootsuyama Y, Ohkoshi S, Nakazawa T, Sekiya H, et al. (1992) Characterization of hypervariable regions in the putative envelope protein of hepatitis C virus. *Biochem Biophys Res Commun* 189: 119-127.
268. Nakazawa T, Kato N, Ootsuyama Y, Sekiya H, Fujioka T, et al. (1994) Genetic alteration of the hepatitis C virus hypervariable region obtained from an asymptomatic carrier. *Int J Cancer* 56: 204-207.
269. Huang CC, Tang M, Zhang MY, Majeed S, Montabana E, et al. (2005) Structure of a V3-containing HIV-1 gp120 core. *Science* 310: 1025-1028.
270. Kwong PD, Wyatt R, Robinson J, Sweet RW, Sodroski J, et al. (1998) Structure of an HIV gp120 envelope glycoprotein in complex with the CD4 receptor and a neutralizing human antibody. *Nature* 393: 648-659.
271. Wyatt R, Kwong PD, Desjardins E, Sweet RW, Robinson J, et al. (1998) The antigenic structure of the HIV gp120 envelope glycoprotein. *Nature* 393: 705-711.
272. Wyatt R, Moore J, Accola M, Desjardin E, Robinson J, et al. (1995) Involvement of the V1/V2 variable loop structure in the exposure of human immunodeficiency virus type 1 gp120 epitopes induced by receptor binding. *J Virol* 69: 5723-5733.
273. Krey T, d'Alayer J, Kikuti CM, Saulnier A, Damier-Piolle L, et al. (2010) The disulfide bonds in glycoprotein E2 of hepatitis C virus reveal the tertiary organization of the molecule. *PLoS Pathog* 6: e1000762.

274. McCaffrey K, Gouklani H, Boo I, Pountourios P, Drummer HE (2010) The variable regions of Hepatitis C Virus glycoprotein E2 have an essential structural role in glycoprotein assembly and virion infectivity. *J Gen Virol*.
275. Forns X, Thimme R, Govindarajan S, Emerson SU, Purcell RH, et al. (2000) Hepatitis C virus lacking the hypervariable region 1 of the second envelope protein is infectious and causes acute resolving or persistent infection in chimpanzees. *Proc Natl Acad Sci U S A* 97: 13318-13323.
276. Goffard A, Callens N, Bartosch B, Wychowski C, Cosset FL, et al. (2005) Role of N-linked glycans in the functions of hepatitis C virus envelope glycoproteins. *J Virol* 79: 8400-8409.
277. Rey FA, Heinz FX, Mandl C, Kunz C, Harrison SC (1995) The envelope glycoprotein from tick-borne encephalitis virus at 2 Å resolution. *Nature* 375: 291-298.
278. Roehrig JT, Bolin RA, Kelly RG (1998) Monoclonal antibody mapping of the envelope glycoprotein of the dengue 2 virus, Jamaica. *Virology* 246: 317-328.
279. Voss JE, Vaney MC, Duquerroy S, Vonrhein C, Girard-Blanc C, et al. (2010) Glycoprotein organization of Chikungunya virus particles revealed by X-ray crystallography. *Nature* 468: 709-712.
280. Allison SL, Stiasny K, Stadler K, Mandl CW, Heinz FX (1999) Mapping of functional elements in the stem-anchor region of tick-borne encephalitis virus envelope protein E. *J Virol* 73: 5605-5612.
281. MacArthur MW, Thornton JM (1991) Influence of proline residues on protein conformation. *J Mol Biol* 218: 397-412.
282. Lavillette D, Pecheur EI, Donot P, Fresquet J, Molle J, et al. (2007) Characterization of fusion determinants points to the involvement of three discrete regions of both E1 and E2 glycoproteins in the membrane fusion process of hepatitis C virus. *J Virol* 81: 8752-8765.
283. Whidby J, Mateu G, Scarborough H, Demeler B, Grakoui A, et al. (2009) Blocking hepatitis C virus infection with recombinant form of envelope protein 2 ectodomain. *J Virol* 83: 11078-11089.
284. Sjoberg M, Garoff H (2003) Interactions between the transmembrane segments of the alphavirus E1 and E2 proteins play a role in virus budding and fusion. *J Virol* 77: 3441-3450.
285. Garry RF, Dash S (2003) Proteomics computational analyses suggest that hepatitis C virus E1 and pestivirus E2 envelope glycoproteins are truncated class II fusion proteins. *Virology* 307: 255-265.
286. Drummer HE, Boo I, Pountourios P (2007) Mutagenesis of a conserved fusion peptide-like motif and membrane-proximal heptad-repeat region of hepatitis C virus glycoprotein E1. *J Gen Virol* 88: 1144-1148.
287. Spadaccini R, D'Errico G, D'Alessio V, Notomista E, Bianchi A, et al. (2010) Structural characterization of the transmembrane proximal region of the hepatitis C virus E1 glycoprotein. *Biochim Biophys Acta* 1798: 344-353.

288. Allison SL, Schalich J, Stiasny K, Mandl CW, Heinz FX (2001) Mutational evidence for an internal fusion peptide in flavivirus envelope protein E. *J Virol* 75: 4268-4275.
289. Gething MJ, Doms RW, York D, White J (1986) Studies on the mechanism of membrane fusion: site-specific mutagenesis of the hemagglutinin of influenza virus. *J Cell Biol* 102: 11-23.
290. Harter C, James P, Bachi T, Semenza G, Brunner J (1989) Hydrophobic binding of the ectodomain of influenza hemagglutinin to membranes occurs through the "fusion peptide". *J Biol Chem* 264: 6459-6464.
291. Garoff H, Frischauf AM, Simons K, Lehrach H, Delius H (1980) Nucleotide sequence of cDNA coding for Semliki Forest virus membrane glycoproteins. *Nature* 288: 236-241.
292. Levy-Mintz P, Kielian M (1991) Mutagenesis of the putative fusion domain of the Semliki Forest virus spike protein. *J Virol* 65: 4292-4300.
293. Delos SE, Gilbert JM, White JM (2000) The central proline of an internal viral fusion peptide serves two important roles. *J Virol* 74: 1686-1693.
294. Perez-Berna AJ, Moreno MR, Guillen J, Bernabeu A, Villalain J (2006) The membrane-active regions of the hepatitis C virus E1 and E2 envelope glycoproteins. *Biochemistry* 45: 3755-3768.
295. Dreux M, Pietschmann T, Granier C, Voisset C, Ricard-Blum S, et al. (2006) High density lipoprotein inhibits hepatitis C virus-neutralizing antibodies by stimulating cell entry via activation of the scavenger receptor BI. *J Biol Chem* 281: 18285-18295.
296. Keck ZY, Sung VM, Perkins S, Rowe J, Paul S, et al. (2004) Human monoclonal antibody to hepatitis C virus E1 glycoprotein that blocks virus attachment and viral infectivity. *J Virol* 78: 7257-7263.
297. Pietschmann T, Kaul A, Koutsoudakis G, Shavinskaya A, Kallis S, et al. (2006) Construction and characterization of infectious intragenotypic and intergenotypic hepatitis C virus chimeras. *Proc Natl Acad Sci U S A* 103: 7408-7413.
298. Lorenz IC, Allison SL, Heinz FX, Helenius A (2002) Folding and dimerization of tick-borne encephalitis virus envelope proteins prM and E in the endoplasmic reticulum. *J Virol* 76: 5480-5491.
299. Koutsoudakis G, Kaul A, Steinmann E, Kallis S, Lohmann V, et al. (2006) Characterization of the early steps of hepatitis C virus infection by using luciferase reporter viruses. *J Virol* 80: 5308-5320.
300. Krieger SE, Zeisel MB, Davis C, Thumann C, Harris HJ, et al. (2010) Inhibition of hepatitis C virus infection by anti-claudin-1 antibodies is mediated by neutralization of E2-CD81-claudin-1 associations. *Hepatology* 51: 1144-1157.
301. Agnello V, Abel G, Elfahal M, Knight GB, Zhang QX (1999) Hepatitis C virus and other flaviviridae viruses enter cells via low density lipoprotein receptor. *Proc Natl Acad Sci U S A* 96: 12766-12771.

302. Molina S, Castet V, Fournier-Wirth C, Pichard-Garcia L, Avner R, et al. (2007) The low-density lipoprotein receptor plays a role in the infection of primary human hepatocytes by hepatitis C virus. *J Hepatol* 46: 411-419.
303. Hsu M, Zhang J, Flint M, Logvinoff C, Cheng-Mayer C, et al. (2003) Hepatitis C virus glycoproteins mediate pH-dependent cell entry of pseudotyped retroviral particles. *Proc Natl Acad Sci U S A* 100: 7271-7276.
304. Rudenko G, Deisenhofer J (2003) The low-density lipoprotein receptor: ligands, debates and lore. *Curr Opin Struct Biol* 13: 683-689.
305. Burlone ME, Budkowska A (2009) Hepatitis C virus cell entry: role of lipoproteins and cellular receptors. *J Gen Virol* 90: 1055-1070.
306. Hemler ME (2005) Tetraspanin functions and associated microdomains. *Nat Rev Mol Cell Biol* 6: 801-811.
307. Kitadokoro K, Galli G, Petracca R, Falugi F, Grandi G, et al. (2001) Crystallization and preliminary crystallographic studies on the large extracellular domain of human CD81, a tetraspanin receptor for hepatitis C virus. *Acta Crystallogr D Biol Crystallogr* 57: 156-158.
308. Higginbottom A, Quinn ER, Kuo CC, Flint M, Wilson LH, et al. (2000) Identification of amino acid residues in CD81 critical for interaction with hepatitis C virus envelope glycoprotein E2. *J Virol* 74: 3642-3649.
309. Petracca R, Falugi F, Galli G, Norais N, Rosa D, et al. (2000) Structure-function analysis of hepatitis C virus envelope-CD81 binding. *J Virol* 74: 4824-4830.
310. Etienne-Manneville S, Hall A (2002) Rho GTPases in cell biology. *Nature* 420: 629-635.
311. Shigeta M, Sanzen N, Ozawa M, Gu J, Hasegawa H, et al. (2003) CD151 regulates epithelial cell-cell adhesion through PKC- and Cdc42-dependent actin cytoskeletal reorganization. *J Cell Biol* 163: 165-176.
312. Delaguillaumie A, Lagaudriere-Gesbert C, Popoff MR, Conjeaud H (2002) Rho GTPases link cytoskeletal rearrangements and activation processes induced via the tetraspanin CD82 in T lymphocytes. *J Cell Sci* 115: 433-443.
313. Rhainds D, Brissette L (2004) The role of scavenger receptor class B type I (SR-BI) in lipid trafficking. defining the rules for lipid traders. *Int J Biochem Cell Biol* 36: 39-77.
314. Glass C, Pittman RC, Civen M, Steinberg D (1985) Uptake of high-density lipoprotein-associated apoprotein A-I and cholesterol esters by 16 tissues of the rat in vivo and by adrenal cells and hepatocytes in vitro. *J Biol Chem* 260: 744-750.
315. Glass C, Pittman RC, Weinstein DB, Steinberg D (1983) Dissociation of tissue uptake of cholesterol ester from that of apoprotein A-I of rat plasma high density lipoprotein: selective delivery of cholesterol ester to liver, adrenal, and gonad. *Proc Natl Acad Sci U S A* 80: 5435-5439.

316. Krieger M (1999) Charting the fate of the "good cholesterol": identification and characterization of the high-density lipoprotein receptor SR-BI. *Annu Rev Biochem* 68: 523-558.
317. Huang ZH, Mazzone T (2002) ApoE-dependent sterol efflux from macrophages is modulated by scavenger receptor class B type I expression. *J Lipid Res* 43: 375-382.
318. Huang ZH, Gu D, Lange Y, Mazzone T (2003) Expression of scavenger receptor BI facilitates sterol movement between the plasma membrane and the endoplasmic reticulum in macrophages. *Biochemistry* 42: 3949-3955.
319. Ji Y, Jian B, Wang N, Sun Y, Moya ML, et al. (1997) Scavenger receptor BI promotes high density lipoprotein-mediated cellular cholesterol efflux. *J Biol Chem* 272: 20982-20985.
320. Jian B, de la Llera-Moya M, Ji Y, Wang N, Phillips MC, et al. (1998) Scavenger receptor class B type I as a mediator of cellular cholesterol efflux to lipoproteins and phospholipid acceptors. *J Biol Chem* 273: 5599-5606.
321. Catanese MT, Ansuini H, Graziani R, Huby T, Moreau M, et al. (2010) Role of scavenger receptor class B type I in hepatitis C virus entry: kinetics and molecular determinants. *J Virol* 84: 34-43.
322. Maillard P, Huby T, Andreo U, Moreau M, Chapman J, et al. (2006) The interaction of natural hepatitis C virus with human scavenger receptor SR-BI/Cla1 is mediated by ApoB-containing lipoproteins. *FASEB J* 20: 735-737.
323. von Hahn T, Lindenbach BD, Boullier A, Quehenberger O, Paulson M, et al. (2006) Oxidized low-density lipoprotein inhibits hepatitis C virus cell entry in human hepatoma cells. *Hepatology* 43: 932-942.
324. von Hahn T, Rice CM (2008) Hepatitis C virus entry. *J Biol Chem* 283: 3689-3693.
325. Kapadia SB, Barth H, Baumert T, McKeating JA, Chisari FV (2007) Initiation of hepatitis C virus infection is dependent on cholesterol and cooperativity between CD81 and scavenger receptor B type I. *J Virol* 81: 374-383.
326. Shin K, Fogg VC, Margolis B (2006) Tight junctions and cell polarity. *Annu Rev Cell Dev Biol* 22: 207-235.
327. Chiba H, Osanai M, Murata M, Kojima T, Sawada N (2008) Transmembrane proteins of tight junctions. *Biochim Biophys Acta* 1778: 588-600.
328. Itoh M, Furuse M, Morita K, Kubota K, Saitou M, et al. (1999) Direct binding of three tight junction-associated MAGUKs, ZO-1, ZO-2, and ZO-3, with the COOH termini of claudins. *J Cell Biol* 147: 1351-1363.
329. McCarthy KM, Francis SA, McCormack JM, Lai J, Rogers RA, et al. (2000) Inducible expression of claudin-1-myc but not occludin-VSV-G results in aberrant tight junction strand formation in MDCK cells. *J Cell Sci* 113 Pt 19: 3387-3398.
330. Li Y, Fanning AS, Anderson JM, Lavie A (2005) Structure of the conserved cytoplasmic C-terminal domain of occludin: identification of the ZO-1 binding surface. *J Mol Biol* 352: 151-164.

331. Meertens L, Bertaux C, Cukierman L, Cormier E, Lavillette D, et al. (2008) The tight junction proteins claudin-1, -6, and -9 are entry cofactors for hepatitis C virus. *J Virol* 82: 3555-3560.
332. Harris HJ, Farquhar MJ, Mee CJ, Davis C, Reynolds GM, et al. (2008) CD81 and claudin 1 coreceptor association: role in hepatitis C virus entry. *J Virol* 82: 5007-5020.
333. Coyne CB, Shen L, Turner JR, Bergelson JM (2007) Coxsackievirus entry across epithelial tight junctions requires occludin and the small GTPases Rab34 and Rab5. *Cell Host Microbe* 2: 181-192.
334. Coyne CB, Bergelson JM (2006) Virus-induced Abl and Fyn kinase signals permit coxsackievirus entry through epithelial tight junctions. *Cell* 124: 119-131.
335. Jardetzky TS, Lamb RA (2004) Virology: a class act. *Nature* 427: 307-308.
336. Colman PM, Lawrence MC (2003) The structural biology of type I viral membrane fusion. *Nat Rev Mol Cell Biol* 4: 309-319.
337. Wilson IA, Skehel JJ, Wiley DC (1981) Structure of the haemagglutinin membrane glycoprotein of influenza virus at 3 Å resolution. *Nature* 289: 366-373.
338. Wiley DC, Wilson IA, Skehel JJ (1981) Structural identification of the antibody-binding sites of Hong Kong influenza haemagglutinin and their involvement in antigenic variation. *Nature* 289: 373-378.
339. Bullough PA, Hughson FM, Skehel JJ, Wiley DC (1994) Structure of influenza haemagglutinin at the pH of membrane fusion. *Nature* 371: 37-43.
340. Chen J, Lee KH, Steinhauer DA, Stevens DJ, Skehel JJ, et al. (1998) Structure of the hemagglutinin precursor cleavage site, a determinant of influenza pathogenicity and the origin of the labile conformation. *Cell* 95: 409-417.
341. Daniels RS, Downie JC, Hay AJ, Knossow M, Skehel JJ, et al. (1985) Fusion mutants of the influenza virus hemagglutinin glycoprotein. *Cell* 40: 431-439.
342. Eckert DM, Kim PS (2001) Mechanisms of viral membrane fusion and its inhibition. *Annu Rev Biochem* 70: 777-810.
343. Kielian M (2006) Class II virus membrane fusion proteins. *Virology* 344: 38-47.
344. Garoff H, Wilschut J, Liljestrom P, Wahlberg JM, Bron R, et al. (1994) Assembly and entry mechanisms of Semliki Forest virus. *Arch Virol Suppl* 9: 329-338.
345. Akahata W, Yang ZY, Andersen H, Sun S, Holdaway HA, et al. (2010) A virus-like particle vaccine for epidemic Chikungunya virus protects nonhuman primates against infection. *Nat Med* 16: 334-338.
346. Modis Y, Ogata S, Clements D, Harrison SC (2003) A ligand-binding pocket in the dengue virus envelope glycoprotein. *Proc Natl Acad Sci U S A* 100: 6986-6991.

347. Modis Y, Ogata S, Clements D, Harrison SC (2005) Variable surface epitopes in the crystal structure of dengue virus type 3 envelope glycoprotein. *J Virol* 79: 1223-1231.
348. Lescar J, Roussel A, Wien MW, Navaza J, Fuller SD, et al. (2001) The Fusion glycoprotein shell of Semliki Forest virus: an icosahedral assembly primed for fusogenic activation at endosomal pH. *Cell* 105: 137-148.
349. Roussel A, Lescar J, Vaney MC, Wengler G, Rey FA (2006) Structure and interactions at the viral surface of the envelope protein E1 of Semliki Forest virus. *Structure* 14: 75-86.
350. Bressanelli S, Stiasny K, Allison SL, Stura EA, Duquerroy S, et al. (2004) Structure of a flavivirus envelope glycoprotein in its low-pH-induced membrane fusion conformation. *Embo J* 23: 728-738.
351. Modis Y, Ogata S, Clements D, Harrison SC (2004) Structure of the dengue virus envelope protein after membrane fusion. *Nature* 427: 313-319.
352. Backovic M, Jardetzky TS (2009) Class III viral membrane fusion proteins. *Curr Opin Struct Biol* 19: 189-196.
353. Roche S, Bressanelli S, Rey FA, Gaudin Y (2006) Crystal structure of the low-pH form of the vesicular stomatitis virus glycoprotein G. *Science* 313: 187-191.
354. Roche S, Rey FA, Gaudin Y, Bressanelli S (2007) Structure of the prefusion form of the vesicular stomatitis virus glycoprotein G. *Science* 315: 843-848.
355. Fredericksen BL, Whitt MA (1995) Vesicular stomatitis virus glycoprotein mutations that affect membrane fusion activity and abolish virus infectivity. *J Virol* 69: 1435-1443.
356. Zhang L, Ghosh HP (1994) Characterization of the putative fusogenic domain in vesicular stomatitis virus glycoprotein G. *J Virol* 68: 2186-2193.
357. Mothes W, Boerger AL, Narayan S, Cunningham JM, Young JA (2000) Retroviral entry mediated by receptor priming and low pH triggering of an envelope glycoprotein. *Cell* 103: 679-689.
358. Chandran K, Sullivan NJ, Felbor U, Whelan SP, Cunningham JM (2005) Endosomal proteolysis of the Ebola virus glycoprotein is necessary for infection. *Science* 308: 1643-1645.
359. Li K, Zhang S, Kronqvist M, Wallin M, Ekstrom M, et al. (2008) Intersubunit disulfide isomerization controls membrane fusion of human T-cell leukemia virus Env. *J Virol* 82: 7135-7143.
360. Wallin M, Ekstrom M, Garoff H (2004) Isomerization of the intersubunit disulphide-bond in Env controls retrovirus fusion. *Embo J* 23: 54-65.
361. Morikawa K, Zhao Z, Date T, Miyamoto M, Murayama A, et al. (2007) The roles of CD81 and glycosaminoglycans in the adsorption and uptake of infectious HCV particles. *J Med Virol* 79: 714-723.
362. Marukian S, Jones CT, Andrus L, Evans MJ, Ritola KD, et al. (2008) Cell culture-produced hepatitis C virus does not infect peripheral blood mononuclear cells. *Hepatology* 48: 1843-1850.

363. Center RJ, Kobe B, Wilson KA, Teh T, Howlett GJ, et al. (1998) Crystallization of a trimeric human T cell leukemia virus type 1 gp21 ectodomain fragment as a chimera with maltose-binding protein. *Protein Sci* 7: 1612-1619.
364. Evan GI, Lewis GK, Ramsay G, Bishop JM (1985) Isolation of monoclonal antibodies specific for human c-myc proto-oncogene product. *Mol Cell Biol* 5: 3610-3616.
365. He J, Choe S, Walker R, Di Marzio P, Morgan DO, et al. (1995) Human immunodeficiency virus type 1 viral protein R (Vpr) arrests cells in the G2 phase of the cell cycle by inhibiting p34cdc2 activity. *J Virol* 69: 6705-6711.
366. Chang LJ, Urlacher V, Iwakuma T, Cui Y, Zucali J (1999) Efficacy and safety analyses of a recombinant human immunodeficiency virus type 1 derived vector system. *Gene Ther* 6: 715-728.
367. Sambrook J, Fritsch, E., Maniatis, T. (1989) *Molecular Cloning: A Laboratory Manual*: Cold Spring Harbour Laboratory Press.
368. Keck ZY, Li TK, Xia J, Bartosch B, Cosset FL, et al. (2005) Analysis of a highly flexible conformational immunogenic domain a in hepatitis C virus E2. *J Virol* 79: 13199-13208.
369. Chesebro B, Wehrly K, Nishio J, Perryman S (1992) Macrophage-tropic human immunodeficiency virus isolates from different patients exhibit unusual V3 envelope sequence homogeneity in comparison with T-cell-tropic isolates: definition of critical amino acids involved in cell tropism. *J Virol* 66: 6547-6554.
370. Toohey K, Wehrly K, Nishio J, Perryman S, Chesebro B (1995) Human immunodeficiency virus envelope V1 and V2 regions influence replication efficiency in macrophages by affecting virus spread. *Virology* 213: 70-79.
371. Lindenbach BD (2009) Measuring HCV infectivity produced in cell culture and in vivo. *Methods Mol Biol* 510: 329-336.
372. Holmgren A (1979) Thioredoxin catalyzes the reduction of insulin disulfides by dithiothreitol and dihydrolipoamide. *J Biol Chem* 254: 9627-9632.
373. Azimi I, Matthias LJ, Center RJ, Wong JW, Hogg PJ (2010) The disulfide bond that constrains the HIV-1 gp120 V3 domain is cleaved by thioredoxin. *J Biol Chem*.
374. Barbouche R, Miquelis R, Jones IM, Fenouillet E (2003) Protein-disulfide isomerase-mediated reduction of two disulfide bonds of HIV envelope glycoprotein 120 occurs post-CXCR4 binding and is required for fusion. *J Biol Chem* 278: 3131-3136.
375. Markovic I, Stantchev TS, Fields KH, Tiffany LJ, Tomic M, et al. (2004) Thiol/disulfide exchange is a prerequisite for CXCR4-tropic HIV-1 envelope-mediated T-cell fusion during viral entry. *Blood* 103: 1586-1594.
376. Matthias LJ, Yam PT, Jiang XM, Vandegraaff N, Li P, et al. (2002) Disulfide exchange in domain 2 of CD4 is required for entry of HIV-1. *Nat Immunol* 3: 727-732.

377. Fenouillet E, Lavillette D, Loureiro S, Krashias G, Maurin G, et al. (2008) Contribution of redox status to hepatitis C virus E2 envelope protein function and antigenicity. *J Biol Chem* 283: 26340-26348.
378. Grove J, Nielsen S, Zhong J, Bassendine MF, Drummer HE, et al. (2008) Identification of a residue in hepatitis C virus E2 glycoprotein that determines scavenger receptor BI and CD81 receptor dependency and sensitivity to neutralizing antibodies. *J Virol* 82: 12020-12029.
379. Holmgren A (1985) Thioredoxin. *Annu Rev Biochem* 54: 237-271.
380. Zhu P, Chertova E, Bess J, Jr., Lifson JD, Arthur LO, et al. (2003) Electron tomography analysis of envelope glycoprotein trimers on HIV and simian immunodeficiency virus virions. *Proc Natl Acad Sci U S A* 100: 15812-15817.
381. Sougrat R, Bartesaghi A, Lifson JD, Bennett AE, Bess JW, et al. (2007) Electron tomography of the contact between T cells and SIV/HIV-1: implications for viral entry. *PLoS Pathog* 3: e63.
382. Meertens L, Bertaux C, Dragic T (2006) Hepatitis C virus entry requires a critical postinternalization step and delivery to early endosomes via clathrin-coated vesicles. *J Virol* 80: 11571-11578.
383. Krey T, Thiel HJ, Rumenapf T (2005) Acid-resistant bovine pestivirus requires activation for pH-triggered fusion during entry. *J Virol* 79: 4191-4200.
384. Durantel D, Branza-Nichita N, Carrouee-Durantel S, Butters TD, Dwek RA, et al. (2001) Study of the mechanism of antiviral action of iminosugar derivatives against bovine viral diarrhea virus. *J Virol* 75: 8987-8998.
385. Lazar C, Zitzmann N, Dwek RA, Branza-Nichita N (2003) The pestivirus E(rns) glycoprotein interacts with E2 in both infected cells and mature virions. *Virology* 314: 696-705.
386. Thiel HJ, Stark R, Weiland E, Rumenapf T, Meyers G (1991) Hog cholera virus: molecular composition of virions from a pestivirus. *J Virol* 65: 4705-4712.
387. Weiland E, Stark R, Haas B, Rumenapf T, Meyers G, et al. (1990) Pestivirus glycoprotein which induces neutralizing antibodies forms part of a disulfide-linked heterodimer. *J Virol* 64: 3563-3569.
388. Grauschopf U, Winther JR, Korber P, Zander T, Dallinger P, et al. (1995) Why is DsbA such an oxidizing disulfide catalyst? *Cell* 83: 947-955.
389. Ferrari DM, Soling HD (1999) The protein disulphide-isomerase family: unravelling a string of folds. *Biochem J* 339 (Pt 1): 1-10.
390. Martin JL (1995) Thioredoxin--a fold for all reasons. *Structure* 3: 245-250.
391. Chivers PT, Prehoda KE, Raines RT (1997) The CXXC motif: a rheostat in the active site. *Biochemistry* 36: 4061-4066.
392. Huber-Wunderlich M, Glockshuber R (1998) A single dipeptide sequence modulates the redox properties of a whole enzyme family. *Fold Des* 3: 161-171.

393. Mossner E, Huber-Wunderlich M, Glockshuber R (1998) Characterization of *Escherichia coli* thioredoxin variants mimicking the active-sites of other thiol/disulfide oxidoreductases. *Protein Sci* 7: 1233-1244.
394. Quan S, Schneider I, Pan J, Von Hacht A, Bardwell JC (2007) The CXXC motif is more than a redox rheostat. *J Biol Chem* 282: 28823-28833.
395. Hadlock KG, Lanford RE, Perkins S, Rowe J, Yang Q, et al. (2000) Human monoclonal antibodies that inhibit binding of hepatitis C virus E2 protein to CD81 and recognize conserved conformational epitopes. *J Virol* 74: 10407-10416.
396. Chivers PT, Laboissiere MC, Raines RT (1996) The CXXC motif: imperatives for the formation of native disulfide bonds in the cell. *Embo J* 15: 2659-2667.
397. Krause G, Lundstrom J, Barea JL, Pueyo de la Cuesta C, Holmgren A (1991) Mimicking the active site of protein disulfide-isomerase by substitution of proline 34 in *Escherichia coli* thioredoxin. *J Biol Chem* 266: 9494-9500.
398. Lundstrom J, Krause G, Holmgren A (1992) A Pro to His mutation in active site of thioredoxin increases its disulfide-isomerase activity 10-fold. New refolding systems for reduced or randomly oxidized ribonuclease. *J Biol Chem* 267: 9047-9052.
399. Appenzeller-Herzog C, Ellgaard L (2008) The human PDI family: versatility packed into a single fold. *Biochim Biophys Acta* 1783: 535-548.
400. Bardwell JC, McGovern K, Beckwith J (1991) Identification of a protein required for disulfide bond formation in vivo. *Cell* 67: 581-589.
401. Givol D, Goldberger RF, Anfinsen CB (1964) Oxidation and Disulfide Interchange in the Reactivation of Reduced Ribonuclease. *J Biol Chem* 239: PC3114-3116.
402. Johnson S, Michalak M, Opas M, Eggleton P (2001) The ins and outs of calreticulin: from the ER lumen to the extracellular space. *Trends Cell Biol* 11: 122-129.
403. Cocquerel L, Voisset C, Dubuisson J (2006) Hepatitis C virus entry: potential receptors and their biological functions. *J Gen Virol* 87: 1075-1084.
404. Hussy P, Faust H, Wagner JC, Schmid G, Mous J, et al. (1997) Evaluation of hepatitis C virus envelope proteins expressed in *E. coli* and insect cells for use as tools for antibody screening. *J Hepatol* 26: 1179-1186.
405. Lorent E, Bierau H, Engelborghs Y, Verheyden G, Bosman F (2008) Structural characterisation of the hepatitis C envelope glycoprotein E1 ectodomain derived from a mammalian and a yeast expression system. *Vaccine* 26: 399-410.
406. Gregory MS-J (2003) Thioredoxin and oxidative stress: Griffith University. 139 p.
407. Marino SM, Gladyshev VN (2009) A structure-based approach for detection of thiol oxidoreductases and their catalytic redox-active cysteine residues. *PLoS Comput Biol* 5: e1000383.

408. Stanley P, Caillibot V, Siminovitch L (1975) Selection and characterization of eight phenotypically distinct lines of lectin-resistant Chinese hamster ovary cell. *Cell* 6: 121-128.
409. Dubuisson J, Duvet S, Meunier JC, Op De Beeck A, Cacan R, et al. (2000) Glycosylation of the hepatitis C virus envelope protein E1 is dependent on the presence of a downstream sequence on the viral polyprotein. *J Biol Chem* 275: 30605-30609.
410. Holmgren A, Soderberg BO, Eklund H, Branden CI (1975) Three-dimensional structure of *Escherichia coli* thioredoxin-S2 to 2.8 Å resolution. *Proc Natl Acad Sci U S A* 72: 2305-2309.
411. Forman-Kay JD, Clore GM, Wingfield PT, Gronenborn AM (1991) High-resolution three-dimensional structure of reduced recombinant human thioredoxin in solution. *Biochemistry* 30: 2685-2698.
412. Mittard V, Blackledge MJ, Stein M, Jacquot JP, Marion D, et al. (1997) NMR solution structure of an oxidised thioredoxin h from the eukaryotic green alga *Chlamydomonas reinhardtii*. *Eur J Biochem* 243: 374-383.
413. Katti SK, LeMaster DM, Eklund H (1990) Crystal structure of thioredoxin from *Escherichia coli* at 1.68 Å resolution. *J Mol Biol* 212: 167-184.
414. Bushweller JH, Billeter M, Holmgren A, Wuthrich K (1994) The nuclear magnetic resonance solution structure of the mixed disulfide between *Escherichia coli* glutaredoxin(C14S) and glutathione. *J Mol Biol* 235: 1585-1597.
415. Eklund H, Ingelman M, Soderberg BO, Uhlin T, Nordlund P, et al. (1992) Structure of oxidized bacteriophage T4 glutaredoxin (thioredoxin). Refinement of native and mutant proteins. *J Mol Biol* 228: 596-618.
416. Sodano P, Xia TH, Bushweller JH, Bjornberg O, Holmgren A, et al. (1991) Sequence-specific ¹H n.m.r. assignments and determination of the three-dimensional structure of reduced *Escherichia coli* glutaredoxin. *J Mol Biol* 221: 1311-1324.
417. Xia TH, Bushweller JH, Sodano P, Billeter M, Bjornberg O, et al. (1992) NMR structure of oxidized *Escherichia coli* glutaredoxin: comparison with reduced *E. coli* glutaredoxin and functionally related proteins. *Protein Sci* 1: 310-321.
418. Ji X, Zhang P, Armstrong RN, Gilliland GL (1992) The three-dimensional structure of a glutathione S-transferase from the mu gene class. Structural analysis of the binary complex of isoenzyme 3-3 and glutathione at 2.2-Å resolution. *Biochemistry* 31: 10169-10184.
419. Reinemer P, Dirr HW, Ladenstein R, Huber R, Lo Bello M, et al. (1992) Three-dimensional structure of class pi glutathione S-transferase from human placenta in complex with S-hexylglutathione at 2.8 Å resolution. *J Mol Biol* 227: 214-226.
420. Reinemer P, Dirr HW, Ladenstein R, Schaffer J, Gallay O, et al. (1991) The three-dimensional structure of class pi glutathione S-transferase in complex with glutathione sulfonate at 2.3 Å resolution. *Embo J* 10: 1997-2005.

421. Sinning I, Kleywegt GJ, Cowan SW, Reinemer P, Dirr HW, et al. (1993) Structure determination and refinement of human alpha class glutathione transferase A1-1, and a comparison with the Mu and Pi class enzymes. *J Mol Biol* 232: 192-212.
422. Martin JL, Bardwell JC, Kuriyan J (1993) Crystal structure of the DsbA protein required for disulphide bond formation in vivo. *Nature* 365: 464-468.
423. Epp O, Ladenstein R, Wendel A (1983) The refined structure of the selenoenzyme glutathione peroxidase at 0.2-nm resolution. *Eur J Biochem* 133: 51-69.
424. Goldberger RF, Epstein CJ, Anfinsen CB (1963) Acceleration of reactivation of reduced bovine pancreatic ribonuclease by a microsomal system from rat liver. *J Biol Chem* 238: 628-635.
425. van Lith M, Karala AR, Bown D, Gatehouse JA, Ruddock LW, et al. (2007) A developmentally regulated chaperone complex for the endoplasmic reticulum of male haploid germ cells. *Mol Biol Cell* 18: 2795-2804.
426. Haugstetter J, Blicher T, Ellgaard L (2005) Identification and characterization of a novel thioredoxin-related transmembrane protein of the endoplasmic reticulum. *J Biol Chem* 280: 8371-8380.
427. Kikuchi M, Doi E, Tsujimoto I, Horibe T, Tsujimoto Y (2002) Functional analysis of human P5, a protein disulfide isomerase homologue. *J Biochem* 132: 451-455.
428. Sugiura Y, Araki K, Iemura S, Natsume T, Hoseki J, et al. (2010) Novel thioredoxin-related transmembrane protein TMX4 has reductase activity. *J Biol Chem* 285: 7135-7142.
429. Kleemann R, Kapurniotu A, Frank RW, Gessner A, Mischke R, et al. (1998) Disulfide analysis reveals a role for macrophage migration inhibitory factor (MIF) as thiol-protein oxidoreductase. *J Mol Biol* 280: 85-102.
430. Laloi C, Rayapuram N, Chartier Y, Grienenberger JM, Bonnard G, et al. (2001) Identification and characterization of a mitochondrial thioredoxin system in plants. *Proc Natl Acad Sci U S A* 98: 14144-14149.
431. Pigiet VP, Schuster BJ (1986) Thioredoxin-catalyzed refolding of disulfide-containing proteins. *Proc Natl Acad Sci U S A* 83: 7643-7647.
432. Yazdanparast R, Andrews PC, Smith DL, Dixon JE (1987) Assignment of disulfide bonds in proteins by fast atom bombardment mass spectrometry. *J Biol Chem* 262: 2507-2513.
433. Mezghrani A, Fassio A, Benham A, Simmen T, Braakman I, et al. (2001) Manipulation of oxidative protein folding and PDI redox state in mammalian cells. *Embo J* 20: 6288-6296.
434. Frutiger S, Hughes GJ, Paquet N, Luthy R, Jaton JC (1992) Disulfide bond assignment in human J chain and its covalent pairing with immunoglobulin M. *Biochemistry* 31: 12643-12647.
435. Matsuo Y, Akiyama N, Nakamura H, Yodoi J, Noda M, et al. (2001) Identification of a novel thioredoxin-related transmembrane protein. *J Biol Chem* 276: 10032-10038.

436. Meng X, Zhang C, Chen J, Peng S, Cao Y, et al. (2003) Cloning and identification of a novel cDNA coding thioredoxin-related transmembrane protein 2. *Biochem Genet* 41: 99-106.
437. Liu S, Lu H, Niu J, Xu Y, Wu S, et al. (2005) Different from the HIV fusion inhibitor C34, the anti-HIV drug Fuzeon (T-20) inhibits HIV-1 entry by targeting multiple sites in gp41 and gp120. *J Biol Chem* 280: 11259-11273.